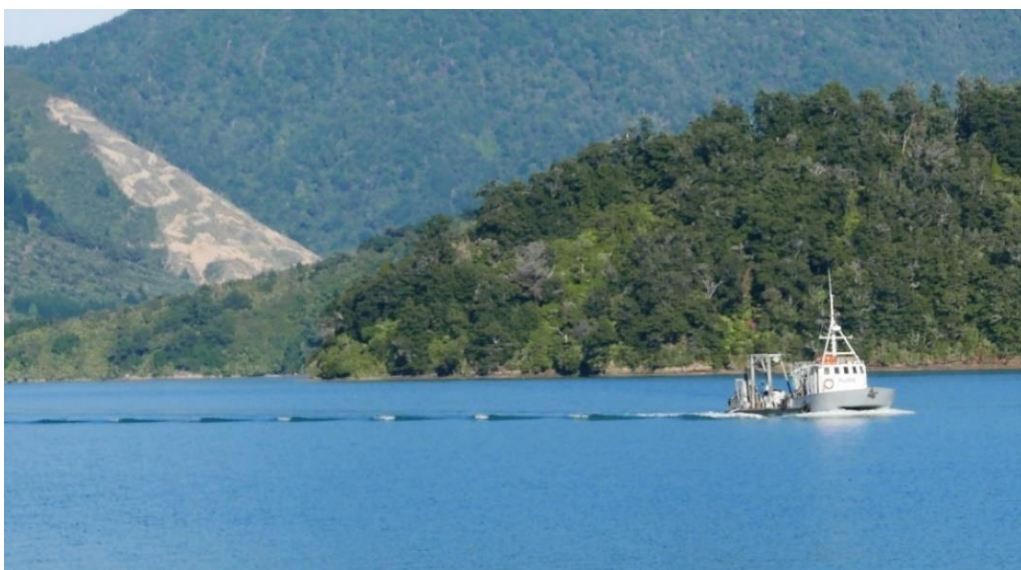


Sources of fine sediment and contribution to sedimentation in the inner Pelorus Sound/Te Hoiere

Prepared for Marlborough District Council

September 2021



Prepared by:

Andrew Swales,
Max M. Gibbs,
Sean Handley,
Greg Olsen,
Ron Ovenden,
Sanjay Wadhwa
Julie Brown




For any information regarding this report please contact:

Dr Andrew Swales
Programme Leader - Catchments to Estuaries
Coastal and Estuarine Physical Processes Group
856 7026
andrew.swales@niwa.co.nz

National Institute of Water & Atmospheric Research Ltd
PO Box 11115
Hamilton 3251

Phone +64 7 856 7026

NIWA CLIENT REPORT No: 2021291HN
Report date: September 2021
NIWA Project: MDC17201

Quality Assurance Statement		
	Reviewed by:	Dr Andrew Hughes
	Formatting checked by:	Alex Quigley Carole Evans
	Approved for release by:	Dr Neale Hudson

© All rights reserved. This publication may not be reproduced or copied in any form without the permission of the copyright owner(s). Such permission is only to be given in accordance with the terms of the client's contract with NIWA. This copyright extends to all forms of copying and any storage of material in any kind of information retrieval system.

Whilst NIWA has used all reasonable endeavours to ensure that the information contained in this document is accurate, NIWA does not give any express or implied warranty as to the completeness of the information contained herein, or that it will be suitable for any purpose(s) other than those specifically contemplated during the Project or agreed by NIWA and the Client.

Contents

Executive summary	5
1 Introduction	9
1.1 Background to study.....	9
1.2 Study objectives.....	10
1.3 Study area	11
2 Methods.....	30
2.1 CSSI sediment source tracing - overview.....	30
2.2 Sediment source library.....	33
2.3 Soil and sediment sampling methods.....	39
2.4 Bulk carbon and fatty acid analyses	43
2.5 Source isotopic polygons	43
2.6 Multivariate ordination – source and tracer selection.....	49
2.7 Sediment source modelling	51
2.8 Sediment composition.....	54
2.9 Sediment accumulation rates.....	54
2.10 Mollusc death assemblage (DA) analysis.....	55
3 Results	59
3.1 Sources of sediment deposited in river system.....	59
3.2 Havelock Estuary sediment cores	65
3.3 Mahau Sound sediment cores	65
3.4 Sources of sediment accumulating in Mahau Sound	71
3.5 Sediment characteristics and mollusc death assemblage	76
4 Discussion	82
4.1 Changes in sediment accumulation rates.....	82
4.2 Sources of river sediment deposits	83
4.3 Sources of sediment accumulating in the inner Pelorus Sound	88
4.4 Mollusc death assemblage	95
5 Concluding remarks	99
5.1 Legacy sediment and future management.....	99
6 Acknowledgements	102

7	References.....	103
Appendix A	Historical record of severe weather events	117
Appendix B	Havelock Harbour Board Report – 20 April 1953.....	120
Appendix C	Summary of CSSI method	126
Appendix D	Soil sampling method	133
Appendix E	Estuarine core sites and composition analysis	134
Appendix F	Source library for Pelorus River and Mahau Sound	136
Appendix G	Mixing models	140
Appendix H	Radioisotope dating	145
Appendix I	River sediment source proportion statistics from mixing model results.....	151
Appendix J	MDC Pelorus Sound TSS Monitoring.....	156
Appendix K	Soil proportion (%) statistics for Mahau cores	158
Appendix L	Source proportion yields (% km²) by land use area for Pelorus-Rai, Kaituna and Cullens Creek catchments.	178

Tables

Table 1-1:	Present-day catchment land use in the Pelorus, Rai and Kaituna catchments.	15
Table 2-1:	Bulk carbon and fatty acid (FA) tracers usable in isotopic biplot polygon test.	45
Table 2-2:	Land use area (km ²) for modelled sediment sources – Land Cover Data Base (LCDB) versions 2 to 4.	53
Table 2-3:	Time periods used to section and process sediment cores as per Handley et al. (2017).	56
Table 3-1:	Summary of the mean proportional contributions of sediment from the tributaries into the main stem of the river downstream of the confluence.	59
Table 3-2:	Calculation of the proportional sediment contribution from each tributary to the Pelorus River at the mouth.	60
Table 3-3:	Conversion of the CSSI estimates of sediment yield proportions (% , Table 3.2) into sediment yields (SY, t yr ⁻¹) and specific sediment yields (SSY, t km ⁻² /yr ⁻¹).	62
Table 3-4:	Series 1 modelling. Proportional mean soil contributions (±SD) by land use to individual rivers from their catchments.	63
Table 3-5:	Series 2 Modelling: Proportional mean soil contributions (±SD) by land use to individual rivers from their catchments.	63

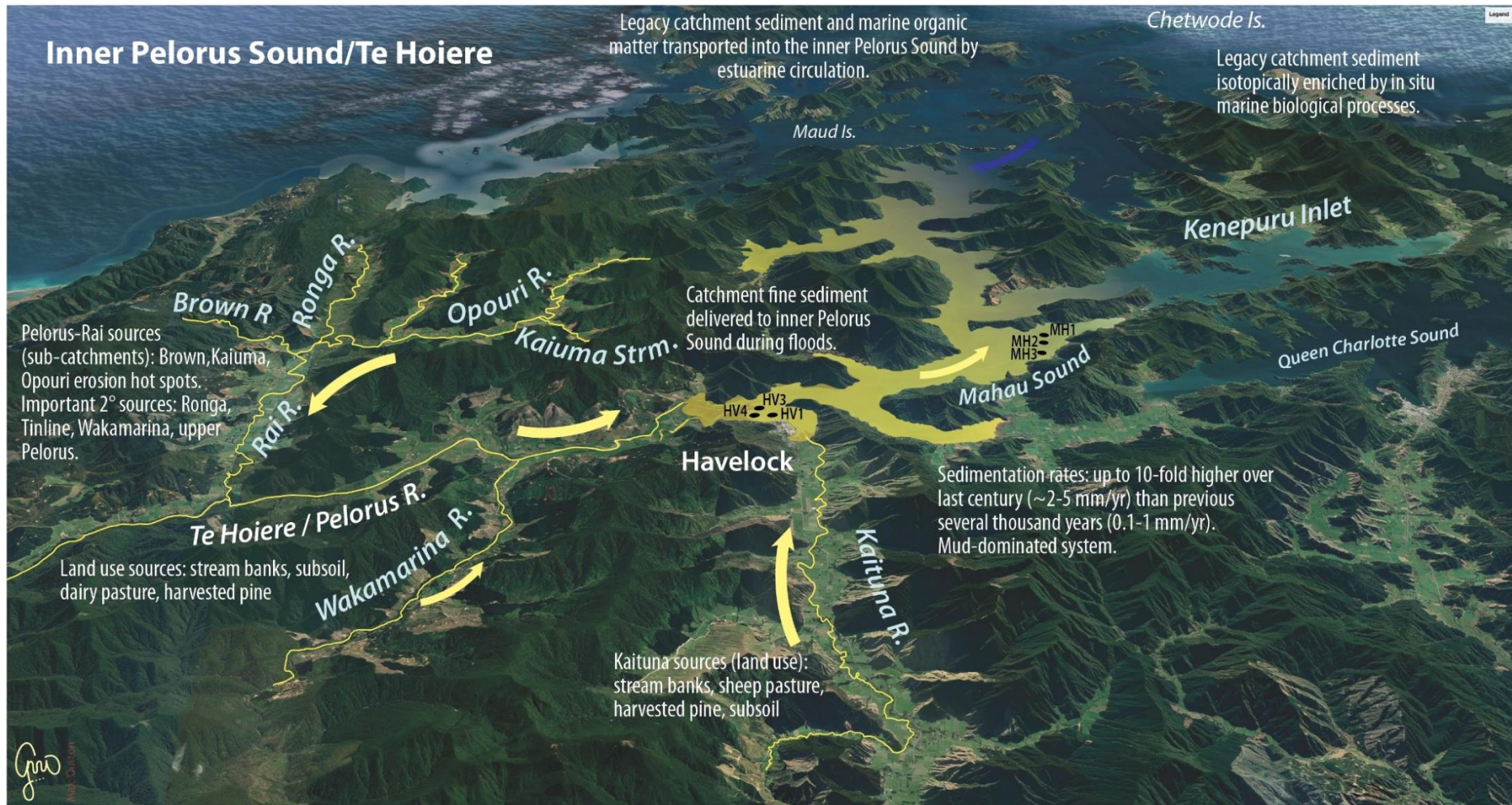
Table 3-6:	Proportional mean soil contributions (\pm SD) by land use in the lower Kaituna River.	64
Table 3-7:	Summary of catchment source contribution (%) to sediment accumulation in Mahau Sound since early 1900s.	72
Table 3-8:	Source proportion yields (% km ⁻²) for land use classes and yield ratios relative to native forest based on Land Cover Data Base (LCDB) versions 2 to 4.	75
Table 3-9:	Mollusc species contributing most of shell by % weight of the total from all three sediment cores.	79
Table A-1:	Historical records of severe weather events (1868-2000) in the Pelorus/Te Hoiere and Kaituna catchments and Pelorus Sound.	117
Table F-1:	Land use library isotopic data from sites as shown in Figure 2-4.	136
Table G-1:	Pelorus River summary of MixSIAR model convergence.	142
Table G-2:	Mahau core MH-1 summary of MixSIAR model convergence.	142
Table G-3:	Mahau core MH-2 summary of MixSIAR model convergence.	143
Table G-4:	Mahau core MH-3 summary of MixSIAR model convergence.	144
Table I-1:	Soil proportion statistics from two-endmember mixing model analysis of the river confluences (tributaries and main stem).	151
Table J-1:	Summary statistics for TSS (g m ⁻³) at selected MDC WQ monitoring sites.	157

Figures

Figure 1-1:	Kaituna river in flood, 15 November 2016.	12
Figure 1-2:	Intact coastal margin adjoining old-growth complex floodplain forest, Tennyson Inlet, Pelorus Sound/Te Hoiere.	14
Figure 1-3:	Havelock township (ca. 1890s).	15
Figure 1-4:	Sluice dredging 1870s and 1910s in the Whakamarino Valley.	17
Figure 1-5:	Rai Valley Co-operative Dairy Factory 1909 note the cleared hillsides.	17
Figure 1-6:	Pine plantations in the Rai-Whangamoia State Forest.	18
Figure 1-7:	Areas of newly-established pine forest in the Rai-Whangamoia State Forest (1950).	19
Figure 1-8:	First harvest of timber from the Rai State Forest, circa 1980.	20
Figure 1-9:	Land use in the catchments of the inner Pelorus Sound.	22
Figure 1-10:	Pelorus-Rai catchment land use capability.	23
Figure 1-11:	Modelled mean current speed at 5 m depth in Pelorus Sound/Te Hoiere.	24
Figure 1-12:	Sentinel-2 satellite image of the Marlborough Sounds, 21 May 2017.	26
Figure 1-13:	Havelock Estuary - distribution of intertidal habitat types.	27
Figure 1-14:	Hydrographic chart of Havelock estuary - H.M.S Pandora (1854).	28
Figure 1-15:	Aerial photographs of Havelock Estuary, 13 April 1942 and 31 December 2015.	29
Figure 2-1:	CSSI sediment source tracing.	31
Figure 2-2:	Subsoil sampling Site 3 road cutting (March 2017).	36
Figure 2-3:	Example of streambank erosion in the Rai River catchment (December 2016).	36
Figure 2-4:	Location of river sediment deposit sampling sites.	37

Figure 2-5:	Schematic diagram of the Pelorus River system showing the tributaries modelled and the location of sediment sampling relative to each confluence.	38
Figure 2-6:	Location of river, estuarine sediment cores and marine sediment sampling sites.	39
Figure 2-7:	A flood sediment deposit sampled from the top of the riverbank.	40
Figure 2-8:	Location of sediment core sites in Havelock Estuary and Mahau Sound.	41
Figure 2-9:	Sediment coring in Mahau Sound.	42
Figure 2-10:	Examples of isotopic biplot polygon plots for all land use sources in the lower Pelorus River (a,b,c) and the lower Kaituna River (d).	44
Figure 2-11:	Isotopic biplots of average FA $\delta^{13}\text{C}$ values (C14:0 with C20:0 and C22:0) for potential sediment sources and estuarine sediment mixtures in dated cores.	47
Figure 2-12:	Isotopic biplots of average FA $\delta^{13}\text{C}$ values (C14:0 with C24:0 and C26:0) for potential sediment sources and estuarine sediment mixtures in dated cores.	48
Figure 2-13:	Canonical Analysis of Principal Coordinates (CAP) plot – ten sources and nine tracers.	50
Figure 2-14:	Canonical Analysis of Principal Coordinates (CAP) plot – seven sources and five tracers.	51
Figure 2-15:	Functional feeding traits of species sampled in the mollusc death assemblage.	58
Figure 3-1:	Summation plot comparing proportional soil source contributions (%) from each land use in the tributaries and the main stem of the Pelorus River.	64
Figure 3-2:	Mean land use soil contributions to a) the Pelorus River and b) the Kaituna River at the lowest site.	64
Figure 3-3:	Havelock Estuary cores – ages of sediment layers and sediment accumulation rates (SAR).	65
Figure 3-4:	Core MH-1 (subtidal: Mahau Sound): 0-128 cm.	66
Figure 3-5:	Core site MH-1 (Mahau Sound) – ages of sediment layers, sediment accumulation rates (SAR), and sediment properties.	67
Figure 3-6:	Core MH-2 (subtidal: Mahau Sound): 0-143 cm.	68
Figure 3-7:	Core site MH-2 (Mahau Sound) – ages of sediment layers, sediment accumulation rates (SAR), and sediment properties.	69
Figure 3-8:	Core MH-3 (subtidal: Mahau Sound): 0-150 cm.	70
Figure 3-9:	Core site MH-3 (Mahau Sound) – ages of sediment layers, sediment accumulation rates (SAR), and sediment properties.	71
Figure 3-10:	All sources of sediment accumulating in Mahau Sound (Inner Pelorus) since the early 20th century determined from CSSI analysis of dated cores.	73
Figure 3-11:	Catchment sources of sediment accumulating in Mahau Sound (Inner Pelorus) since the early 20 th century determined from CSSI analysis of dated cores.	74
Figure 3-12:	a) Results of multivariate death assemblage and sediment analyses.	77
Figure 3-13:	Sediment characteristics derived from sections of three replicate cores taken in Mahau Sound, plotted by time-period. .	78

Figure 3-14:	Distance based redundancy (dbRDA) plot of death assemblage species (shell volumes) to discriminate time periods against predictor sediment characteristics.	80
Figure 3-15:	The mean proportion of mollusc feeding traits calculated from all cores expressed by shell volume (mL/yr).	80
Figure 3-16:	Mean number of mollusc species calculated from presence/absence from each date period across all replicate core sections.	81
Figure 4-1:	Sources of sediment by land use deposited at confluences and contributions (%) from major tributaries in the Pelorus-Rai and Kaituna catchments.	86
Figure 4-2:	Examples of understory plant communities in (a) native forest, and (b) mature pine forest.	87
Figure 4-3:	Resuspension potential (threshold = 0.1 Pa) for fine sediment in the Marlborough Sounds. .	89
Figure 4-4:	Potential for benthic sediment disturbance by waves in the Marlborough Sounds.	91
Figure 4-5:	Proportional soil contributions from surface sediment from each source.	92
Figure 4-6:	LCDB Version 5 (2018) – landcover in the Pelorus Sound catchment.	94
Figure 4-7:	Hjulström Curve.	98
Figure C-1:	Historical change in atmospheric $\delta^{13}\text{C}$ (per mil) (1570–2010 AD) due to release of fossil carbon.	131
Figure J-1:	Locations of MDC water quality monitoring sites in Pelorus Sound.	156
Figure J-2:	Time series of total suspended solids (TSS, g m^{-3}) at MDC water quality monitoring sites in Pelorus Sound (July 2012 to July 2021).	157



Graphical abstracts: key study findings – views from the catchment (**top**) and looking towards Havelock (**bottom**) from outer Pelorus Sound/Te Hoiere.

Inner Pelorus Sound/Te Hoiere

Sedimentation rates: up to 10-fold higher over last century (~2-5 mm/yr) than previous several thousand years (0.1-1 mm/yr).
Mud-dominated system.

Large cockles in pre-human times suggest system was more stable & waters less turbid. Large cockles now rare in subtidal habitats.

Fine-sediment laden river plumes dispersed in seaward-flowing surface layer. Deposition in low-energy subtidal environments.

Legacy catchment sediment:

- Isotopically enriched by in situ marine biological processes.
- Resuspended sediment and marine organic matter transported into the inner Pelorus Sound by estuarine circulation.

Kaituna R.

Te Hoiere / Pelorus R.

Rai R.

Havelock

Mahau Sound

MH3
MH2
MHT

Queen Charlotte Sound

Kenepuru Inlet

Sentinel-2 satellite image 21 May 2017



Executive summary

Marlborough District Council commissioned a study of the inner Pelorus Sound/Te Hoiere to improve understanding of how land use activities and associated soil erosion have impacted on sediment accumulation rates (SAR) and composition, and to identify sources of deposited sediment. This study builds on a previous work by Handley et al. (2017) in Kenepuru Inlet and Beatrix Bay. The specific objectives of the study were to:

- Determine SAR in the inner Pelorus Sound over recent decades and how these rates compare to pre-human (background) rates.
- Identify sources of sediment (by land use) that are accumulating in the inner Sound and how these have changed over time.
- Identify sources of sediment that are over-represented as a proportion of land use area in the Pelorus and Kaituna catchments.

The compound specific stable isotope (CSSI) sediment-tracing technique developed by NIWA was used to determine sources of sediment accumulating in the inner Pelorus Sound. The CSSI method employs the isotopic (i.e., $\delta^{13}\text{C}$) signatures of fatty-acid (FA) biomarkers secreted by plant root systems. These FA are naturally bound to soil particles and are used to identify different plant communities (i.e., plant community soil signatures are used as proxies for each land use).

Samples of soils and sediment from potential sources and sediment deposits from rivers and the inner Pelorus Sound were collected in several phases during February 2017 to December 2019. Sampling included topsoils (i.e., land uses), subsoils, river and streambank sediment, fine-sediment deposits in river channels, sediment cores from Mahau Sound, and surficial marine sediment from the entrance to Pelorus Sound (i.e., Chetwode Islands/Nukuwaiata and Te Kakaho). These samples were used to: (1) assemble a library of FA biotracer data for potential soil/sediment sources and sediment mixtures from the river and estuarine receiving environments, and employed with mixing models, (2) determine the contributions of various sources to present-day sedimentation in the rivers and fine sediment deposition in Mahau Sound since the early 1900s.

Sediment accumulation rates in Havelock Estuary and Mahau Sound over the last ~century were estimated using two independent radioisotope dating methods (i.e., lead-210 [^{210}Pb] and caesium-137 [^{137}Cs]). Pre-historic SAR in the Mahau Sound were derived from radiocarbon (^{14}C) dating of cockle-shell valves. Abundant shellfish remains preserved in cores from one of three sites sampled in Mahau (site MH-3) (site: MH-3) were analysed along with environmental variables to identify drivers of changes in shellfish communities over time.

The main conclusions of the study are:

- Baseline pre-human SAR ($0.2\text{--}0.3\text{ mm yr}^{-1}$), extending back some ~2,000 years were very low, comparable with previous estimates in Kenepuru Inlet and Beatrix Bay (Handley et al. 2017). This sediment is entirely composed of mud containing some shell remains.
- In contrast, European-era SAR in Mahau Sound have averaged $3.8\text{ to }4.1\text{ mm yr}^{-1}$ since the early-1900s representing a ten-fold increase. The Mahau Sound SAR are also up to 90% higher (i.e., $+1.8\text{ mm yr}^{-1}$) than the recommended ANZECC default guideline value of **no more than 2 mm yr^{-1} above the natural annual sedimentation rates** (i.e., native-forest catchment, Townsend and Lohrer, 2015). These SAR are similar to values in the

outer Pelorus Sound (1.8–4.6 mm yr⁻¹, Handley et al. 2017) over the last century, and within the range of values measured in North Island estuaries (2.3–5.5 mm yr⁻¹).

- Lower sediment accumulation rates in the intertidal Havelock Estuary (2.2–3.6 mm yr⁻¹) over the last ~50 years are consistent with relatively limited sediment accommodation volume.
- Major sources of deposited fine sediment at the outlets of subcatchments were streambank sediment (range of mean soil proportion: 26–44%), and subsoils (28–37%). Stream-bank erosion is pronounced in the Kaituna (53%) and Tinline, upper Rai and Whakamarino (Wakamarina) subcatchments. Subsoil erosion “hotspots” occur in the Tinline, Whakamarino and upper Rai subcatchments (i.e., Tunakino, Opouri). Dairy pasture topsoils (range: 8–32%) and harvested pine (range: 5–19%) were also substantial sources of deposited fine sediment in the rivers. Harvested pine topsoil contributions were highest at the outlets of the Upper Pelorus, Brown, Ronga and Kaiuma (Opouri) subcatchments (17–19%). Sheep pasture topsoils accounted for 14% of the river sediment deposited near the outlet of the Kaituna River. Contributions of topsoils from native forest (range: 2–6%) and kanuka scrub (range: 2–8%) to river sediment deposits were uniformly low across all sampling sites in the Pelorus-Rai and Kaituna catchments. Comparison of specific sediment yields provided by the CSSI method and NIWA’s NZ River Map tool (national-scale multivariate statistical model, Booker and Whitehead, 2017) identified two subcatchments with excessive soil erosion. These were the Brown and Kaiuma subcatchments located in the Rai. This assessment was based on comparison of the two independent suspended sediment yield (SSY) estimates provided by CSSI and NZRM as a ratio (i.e., SSY_{CSSI}/SSY_{NZRM}). The CSSI-based SSY represents a **recent time period** prior to sampling whereas the NZRM SSY represents a long-term average value. A ratio substantially higher than one indicates that excessive erosion is occurring in the catchment during the time period that the sampled river sediment was deposited.
- A large proportion (i.e., ~70%) of sediment accumulating in Mahau Sound over the last century has an isotopically enriched marine signature. The consistent and uniform nature of this source contribution over time is notable. Ten-fold higher SAR in Pelorus Sound over the last ~century (c.f. previous 3,400 years), coincides with large-scale catchment disturbance. Estuarine processes that re-suspend and re-circulate fine sediment also create a natural sediment trap within Pelorus Sound. Along with sediment recirculation within the system, the historical increase in SAR indicates that isotopically enriched legacy catchment sediment as well as marine organic matter (e.g., phytoplankton) transported into Mahau Sound is the likely ultimate source of this marine sediment. This legacy sediment is defined primarily by its distinctive isotopically enriched C14:0 fatty-acid signature (i.e., by 4–12 per mil, ‰) in comparison to catchment sediment. Marine plants (e.g., microphytobenthos) have altered the isotopic signature of this legacy catchment sediment over time.
- Handley et al. (2017) similarly identified the “**Havelock Inflow**” sampled from the estuary as a major source of sediment depositing in Kenepuru Sound and Beatrix Bay. This inflow sediment has a C14:0 FA isotopic value consistent with the marine source described in the present study. Re-analysis of the Havelock Inflow data using the source library from the present study indicates that the inflow sediment is largely

composed of marine (legacy) sediment (mean: 86%), subsoil (10%), with total contributions from topsoils (land use) being less than 4%.

- **Subsoils** are the largest contributor of catchment-derived sediment depositing in Mahau Sound over the last ~century, averaging 14% to 17% of the total sedimentation across the three core sites. The land uses associated with these subsoils cannot be determined using the isotopic values of the FA biotracers. Subsoils are likely to be derived from steep land areas after removal of forest canopy and topsoils. Potential subsoil sources also include cutting for roads and tracks and side casting material, with bare or sparse vegetation cover, where subsoils are exposed to surface erosion by rainfall and runoff, as well as landslides during high-intensity rainfall events.
- **Streambank** erosion is the second largest source of catchment-derived sediment accumulating in Mahau Sound, accounting for 8% to 10% of the total.
- **Native forest and harvested pine forest** (post-1979/1980) account for similarly small proportions of the sediment accumulation in Mahau Sound, averaging 1.8–2.3% of the total. Sediment contributions from Kanuka scrub average 1.3–1.5% and the Scrub and Pasture (combined sources) only 1.1–1.3%. Although these sources account for a relatively small proportion of the total (with marine source included), large differences in land use areas suggest that specific sediment yields vary markedly. Source proportions (%) normalised by the matching land use areas, LCDB-2 to -4) were used to calculate yields (% km⁻²) for matching years in the cores. This enabled direct comparison of source yields for land uses relative to native forest.
- **Large cockles** (tuangi, diameter >5 cm) in cores from site MH-3 date to the pre-human period and indicate that the system was likely more stable and less turbid. Large cockles and seagrass meadows in subtidal habitats are now rare in the Marlborough Sounds. Unlike Kenepuru Sound, where shell deposition increased up until the 1950s (Handley et al. 2017), the Mahau core shows a decline in shell deposition (mostly large subtidal cockles/tuangi). This decline followed the arrival of Māori (ca. 1300AD). Mollusc species diversity has declined to its lowest point in recent (surficial) sediment.
- Evidence of large storms (post-2001) were not detected in the Mahau Sound cores. This reflects the temporal resolution of the core records (i.e., greater than annual) and relatively uniform characteristics of the fine sediment accumulating in Mahau Sound.
- The study catchments are relatively small (i.e., <1,000 km²), so that time lags in sediment delivery to Havelock Estuary primarily depend on sediment characteristics. The potential time-lag in delivery during large storms was considered for major sediment-size fractions. Fine sediment (<62.5 microns) is the most ecologically damaging fraction and is readily maintained in suspension due to its relatively low settling velocity (i.e., 0.1–2 mm s⁻¹). Therefore, a large proportion of the fine-sediment load will be discharged to Havelock Estuary during floods, unless deposited during over-bank flow conditions (e.g., flood plain, vegetated areas).

This study has shed new light on sedimentation and the sources of sediment accumulating in the inner Pelorus Sound/Te Hoiere ecosystem. It has revealed the complex cumulative effect of intensive land use in the contributing catchments over the period of human settlement. Effects of increased soil erosion and sedimentation have ranged in scale, from localised impacts on cockle beds from early Māori activities in Mahau Sound, to extensive catchment-wide soil erosion and sedimentation

since European settlement. Gold mining, native forest clearance, pastoral farming, and more recent widespread harvesting of *Pinus radiata* plantations (~1980– present), have all left their legacy in the coastal waters of the Sound. A recurring theme underlying the increase in the sediment accumulation rates over the past century is that clear-felling and uniformity in land use exacerbates sediment loads delivered to waterways. This information will be valuable to catchment managers and communities working alongside each other in the Te Hoiere restoration project in determining outcomes for the land and coastal environments.

1 Introduction

1.1 Background to study

The Pelorus Sound (Te Hoiere) is a 50 km long and relatively deep (c. 40 m) drowned-river valley estuary. Te Hoiere is valued by the people of Marlborough for its natural character, marine habitats, recreational opportunities, economic and cultural significance. These values have been affected in recent decades by land-use intensification that has increased sediment, nutrient and microbial loads to Pelorus Sound and marine activities that disturb or degrade benthic ecosystems (Robertson and Stevens, 2009, Handley et al. (2017). Te Hoiere is also the centre of New Zealand's \$200 million per annum mussel aquaculture industry (Handley et al. 2017).

ANZECC guidance for sedimentation in estuaries recommends: (1) a default guideline value (DGV) of no more than 2 mm yr⁻¹ above the natural annual sedimentation rate (i.e., for a native-forest catchment), and (2) "*estuarine sedimentation and its effects should be better linked to catchment processes*".... to..." *facilitate a clearer understanding of erosion pathways and thereby improved targeted management responses*" (Townsend and Lohrer, 2015). The DGV is based on knowledge of event-scale effects adapted for annual sedimentation rates.

The National Policy Statement for Freshwater Management (NPS-FM, 2017) has recently been superseded by new policies introduced in the "*Action for healthy waterways – decisions on the national direction and regulations for freshwater management*" (Ministry for the Environment, 2020). The current NPS-FM (2020) signals a new direction for freshwater management with the key objectives of:

1. stopping further degradation of New Zealand's freshwater resources and make immediate improvements so that water quality is materially improving within five years, and
2. reversing past damage to bring New Zealand's freshwater resources, waterways and ecosystems to a healthy state within a generation.

The NPS-FM (2020) recognises that land use intensification has contributed to major degradation of estuaries and that sediment is one of the most prominent environmental stressors in New Zealand freshwater and estuarine environments. Councils are required to develop plans that address degradation of freshwater and estuaries (enact by 2026) and to shift the emphasis from effects- to limits-based management.

Nearshore coastal waters, especially estuaries, have been increasingly degraded by excessive land-derived contaminants, in particular sediment, nutrients and urban-derived stormwater contaminants. This degradation has been exacerbated by land-use intensification, urban expansion and coastal development (Schiel and Howard-Williams, 2016). Sediment has been ranked in the top three threats to New Zealand's marine habitats, along with ocean acidification and global warming (MacDiarmid et al. 2012). Although soil erosion and deposition in New Zealand estuarine and coastal marine receiving environments is a natural process, the rate at which sedimentation is now occurring is ten-fold higher than before human activities disturbed the natural land cover (e.g., Swales et al. 2002a, Thrush et al. 2004, Hunt, 2019). In New Zealand, increases in sediment loads to estuaries and coastal ecosystems coincided with large-scale deforestation, which followed the arrival of people about 700 years ago (Wilmshurst et al. 2008).

Soil erosion rates in New Zealand are naturally high by global standards due to steep terrain, weathered and erodible rocks, generally high rainfall and frequency of high-intensity rainstorms (Basher, 2013). Historical catchment deforestation, large-scale conversion to pastoral agriculture and land-use intensification and catchment disturbance have increased erosion rates. Important erosion processes include rainfall-triggered shallow landslides, earthflows and slumps, gully and surface erosion (i.e., sheet, rill) and streambank erosion. Landslide occurrence is reduced by 70 to 90% by closed-canopy woody vegetation and maintenance of groundcover on hillslopes is an important factor reducing surface erosion (Basher, 2013).

Deforestation in New Zealand accelerated following European settlement in the mid-1800s. Timber extraction, mining and land conversion to pastoral agriculture and associated burning triggered large increases in fine sediment yields from catchments. During the peak period of deforestation from the mid-1800s to early 1900s, sediment accumulation rates (SAR) in many New Zealand estuaries increased by a factor of ten or more. This influx of fine sediment resulted in a shift from sandy to more turbid, intertidal and muddy environments, degrading ecosystems (Thrush et al. 2004). Studies mainly in North Island estuaries indicate that in pre-Polynesian times (i.e., before 1300 A.D.) SAR averaged 0.1–1 millimetre per year (mm yr^{-1}). Sedimentation rates over the last century have averaged 2–5 mm yr^{-1} in these same systems (e.g., Bentley et al. 2014, Handley et al. 2017, Hume and McGlone, 1986, Sheffield et al. 1995, Swales et al. 1997, 2002a, 2002b, 2005, 2012, 2016a). This work has also documented the environmental changes that have resulted from increased catchment sediment yields following large-scale catchment deforestation that began in the mid-1800s. Effects include accelerated rates of infilling, shifts in sediment type from sand to mud and former subtidal habitats have become intertidal.

In the context of the present study, significant changes appear to have occurred to the benthos of Pelorus Sound, including loss of extensive intertidal and subtidal green-lipped mussel reefs, loss of biogenic habitats, and contingent changes to sediment structure. Factors most likely to have driven these changes are over-fishing of shellfish stocks (dredging and hand-picking), contact fishing methods (shellfish dredging and finfish trawling), increased delivery of sediment from catchments that have undergone significant land use change, and ongoing aquaculture and forestry developments (Handley, 2015, Handley et al. 2017, Urlich and Handley, 2020b).

1.2 Study objectives

Marlborough District Council (MDC) commissioned NIWA to undertake a study of sediment accumulation rates (SAR) and sources of sediment accumulating in the inner Pelorus Sound/Havelock Estuary. The specific objectives of the study were to:

- Determine the rate that sediment has accumulated in the inner Pelorus Sound/Havelock estuary over recent decades and how do these compare to pre-human “background” rates (Sections 3.2 and 3.3).
- Identify the sources of sediment (by land use) that is accumulating in the estuary (Section 3.4).
- Estimate the relative proportions of sediment from different land uses (Section 3.1).
- Reconstruct how the sources of sediment (by land use) have changed over time (Section 3.4).
- Identify if there are any sediment sources that are over-represented as a proportion of land use area in the Pelorus and Kaituna catchments (Section 4.2).

Additional questions were addressed contingent on the degree of preservation and temporal resolution of environmental changes preserved in the estuarine sediment. To this end, core sites were selected using existing information, local knowledge and our expertise to maximise the likelihood of collecting high-quality cores. The additional questions were:

- Can the effects of large storms since 2001 be detected in estuarine sediment?
- What is the relative contribution of these storm events to the overall sedimentation rate?
- Is there a time-lag in sediment transport from large storms?

The results of this study will be used to inform integrated catchment-estuary management of the Pelorus system.

1.3 Study area

1.3.1 Geology, soils and climate

Pelorus Sound/Te Hoiere is part of the extensive drowned-river valley estuarine system of the Marlborough Sounds. This system consists of a series of narrow river valleys that were flooded by rising sea levels that are some 120 m higher today than at the end of the last ice age 14,000 years ago (Cotton, 1955, Hayward et al. 2010). The Pelorus system is gradually subsiding due to regional tectonic processes. Analysis of sediment cores collected from Havelock Basin and Mahau Sound (Inner Pelorus) indicate a subsidence rate of 0.7–0.8 mm yr⁻¹ over the last 6000 to 7000 years (Hayward et al. 2010).

The basement rock of the Marlborough Sounds is composed of metasedimentary rocks of Permian-Jurassic age that form a series of uplifted, north-west tilted blocks that are separated by north-east trending faults (Brown, 1981, Lauder 1987). The Caples terrane is extensive in the Marlborough Sounds (previously mapped in the Marlborough Region as the Pelorus Group, Lauder, 1987). This “consists of well bedded indurated sandstone and siltstone with thick sequences of coarse sandstone” and “become increasingly schistose southeast towards the Wairau Valley” (Rattenbury et al. 1998).

Hillslopes are typically moderately steep to steep (13–30°) and steep (30–38°). Flat and rolling land (slopes 0–12°) comprises less than 10% of the total land area of the Marlborough Sounds and occur mainly as alluvial flats and fans at the heads of larger bays and shallow inlets (Walls and Laffan, 1986). In the Marlborough Sounds (as is the case elsewhere in New Zealand), steepland soils are prone to mass failure/slips and sheet and rill erosion when vegetation cover is removed and/or soils are disturbed (e.g., Hicks, 1991, Fahey and Coker, 1992, DeRose et al. 1993, Basher 2013). In the Marlborough Sounds these ultic soils are primarily composed of silt and silt-clay loams with up to 45% clay content (DSIR 1968, Laffan and Daly 1985).

The climate of the Marlborough Sounds varies from mild to cool (Walls and Laffan, 1986). Average annual rainfall in the Marlborough Sounds varies between 1600 and 1800 mm per year, increasing markedly with altitude. Spatial patterns in rainfall reflect the complex topography of the region, which influences airflows and resulting precipitation (Chappell, 2016). Monthly rainfall normals in the Pelorus area vary from 89 mm (Feb) to 215 mm (October) (Station: Havelock-2). Rainfall frequency in the Marlborough region is also highest in the Pelorus Sound with an average of 117 days per year with rainfall >1 mm (Chappell, 2016). Heavy rainfall typically occurs in the Marlborough Sounds and the Richmond Range under north-westerly flows, with the region experiencing numerous extreme

weather events, with significant damage and disruption caused by landslides, scouring of channels and flooding (Laffan, 1980, Chappell, 2016).

The Pelorus-Rai and Kaituna rivers account for a large proportion of the catchment area discharging to the inner Pelorus Sound. The Pelorus-Rai has a catchment area of $\sim 888 \text{ km}^2$, which is about 84% of the total catchment area (1063 km^2 , LCDB-5) draining to the inner Pelorus Sound. The remaining 16% comes from the Kaituna ($\sim 147 \text{ km}^2$) and Cullens (28 km^2) river catchments. The Pelorus River receives sediment from four subcatchments via major tributary streams (i.e., Upper Pelorus River, Tinline River, Rai River and Whakamarino River), and these contribute about 73% of the total estimated suspended sediment load (NZ River Maps, Booker and Whitehead, 2017). NIWA's NZ River Maps is a national-scale multi-variate statistical model based on data provided by the River Environment Classification (REC-1). The Rai River catchment ($\sim 212 \text{ km}^2$) is the largest tributary of the Pelorus River.

Large floods in the Pelorus-Rai and Kaituna catchments often result in inundation of pasture and croplands by sediment-laden flood waters (Figure 1-1). Historically significant storm events resulting in landslides and flooding in the Pelorus catchment since 1868 are summarised in **Appendix A**



Figure 1-1: Kaituna river in flood, 15 November 2016. Sediment-laden flood waters inundating low-lying farmland, with the Havelock estuary and Cullens Point visible in the distance. Source: Marlborough District Council.

1.3.2 Plant communities and land use change

Present day land use in the Pelorus-Rai and Kaituna catchments is dominated by native forest (70%) and smaller areas of exotic forestry (13.2%), dairying (high producing exotic grassland, 7.3%), low producing exotic grassland/pasture (4.8%) and scrub (1%). Dairy farms presently cover some 76 km² of the flood plain and 2 km² of coastal flats of the Pelorus and Kaituna catchments, respectively (source: LCDB-5, 2018/19, Table 1-2). The Pelorus and Kaituna Rivers discharge an estimated ~259,000 tonnes per year of suspended sediment to the Havelock estuary annually, with ~90% of this load delivered by the Pelorus River (NZ River Maps, Booker and Whitehead 2017).

The climate, topography and soils of the Marlborough Sounds favoured the development of native forests, dominated by beech (Walls and Laffan 1986). Broadleaf forests co-occurred in moister or warmer conditions in gullies and on hillslopes at lower altitudes, along with an increasing density of podocarps, with kahikatea, rimu, totara, matai and miro particularly dominant on flood plains and coastal flats (Figure 1-2). Manuka, kanuka and bracken, are characteristic of native scrub regenerating after deforestation (Walls and Laffan 1986).

Disturbance of these native plant communities by people began soon after Māori arrival in New Zealand, around 1300 AD (Prickett 1982, Wilmshurst et al. 2008). Pockets of forest were cleared mainly by fire. Archaeological evidence, including middens, dwelling sites, defensive earthworks, storage pits and gardens are abundant in the area and indicate that Māori activities modified the environment (Walls and Laffan 1986, Challis 1991).

The record of deforestation, establishment of pastoral agriculture and production forestry and impacts of other activities, in particular gold mining, following European settlement has been reconstructed from several sources. These include first-person accounts from 19th century explorers, National Library of New Zealand's on-line Papers Past database, historical photographs, local and family histories, technical reports, and the scientific literature.

European modification of the Pelorus catchment got underway in earnest in 1864 with the commencement of goldmining and forest harvesting. Subsequent deforestation and establishment of pastoral agriculture has modified the landscape and ecosystems, with more than half of the original native forest cleared. Timber extraction has occurred in most valleys, coastal flats, and lower hillslopes (Figure 1-3). Farming practices have changed with the prevailing economic conditions (Walls and Laffan 1986).

The history of the Pelorus catchment following the arrival of people is divided into four major time periods, with different predominant land use patterns:

- **Subsistence c.1300 – 1864:** Encompasses the arrival of Māori and up to the onset of European settlement and the subsequent disturbance of forest ecosystems.
- **Transformation 1864 – 1915:** Describes the first major landscape transformation driven by gold, timber and pastoralism.
- **Pastoralism 1915 – 1985:** Covers the period of WWI, the Great Depression in the 1930s, WWII, and the post-war years leading up to the structural economic changes of the fourth Labour government. Sheep farming characterised the hill country, with frequent burn-offs of regenerating scrub. Land use on the relatively productive alluvial flood plains in the Pelorus and Cullens Creek catchments was dominated by dairy farming in small ballot farms.

- **Intensification 1985 – present:** Outlines the most recent land conversions to extensive radiata pine (*Pinus radiata*) plantations on hill country, particularly in the Rai, Pelorus and Whakamarino valleys. Dairy farming intensified as irrigation became more widespread from the early 2000s. Sheep and deer farming occur throughout the Kaituna catchment on the lower hillslopes and valleys.



Figure 1-2: Intact coastal margin adjoining old-growth complex floodplain forest, Tennyson Inlet, Pelorus Sound/Te Hoiere. This vegetation sequence is characteristic of the pre-European mountains to sea ecosystems that existed in the Pelorus system. Photo credit: Steve Urlich.



Figure 1-3: Havelock township (ca. 1890s). The hills around the town had been cleared of its original forest cover. Note the pines planted on the lower slopes in the foreground. Examination of high-resolution image online <https://natlib.govt.nz/photos?text=Tyree+Havelock> shows older trees have had lower branches pruned. Source: Tyree collection – Alexander Turnbull Library 10x8-0420-G.

Table 1-1: Present-day catchment land use in the Pelorus, Rai and Kaituna catchments. Source: LCDB-5 (2018) with areas for the most common land uses by area shown. Note: indigenous forest (LCDB classification) is referred to as native forest in this report.

Land use	Pelorus (Area, km ²)	Rai (Area, km ²)	Kaituna (Area, km ²)
Indigenous Forest	527.20	112.36	47.07
Broadleaved Indigenous Hardwoods	20.55	8.76	10.04
Manuka and/or Kanuka	9.10	2.09	8.24
Exotic Forest	59.78	31.58	28.68
Exotic Forest – Harvested	11.65	4.00	0.81
High-producing exotic grassland	29.81	45.93	2.09
Low-producing exotic grassland	3.16	1.07	46.01
Gorse and/or Broom	4.12	4.22	0.60
Fernland	0.63	0.15	1.70
Total areas	665.89	210.16	145.24

The following sections are a summary of land-use changes and broad-scale environmental effects. Previous work by Handley (2015) and Handley et al. (2017) describe environmental changes in Pelorus Sound. The history of pine forestry in the catchments can be found in Urlich and Handley (2020) and Urlich (2020).

Subsistence land use: c. 1300 – 1864

Subsistence harvesting by Māori was unlikely to have resulted in widespread physical damage to marine ecosystems (Leach, 2006). However, use of fire, localised coastal land clearance for dwellings and cultivation has been shown to affect benthic productivity in Tasman and Golden Bays (Handley et al. 2020). Sediment cores from Kenepuru Sound, that span the period from before Māori settlement showed no detectable changes before European settlement, native-forest clearance and subsequent land-use activities from the late 1800s (Handley et al. 2017). Early European explorers describe intact forests and wetlands in the Kaituna and Pelorus catchments and Pelorus Sound, and a diversity of bird and fish species (Wakefield in Ward 1840, Drury 1854).

Transformation: 1864 – 1915

Havelock township was established after the discovery of gold in 1864 at the Whakamarino (Wakamarina) River that flows into the lower Pelorus at Canvastown (Hector, 1872, Brayshaw 1964). The goldrush was the start of a radical transformation of the ecosystems of the Pelorus and Kaituna catchments, including the estuary and Mahakipaoa Arm. Logging of native forest commenced soon after (Paton 1982). Establishment of pastoral farming followed deforestation (McIntosh, 1940, Bowie, 1963, Lauder, 1987). Frequent fires to burn off primary native forests and secondary regrowth to clear areas for pasture occurred for almost a century from the late 1800s. This practice, as well as intense rainfall events, contributed to soil erosion by removing soil-stabilising root networks. Forest canopies also substantially reduces the velocity (i.e., resulting kinetic energy) and volume of rainfall impact on the soil surface during storms, thereby influencing soil erosion (e.g., Li et al. 2019). Therefore, large-scale deforestation and removal of the protective forest canopy would have also contributed directly to soil erosion. The Opouri valley forest was the last to be milled. Cleared land was quickly converted to dairy paddocks on the floodplains (Figure 1-5) and sheep pasture on the hillier terrain (Bowie, 1963).

Monterey Pine (*Pinus radiata*) were introduced to the Pelorus area by the early 1890s (Handley 2015, Urlich and Handley 2020). Increased awareness of pine for timber production can be traced to the 1913 Royal Commission on Forestry (Hegan, 1993). Harvesting of woodlots and shelterbelts would have been localised, and possibly in a progressive on-demand manner. Sediment run off from this activity would have been relatively minor compared to soil erosion from other sources, such as clearance of native forest, gold mining, slips under newly created pastureland on hill country, and bank erosion from dairy cattle on the flood plains.



Figure 1-4: Sluice dredging 1870s and 1910s in the Whakamarino Valley. Left: Deep Creek being excavated down to bedrock. Much of the creek's flow washed the gold-bearing gravels that were shovelled into the wooden flume boxes. Courtesy Marlborough Museum 2009.067.0015. Right: Nelson and Mayo's high-pressure sluicing claim in 1911 in the Whakamarino. The jet was swung to erode the terrace gravels quickly. The force of the jet can be gauged by the men on the right. Courtesy Marlborough Museum: 2009.067.0001.

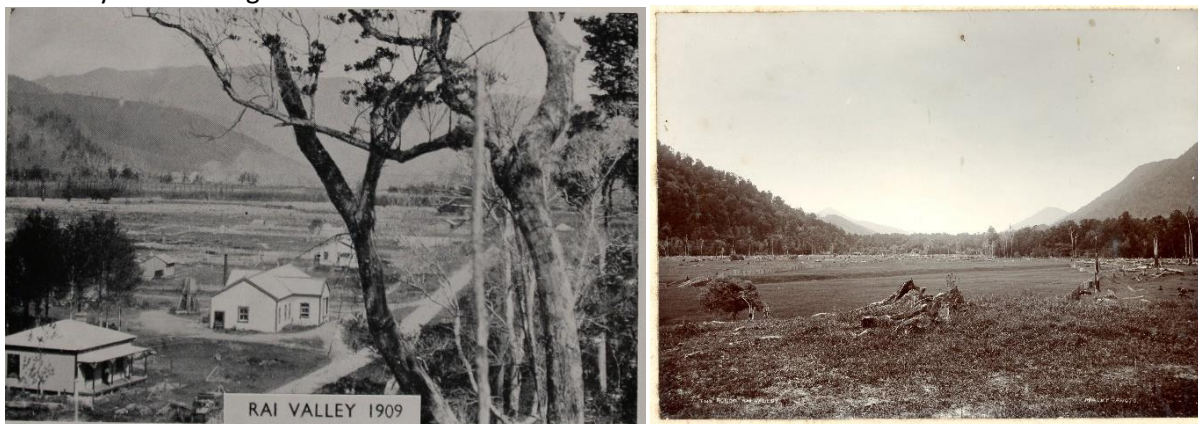


Figure 1-5: Rai Valley Co-operative Dairy Factory 1909 note the cleared hillsides. Left: Early dairy farming, Ronga Valley (ca. 1910s) with cows visible to the right (Macey Photo). Courtesy: Marlborough Museum: 2009.067.0001.

Pastoralism: 1915–1985

Soil erosion on hill country following earlier deforestation had become a significant issue by the mid-20th century: *"The history of one is typical of all. In the Rai, for example, the sawmilling was followed by the grassing down of the bush burn and the introduction of sheep. The heavy rain leached out the fertility and the process of erosion denuded the steep hill faces of soil."* (p277, McIntosh (1940)). After heavy rains, surface slips were common on the unstable soils and after burn-offs. Regenerating fern and scrub on south-facing hills was frequently burnt from the late 1800s to the early 1980s (MDC, 1992). This practice was used for small-scale burns to prepare areas logged of native timber into pasture and to convert secondary regrowth back into pasture or into plantations (McIntosh 1940, Bowie 1963). Significant conflagrations and wildfires could last for weeks (The Rai Valley Centennial Committee, 1981). After WWII, reversion on pastoral hill country following fire was somewhat counteracted by aerial topdressing and grass seeding to raise soil fertility and restore pasture (Beggs 1962, Peden 2008). The productivity of this marginal hill country pasture was maintained by

topdressing in many parts of New Zealand due to buoyant economic conditions (1950s – 1970s) and government subsidies (1970s – mid-1980s, Peden 2008). In the Kaituna, Canvastown and Rai areas, dairy cows were run on the flats and Romney sheep on hill country. Regrowth of bracken, tauhinau and Spanish heath was an ongoing issue for pastoral farmers (Beggs, 1962).

Large-scale plantation forestry also began in the Pelorus catchment during WW II. The potential for increased planting of *Pinus radiata* as an alternative to pastoral farming on the marginal hill country was being realised. The State Forest Service began planting *P. radiata*, Douglas fir (*Pseudotsuga menziesii*), and Corsican pine (*Pinus nigra*) in the Rai/Whangamoā area in 1940 (Figure 1-7 and Figure 1-8). This gathered momentum (Huddleston in Urlich and Handley 2020), with loans authorised by the Forestry Encouragement Act 1962 (Sutherland, 2011). Farm blocks up to ca. 100 hectares were planted in pine and in previously burnt areas pine trees (Eric Huddleston and Vern Harris in Urlich and Handley, 2020) stabilised the hillslopes prior to harvest, and helped to phase out the practice of scrub burning on hill country. The renamed New Zealand Forest Service began planting hillsides within the Tinline Valley in the Upper Pelorus in the 1960s, and then the Whakamarino in the 1970s (MDC 1992). The forest service also planted forests on steep hill country above Tory Channel and around Port Underwood from the 1960s to 1986 (MDC, 1992).

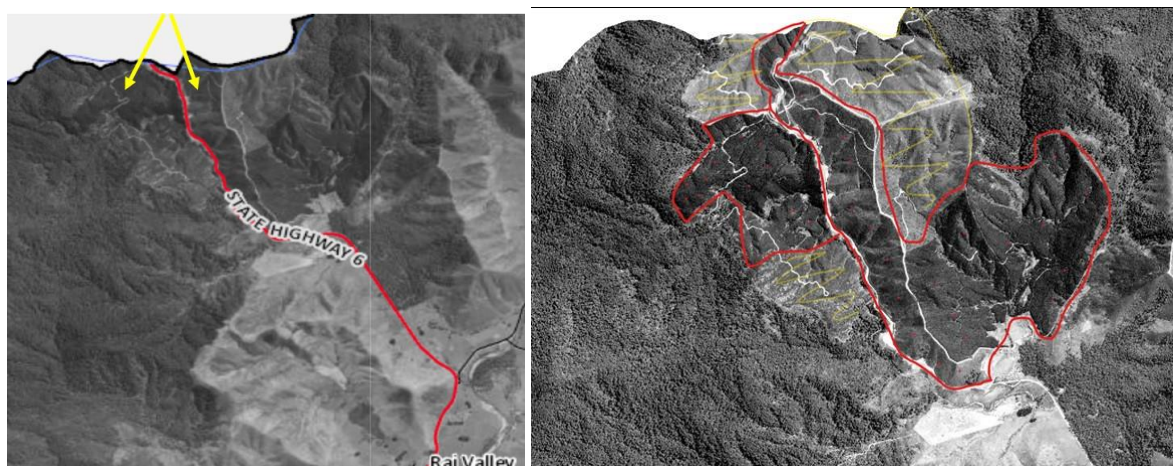


Figure 1-6: Pine plantations in the Rai-Whangamoā State Forest. Arrows show these locations (left), adjacent to State Highway 6, Rai Valley to Nelson, on eastern side of Rai Saddle, 1958. Enlarged view (right) also shows planted and bare areas. Aerial images georeferenced from survey SN1208 16/10/1958 from <https://www.marlborough.govt.nz/services/maps/historic-aerial-photos>



Figure 1-7: Areas of newly-established pine forest in the Rai-Whangamoia State Forest (1950). The photo shows the extent of new plantings, including Corsican pine (*Pinus laricio*). Source: NZ Forest Service records, courtesy of Mr Eric Huddleston.

Harvesting of pine gradually increased as the first plantation timber from Rai State Forest was harvested in ca. 1979 (Huddleston, in Ulrich and Handley, 2020) (Figure 1-8). Bulldozers and skidders were phased in for earthworks and moving harvested trees, then diggers with backhoes as technology advanced. These machines cause extensive soil disturbance (Mr Eric Huddleston, in his memory).



Figure 1-8: First harvest of timber from the Rai State Forest, circa 1980. Precise date of photo not recorded. Note: JB number plate series issued 1978. Photo courtesy of Mr Eric Huddleston.

In the late 1970s, the Marlborough Catchment and Regional Water Board considered the potential effects on the Brown River and Havelock Estuary from the impending pine harvest of the Rai State Forest (Bargh, 1977). Increased stream turbidity and possible effects on recreation, wildlife, and commercial wet fish catches were identified. Adverse effects of fine sediment on mussel spat were inferred, with reference made to a ‘massive sedimentation’ event in 1976 suggested as affecting spat production (Clarke, 1977 cited in Bargh, 1977). Sedimentation was acknowledged as a natural process but thresholds above which adverse environmental effects occur were unknown (Bargh, 1977). The Catchment Board were however clear that: *“Sediment originating from forest harvesting operations needs to be strictly controlled...as they may cause detrimental changes to life in the river system or in Pelorus Sound”* (Bargh 1977: p 4-5). The potential for cumulative effects of harvesting was also recognised: *“In the long term...pollutants from forest harvesting in this catchment (Brown River), in conjunction with pollutants from forestry operations in other catchments draining into the Pelorus river, may cause detrimental changes to life in the river system or in Pelorus Sound”* (Bargh 1977: p5).

In the Havelock Estuary, dredging to widen and deepen shipping channels had been an ongoing activity dating back to before 1910 (Handley et al. 2017). The most intensive works were undertaken during the 1950s when the blind channel leading directly from Cullen Point to the Harbour Wharf was deepened and the side cut from the Kaituna River channel was closed. A proposal to build a 135 yards long wharf was also considered in the 1950s (**Appendix B**). Excessive sedimentation was acknowledged by the harbour board as an issue affecting the infilling of previous dredging. Introduced estuarine cordgrass (*Spartina townsendii*) was planted in 1948, and a further 1500 plants established in 1952 to “hold up most of the silt brought down by floods”.

Dredging works also occurred in the 1980s to develop the marina, deepen the harbour and shipping channel (M. Gibbs, NIWA, pers obs.). This created a large spoil mound at the north-eastern end of the harbour break wall.

Intensification: 1985 – present

Establishment of plantation pine forest on hill country continued in the 1980s due to tax concessions, favourable returns, and reduced profitability of pastoral farming (MDC 1992, Sutherland 2000). By 1992, some 9,100 ha of plantation pine forest had been planted in the Pelorus and Kaituna catchments and increased to 14,109 ha in 2018/19 (Figure 1-9). Today, the flood plains in the Pelorus and Cullens Creek catchments are dominated by dairy farming (Figure 1-9). Irrigation became more widespread after the drought of 2001, which also increased production. Sheep and deer farming occur throughout the Kaituna catchment on the lower hillslopes and valleys. There is less native forest proportionately in the Kaituna compared to the Pelorus, where largely intact forest stretches occur up to the montane areas of the Richmond Range.

Dairy farming occurs on the more stable and productive LUC Class 1-3 alluvial soils (Figure 1-10). About 75% of Marlborough's dairy farms are in the wider Pelorus and Cullens Creek catchments (MDC, 2016). In 1988 there were 14,783 dairy cattle in the Marlborough region (MDC, 1994). By 2002, dairy cattle numbers had more than doubled to 32,256 (Statistics NZ, 2021) when MDC implemented a non-regulatory programme to reduce sedimentation and improve water quality (Neal, 2018). This has included work with farmers to reduce access of dairy cows to watercourses by requiring direct stream crossings to be phased out. For example, stream crossings in the Pelorus catchment have been reduced from 149 in 2002 to 13 in 2018, with all of the remaining crossings located in the Rai Valley. Marlborough District Council State of Environment reporting in the mid-2000's calculated that the number of cow movements across the Rai River system was approximately 3 million per dairy season (MDC, 2008). Dairy industry support for fencing off waterways over the last decade may also have reduced streambank erosion.

Land use intensification has coincided with an increase in radiata pine harvesting from 2000 onwards (Urlich and Handley, 2020). Google Earth time-lapse of satellite imagery shows an increase in harvesting as ex-State Forest plantations and smaller forestry encouragement blocks (planted during 1960s – 1980s) progressively matured. The risk of soil erosion from these steep land, highly erodible soils is elevated during the 1- to 6-year period following tree removal/harvesting (Phillips et al. 2012) and establishment of the next rotation and/or seral vegetation. Therefore, the 'window of vulnerability' (O'Loughlin and Watson, 1979) for soil erosion and sedimentation across the landscape is near-continuous. This process provides an ongoing potential source of sediment accumulating in marine receiving environments in the Marlborough Sounds (Johnson et al. 1981, Fahey and Coker, 1992, Handley et al. 2017, Urlich and Handley, 2020).

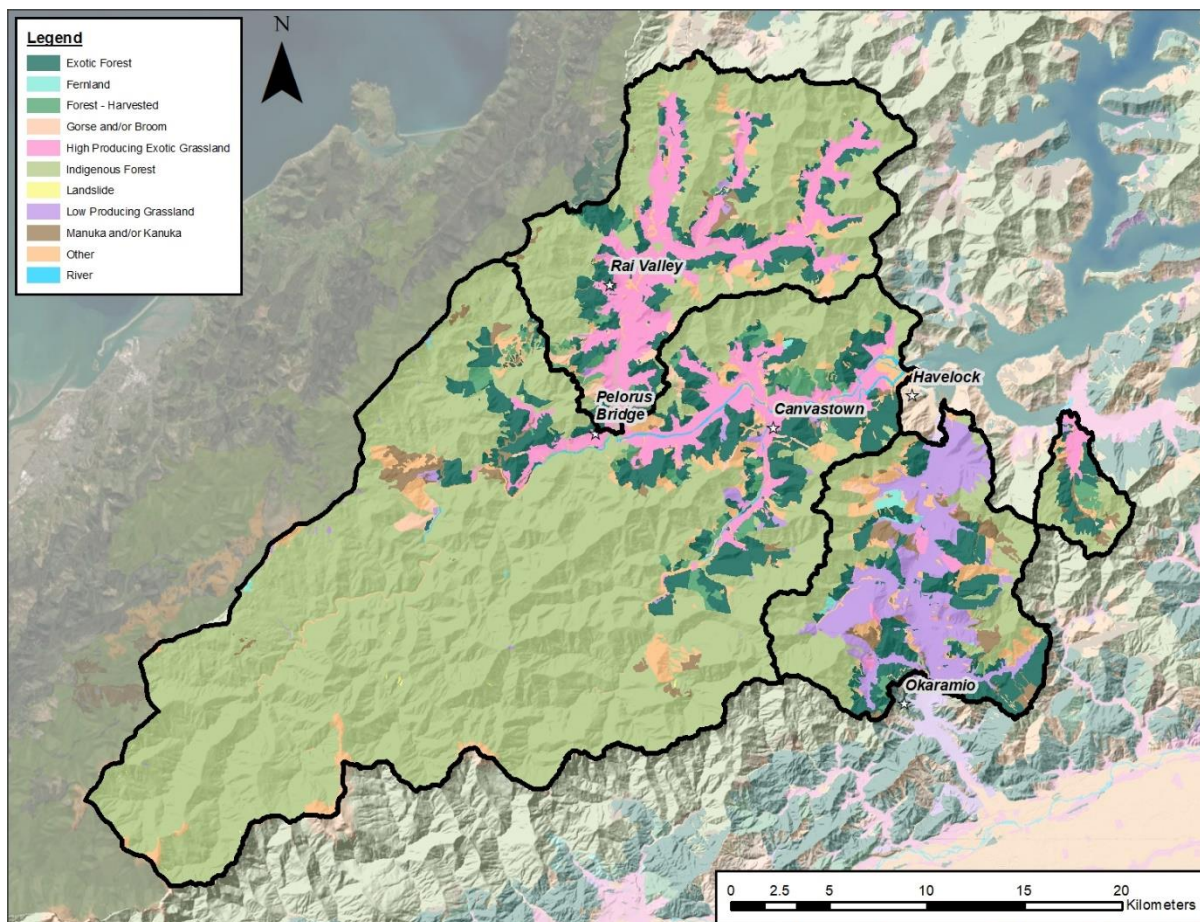


Figure 1-9: Land use in the catchments of the inner Pelorus Sound. Source: LCDB-5 (2018).

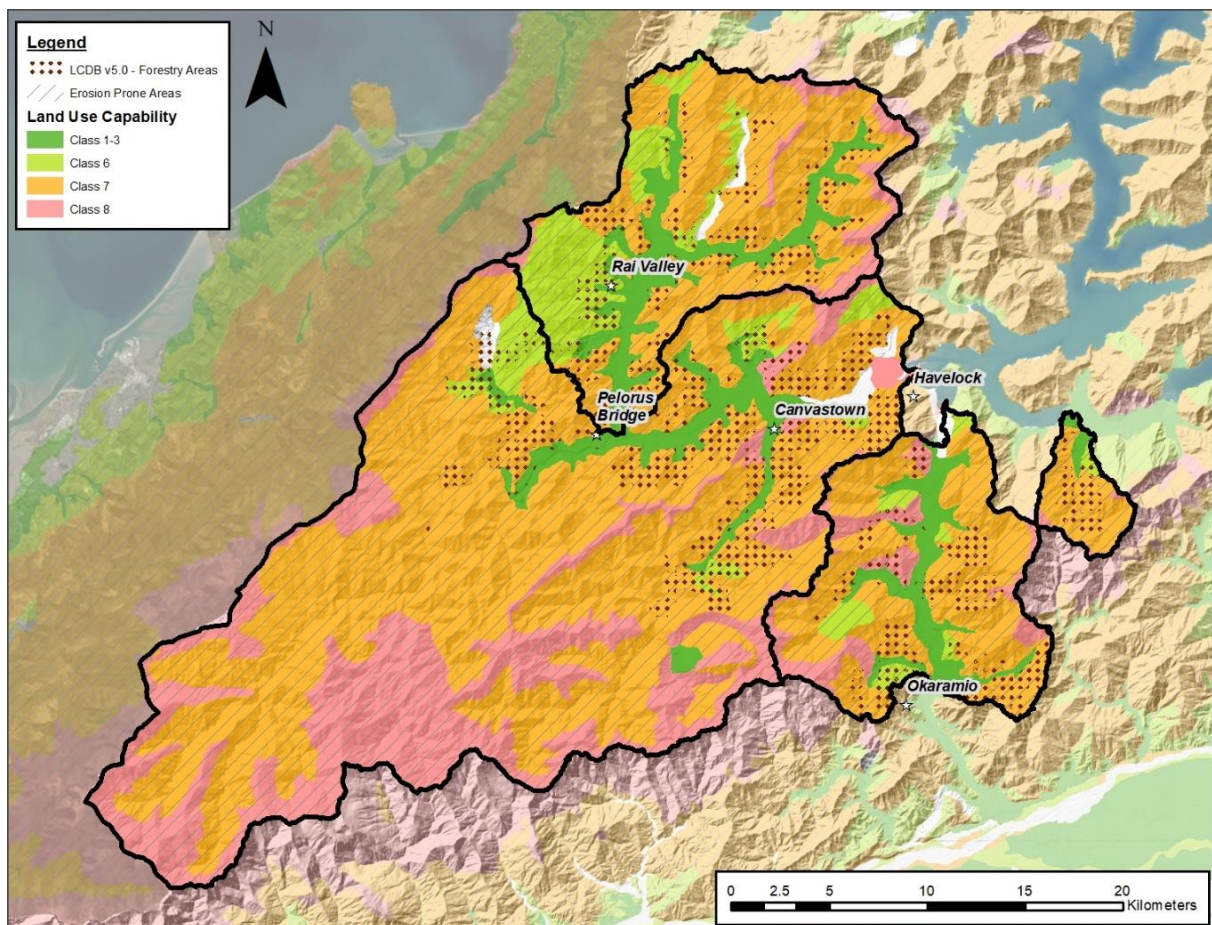


Figure 1-10: Pelorus-Rai catchment land use capability. Key: Highly suitable for arable cropping and pastoral grazing (Class 1-3), Low suitability for pasture or forestry (Class 6–7); Unsuitable for pasture or forestry (Class 8). The dotted lines represent plantation forestry from LCDB 5. Source: MDC.

1.3.3 Estuary hydrodynamics and sediment processes

The dispersal and fate of sediment-laden river plumes in the Pelorus Sound is influenced by complex tidal, estuarine and wind-driven circulation processes. Suspended sediment concentrations are persistently higher in the inner Sound due to the influence of sediment discharge from the nearby Pelorus-Rai and Kaituna Rivers and sediment resuspension by tidal currents and estuarine circulation that traps sediment (Carter, 1976). Broekhuizen et al. (2015) describes the main features of estuarine hydrodynamics in Pelorus Sound:

- Mean current speeds are highest in the tidal channels (i.e., $0.2\text{--}0.3\text{ m s}^{-1}$) and weakest in the inlets, bays and subtidal flats that flank the channels (i.e., $<0.05\text{ m s}^{-1}$, Figure 1-11).
- transport of suspended particles in the Pelorus Sound is primarily driven by two-layer estuarine circulation, with freshwater discharge primarily from the Pelorus River. This stratified estuarine circulation drives a consistent landward-directed inflow in the bottom layer (up to 0.1 m s^{-1}) and a seaward-directed surface outflow ($\sim 0.2\text{ m s}^{-1}$).
- Estuarine circulation is weaker during periods of low freshwater inflows, which results in longer residence times.

- Freshwater discharges during floods influences the entire Sound, with stratification generally driven by salinity (Carter 1976, Vincent et al. 1989, Gibbs et al. 1991). Under storm conditions, the surface layer carries a substantial load of terrigenous sediment from the Pelorus River. Sediment is deposited along the length of the Sound and embayments, including Kenepuru Sound, and seaward to the Chetwode Islands at the sea entrance to the Sound (Figure 1-11, Figure 1-12).
- Warmer surface temperatures in summer can strengthen stratification when river flows are generally low. Sediment is transported to the head of Pelorus Sound under low flow conditions that account for most of the river-flow duration. The mean residence time for the Pelorus channel is approximately 50 days (Broekhuizen et al. 2015).

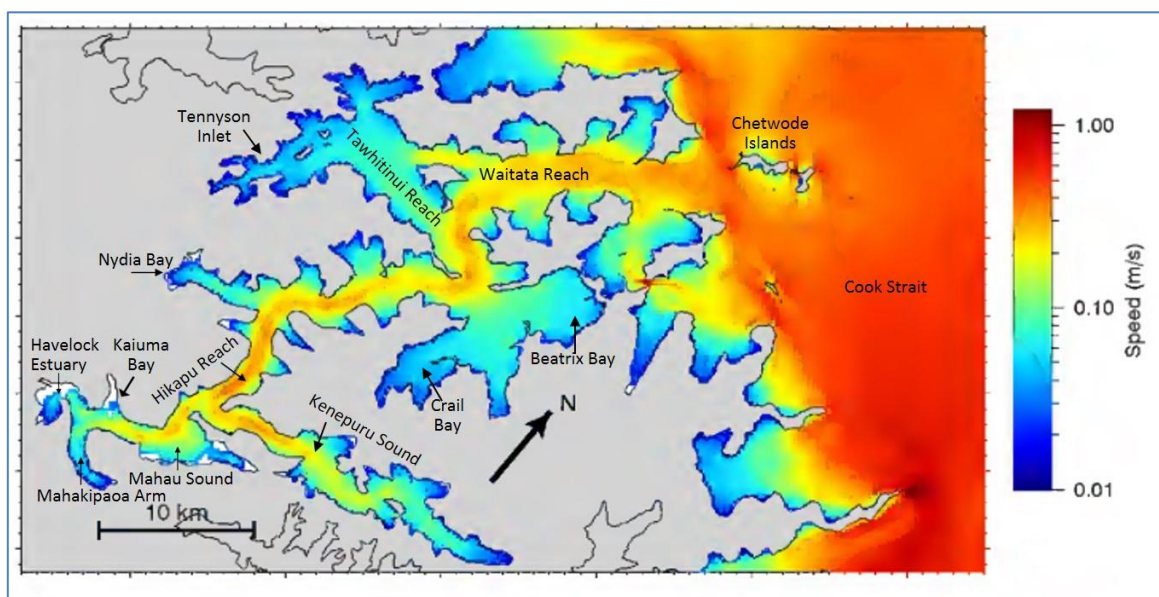


Figure 1-11: Modelled mean current speed at 5 m depth in Pelorus Sound/Te Hoiere. Simulation based on one year's hourly data from a hydrodynamic model (200 m grid). The scale bar is logarithmic, with blue shading representing areas of low current speeds. Mean currents speeds of several cm s^{-1} are characteristic of the upper reaches of bays. Modified from Figure 3-8, Broekhuizen et al. (2015).

Deposition of clay-rich eroded soils transported with river plumes is likely to occur rapidly on mixing with seawater (O'Loughlin 1979, Coker 1994). Laboratory tests on Kenepuru series soils, which underlie many forestry areas in the Sounds, showed rapid flocculation of suspended clays (O'Loughlin 1979, Ulrich, 2015). Fine-sediment depo-centres occur in the inner Sound and near its entrance. Deposition in the inner Sound is associated with the Pelorus river delta and landward directed sediment-transport during periods of low freshwater discharge. Sediment transported into the Sound from Cook Strait are also trapped at the Sound's seaward entrance, thereby operating as a "double-ended sediment trap" (Carter, 1976). The biogenic component of this sediment is primarily derived from individual and colonial diatoms, which constitute up to 20–33% of the suspended sediment at the entrance of Pelorus Sound (Carter, 1976). A typical lower resuspension threshold for unconsolidated clay-rich sediment under tidal currents is $0.1 \text{ newton m}^{-2}$, (0.1 pascal [Pa]). The critical stress for resuspension increases as cohesive bed sediment consolidate, with a value of about 0.4 Pa after consolidation (Hadfield, 2015). Thus, the potential for sediment deposition and resuspension depends on sediment characteristics and local hydrodynamic conditions (i.e., bottom

shear stress). Fine river-borne sediment will preferentially accumulate in sheltered embayments and in the inner Sound where tidal currents are weak (Hadfield et al. 2014, Broekhuizen et al. 2015).

Sediment accumulation rates in Kenepuru Inlet and Beatrix Bay, indicate time-average SAR of 1.8–4.6 mm yr⁻¹ since the early–mid 1900s (Handley et al. 2017). These rates are as much as ten-fold higher than over the several thousand years prior to European period (Handley et al. 2017). Subsidence driven by regional tectonic processes in the inner Sound of 0.7–0.8 mm yr⁻¹ over the last 6,000 to 7,000 years (Hayward et al. 2010), as well as sea level rise around the NZ coast (1.7 mm ±0.1 yr⁻¹ (Hannah and Bell, 2012) since the early-1900s have created sediment accommodation volume in the Sound, as it has progressively infilled with sediment.



Figure 1-12: Sentinel-2 satellite image of the Marlborough Sounds, 21 May 2017. This image shows the extent and relative concentration of fine-sediment laden plumes discharged by Pelorus River into Pelorus Sound. This is in sharp contrast to the less turbid waters of the adjacent Queen Charlotte Sound. Landsat 8 image courtesy of Ben Knight (Cawthron Institute).

Havelock Estuary is located at the head of Pelorus Sound at the outlet of the Pelorus and Kaituna Rivers. The Havelock Estuary is a shallow, macrotidal basin (2.17 m spring tidal range) with several poorly flushed tidal arms. The intertidal zone is dominated by saltmarsh (25%) and unvegetated intertidal flats (46%). Seagrass (>20% cover) accounts for less than 2% of the estuary area (Figure 1-13). Surficial sediment is dominated by mud (~70%). Mean freshwater discharges from the Pelorus-Rai and Kaituna Rivers are $45 \text{ m}^3 \text{ s}^{-1}$ and $3.7 \text{ m}^3 \text{ s}^{-1}$ respectively (Robertson, 2019a). Sediment accretion rates over the last several years have been measured on buried plates at four sites in the main intertidal basin of Havelock Estuary (Robertson, 2019b). These measurements indicate rates of mud accumulation of from less-than 1 mm yr^{-1} to as much as 6.5 mm yr^{-1} . High sedimentation rates and the high mud content of deposited sediment in Havelock Estuary remain the main driver of ecological effects in Havelock estuary (Robertson, 2019b).

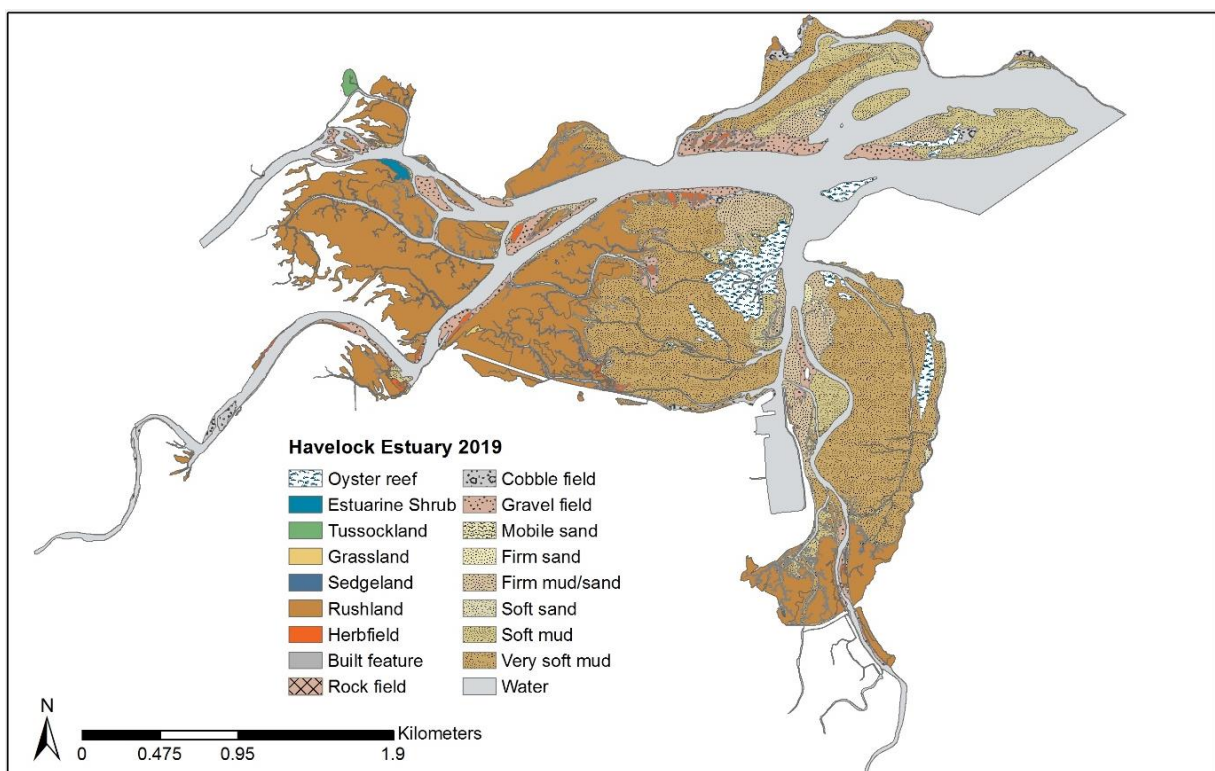


Figure 1-13: Havelock Estuary - distribution of intertidal habitat types. Source: Robertson (2019a).

Historical information suggests that mud deposition was occurring in Havelock Estuary before European settlement. The hydrographic survey of H.M.S. Pandora (1854) documents soft mud flats and banks in the estuary and also on intertidal banks in the inner Pelorus Sound (Figure 1-14). Longer-term measurements of sedimentation in the inner Pelorus Sound by Handley et al. (2017) employed radioisotope dating of cores collected at six sites in Kenepuru Sound. These records indicate substantial increases in sediment accumulation rates (SAR) and changes in shellfish community composition following European settlement and subsequent catchment disturbance. Lead-210 (^{210}Pb) dating of European period sediment indicate apparent SAR of $1.8\text{--}4.6 \text{ mm yr}^{-1}$ over the last 74–120 years. These rates are as much as an order of magnitude (10 x) higher than over the ~1000–3000 years prior to European settlement. These sedimentary records also show that mud deposition is not a recent phenomenon in Kenepuru Sound, with pure mud accumulating (mean particle size ~10 microns) over the last several thousand years (Handley et al. 2017).

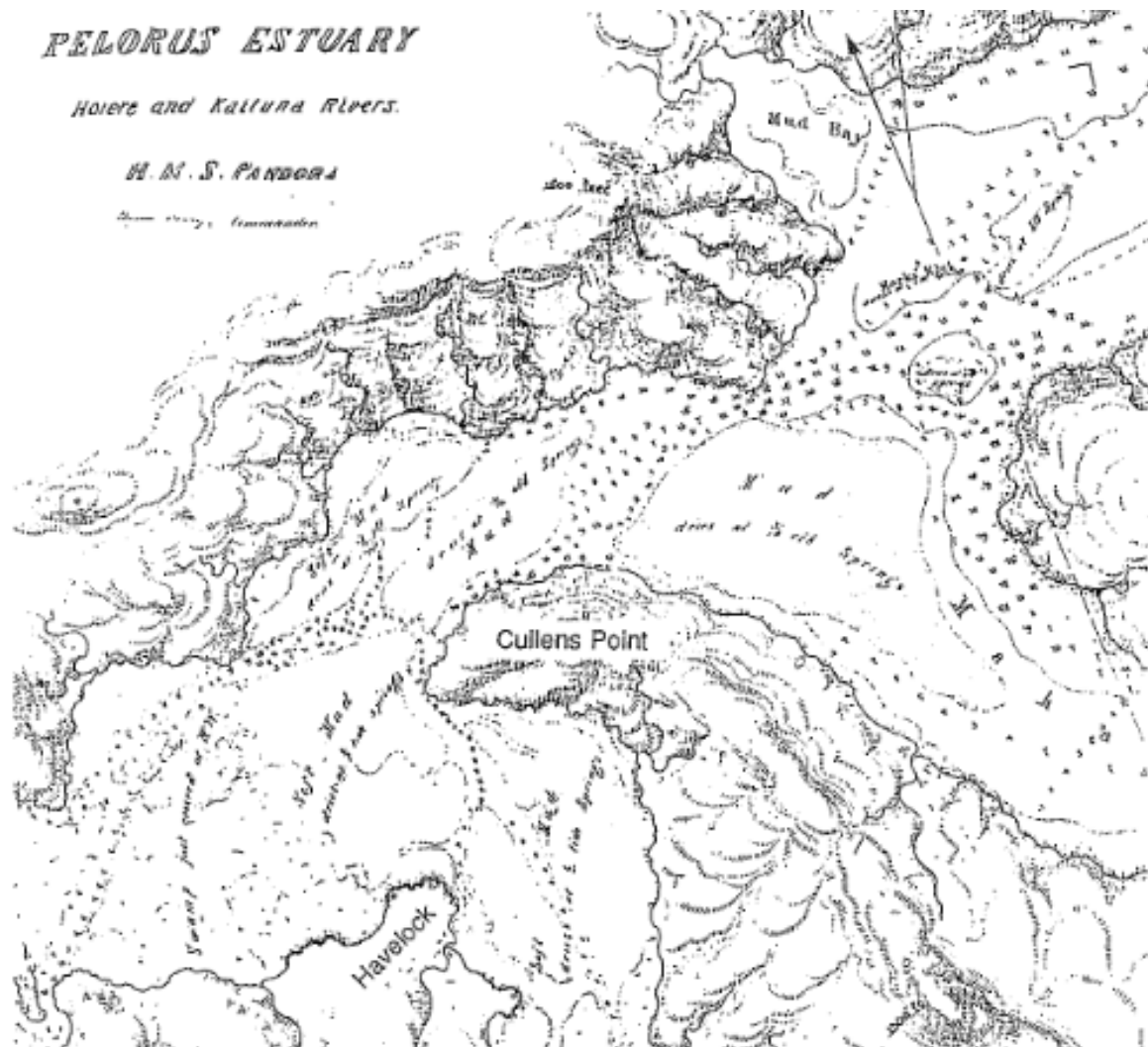


Figure 1-14: Hydrographic chart of Havelock estuary - H.M.S Pandora (1854). The chart shows the extent of mud flats and delta deposits prior to catchment disturbance following European settlement. Scale: 1:30,000. Reproduced from Lauder (1987).

Havelock Estuary has been substantially modified over the last 160 years, associated with its role as a port and in more recent years as the service centre for the aquaculture industry. Modifications since Havelock township's establishment (1860) have included dredging and construction of navigation channels and river diversions from the early-1900s (Figure 1-15). More recently, dredging associated with marina development and deepening of the navigation channel in the 1980s (Max. Gibbs, NIWA, pers. obs.) created a dredge-spoil island, located north eastern end of the Harbour break wall. Recent maintenance dredging was carried out in 1995, and spoil dumped on a farm at Twidles Island, Havelock¹. These activities are described in detail by Handley et al. (2017).

¹ Havelock maintenance dredging 950435/U150829, MLDC, 1995.



Figure 1-15: Aerial photographs of Havelock Estuary, 13 April 1942 and 31 December 2015. (top) 1942: image shows the wharf at the end of Cook Street (A), constructed channel connecting the Kaituna River with the wharf area (B); and the channel that now forms the present-day entrance to Havelock Harbour; **(bottom) 2015:** present-day wharf and marina facility, with the dredge-spoil island immediately north of the marina entrance. An area of post-harvest pine forest is visible on the hillslopes flanking the northern side of the Pelorus River mouth. Image elevation: 6.7 km. Source Google Earth.

2 Methods

2.1 CSSI sediment source tracing - overview

Sediment source tracing (aka sediment fingerprinting) is a widely used technique for determining the proportional contributions of catchment soil sources to sediment mixtures transported and deposited in rivers, estuaries and marine environments (e.g., Blake et al. 2012, Wildhaber et al. 2012, Hancock and Revill, 2013, Smith et al. 2018, Gibbs, 2008, 2014, 2020). Sediment tracing techniques calculate source proportions from a whole (e.g., %) rather than absolute quantities. However, by combining source proportion information with sediment yield (t km^{-2}) or sedimentation rate ($\text{t m}^{-2} \text{yr}^{-1}$) data the contribution of various sources can be quantified. The technique has developed rapidly over the last several decades to address research questions and inform catchment management (Owens et al. 2016, Smith et al. 2018). Sediment tracing studies have employed a range of tracers, including sediment properties (i.e., size, shape, colour), fallout radioisotopes (^7Be , ^{137}Cs , excess ^{210}Pb), geochemistry (e.g., trace metal concentrations), pollen, microbes, magnetic susceptibility and organic compounds. Source tracing used together with information on sediment transport can provide insights into landform processes and evolution (Owens et al. 2016).

In the present study, a sediment tracing method developed by NIWA employing compound specific stable isotopes (CSSI) is used to apportion sediment sources. The CSSI sediment tracing technique is based on the natural abundance isotopic signatures of specific organic compounds, primarily fatty acids (FA) (i.e., delta carbon-13, $\delta^{13}\text{C}$, referred to as FA isotopic value) in soils and sediment. In the current study, FA biomarkers were used to determine sources of sediment that has been deposited in the Te Hoiere/inner Pelorus Sound and its major catchments. The unique attribute of the CSSI tracing technique that makes it particularly useful for land management is that sediment sources are identified by plant community (i.e., land use) (Figure 2-1).

The CSSI sediment tracing technique is based on the following key concepts:

- Plants label the soils they grow in with organic compounds, including FAs, that are primarily exuded by their roots (Gibbs 2008).
- Plant FAs are slightly water soluble but highly polar, so that they spread through the soil in the root zone and ionically bind to the soil particles.
- The suite of FA $\delta^{13}\text{C}$ values from carbon chain lengths of 12 (C12:0) to 26 (C26:0) provides a unique 'fingerprint' for different plant communities (i.e., land uses).
- Although the quantity or concentration of FAs in sediment may reduce over time due to microbial decay, the isotopic value does not change (i.e., FA isotopic values are conservative) (e.g., Glaser, 20005, Kohn, 2010).
- Plant FAs label soils irrespective of particle size so that adoption of isotopic values (as opposed to concentration) avoids issues with using concentration due to particle-size dependency (Owens et al. 2016, Smith et al. 2018).
- Changes in the isotopic signatures of FAs in soils occur in response to changes in plant communities over time (e.g., native forest > radiata pine > pasture grass). These changes occur over time scales of months to years (Swales et al. 2020).

- FAs persist in sediment over long time scales (i.e., decades–centuries) (e.g., Gibbs, 2008). By linking these CSSI fingerprints of land use to sediment in depositional environments, this approach has been shown to be useful for determining sources of catchment sediment (e.g., Blake et al. 2012, Wildhaber et al. 2012, Hancock and Revill 2013, Alewell et al. 2016, Upadhayay et al. 2018, Gibbs et al. 2020). The main concepts underpinning CSSI for sediment source tracing are described in more detail in **Appendix C**.

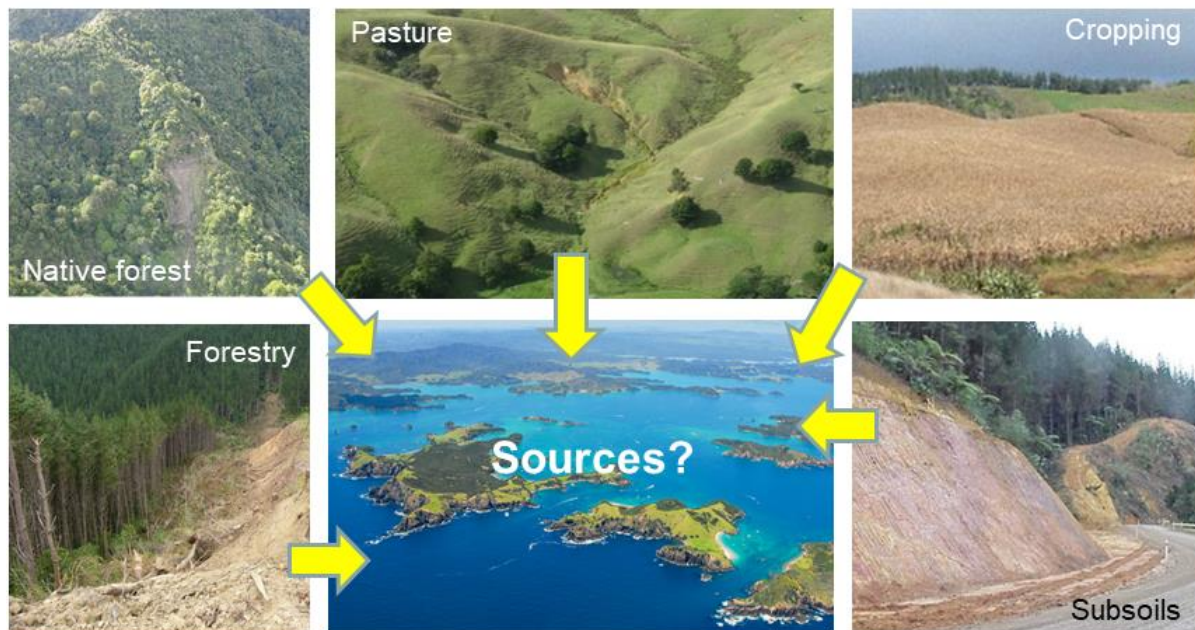


Figure 2-1: CSSI sediment source tracing. A sediment-tracing method based on the concept of compound specific stable isotope (CSSI) signatures of fatty-acid (FA) soil biomarkers that are produced by plants. The isotopic signatures of these biomarkers can be used to identify different plant communities (i.e., land use).

As in the present study, CSSI sediment tracing can be applied in a catchment-to-sea sediment accounting approach. The CSSI sediment-tracing approach can be used to:

- Differentiate sediment sources by land use (i.e., plant community) type.
- Differentiate sediment derived from streambank and subsoil sources from land use sources.
- Determine the contribution of sediment by subcatchment.
- Estimate source-specific sediment yields (e.g., tonnes km⁻²) when percentage source proportions are coupled with sediment yield data, by subcatchment and/or for a specific land use
- Reconstruct changes in the contributions of different sources over time (i.e., decades to centuries) when applied to dated estuarine sediment cores and constrained by a reliable land use history.

Two fundamental decisions are required in any sediment source tracing study:

- **Which potential sources to include?** Potential sources can be selected based on a number of criteria. Land use and topographic maps and land use classifications incorporating information on erosion susceptibility (e.g., slope, soil type, vegetation cover) can be used to identify potential contemporary sources. General understanding of catchment geomorphology can also be applied. For example, streambanks can be important sources of fine sediment in many New Zealand catchments (Basher, 2016, Smith et al. 2019). In production forests, soil erosion risk on hill slopes is substantially higher after harvesting and persists for several years after harvested areas are replanted (Phillips et al. 2012). Council land management officers and scientists can provide catchment-specific information to guide selection of potential sediment sources. Development of a reliable land-use history is also important if the assessment of sediment sources includes reconstruction of historical changes using tracers preserved in sediment cores. The possibility of a missing source(s) can also be identified by plotting source and mixture tracer data. Reviewing knowledge of the system and/or literature can be helpful to identify the potential missing source. Potential sources may also need to be combined if sample variability is such that individual sources cannot be distinguished based on statistical measures (Phillips et al. 2014).
- **Which tracers to use?** Identify the most suitable **suite of tracers** to determine sediment source contributions to a sediment mixture. The standard approach to tracer selection in studies employing a large number of geochemical and radioisotope tracers (e.g., dozens) employs a number of steps. These steps typically include exploratory data analysis (e.g., plotting data to identify outliers, separation of sources by tracer), statistical analysis of tracer discrimination, identification and exclusion of tracers exhibiting non-conservative behaviour and/or sediment-property specific behaviour (e.g., concentration dependency on particle size), and inform tracer selection based on knowledge of hydrological and geochemical processes that control tracer behaviour. The overall objective is to minimise the number of tracers employed in a mixing model employing least-squares optimisation in combination with Monte-Carlo (i.e., random) sampling (Owens et al. 2016), Smith et al. 2018).

In the present study, the Bayesian mixing model, MixSIAR, employing a Markov Chain Monte Carlo (MCMC) sampling approach was used to construct the probability distributions of sources (Stock et al., 2018). A key advantage of MixSIAR is that it can incorporate and account for uncertainty in the isotopic signatures of each source and resulting estimates of source contributions to a sediment mixture. Using this approach, Smith et al. (2018) evaluated tracer selection using synthetic sediment mixtures and found that: (1) the most accurate source apportionment results were achieved by retaining tracers that exhibited conservative behaviour, and (2) selection based on minimising the number of tracers and maximising source discrimination did not produce more accurate results.

A key selection criterion for tracers and sources is that they must conform to the isotopic biplot polygon principle, which is the fundamental basis of isotopic mixing models. Specifically, the $\delta^{13}\text{C}$ values of the mixture samples (i.e., sediment from aquatic receiving environments) must be enclosed with a polygon (two tracers) defined by the $\delta^{13}\text{C}$ values of potential sources (Phillips et al. 2014). Typically, multiple

tracers are employed in modelling of sources to improve the discrimination of sources and confidence in the results.

2.2 Sediment source library

The contribution of catchment and marine sediment to sedimentation in Mahau Sound was evaluated using a FA source library. This library is composed of samples of topsoils from eight land uses, subsoils and a marine sediment (i.e., Chetwode Islands) from a total of 40 sites. Soil samples of each catchment source as well as sediment from river and marine deposits were collected in several phases (February 2017, May and June 2018, December 2019). Soils were sampled at sites that were easily accessible by vehicle and/or foot. The soil samples were used to assemble a FA sediment source library for potential sources of sediment that have accumulated in Mahau Sound since the early 1900s (Figure 2-4). These data were used to:

- Determine the relative contribution of fine sediment (during the 2017-18 sampling period) from different parts of the catchment to river deposits by sampling at major confluences.
- Identify the sources of fine sediment deposited in Mahau Sound and how these have changed since the early 1900s.

2.2.1 Land use sources

Topsoil samples were collected from the range of land uses that have existed in the Pelorus–Rai and Kaituna catchments since the early-1900s. Sources of land use and historical land-use change information include Robertson and Stevens (2009), the review of Handley et al. (2017) and references therein, and Marlborough District Council. Present-day land use data for the Pelorus-Rai and Kaituna catchments were provided by the Land Cover Data Base (Manaaki Whenua Landcare, LCDB). Information on historical changes in land use and dominant plant communities, particularly on the flood plains and lower to mid-slopes, was obtained from central and local government records and the scientific literature (Section 1.3.2). Historical land use information was required to identify major land uses and timing of land use change to inform modelling of sediment sources over the last century.

Land use types included are:

- native forest,
- harvested pine forest (post-1979/1980),
- dairy pasture,
- sheep pasture,
- kanuka scrub,
- gorse and broom scrub, and
- bracken.

Native forest is a major landcover type in the catchments flowing into the inner Pelorus Sound. These forests, dominated by beech and broadleaf hardwoods, presently account for 62% (548 km²) and 39% (57 km²) of landcover in the Pelorus-Rai and Kaituna catchments (LCDB-5, 2017/18). Along with other native plant communities (e.g., tussock grassland, sub-alpine shrubland), these forests represent the original landcover of the Pelorus system that existed before human arrived. As such, soil erosion from these native forest areas will be the most representative of reference conditions (i.e., background rates).

Harvested pine forest is defined as land predominantly with bare ground post-harvest and prior to replanting (LCDB-5 definition). This source was included as a potential sediment source rather than mature pine forest because the harvesting phase of a production forest rotation coincides with the so-called 'window of vulnerability' (O'Loughlin and Watson, 1979) during the 1–6 year period following tree removal (Phillips et al. 2012) for substantially increased soil loss. Forested landscapes (including exotic forests) generally generate less sediment than pasture landscapes (e.g., Eyles and Fahey, 2006, Phillips et al. 2012). However, when plantation forests are harvested there is the potential for increased erosion due soil disturbance, removal of protective ground cover exposing soils to direct rainfall impact and loss of root strength (reinforcement) (e.g., Phillips et al. 2012). This increased vulnerability to soil loss occurs after harvesting, between the decay of harvested tree root systems and the establishment of the next forest rotation. This period of elevated susceptibility to soil erosion varies “depending on site conditions, tree density and other factors” (Phillips et al. 2012). Harvesting of pine forest increased after the first plantation timber from the Rai State Forest was harvested in ca. 1979 (Huddleston, in Ulrich and Handley, 2020). Sediment derived from harvested pine areas can be differentiated from sediment derived from mature pine forest due to differences in the isotopic values of short-chain length FA tracers (i.e., C14 to C18, Swales and Gibbs, 2020). Harvested pine accounted for 1.6% of the total landcover of the Pelorus-Rai and Kaituna catchments in 2017/18 (LCDB-5).

Dairy pasture (high producing exotic grassland) occurs on flood plains and coastal flats, and presently occupies 7.3% (76 km²) and 1.4% (2 km²) in the Pelorus-Rai and Kaituna catchments (LCDB-5, 2017/18). Dairy farming has been practiced in the Pelorus-Rai since the late-1800s (section 1.3.2). Dairy pasture occurs in close proximity to the main stem and major tributaries, so that there are short sediment transport pathways for runoff to streams and rivers.

Sheep pasture (low producing exotic grassland) presently accounts for 31% (46 km²) of land use in the Kaituna catchment, where it occurs on the hillslopes and in the valleys. Sheep pasture accounts for less than 0.5% (4 km²) of landcover in the Pelorus-Rai catchment (LCDB-5, 2017/18). Historically, sheep pasture was a widespread land use in the Pelorus-Rai catchment and was established on hill slopes at an early stage after native forest clearance (i.e., late-1800s). These hillslope pastures were prone to soil erosion in heavy rain (McIntosh, 1940).

Kanuka and/or manuka scrub covers 19.5 km² in the Pelorus-Rai and kaituna catchments. Along with bracken, kanuka and manuka are the main native scrub species in the Marlborough Sounds, and occur on lower–mid hillslopes below 700 m elevation. These native scrub species colonise areas following forest clearance (Walls and Laffan, 1986) and so are key indicator of catchment disturbance.

Gorse and broom were introduced by European settlers primarily for hedging in the late-1800s and would have rapidly become invasive pest plants on open pasture in Te Hoiere, as elsewhere in New Zealand. The spread of gorse through the Pelorus-Rai and Kaituna catchments was facilitated by the regular burn offs for scrub clearance. This land management practice was used for small-scale burns

to prepare areas logged of native timber into pasture and to convert secondary regrowth back into pasture or into plantations (McIntosh 1940, Bowie 1963). This historical information suggests that the area of gorse and broom was substantially higher than today, presently accounting for 5.6% (8.3 km²) of land use in the Kaituna catchment (c.f. Pelorus-Rai, 0.6 km²). Present day area of exotic invasive scrub is also substantially lower than in the mid-1990s (i.e., Pelorus-Rai, 13.6 km², Kaituna 3.4 km², LCDB-1).

Bracken is a widespread and dominant plant in pasture and in the early stages of forest regeneration and occurs on hillslopes below 500 m in the Marlborough Sounds (Walls and Laffan, 1986, Bray 1991). Bracken soils are also a ubiquitous indicator of natural and human-induced forest disturbance. Evidence of long-term cycles of catchment disturbance indicated by Bracken pollen abundance is preserved in sedimentary records (McGlone, 2005). In the Marlborough Sounds, bracken colonises ungrazed pasture within several years (Bray, 1991) and is abundant on forest margins. Regrowth of bracken on marginal hill country pasture was a management issue for farmers after World War 2 (Beggs, 1962).

2.2.2 Subsoil and streambanks

Subsoils consist of weathered regolith that underlie the topsoil (A Horizon) and are exposed at the surface by erosion processes. Unlike most topsoil's, subsoils contain little organic material and typically contain small quantities of FAs exuded from the overlying vegetation, in comparison to topsoils (i.e., 10-fold lower concentrations). Subsoils gradually accumulate these small quantities of FAs that percolate down through the soil profile, associated with past plant communities (i.e., over decades–centuries) as well as integrating contributions from contemporary plant communities. Consequently, the FA isotopic signatures of subsoils can be substantially different from those of the overlying topsoils. Subsoil sources are presented here by samples collected from five sites within the Pelorus (2) and Kaituna (3) catchments. Subsoil erosion processes include hillslope failure and gullying and can be associated with a range of land uses.

Streambanks can be important sources of fine sediment in many New Zealand catchments (Basher, 2016, Smith et al. 2019). Streambank deposits on floodplains are composed of mixtures of sediment eroded from upstream sources that may include both topsoils, subsoils, regolith and streambanks. Streambank samples from active erosion sites were collected at three locations in the Opori, Tunakino and Kaiuma streams.



Figure 2-2: Subsoil sampling Site 3 road cutting (March 2017). Photo: S. Urlich, MDC.



Figure 2-3: Example of streambank erosion in the Rai River catchment (December 2016). Photo: A. Swales, NIWA.

2.2.3 River subcatchments

Sediment from recent flood deposits were collected at the confluence of major tributaries within the Pelorus-Rai and Kaituna catchments (Figure 2-4). Sets of three samples were collected at each confluence – one in the main river channel (i.e., first end member), one in the tributary channel upstream of the confluence (i.e., second end member), and a third downstream of the confluence (i.e., mixture) at sufficient distance (i.e., several hundred metres or after a zone of turbulent mixing). Figure 2-5 shows the location of the sediment samples collected at each river/stream confluence.

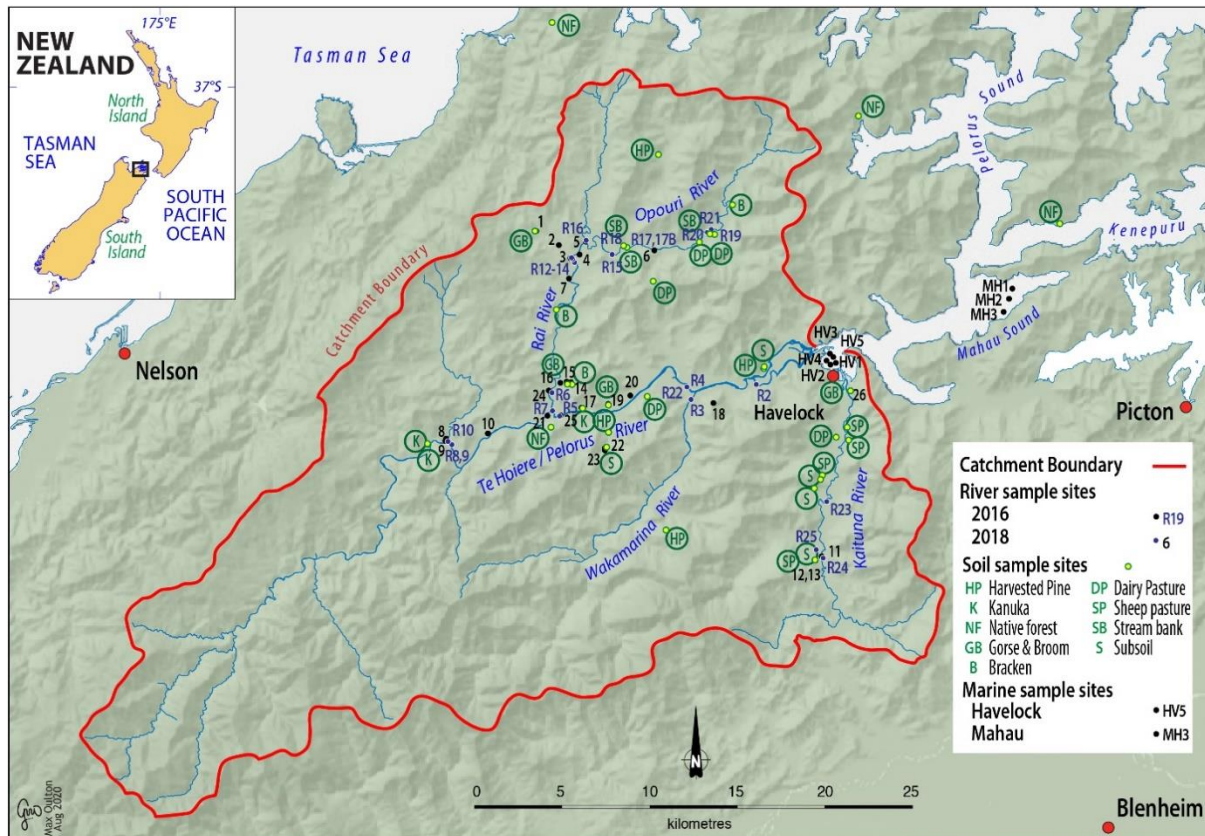


Figure 2-4: Location of river sediment deposit sampling sites. April 2016 and May 2018.

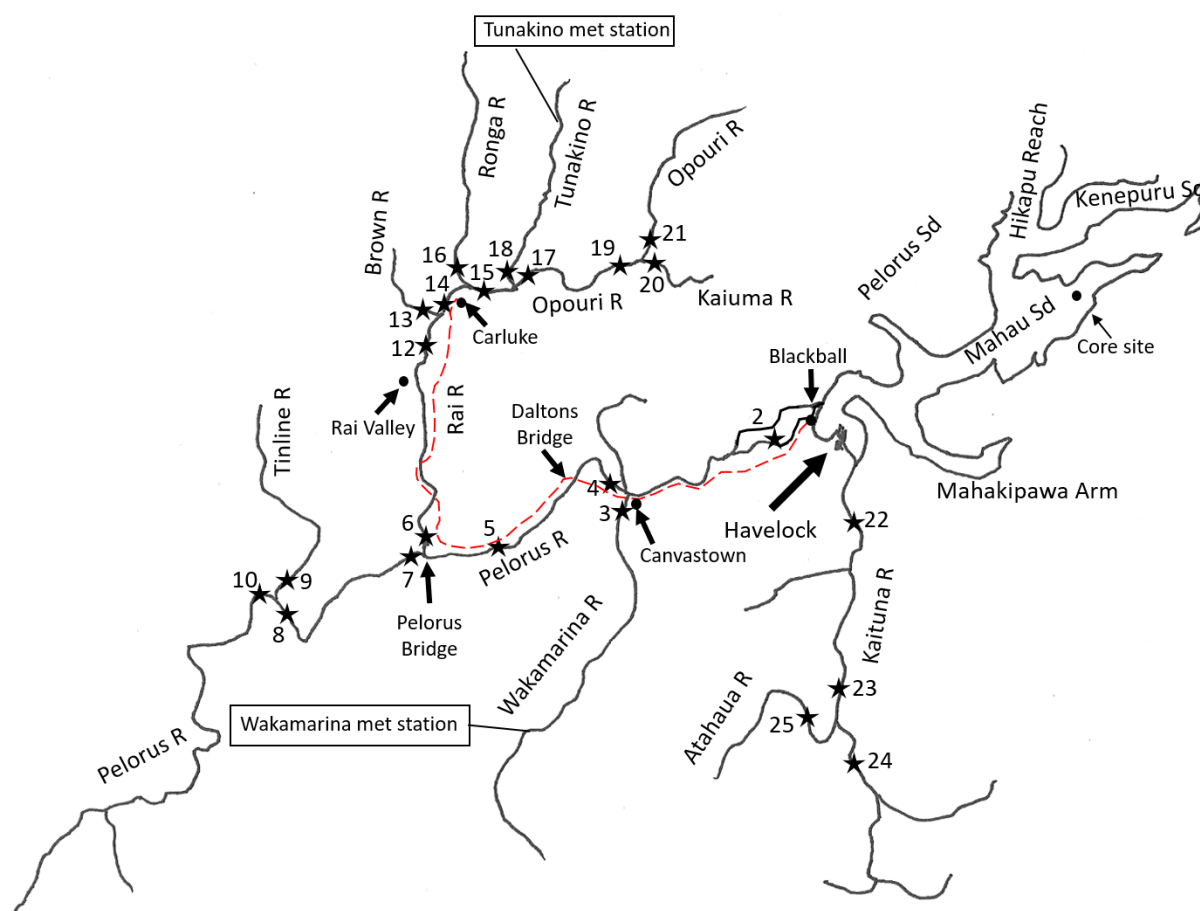


Figure 2-5: Schematic diagram of the Pelorus River system showing the tributaries modelled and the location of sediment sampling relative to each confluence. Schematic diagram of the Pelorus River system showing the tributaries modelled and the location of sediment sampling relative to each confluence. Additional information such as sawmill names and the path taken by Brownlee’s tramway (dashed red line) are also shown. (Numbers around each confluence are those used for modelling and may not correspond with numbers in Figure 2-4).

2.2.4 Marine sediment

Marine sediment samples were collected from the Chetwode Islands (Nukuwaiata and Te Kakaho) on 11 December 2019. The Chetwodes are located ~6 km northeast of the entrance to Pelorus Sound. This is an area of mud deposition associated with accumulation of marine biogenically-enriched fine suspended sediment from Cook Strait (Carter, 1976) and sediment discharged from the Pelorus and Kaituna Rivers during flood events (Handley et al. 2017) (Figure 1-12, Figure 2-6).

CSSI analysis of a sample collected by Handley et al. (2017) from Nukuwaiata Island (i.e., bay on southeast coast) indicated that sediment here has a notably different isotopic signature to catchment soils (i.e., Figure 2-7, Handley et al. 2017). In particular, the C14:0 fatty-acid signature was isotopically enriched (i.e., 4 to 12 per mil, ‰) in comparison to catchment soils. This Chetwode Island $\delta^{13}\text{C}$ FA sediment signature was similar to the “Havelock inflow” sediment sample collected from Havelock Estuary by Handley et al. (2017). Thus, surficial seabed samples were collected using a Van-Veen grab from 8 subtidal sites located along the south-eastern coast of the islands (including the Handley et al. (2017) site), in water depths ranging from 18 to 32 m (Figure 2-6). This provided a robust FA isotopic data set for a marine endmember to model sources of sediment accumulating in the inner Pelorus Sound.

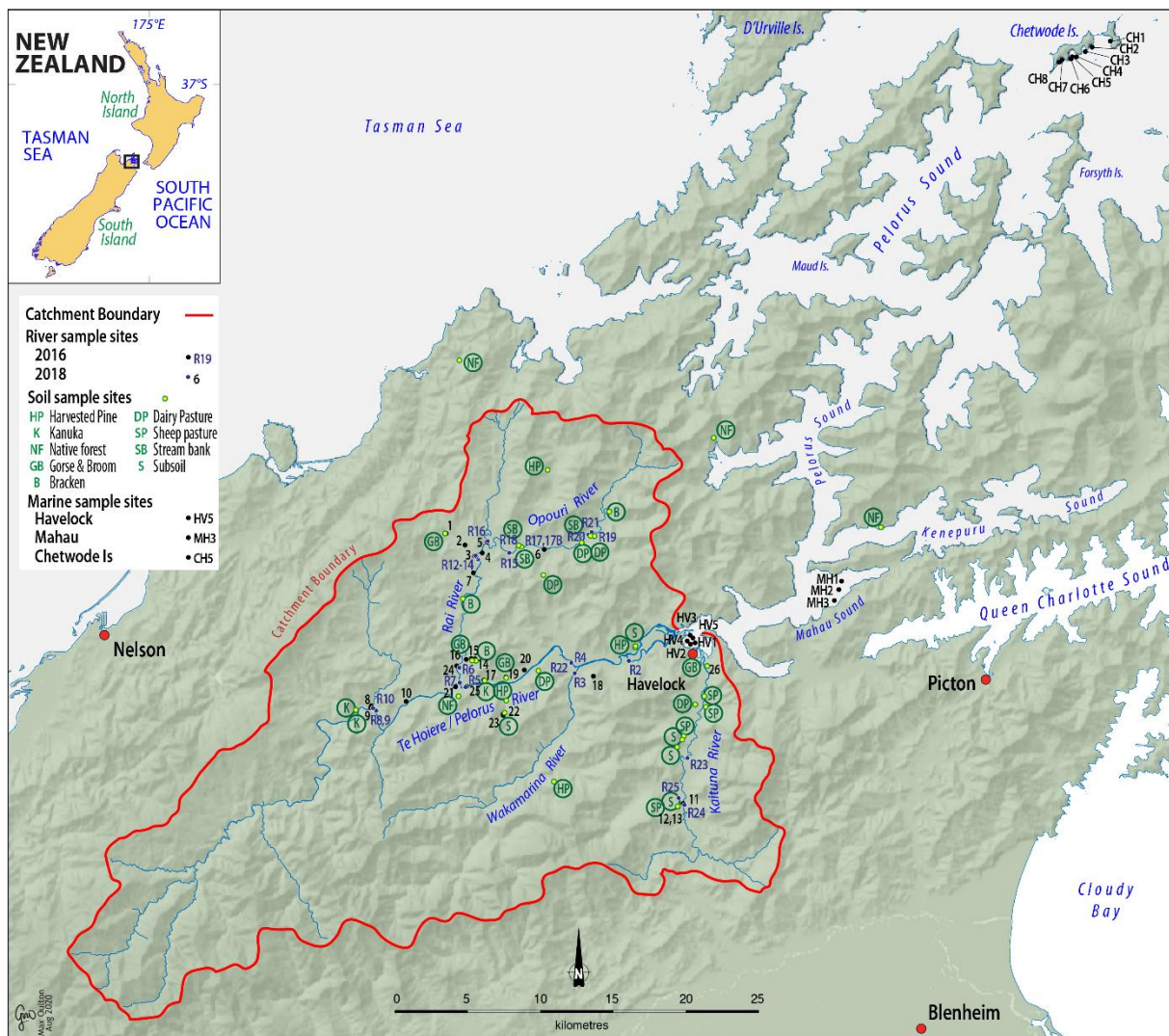


Figure 2-6: Location of river, estuarine sediment cores and marine sediment sampling sites.

2.3 Soil and sediment sampling methods

2.3.1 Topsoil and subsoil

Topsoil and subsoil samples were collected at the sampling sites as composites composed of 10 randomly located subsamples collected within a ~100 m² area (i.e., quadrat). Compositing of subsamples provides an average FA isotopic signature for the land use and also avoids the possibility of a single sample not being representative of a sampling quadrat. Each subsample was collected using a purpose-built hand corer with the top-most 20 mm retained. This ensured that soil subsample volumes were similar and prevented bias in the composite sample. Details of the sampling protocol are described in **Appendix D**.

2.3.2 River sediment

Fine sediment was collected from flood-deposition zones on riverbeds and banks by taking several scrapes of the deposited layer (i.e., typically less than 20 mm) and combining these into a single composite sample. This method recognises that suspended sediment associated with a flood event may be deposited as a layer of variable thickness. This is acceptable as the sediment is homogenised during transport (IAEA, 2019). Recent flood deposits can be discriminated by eye based on sediment

colour and deposit morphology (Figure 2-7). These fine sediment deposits sampled from riverbeds and banks represent a mixture of all of the upstream sources that contributed to the deposit. These recent storm deposits (i.e., within previous several months) were often associated with woody flood debris (Figure 2-7) or behind trees and other obstructions to the river flow where mud was readily deposited. Flood deposition on the upper riverbank generally represents suspended sediment deposited during the early phase of the flood hydrograph recession. Thus, these river sediment deposits provide information on sediment sources over a relatively recent and short time period (i.e., weeks to months) between the flood events and subsequent sample collection.



Figure 2-7: A flood sediment deposit sampled from the top of the riverbank. Rai River, December 2016. Photo: A. Swales, NIWA.

2.3.3 Estuarine sediment cores

Sediment cores were collected from the Inner Pelorus Sound to determine sediment accumulation rates (SAR) and sources of sediment that have accumulated in this estuarine environment over the last century or more. In particular, CSSI analysis of these dated cores enable the timing and persistence of sources to be determined in relation to land use activities over annual to decadal time scales. This longer-term perspective complements the analysis of recent sediment sources based on sampling in the river system.

Sediment cores were collected at multiple sites in the Havelock Estuary on 28 March 2017 (5 sites) and Mahau Sound on 12 December 2017 (3 sites) (Figure 2-8). Replicate sediment cores up to 1 m (Havelock) and 1.6 m long (Mahau) were collected using a 100-mm diameter vibra-corer operated by Diving Services Ltd (Nelson). Longer cores were collected at the Mahau sites because the increased water depths enabled use of longer lengths of PVC core pipe with the vibra-corer.

The Havelock Estuary core sites were spread across the shallow intertidal basin west of Cullen Point (Figure 2-8), with site HV-1 located close to MDC's long-term monitoring site C (Robertson, 2019). Radioisotope dating of cores from three sites (HV-1, HV-2 and HV-4) indicated very low rates of fine-sediment accumulation in the basin as demonstrated by relatively shallow profiles (i.e., 10–20 cm) of excess lead-210 ($^{210}\text{Pb}_{\text{ex}}$) that is the basis for sediment dating. This mainly reflects the limited sediment accommodation volume of these intertidal sites (i.e., below high tide level) (e.g., Swales et al. 2016b).

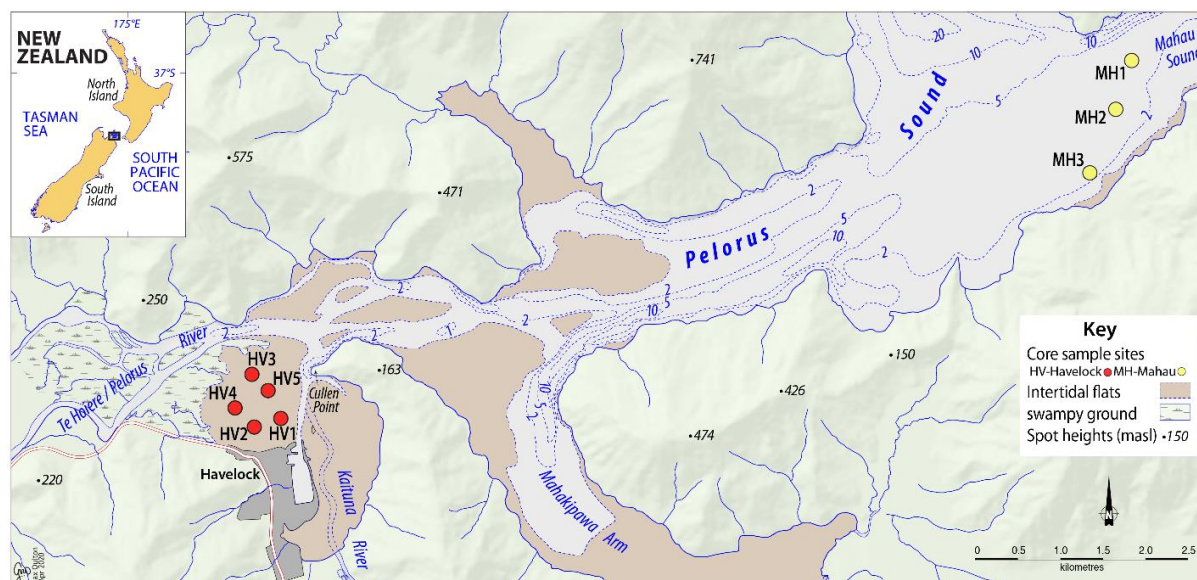


Figure 2-8: Location of sediment core sites in Havelock Estuary and Mahau Sound. Cores collected 28 March (Havelock) and 12 December 2017 (Mahau).

As well as the potential effects of sediment mixing by the activities of animals (i.e., bioturbation), intertidal estuarine sediments in particular are also subject to disturbance and resuspension by fetch-limited waves (Green and Coco, 2014). These result in transport and mixing of sediment deposits and winnowing of fine sediments that are redeposited in low energy environments (e.g., upper-intertidal flat, saltmarshes, subtidal zone). The sediment cores are also sampled in 1-cm depth increments, that is dictated by the requirement to sample sufficient material for accurate dating and sediment source tracing. Thus, as sediment accumulation rates (SAR) decrease, the time-period averaged in each sample increment, increases. Sediment mixing along with low SAR results in low temporal resolution of sediment cores. These effects on the temporal resolution of sedimentary

records are reduced as SAR values increases. Based on these considerations, the sedimentary records obtained from the Havelock basin core sites were not considered suitable for reconstructing a long-term history of sedimentation and sediment sources in the inner Pelorus Sound.

Consequently, nearby subtidal sites that were likely to have higher SAR due to increased sediment accommodation volume and less physical disturbance by waves were identified in Mahau Sound, some seven kilometres east of Havelock Estuary. The three core sites were located within a narrow depth range in the subtidal zone between 3–4 m below chart datum (CD, i.e., lowest astronomical tide). Relatively undisturbed records of mud accumulation can be preserved in such sheltered/fetch-limited subtidal environments. This is because tidal currents on subtidal flats are typically weak. Bed-orbital currents generated under small, short-period waves are also insufficient to resuspend cohesive muds in water depths of more than a few metres (e.g., Green and Coco, 2014). In the nearby Kenepuru Sound, Handley et al. (2017) found that muds have accumulated at several sites at rates of 3–9 mm yr⁻¹ since the early-1900s. Satellite images also indicated that river plumes from the Pelorus and Kaituna rivers are preferentially advected into the Mahau Sound (Figure 1-12) so that deposition of catchment-derived fine sediment in this environment was likely to occur.

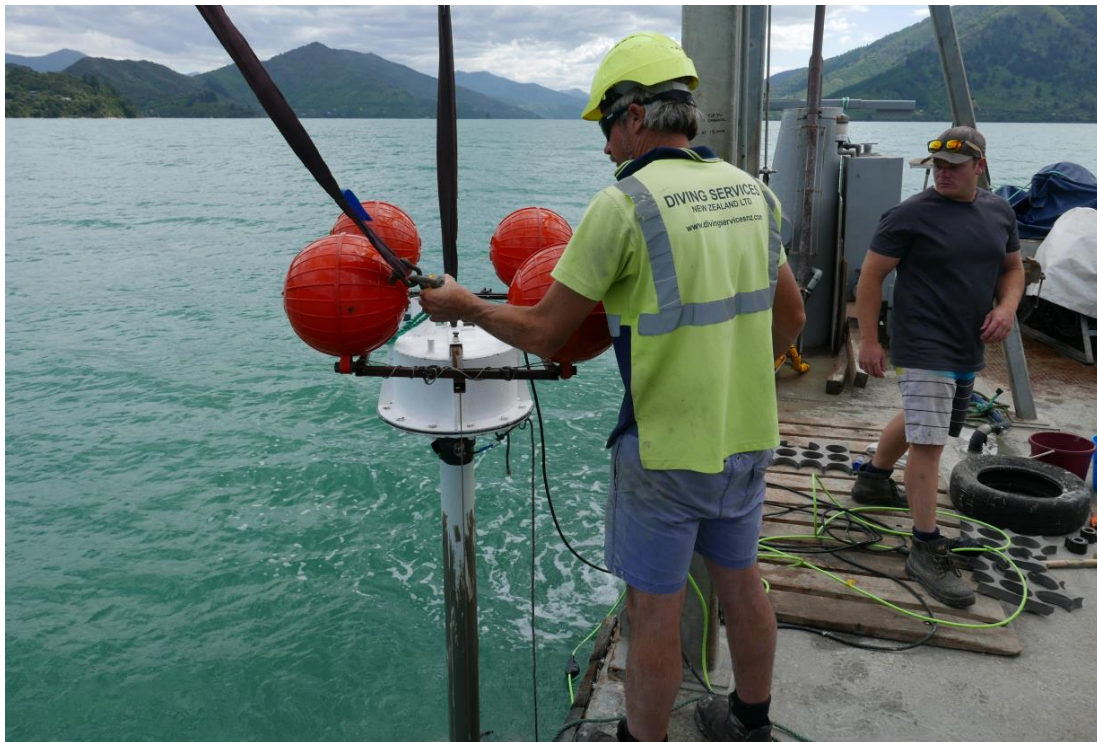


Figure 2-9: Sediment coring in Mahau Sound. Retrieving the vibra-corer from M.V. Pelorus, 12 December 2017. Photo: A. Swales, NIWA.

Replicate cores were collected at each site, with one used for radioisotope dating, particle size and bulk density analyses. A second core was prepared for x-ray imaging and subsequent subsampling for analysis of the $\delta^{13}\text{C}$ values of FA biotracers. Cores with the least compression, as calculated from the driven and retained-core lengths, were selected for these analyses. **Appendix E** provides details of the Havelock and Mahau sediment core sites.

2.4 Bulk carbon and fatty acid analyses

The CSSI sediment-tracing technique employs two different sets of stable isotope signatures:

- Bulk $\delta^{13}\text{C}$ values and percentage carbon (%C) of the whole soil or sediment. These were analysed on a continuous flow, isotope ratio mass spectrometer (IRMS) after acidification to remove inorganic carbonates.
- Compound specific stable isotopes (CSSI) using the $\delta^{13}\text{C}$ values of the carbon atoms in of individual FAs bound to soil and sediment particles.

The FA biomarkers were extracted from a 20 g unacidified aliquot of each sample with dichloromethane (DCM) at 100 °C at 2000 psi in a DIONEX ASE200 accelerated solvent extraction system, using two 5-minute extraction cycles, after which the extracts were combined. Full details of the analytical method and the CSSI technique are included in **Appendix C**. The CSSI source library data for the Pelorus-Rai and Kaituna Rivers, and Mahau Sound sediment deposits are presented in **Appendix F**.

2.5 Source isotopic polygons

The application of the CSSI technique to identify the land use sources of sediments deposited in rivers and estuaries is a complex/multi-step process. Development of source isotopic polygons enclosing sediment mixtures underpins the application of mixing models (Phillips et al. 2014). These “unmixing” models, are used to calculate the proportional contributions of each potential source to a sediment mixture. Modelling results for the sources of river and estuarine sediments of the inner Pelorus Sound are reported in Section 3.

The selection of FA tracers for modelling source soil contributions to river and estuarine sediment mixture deposits was informed by the isotopic biplot polygon principle that underpins the application of isotopic mixing models (Phillips et al. 2014). The fundamental requirement is that the isotopic values of the tracers in a sediment mixture must be enclosed within a polygon (two tracers) or multi-dimensional volume (i.e., three or more tracers) defined by the isotopic values of the potential sources, within their range of uncertainty (e.g., standard deviation).

Modelling sources of river sediment deposits

Comparison of the source library with the deposited river sediment (i.e., mixtures) using biplots indicated that an isotopic system based on the bulk carbon isotope ($\delta^{13}\text{C}$) in combination with the even-numbered mid-chain length FAs (i.e., C20:0, C22:0, C24:0, C26:0) best satisfied the isotopic polygon condition (Phillips et al. 2014). Where sources could not be discriminated from each other within a source polygon (i.e., had consistently similar mean values/groupings), they were merged into a single source. Figure 2-10 shows example biplots for the lower Pelorus River using three tracer pairs, a) $\delta^{13}\text{C}$ versus C20:0, b) $\delta^{13}\text{C}$ versus C22:0 and c) $\delta^{13}\text{C}$ versus C24:0, and d) lower Kaituna River using $\delta^{13}\text{C}$ versus C26:0. All other tracer combinations either had most river samples plotting substantially outside the source polygons and/or the tracers were highly correlated (i.e., no polygon).

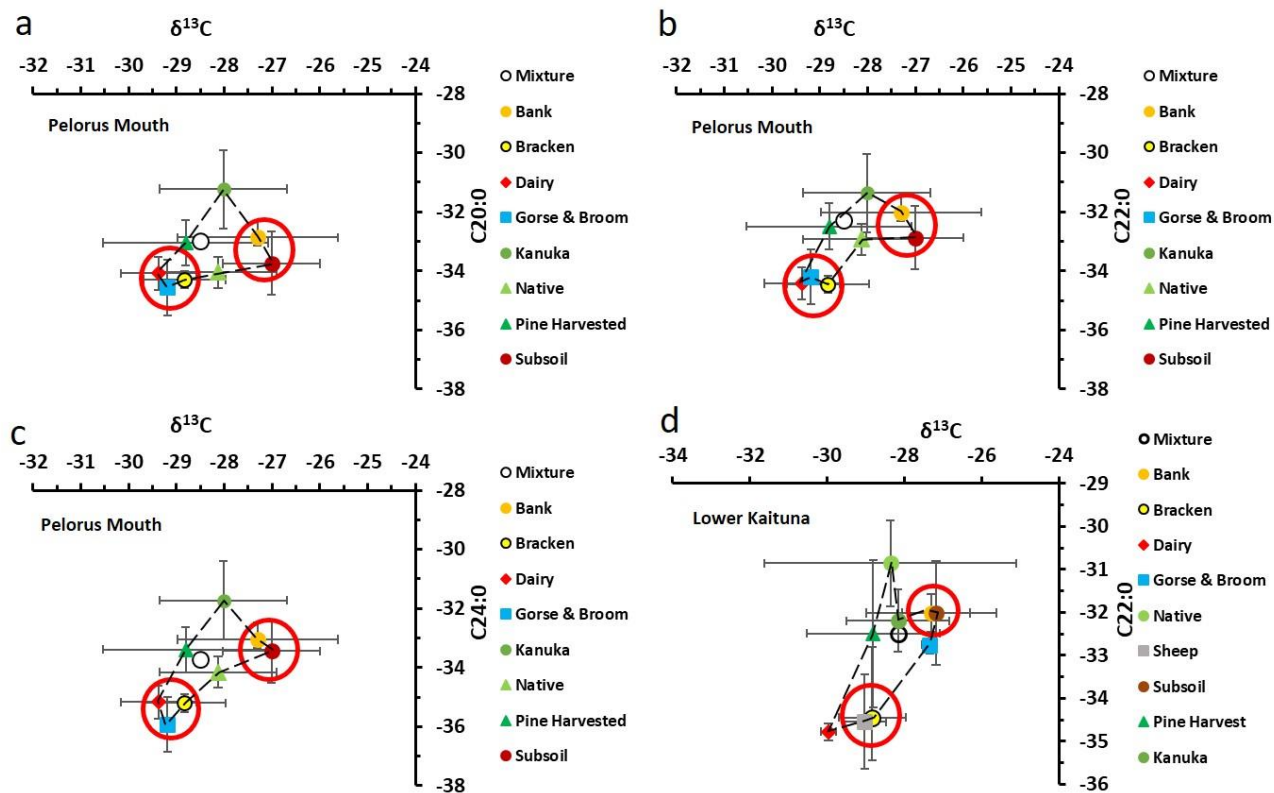


Figure 2-10: Examples of isotopic biplot polygon plots for all land use sources in the lower Pelorus River (a,b,c) and the lower Kaituna River (d). Red circles enclose groups of sources that were merged for the second series of modelling. Although only one example is shown for the Kaituna River (d), that same set of groupings was found for other tracer pairs in the Kaituna River. Note: the dairy source cannot be discriminated from gorse+broom and bracken sources in the Pelorus River system but can be discriminated in the Kaituna River and is modelled as an individual source.

The isotopic values for each land use source were plotted in biplots for the bulk C and FA tracers for each river tributary to determine which tracer set best satisfied the source polygon constraint (See section 2.5, Source Isotopic polygons, Phillips et al. 2014). The example (Figure 2-10) shows the biplots for the lower Pelorus River using three tracer pairs, a) $\delta^{13}\text{C}$ versus C14:0, b) $\delta^{13}\text{C}$ versus C20:0 and c) $\delta^{13}\text{C}$ versus C24:0, and d) for the lower Kaituna River using C14:0 versus C22:0.

Sheep pasture was only included as a potential source in the Kaituna River system as this land use was not observed in the Pelorus-Rai catchment during the sampling/study period. The dairy pasture source was included in mixing models for both river systems because dairy farming was observed in both catchments. The example river mixtures shown in the biplots (Figure 2-10) lie within the bounds of the land uses plotted. Similar plots were made for all possible combinations of tracers and land uses for each tributary. Valid combinations are marked with a tick (Table 2-1).

Table 2-1: Bulk carbon and fatty acid (FA) tracers usable in isotopic biplot polygon test. Ticks indicate those land use tracers that formed a source polygon enclosing the sediment sample (mixture) from each river site (left hand column).

Pelorus River Tributary	$\delta^{13}\text{C}$	C14:0	C16:0	C18:0	C20:0	C22:0	C24:0	C26:0
	‰	‰	‰	‰	‰	‰	‰	‰
Upper Pelorus	✓		✓	✓	✓	✓	✓	
Tinline	✓		✓	✓	✓	✓	✓	
Rai		✓		✓	✓	✓	✓	✓
Wakamarina	✓	✓	✓	✓	✓	✓	✓	✓
Pelorus Mouth	✓	✓	✓	✓	✓	✓	✓	✓
Brown	✓	✓	✓	✓	✓	✓		✓
Ronga	✓	✓	✓	✓	✓	✓		✓
Tunakino	✓			✓	✓	✓	✓	
Kaiuma	✓	✓	✓	✓	✓	✓		✓
Opouri	✓		✓	✓	✓	✓	✓	✓

The source modelling for the Pelorus and Kaituna River sediment deposits was undertaken in two ways to confirm the validity of merging sources as identified in the isotopic biplots (e.g., Figure 2-10). This approach was taken due to the relatively small isotopic distances between the potential sources for the river sediment deposits (i.e., range of average source values less than 4‰). First, all possible land use sources were modelled individually (i.e., series one), which was previously the recommended standard practice (Gibbs, 2014). Secondly, the land use sources were modelled with the merged sources in place of the individual sources that were merged (i.e., series two).

Gibbs (2014) recommended modelling all possible land use sources individually. However, this approach can result in impractically long model run times, particularly using older generation mixing models (e.g., the linear model IsoSource, Phillips and Gregg 2003). Model runs with large numbers of sources and/or sources with similar isotopic values may also fail to converge to a stable solution or produce source proportion estimates with a large range of uncertainty. This is particularly the case for models where the number of sources exceeds the number of tracers (n) by more than $n + 1$ (Phillips et al. 2014, Smith et al. 2018). Although probabilistic mixing models, such as MixSIAR, are not constrained by the $n+1$ rule, their performance is typically degraded as the number of sources increases (Stock et al. 2018). Gibbs (2014) also recommended iterative elimination of sources that produced minimal or no substantial proportional contribution (i.e., < 5%) (e.g., Figure 2-10).

The objective of including both series one and series two modelling run results was to demonstrate the validity of the series two modelling approach for the river sediment deposits. To achieve this, the series one and series two model results were compared by adding the results of the series one average proportions for the individual sources used in the merge. If the merge was valid, the average source proportion for the series 1 and 2 runs values should be essentially the same, within the limits of the mixing model uncertainty.

The validity of merging sources was also independently confirmed using Canonical Analysis of Principal coordinates (CAP) (Section 2.6). CAP considers the correlation structure among variables in the multivariate data set and, in doing so, uncovers important patterns by reference to relevant

hypotheses (e.g., null hypothesis: source soils cannot be separated based on the tracers used). The application of CAP was particularly important for analysis of isotope data for the Mahau Sound sediment deposits. This is because of the larger number of potential sources in comparison to the river sediment deposits, where potential sources can be constrained to a subset of all potential sources (e.g., upstream land uses).

Modelling sources of Mahau Sound sediment deposits

For the Mahau sediment cores, comparison of the source library with the estuarine sediment mixtures showed that an FA isotopic system based on the even-numbered FA biotracer C14:0 in combination with the four mid-chain length FAs (i.e., C20:0, C22:0, C24:0, C26:0) best satisfied the isotopic polygon condition. All other combinations of FAs either had most mixture samples from the cores plotting substantially outside the source polygons and/or the tracers were highly correlated (i.e., no polygon). This was particularly the case for combinations of the longer chain length FAs. Four land-use sources (i.e., sheep, dairy, gorse and broom, bracken) could not be discriminated from each other within the source polygons and were merged into a single source (i.e., Scrub and Pasture). Figure 2-11 and Figure 2-12 present isotopic biplots for each combination of the short-chain C14:0 FA with the long-chain C20 to C26:0 FAs for potential sources with the catchment (i.e., river deposits) and estuarine sediment mixtures. These isotopic biplots show the average FA isotopic values (with one standard deviation) for the potential sources and the individual sediment mixtures. The sediment samples (mixtures) from the Pelorus-Rai and Kaituna Rivers and Mahau Sound cores are largely constrained within the polygons formed by the potential sources. It should be borne in mind that the mixing model incorporates the uncertainty in the average FA isotopic values of each potential source.

The bi-plot analysis indicated that the gorse and broom, bracken, sheep pasture and dairy pasture could not be discriminated from each other due to their similar average $\delta^{13}\text{C}$ FA values and variability (individual dark blue diamond symbols, Figure 2-11 and Figure 2-12). Consequently, these four land use sources were merged into a single “Scrub and pasture” source to incorporate into the mixing model. The harvested pine source was included in the analysis of the Mahau Sound sediment cores for sediment deposition after 1979/1980 when large-scale harvesting of the first rotation of the Rai Forest began.

The marine endmember source (Chetwodes) has C14:0 $\delta^{13}\text{C}$ values that are between 4–12‰ more enriched (i.e., $\delta^{13}\text{C}$ values closer to zero) than the potential catchment sources (Figure 2-11 and Figure 2-12). It is also notable that complete sequences of the final FA tracer suite were preserved in the Mahau sediment cores. This may reflect the anoxic, muddy nature of the sediment accumulating in Mahau Sound that more effectively preserve geolipids such as fatty acids than do sand-rich sediment (Rieley et al. 1991, Bourbonniere and Meyers, 1996). Rapid burial by sedimentation also reduces exposure of organic compounds to microbes concentrated in the surface layer of the substrate (Didyk et al. 1978).

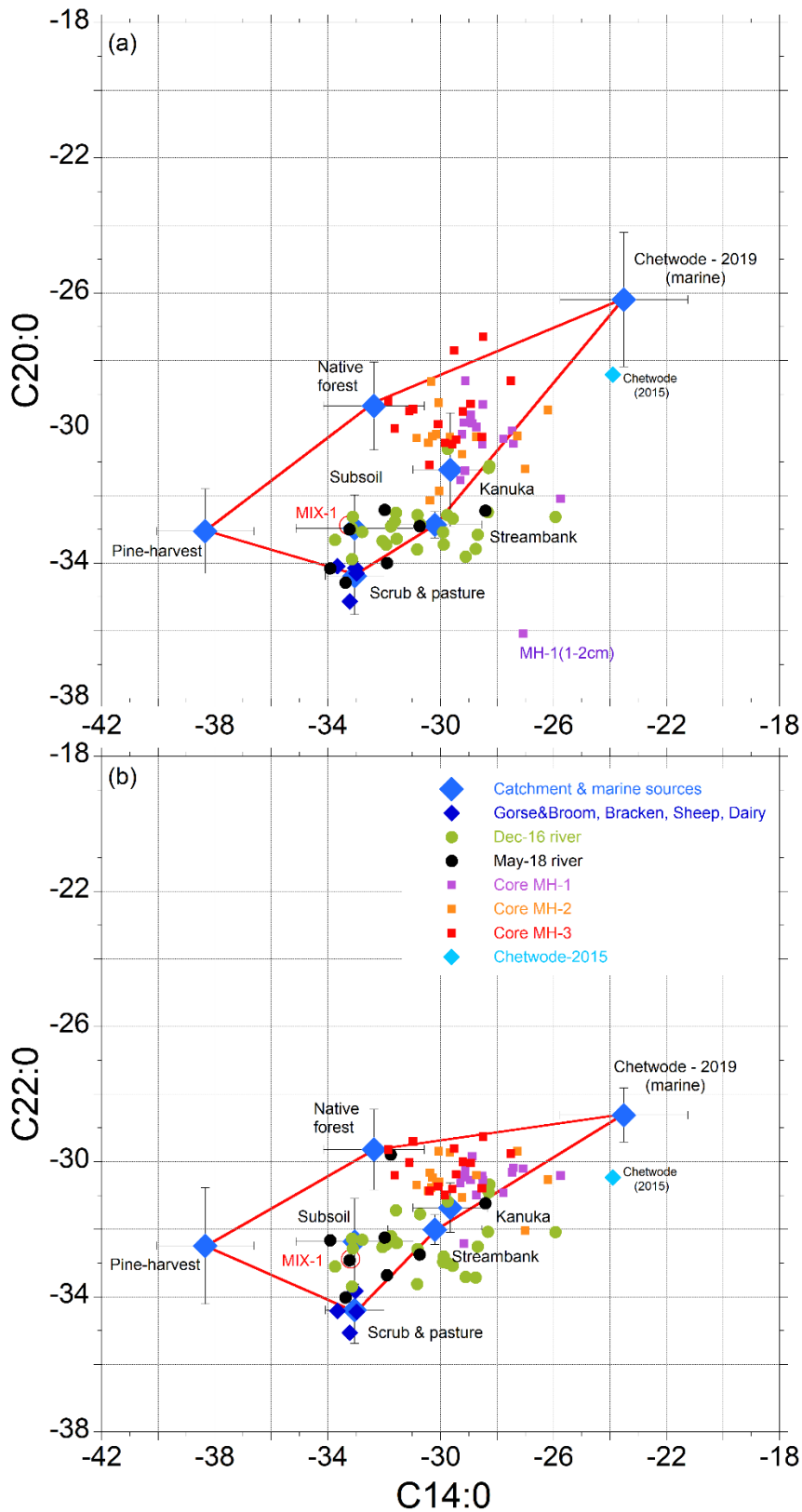


Figure 2-11: Isotopic biplots of average FA $\delta^{13}\text{C}$ values (C14:0 with C20:0 and C22:0) for potential sediment sources and estuarine sediment mixtures in dated cores. Notes: (1) The average $\delta^{13}\text{C}$ values of potential sources are plotted with standard deviations, (2) stable isotope values for estuarine sediment mixtures are Suess-effect corrected to year of core collection (i.e., 2017 AD) with inter-batch corrections applied using standards, (3) The location of river sediment samples in the isotopic space are also shown. Mix 1 is the most downstream river sediment sample collected from the Pelorus River (sample 196/2, May 2018).

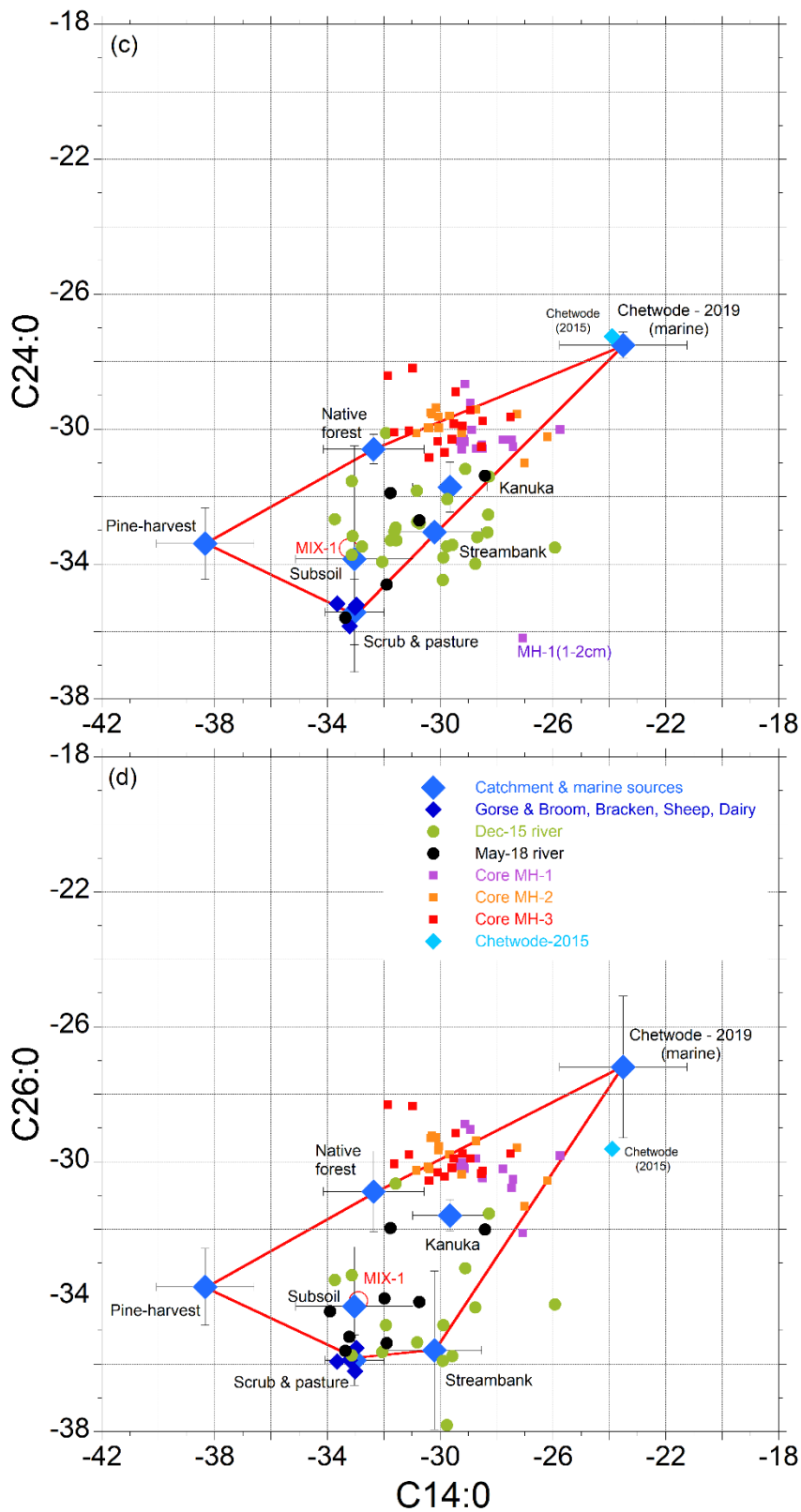


Figure 2-12: Isotopic biplots of average FA $\delta^{13}\text{C}$ values (C14:0 with C24:0 and C26:0) for potential sediment sources and estuarine sediment mixtures in dated cores. Notes: (1) The average $\delta^{13}\text{C}$ values of potential sources are plotted with standard deviations, (2) stable isotope values for estuarine sediment mixtures are Suess-effect corrected to year of core collection (i.e., 2017 AD) with inter-batch corrections applied using standards, (3) The location of river sediment samples in the isotopic space are also shown. Mix 1 is the most downstream river sediment sample collected from the Pelorus River (sample 196/2, May 2018).

2.6 Multivariate ordination – source and tracer selection

The isotopic bi-plot analysis indicated that a sub-set of the available FA tracers (i.e., C20:0, C22:0, C24:0, C26:0) best satisfied the fundamental isotopic polygon condition (i.e., sediment mixtures constrained within source polygons). In addition, the bi-plot analysis indicated that four land-use sources (i.e., sheep, dairy, gorse and broom, bracken) were poorly discriminated from each other and incorporating as individual sources would substantially degrade the mixing-model performance. Consequently, these four sources were merged into a single source (i.e., Scrub and Pasture).

Independent verification of the sources and tracer selection was undertaken using Canonical Axis of Principal Components (CAP) analysis. This multivariate statistical procedure identified the most appropriate combinations of sediment sources and tracers to model the contributions of sources to sediment deposition in the Pelorus River and Mahau Sound.

Multivariate ordination methods (including Principal Components Analysis, PCA) can be used to reduce dimensionality and to visualize patterns in multivariate data. Ordination² procedures can be classified as either constrained or unconstrained in relation to a-priori hypotheses. An unconstrained ordination procedure does not use a priori hypotheses in any way but reduces dimensions on the basis of some general criterion, such as minimizing residual variance (e.g., PCA). Unconstrained methods include PCA and are useful for visualising broad patterns in data sets (Anderson and Willis 2003). PCA is used to find axes that maximise the total variance (or equivalently, that minimises the total residual variation).

Constrained ordinations, on the other hand, use an a-priori hypothesis in some manner to produce the plot, for example concerning differences among groups. **Canonical Analysis of Principal coordinates** (CAP), is a flexible and particularly useful constrained ordination procedure developed for ecology (Anderson and Willis, 2003). It has the advantage of allowing any distance or dissimilarity measure to be used, and also considers the correlation structure among variables in the response data cloud. Thus, like the traditional canonical methods, it can uncover important patterns in the multivariate data by reference to relevant hypotheses (e.g., **null hypothesis**: source soils cannot be separated based on the tracers used). Both PCA and CAP analyses were undertaken using the PRIMER ver. 7 software package (**Plymouth Routines in Multivariate Ecological Research**) (Clarke and Gorley, 2015).

The CAP input data were processed as follows: isotope values were first transformed by multiplying by -1 (CAP cannot be performed on negative values). The data were then examined using Draftsman's plots, which indicated skewed distributions. A "log (x+1)" transform was applied to the data to minimise skewness, following recommended best practice in PRIMER. Data were then normalised, and a Euclidean distance matrix created to perform CAP analyses. Samples with missing data were excluded from the analysis. Initially, all remaining fatty acid tracers and sources were analysed to determine the variation explained. Subsequently, in an iterative approach, were tracers discarded and sources merged, with the objective being to increase the allocation success of the CAP analyses.

CAP analysis was initially conducted using all 10 sources and 9 fatty-acid tracers under the *a-priori hypothesis that the sources are distinct and dissimilar*. This initial analysis produced a total **allocation success of 55.6%** (i.e., mis-classification error: 44.4%). In the next iteration, CAP analysis was performed using the reduced set of five fatty-acid tracers identified from isotopic polygon analysis

² An ordination is a map of the samples, usually in two or three dimensions, in which placement of the samples, is achieved by ordering samples so that similar objects are near each other and dissimilar objects are farther apart (Clarke, K.R., Gorley, R., Somerfield, P.J., Warwick, R. (2014) Change in marine communities: an approach to statistical analysis and interpretation.).

(i.e., (C14:0, C20:0, C22:0, C24:0, C26)). This reduced the allocation success to **48.8%**. Subsequently re-running the CAP analysis with the reduced fatty-acid tracer set and the merged source (Scrub&Pasture), produced a **CAP with 75.6% allocation success**. This result indicated that the inclusion of the merged source (Scrub&Pasture = MERGE[Dairy, Sheep, Gorse & Broom, Bracken]) with the reduced fatty-acid tracer set provided the best selection of sources and tracers for the mixing model.

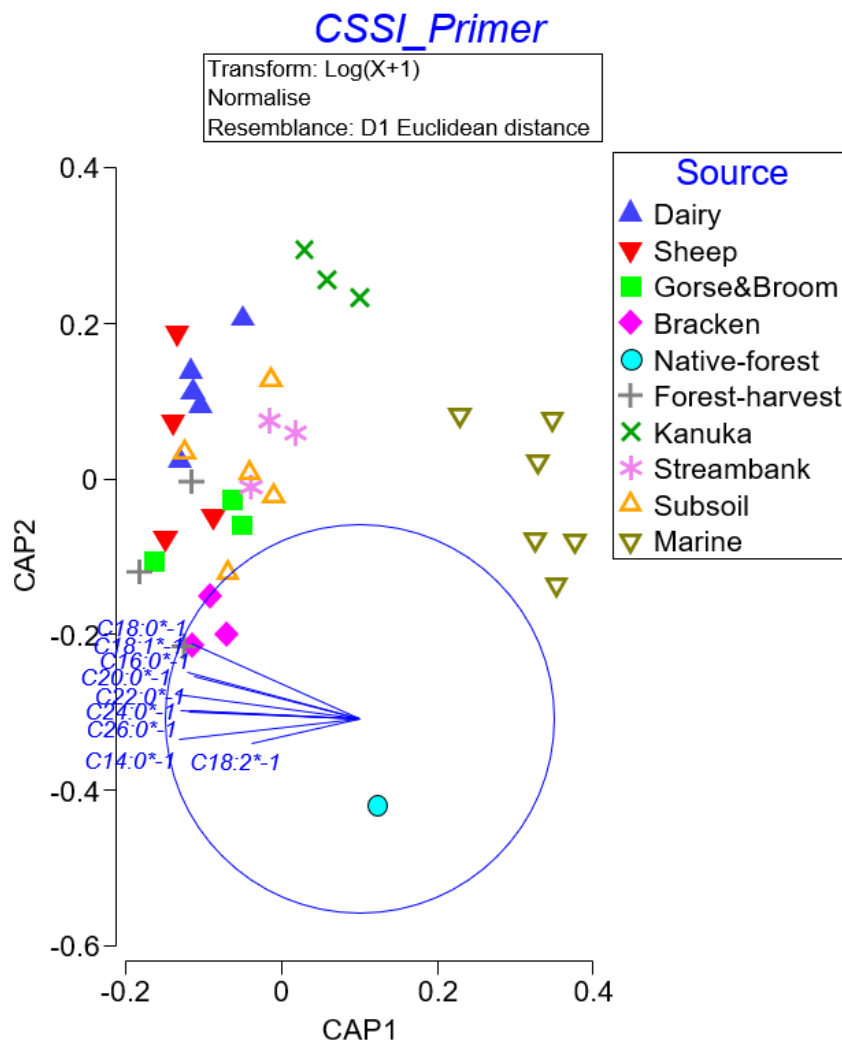


Figure 2-13: Canonical Analysis of Principal Coordinates (CAP) plot – ten sources and nine tracers. The length of the vectors (blue lines) is proportional to the strength of the influence of each tracer on the CAP components. This CAP analysis for 10 sources and 8 tracers has a 56% allocation success.

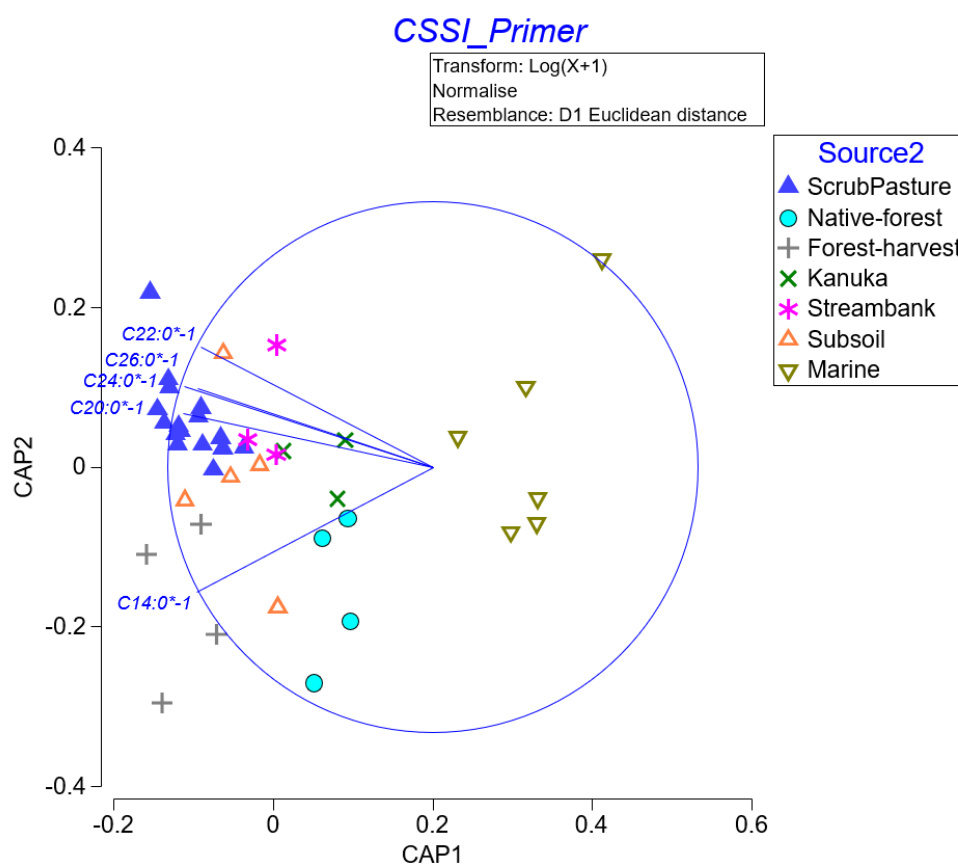


Figure 2-14: Canonical Analysis of Principal Coordinates (CAP) plot – seven sources and five tracers. The length of the vectors (blue lines) is proportional to the strength of the influence of each tracer on the CAP components. This CAP analysis for ten sources and 8 tracers has a 76% allocation success.

The results of the CAP analyses are consistent with the isotopic polygon analysis and supports the selection of sources and tracers. The tracer subset (C14:0, C20:0, C22:0, C24:0, C26) and merging of pasture and scrub plant community sources (source: Scrub+Pasture) substantially improved the allocation success. It should be borne in mind that PCA/CAP analysis does not address a key selection criterion, being that tracers and sources must conform to the isotopic-biplot polygon principle. Specifically, the $\delta^{13}\text{C}$ values of the mixture samples (i.e., sediment deposits) must be enclosed within a polygon (i.e., two tracer biplots) defined by the $\delta^{13}\text{C}$ values of potential sources (Phillips et al. 2014). Failure to comply with this condition is a serious violation of mixing model assumptions (Stock et al. 2018). This is the fundamental basis of isotopic mixing models. The FA tracers employed in the modelling (C14:0 in combination with C20:0, C22:0, C24:0, C26) best satisfy this requirement for mixtures to be enclosed within source polygons.

2.7 Sediment source modelling

2.7.1 River confluences – upstream contributions

The isotopic signatures of the bulk carbon and the FAs extracted from the soil samples were collated with the %C values for each sediment sample, as required for subsequent modelling of source contributions. Samples of river-bed sediment deposits were separated into their confluence triplicates (Section 2.2.3) and the proportional contribution (%) of the tributary at each confluence was determined using a two-endmember linear mixing model. Additional details of the two-endmember mixing model are presented in **Appendix G**.

The catchment area and sediment yield data provided by the NZ River Maps database (NZRM, Whitehead and Booker, 2019) were used with the CSSI results to estimate specific sediment yields (SSY) for each subcatchment. Gibbs et al. (2020) also used NZRM annual sediment yields to inform CSSI modelling of catchment contributions to sedimentation in South Island marine canyons. Sediment yield data incorporated in NZRM is derived from measurements of suspended sediment yields from 233 New Zealand catchments. This includes data from a hydrometric station located in the Pelorus Catchment (Site: Bryants, site # 58902, Hicks et al. 2011).

In order to identify sources of sediment that are over-represented as a proportion of land use area in the Pelorus and Kaituna catchments, the tributary proportional contributions from the CSSI two-endmember modelling were converted from source % proportional values to SSY. This was achieved (using the Kaiuma subcatchment as an example, Table 3-3) by:

- Multiplying the CSSI decimal percentage value with the sediment yield from the whole catchment [decimal percentage value = 0.093, sediment yield from the whole catchment = 237,930 tonnes (NZ River Maps), then $0.093 \times 237,930 = 22,127 \text{ t yr}^{-1}$, which is the sediment yield from the subcatchment).
- Dividing the subcatchment sediment yield ($22,127 \text{ t yr}^{-1}$) by the subcatchment area (NZ River Map database). This gives the SSY value based on the CSSI data (i.e., NZRM subcatchment area = 12.1 km^2) as $22,127 \div 12.1 = 1,829 \text{ t km}^{-2} \text{ yr}^{-1}$. The NZRM SSY value is $105 \text{ t km}^{-2} \text{ yr}^{-1}$.]
- Comparing SSY values between subcatchments. If the ratio of CSSI SSY to NZRM SSY values across subcatchments are close to 1, then no sub-catchment source is over-represented, and erosion is proportional to land area. Where the CSSI SSY/NZRM SSY ratio is substantially greater than 1, then those subcatchments have disproportionately high sediment yields relative to land area. For example, for the Kaiuma subcatchment the, CSSI SSY/NZRM SSY ratio is $1829/105 = 17.4$, which is a ~ 17 times higher sediment yield than the long-term average sediment yield predicted by NZ River Maps). These subcatchments are regarded as erosion hotspots (Gibbs et al. 2014a).

Further description of this method to identify sub-catchments with excessive sediment yields is provided in **Section 3.1.1** to aid interpretation of Table 3-3. below.

2.7.2 Land use sources - modelling

The MixSIAR model (Stock et al. 2018) was used in the present study. MixSIAR incorporates and accounts for uncertainty in the isotopic values of each sediment source as well as their geometry. The geometry is defined by the locations and distances of sources relative to each other and the sediment mixtures in isotopic space. These uncertainties and geometry are reflected in the resulting statistical results of source contributions to a sediment mixture generated by the mixing model. MixSIAR is a Bayesian isotopic mixing model, which incorporates advances in mixing model theory and builds on the earlier MixSIR and SIAR models (Stock and Semmens, 2016, Stock et al. 2018). Additional details of the MixSIAR model as implemented in this study are presented in **Appendix G**.

With the exception of the two-endmember mixing model, mixing models, regardless of tracers used or the mixing system, are based on the same fundamental mixing equation:

$$Y_j = \sum_k p_k \mu_{jk}^S \quad (1)$$

where the tracer value (Y_j) for each of j tracers is equal to the sum of the k sources tracer means (μ_{jk}^s), multiplied by their proportional contribution to the mixture (p_k). This basic equation assumes: (1) all sources contributing to a mixture are known and quantified, (2) tracers are conservative, (3) source, mixture and tracer values are fixed and known, (4) $p_k = \text{unity}$, and (5) source tracer values differ (Stock et al. 2018). An analytical solution to this basic equation requires that the system is not under-determined (i.e., number of tracers $\leq n+1$ sources). Another advantage of MixSIAR is that it employs probability-distribution based solutions for under under-determined systems. These probabilistic models integrate the variability in source and mixture tracer data.

2.7.3 Contributions of disturbed land use sources to estuary sedimentation

The relative sediment contributions of disturbed catchment land use sources were compared with the native/indigenous forest sediment contributions for the same time periods (2001 – 2012). This was undertaken using the average sediment source proportions (% , model run 3) calculated from analysis of the Mahau cores and normalising these % source proportions using land use area (km^2). Landuse area data were extracted from the Land Cover Data Base (Manaaki Whenua Landcare [LCDB], <https://www.landcareresearch.co.nz/publications/innovation-stories/2014-stories/lcdb>) versions 2 through 4. The disturbed land use sources included manuka and/or kanuka (class 52) and forest – harvested (class 64). Soil proportion (%) results for dated sediment core samples that coincided in time with LCDB-2 (2001/2002), LCDB-3 (2008/2009) and LCDB-4 (2012/13) were included. Data from LCDB-1 (1996/97) does not identify harvested pine as a separate land use class. Likewise, data from LCDB-5 (2018/19) was not included because the Mahau cores were collected in 2017, prior to that LCDB update. The source proportion yields ($\% \text{ km}^{-2}$) for the disturbed catchment land uses were then normalised by the matching values (i.e., year and core) for the native forest ($\% \text{ km}^{-2}$) to enable direct comparisons of the source yields relative to native forest.

Two separate analyses were undertaken using: (1) LCDB land use area data for the Pelorus-Rai, Kaituna and Cullens Creek catchments that discharge to the upper reaches of Pelorus Sound, and (2) land use area data for the entire catchment of the Sound to its seaward boundary at Te Akaroa (west point) – Kaitira (east point). The second option is considered most appropriate given the “global” dispersal of fine suspended sediment in river plumes throughout Pelorus Sound by tidal currents and estuarine circulation, as demonstrated by remote sensing (e.g., Figure 1-12) and the transport of large quantities of marine sediment from its seaward mouth to the Sound’s upper reaches, as indicated by the sediment tracing results. Table 2-2 summarises the LCDB land cover area information for the combined Pelorus-Rai and Kaituna catchments and for the entire catchment area of Pelorus Sound. These data show that a large fraction of the gorse and broom and harvested pine land use classes occur in the Pelorus-Rai, Kaituna and Cullens Creek catchments.

Table 2-2: Land use area (km^2) for modelled sediment sources – Land Cover Data Base (LCDB) versions 2 to 4. Land use areas for the combined Pelorus-Rai and Kaituna catchments (Catch-1) and for the entire land catchment of Pelorus Sound (Catch-2).

LCDB Survey	Year	Native forest (km^2)		Manuka/Kanuka (km^2)		Harvested Pine (km^2)	
		Catch-1	Catch-2	Catch-1	Catch-2	Catch-1	Catch-2
4	2012/13	694.9	935.8	21.6	125.9	21.2	25.9
3	2008/09	696.2	935.9	22.2	127.2	11.8	17.7
2	2001/02	696.2	935.9	24.3	130.1	5.7	11.4

2.8 Sediment composition

Sediment cores were processed in the laboratory at NIWA's Hamilton campus. This work included preparing cores for x-ray imaging and subsampling the cores for dating, as described below. Stable isotope analysis for sediment source tracing and determination of basic sediment properties was only undertaken for cores collected from Mahau Sound. Information on the composition and stratigraphy of the sediment cores was provided by x-ray imaging (**Appendix E**). An x-ray image or x-radiograph provided information on the fine-scale sedimentary fabric of sediment deposits. Density differences (due to particle size and composition, porosity) between layers of silt and sand or animal burrows that are infilled with mud make these often-subtle features easily recognisable in the x-ray image even though they may not be visible to the naked eye. Particle size distributions (PSD, 0.1–300, 10–2000 μm) of sediment-core samples were determined using an Eye-Tech stream-scanning laser system, employing the time-of-transition (TOT) method to measure the diameters of individual particles (e.g., Jantschick et al. 1992). Dry-bulk sediment density (ρ_b) profiles were determined for each core.

2.9 Sediment accumulation rates

Sediment accumulation rates were estimated from radioisotope dating of the sediment cores. Radioisotopes are strongly attracted to the surfaces of clays and silt particles and this makes them particularly useful as “mud meters” (Sommerfield et al. 1999).

In the present study, sediment accumulation rates (SAR) over the last several decades to century were quantified based on caesium-137 (^{137}Cs) and lead-210 (^{210}Pb) dating (Wise, 1977, Robbins and Edgington, 1975, Olsen et al. 1981, Richie and McHenry, 1989). Radiocarbon (^{14}C) dating was used to calculate long-term SAR over the last ~2,000 years, up to but not including the time period since the early 1900s (i.e., ^{210}Pb dating). The short-lived radioisotope beryllium-7 (^7Be) provided information on the depth of the surface mixed layer (SML) (Sommerfield et al. 1999). The SML is the surface layer in which seabed sediment is mixed by the activities of benthic animals and current- and/or wave-driven sediment reworking. These radioisotope dating techniques are described in detail in **Appendix H**.

Sediment dating using two or more independent methods offsets the limitations of any one approach. This is important when interpreting sediment profiles from estuaries because of the potential confounding effects of sediment mixing by physical and biological processes (Smith, 2001). Sediment mixing by physical and biological processes in the surface mixed layer (SML) results in uniform radioisotope activities. Because of differences in ^7Be and ^{210}Pb decay rates, these radioisotopes provide quantitative information about the depth and rate of sediment mixing. This is important when considering the fate of fine sediment in estuaries or coastal waters.

The activity of excess ^{210}Pb , ^{137}Cs and ^7Be in each core was determined by gamma spectrometry of 40–60 g dry samples (1-cm slices) of sediment taken at increasing depths from each core. The radioisotope activity of a sediment sample is expressed as Becquerel (number of disintegrations per second) per kilogram (Bq kg^{-1}). The radioactivity of samples was counted at the ESR National Radiation Laboratory for 23 hours using a Canberra Model BE5030 hyper-pure germanium detector. Initial core samples were analysed for ^7Be within ~30 days to minimise loss of this shorter-lived radioisotope. The activities of all radioisotopes are corrected to the date of sampling. The excess ^{210}Pb activity ($^{210}\text{Pb}_{\text{ex}}$) used for sediment dating was determined from the ^{226}Ra ($t_{1/2}$ 1622 yr) activity. The uncertainty ($U_{2\sigma}$) of the $^{210}\text{Pb}_{\text{ex}}$ activities was calculated as:

$$U_{2\sigma} = \sqrt{({}^{210}\text{Pb}_{2\sigma})^2 + ({}^{226}\text{Ra}_{2\sigma})^2} \quad (2)$$

where ${}^{210}\text{Pb}_{2\sigma}$ and ${}^{226}\text{Ra}_{2\sigma}$ are the two standard deviation uncertainties in the total ${}^{210}\text{Pb}$ and ${}^{226}\text{Ra}$ concentrations at the 95% confidence level. The main source of uncertainty in the measurement of radioisotope activities relates to the counting statistics (i.e., variability in the rate of radioactive decay). This source of uncertainty is reduced by increasing the sample size and the counting time. The excess ${}^{210}\text{Pb}$ profiles in each core were used to determine time-averaged SAR from regression analysis of natural-log transformed data. The maximum depth of ${}^{137}\text{Cs}$ in the cores was used to estimate time-averaged SAR since the early 1950s. This included a correction for downward mixing of ${}^{137}\text{Cs}$, based on the maximum depth of ${}^7\text{Be}$. In New Zealand, ${}^{137}\text{Cs}$ deposition from the atmosphere was first detected in 1953 (Matthews, 1989). It should be noted that the maximum depth of detectable ${}^{137}\text{Cs}$ in sediment cores may coincide more closely with the early-1960s when peak atmospheric deposition of ${}^{137}\text{Cs}$ occurred in NZ (i.e., 1963/64). This is because of the low initial ${}^{137}\text{Cs}$ activity in the mid-1950s, radioactive decay since that time (i.e., 2 half-lives = 60 years) and instrumental minimum detection limits.

2.9.1 AMS ${}^{14}\text{C}$ dating

Estimates of pre-historic SAR in the Mahau Sound were derived from atomic mass spectrometry (AMS) radiocarbon (${}^{14}\text{C}$) dating of articulated shell valves of the common suspension-feeding bivalve *Austrovenus stutchburyi* (cockle). Shell valves from three individuals in a shell layer (82–91 cm) preserved in core MH-3D were selected for dating (**Appendix H**, Table H-1). The calculated ${}^{14}\text{C}$ SAR are compared with ${}^{14}\text{C}$ SAR determined for dated cores collected in the nearby Kenepuru Inlet (Handley et al. 2017). The fact that the shell valves of the individual animals remained articulated with surface ornamentation intact suggests that the animals died in situ and/or were not transported far beyond their place of origin. The New Zealand cockle is particularly suitable for radiocarbon dating as they have ${}^{14}\text{C}$ concentrations in their carbonate that are similar to those found in marine shellfish (Hogg et al. 1998). This means that marine reservoir effects (i.e., “old” carbon in ocean waters mixing with coastal waters) can be accounted for using the marine ${}^{14}\text{C}$ calibration curve (Petchy et al. 2008).

2.10 Mollusc death assemblage (DA) analysis

To investigate long term changes in the fauna living within the sediments in Mahau Sound, we analysed the preserved remains of shellfish (death assemblage) that were extracted from sediment cores. Decadal to century-scale changes in the quantity and species composition can be used to interpret effects of human colonisation and land use changes on the marine environment.

To analyse the mollusc death assemblage preserved in the Mahau cores, the age of sediment deposited within the sediment column was first obtained via fallout radioisotopes (${}^{210}\text{Pb}$, ${}^{137}\text{Cs}$) and carbon radioisotopes (Section 2.8). Our intent was to partition the cores into historic time periods of interest to compare with the previous results from Kenepuru Sound and Beatrix Bay (Handley et al. 2017). As with the previous study, to maximise the quantity of shell available for analysis, it was decided to process whole sections of the cores. Each core section was analysed by volume between predicted sediment depth/age ranges (Table 2-3).

To extract shells, gravels, and wood material present, each core section was gently washed through a 1 mm sieve. The shells, wood and gravel were weighed after they had been air dried to constant weight at 60°C. We identified all shells to lowest practical taxonomic level and weighed all shell fragments. Shell fragments were included in our analyses under the assumption that bottom-contact

fishing methods (e.g., dredging, trawling) and feeding from large fish would damage molluscs, creating fragments of whole live and dead mollusc shells.

Table 2-3: Time periods used to section and process sediment cores as per Handley et al. (2017).

Time period (AD)	Description
1975–2015	Recent period, post-green-lipped mussel fishery.
1950–1974	Commercial fishing, chemical agriculture period.
1860–1949	European colonisation, mining, forest milling, farming period.
1300–1859	Māori period.
500–1299	Pre-human period.

Percent weight of shell and gravel were calculated from the volume of the core analysed per time period, after conversion to equivalent volume. Rock gravel, charcoal and wood were converted to volume based on specific densities of 2.7, 0.21 and 0.76 tonne/m³, respectively³. Mollusc shells were converted to volume based on regression of oyster shell weights to volume calculated from unpublished data collected during a study of Pacific oyster *Crassostrea gigas* condition indices (Handley, 1998). This conversion was used under the assumptions that carbonate volume of oyster shells does not differ significantly to those of other mollusc species and that volume of shells accurately represents biomass of each species. Estimates of biomass have been shown to accurately estimate species dominance when compared with numerical estimates (Staff et al. 1985), and size based methods used to estimate species biomass have also been recently validated (Eklöf et al. 2017). The shell, gravel and wood estimates were standardised to percent material accumulating per year. This was achieved by back calculating the number of years each core section represented and dividing the percent volume of material deposited in each core section by the estimated years that deposited them.

2.10.1 Statistical analyses

Exploratory analyses and relationships among death assemblage (DA) and sediment characteristics were assessed using non-metric multidimensional scaling (nMDS, Kruskal and Wish, 1978). Non-metric multi-dimensional scaling is an extremely robust method of ordination that can be done on the basis of any measure of dissimilarity (including the Bray-Curtis measure, used here). The algorithm essentially attempts to plot the points (e.g., species composition from each time period) on the basis of the relative dissimilarities between them in an arbitrary number of Euclidean dimensions. For example, one chooses *a priori*, to see an ordination or “map” of the samples in, say, two dimensions in Euclidean space. The algorithm starts by placing the points in a random orientation. It then iteratively moves or “jitters” the points around relative to one another so as to minimize the discrepancy between the inter-point Euclidean distances on the 2-d plot and their original Bray-Curtis dissimilarities. A measure of this discrepancy is called “stress” and the algorithm

³ <https://www.eoas.ubc.ca/ubcgif/iag/foundations/properties/density.htm>

<https://www.aqua-calc.com/page/density-table/substance/charcoal>

The density of wood was calculated from the average density of kanuka, red beech, rimu, and southern rata from:

<https://www.tanestrees.org.nz/species-profiles/>, <http://nzforests.co.nz/native-timber/rata/>, <http://www.nzwood.co.nz/forestry-2/red-beech/>

works to find a solution that minimises stress. Several random starts are usually needed in order to obtain a global (as opposed to a local) minimum in the value of stress.

The axes produced in non-metric MDS are arbitrary and bear no known relationship to the original variables. This is why these plots do not have any labels on their axes. It also means that the axes can be rotated, inverted, expanded or contracted, without altering their meaning. Each MDS plot in the text reports a measure of stress, because stress indicates how accurately the MDS plot reflects the original relative Bray Curtis (or other) dissimilarities among the points. As a general rule of thumb, stress values less than 0.2 provide a good representation of the original dissimilarities among the points. The interpretability of MDS plots with stress values of 0.2 or greater should be considered cautiously.

When viewing an MDS plot, the relative distances between points indicate their relative similarity with respect to the composition and abundance of assemblages. In general, the points on the plot are labelled according to their membership in groups. For example, individual core samples are labelled by their estimated age. Of interest is to see whether the samples belonging to the same core age period are clustered together on the plot and are cleanly separated from other samples belonging to other ages. This would suggest that core samples differ in their communities of organisms. On the other hand, if samples from different core ages are well-mixed in the diagram, this would suggest no clear differences in assemblages from different core ages.

Relationships between the death assemblage composition and predictor variables (i.e., volume estimates of gravel, sediment grain size classes, wood and charcoal content, and sediment accumulation rates) were examined. This was undertaken using forward selection of the multivariate multiple regression using the DistLM routine (distance based linear model, Legendre and Anderson, 1999, McArdle and Anderson, 2001) and distance-based redundancy analysis (dbRDA, Legendre and Anderson, 1999). DistLM is a routine for analysing and modelling the relationship between a multivariate data cloud, as described by a resemblance matrix, and one or more predictor variables. The routine allows for predictor variables to be fit individually or together in specific sets. DistLM can provide quantitative measures and tests of the variation explained by one or more predictor variables. The fitted model can then be visualised in multidimensional space using the dbRDA routine.

To visualise the abundance, or in this case the volume estimate of shells deposited for a particular species or assemblage of species within a time period, each corresponding ordination point or circle (“bubble”) is represented by a size proportional to that abundance (volume), based on its original scaling. Relationships between species composition, environmental variables, and functional feeding modes were visualised using vector biplots of Spearman’s correlations. The length of the biplot vectors represent the correlation score where $p > 0.4$ and the direction of each vector indicates the direction within the plot that variable increases. Multivariate analyses were completed using the procedures in PERMANOVA+ for PRIMER (Anderson et al. 2008).

2.10.2 Death assemblage functional feeding analysis

To explore changes to the mollusc community over time, we analysed functional feeding traits. To achieve this, an index was derived by multiplying the percent volume represented by each mollusc species by a score assigned to each of five functional feeding traits: suspension feeders, deposit feeders, scavengers, grazers, and predators (e.g., Handley et al. 2014). A diagram outlining the feeding traits using examples of species sampled in DA cores is in Figure 2-15. Sediment characteristics including carbonate content were also averaged and plotted to investigate temporal trends.

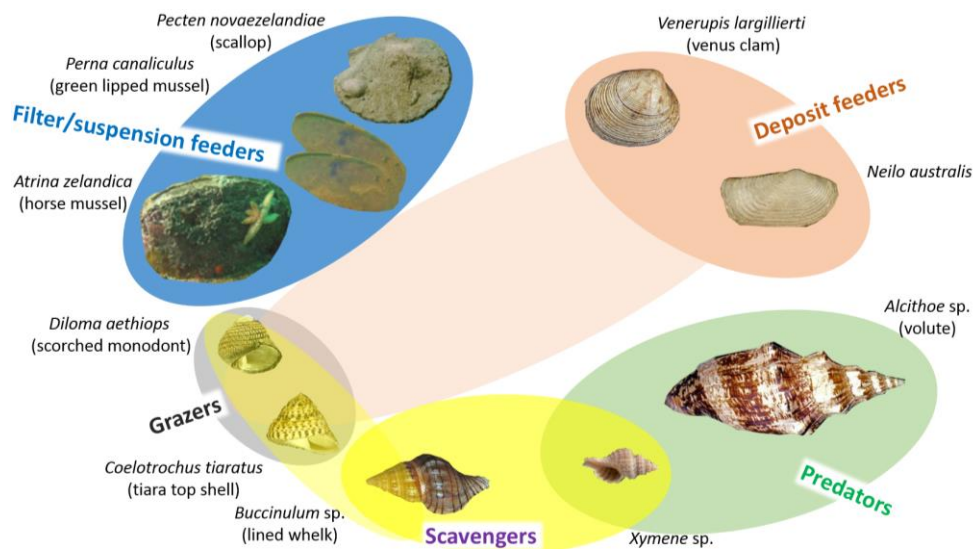


Figure 2-15: Functional feeding traits of species sampled in the mollusc death assemblage. Filter or suspension feeders take food from the water column (e.g., phytoplankton), deposit feeders ingest food from the surface of sediment around them, predators consume other animals, scavengers consume carrion (dead animals), and grazers eat plants and organisms that can be scraped off hard surfaces. Note: some species use multiple feeding modes, depending on food availability indicated by overlapping polygons.

3 Results

3.1 Sources of sediment deposited in river system

3.1.1 Tributary contributions

The two-endmember mixing model results for the individual bulk C and FA isotopic values sediment tracers in each downstream sediment mixture at each river confluence were averaged (**Appendix I**). This provided the most robust estimate of the proportional % sediment contribution from each tributary. For example, there were five possible combinations of source and mixture samples for the Tinline River confluence with the Pelorus River. These combinations produced thirteen valid estimates of the proportional contribution of sediment from the Tinline River into the Pelorus River as measured downstream of the confluence. This analysis indicated that about 30% of the sediment came from the Tinline River and 70% (to nearest whole %) was sourced from the Pelorus River upstream of the confluence. The uncertainty at one standard deviation was $\pm 6.8\%$. The results of all confluence assessments are presented in Table 3-1.

Table 3-1: Summary of the mean proportional contributions of sediment from the tributaries into the main stem of the river downstream of the confluence. Proportions estimated by two end-member mixing model assessment using all available source and mixture sample combinations for each confluence. The SD is the standard deviation of all two-endmember model results for the catchment modelled. Where replicate sampling allowed several iterations of the two-endmember model, SD is the average standard deviation of all results. Refer to table 1 in Appendix I.

Main stem	%	Tributary	%	SD	n
Pelorus	70.3	Tinline	29.7	6.8	13
Pelorus	37.5	Rai	62.5	12.7	17
Pelorus	85.6	Wakamarina	14.4	6.8	5
Rai	61.1	Brown	38.9	11.5	5
Opouri	76.0	Ronga	24.0	14.0	3
Opouri	86.5	Tunakino	13.5	2.0	4
Opouri	56.6	Kaiuma	43.4	16.3	8
Kaituna	69.3	Atahaua	30.7	10.4	9

The results in Table 3-1 were used to calculate the proportion of total sediment (%) from each subcatchment contributing to the Pelorus River at the downstream site, Site 2. Assuming that all sediment is transported past this site, the “Tributary % total yield” values were scaled to total 100%.

Table 3-2: Calculation of the proportional sediment contribution from each tributary to the Pelorus River at the mouth. Tributary contribution values are from Table 3-1. The Rai River tributary contributions have been calculated using the Rai River main stem data. (“Residual %” is the proportion remaining in the main stem upstream of each confluence after removing the “Tributary %”. The “Tributary %” is the contribution (i.e., scaled proportion) of each subcatchment summing to 100% at the Pelorus River mouth)

River	Residual % in main stem	Tributary % contribution	Tributary % of total yield
Pelorus R main stem	100.0		
Wakamarina	100.0	14.4	14.4
Rai	85.6	62.5	53.5
Tinline	32.1	29.7	9.5
Upper Pelorus	22.6		22.6
Rai mainstem	53.5		
Brown	53.5	38.9	20.8
Ronga	32.7	24.0	7.8
Tunakino	24.8	13.5	3.4
Kaiuma	21.5	43.4	9.3
Opouri	12.2	-	12.2

The “Tributary % of total yield” values from the CSSI analysis (Table 3-2) were converted to sediment yield values (SY, t yr⁻¹ Table 3-3) by multiplying the decimal % value for each subcatchment by the total sediment yield for the entire Pelorus River catchment using the annual average SY (NZRM database). The sediment yields were then converted to specific sediment yields (SSY, t km⁻² yr⁻¹) based on the subcatchment area. The ratio of the CSSI SSY to the NZRM SSY values provides an indication of which subcatchments are producing excessive amounts of sediment based on the analysis of the sampled sediment deposits. A summary of the method with an example to aid interpretation of Table 3-3 is provided below.

Explanation:

To identify where excessive soil erosion is occurring in a catchment, a reference value is used that quantifies the expected average rate of erosion in each sub-catchment. In this study, we have used mean annual specific sediment yields (SSY) provided by NZ River Maps (NZRM, Booker and Whitehead, 2017). NZRM incorporates SSY estimates from Hicks et al. (2011) erosion terrain model that is underpinned by sediment yield data from 233 New Zealand catchments. These data include measurements from the Bryants hydrometric station (site 58902) located in the Pelorus Catchment (Hicks et al. 2011). This mean annual SSY estimate is based on a multi-variable statistical analysis, that incorporates drivers (rainfall and runoff) and supply factors, related to geology, soils, erosion processes and slope. Land cover and climate variability are not explicitly included in the erosion terrain model. The CSSI sediment-tracing technique provides an estimate of SSY for each sub-catchment that is independent of the multi-variate NZ River Maps model. The CSSI-based SSY also represents a **recent time period** prior to sampling whereas the NZRM SSY represents a long-term average value. These two independent SSY estimates can then be compared as ratios (i.e., SSY_{CSSI}/SSY_{NZRM}).

Interpretation:

An SSY ratio of unity (i.e., 1) means that SSY values determined by both methods are identical and indicates that there is no excessive erosion in that catchment. A ratio higher than unity indicates that excessive erosion is occurring in the catchment during the time period when the sampled river sediment was deposited. The magnitude of the SSY ratio greater than unity indicates how excessive the erosion rate is. This information can be used to identify erosion hot spots where: (1) the SSY ratio moderately exceeds an expected range and further investigations maybe required, or (2) implementing soil conservation measures where the SSY ratio substantially exceeds the expected range (see examples below).

Examples: an SSY ratio of 1.5 means soil erosion is producing 1.5 times as much sediment as expected relative to the mean annual SSY value calculated by NZ River Maps. This maybe within the SSY range “expected” for a steepland catchment. The expected range may have been set at (for example) 1-2 times the mean annual value. Consequently, catchment management can focus on the hot spots with ratios substantially greater than an expected range that recognises some level of year-to-year variability associated with climate. In this study, SSY ratios as high as ~22 are an order of magnitude higher than the mean annual value and can reasonably be considered to be excessive. Conversely, there are SSY ratios less than 1, which indicates that those subcatchments are producing less sediment than expected relative to the mean annual value.

Table 3-3: Conversion of the CSSI estimates of sediment yield proportions (% , Table 3.2) into sediment yields (SY, t yr⁻¹) and specific sediment yields (SSY, t km⁻²/yr⁻¹). Land areas and sediment yields were extracted from the NZ River Maps database (NZRM, Booker and Whitehead, 2017). The ratio of CSSI SSY to NZRM SSY values for each subcatchment indicates subcatchments that are producing excessive amounts of sediment (high values,) and those that are producing much less sediment than would be expected based on their area (ratios < 1).

Tributary	NZ River Maps			CSSI Results			
	Catchment area (km ²)	SY (t yr ⁻¹)	SSY (t km ⁻² yr ⁻¹)	Tributary % of total yield	SY (t yr ⁻¹)	SSY (t km ⁻² yr ⁻¹)	CSSI SSY/ NZRM SSY Ratio
Pelorus River							
Opouri	40.6	5439	134	12.2	29027	715	5.3
Kaiuma	12.1	1268	105	9.3	22127	1829	17.4
Tunakino	32.8	4275	130	3.4	8090	247	1.9
Ronga	32.8	4310	131	7.8	18559	566	4.3
Brown	12.9	2186	169	20.8	49489	3836	22.7
Pelorus (upper)	274	116019	423	22.6	53772	196	0.5
Tinline	54.4	6806	125	9.5	22603	416	3.3
Wakamarina	188	69657	371	14.4	34262	182	0.5
Area measured	647.7						
Total catchment	888	237930	268	100	237930		
Kaituna River							
Kaituna (upper)	58.4	6153	105	69.3	14286	245	2.3
Atahaua	29.8	6225	209	30.7	6328	212	1.0
Area Measured	88.2						
Total Catchment	147	20614	140	100	20614		

3.1.2 Land use contributions to river deposits

The series 1 source modelling incorporated all possible land use sources (Table 3-4), whereas the series-2 modelling (Table 3-5) merged sources where the individual sources had similar tracer signatures. As described in Section 2.5, some sources were merged based on examination of isotopic biplots (e.g., Figure 2-10). Table 3-4 and Table 3-5 present the % soil proportion results as averages with standard deviations for individual and merged sediment sources in the Pelorus River system, and Table 3-6 provides the same information for the Kaituna River.

Table 3-4: Series 1 modelling. Proportional mean soil contributions (\pm SD) by land use to individual rivers from their catchments. Series 1 modelling used all land uses as separate sources.

Source	Streambank	Bracken	Dairy	Gorse and Broom	Kanuka	Native	Pine Harv	Subsoil
UpperPel_R	35.7 (21.4)	4.7 (4.8)	6.5 (5.8)	4.8 (4.3)	6.5 (5.0)	2.6 (2.8)	11.6 (9.6)	27.9 (19.7)
Tinline_R	44.3 (24.3)	1.8 (2.0)	2.5 (2.8)	1.5 (1.6)	9.9 (5.8)	1.7 (2.1)	7.5 (8.5)	30.7 (20.8)
Rai_R	30.4 (18.9)	8.1 (7.1)	6.1 (5.4)	8.6 (6.0)	1.3 (1.2)	2.2 (1.9)	6.3 (5.8)	37.0 (19.4)
Wakamarina_R	41.8 (21.6)	4.1 (3.7)	4.3 (4.2)	3.3 (2.8)	2.2 (1.6)	2.0 (1.7)	6.9 (6.5)	35.4 (20.9)
Pelorus_R	36.2 (20.5)	4.8 (4.8)	6.2 (5.6)	4.8 (4.9)	6.2 (4.2)	2.1 (2.1)	11.7 (9.4)	27.9 (19.3)
Opouri_R	40.7 (23.7)	2.4 (2.7)	6.5 (5.7)	2.3 (2.2)	2.0 (2.6)	0.9 (1.1)	8.0 (8.6)	37.2 (24.0)
Kaiuma_R	36.6 (20.8)	5.3 (5.5)	6.4 (5.9)	6.2 (5.9)	3.2 (2.7)	2.3 (2.1)	10.5 (8.9)	29.4 (20.0)
Tunakino_R	42.0 (22.5)	3.2 (3.1)	3.8 (3.8)	2.5 (2.4)	4.0 (3.0)	2.4 (2.7)	8.0 (8.2)	34.1 (21.0)
Ronga_R	36.2 (22.2)	4.1 (4.2)	8.5 (7.6)	4.4 (4.4)	3.0 (3.0)	1.4 (1.5)	10.9 (9.8)	31.5 (22.1)
Brown_R	26.0 (18.6)	6.4 (7.1)	8.2 (7.8)	5.6 (5.5)	1.9 (1.8)	5.7 (4.9)	14.0 (11.4)	32.1 (20.9)

Table 3-5: Series 2 Modelling: Proportional mean soil contributions (\pm SD) by land use to individual rivers from their catchments. Series 2 modelling used the same tracers as for Table 3-4 but merged land use sources for Dairy pasture (= Dairy+GorseandBroom+Bracken) and merged Subsoil+streambank as identified in Figure 2-10a-c.

Source	Subsoil + Streambank	Dairy Pasture	Kanuka	Native	Pine Harvest
Upper Pelorus R.	52.2 (23.1)	16.8 (12.6)	6.3 (5.7)	5.7 (6.0)	19.0 (15.3)
Tinline_R	75.2 (18.7)	3.8 (4.1)	8.0 (6.8)	2.7 (3.7)	10.2 (12.0)
Rai_R	48.8 (22.0)	32.5 (17.1)	1.9 (1.9)	3.8 (3.5)	13.1 (12.4)
Wakamarina_R	66.8 (17.7)	16.0 (10.7)	2.2 (2.1)	3.6 (3.2)	11.4 (11.4)
Pelorus_R	54.4 (21.8)	19.1 (13.3)	4.5 (3.8)	3.9 (3.6)	18.1 (14.3)
Rai R. Tributary					
Opouri_R	68.4 (17.2)	15.5 (11.3)	2.4 (2.4)	1.8 (1.8)	11.9 (11.7)
Kaiuma_R	54.1 (21.9)	22.9 (15.3)	2.9 (2.8)	3.5 (3.3)	16.6 (14.0)
Tunakino_R	67.8 (19.8)	9.9 (8.1)	4.3 (4.6)	5.5 (6.0)	12.4 (11.8)
Ronga_R	52.4 (22.2)	25.1 (16.7)	2.9 (2.8)	2.6 (2.6)	16.9 (14.2)
Brown_R	41.3 (21.7)	30.8 (16.4)	3.0 (2.9)	5.6 (4.9)	19.3 (15.4)
Rai_R	48.8 (22.0)	32.5 (17.1)	1.9 (1.9)	3.8 (3.5)	13.1 (12.4)

Table 3-6: Proportional mean soil contributions (\pm SD) by land use in the lower Kaituna River. Series 2 (#2) modelling used the same tracers as for series 1 (#1) modelling but combined land uses sources for sheep pasture with bracken (= Sheep+Bracken) and combined Subsoil+streambank.

	Kaituna R	Streambank	Bracken	Dairy	GandB	Kanuka	Native	PineHarv	Sheep	Subsoil
Model #1	53.2 (16.9)	3.4 (3.4)	4.9 (3.8)	8.2 (7.3)	1.2 (1.1)	1.5 (1.6)	6.7 (6.3)	7.9 (6.2)	13.0 (11.4)	
				Dairy	GandB	Kanuka	Native	PineHarv	SheepandBr	SubsoilandBank
Model #2			7.9 (7.0)	12.2 (10.8)	1.8 (1.8)	2.7 (3.1)	5.5 (5.7)	14.2 (11.4)	55.8 (18.8)	

A summation plot (Figure 3-1) and a plot of mean soil source contributions (%) from tributaries into the Pelorus River (Figure 3-2) show that subsoil and bank erosion are the major sources of sediment deposited in the rivers during the period of sampling, contributing almost 60%. The combined Dairy pasture/Gorse and Broom/Bracken contributed ~18% and Pine harvest ~15%. Conversely, kanuka (4.0%) and native forest (3.9%) were relatively minor contributors to sediment deposited in the Pelorus-Rai River.

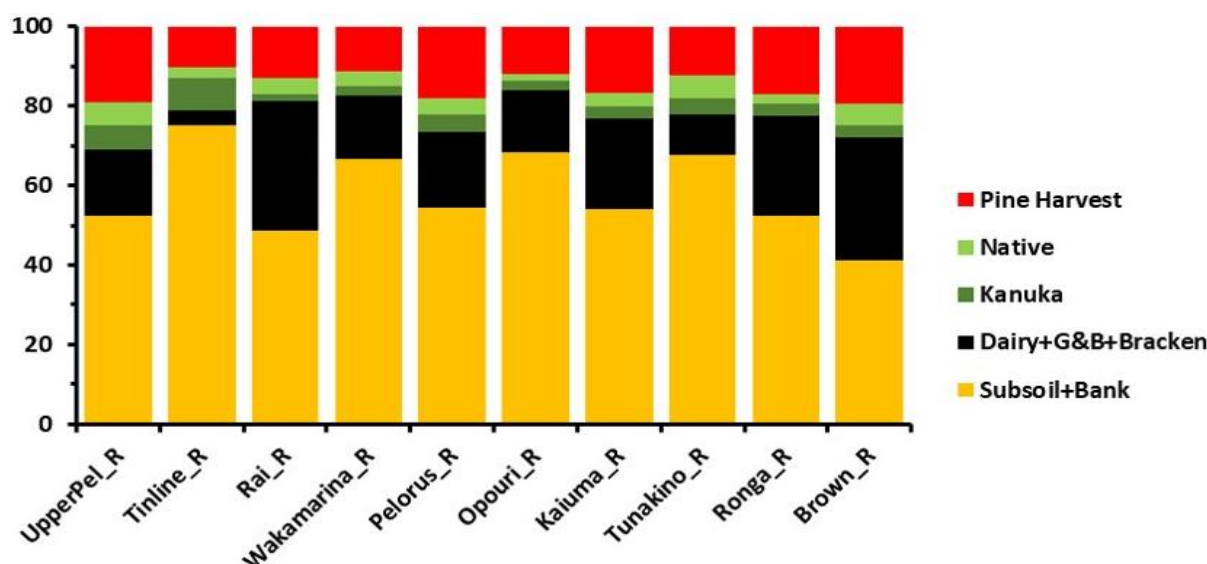


Figure 3-1: Summation plot comparing proportional soil source contributions (%) from each land use in the tributaries and the main stem of the Pelorus River.

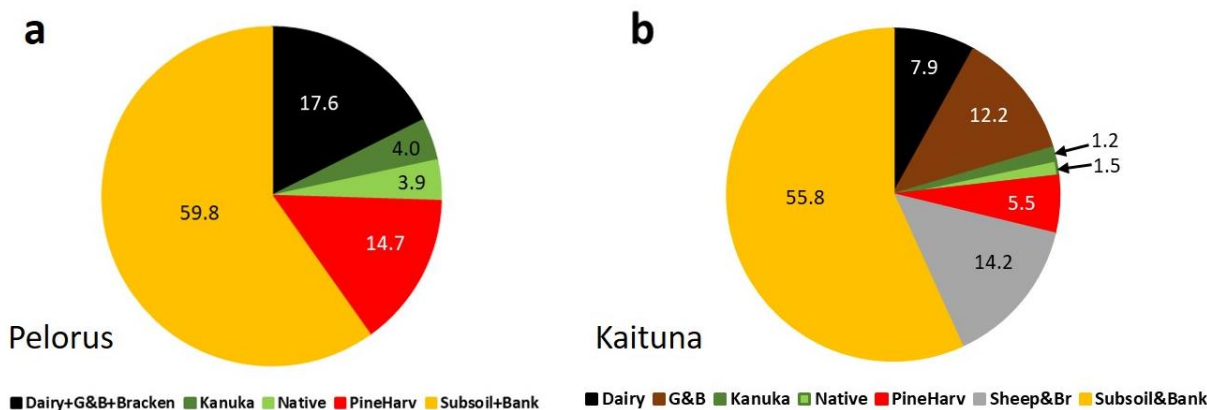


Figure 3-2: Mean land use soil contributions to a) the Pelorus River and b) the Kaituna River at the lowest site. Data using combined sources.

3.2 Havelock Estuary sediment cores

Cores from sites HV-1, HV-3 and HV-4 located on the intertidal flats in Havelock estuary's central basin were selected for radioisotope dating (Figure 2-8). The log-linear regression fits to the excess lead-210 ($^{210}\text{Pb}_{\text{ex}}$) profiles yielded apparent time-averaged SAR of 2.2 mm yr⁻¹ (HV-1, HV-4) and 3.6 mm yr⁻¹ (HV-3) (Figure 3-3). The regression fit for HV-1 is relatively poor ($r^2 = 0.72$, $n = 4$, $P = 0.1$) and only slightly improved for the other two core sites (i.e., $r^2 = 0.85$, 0.92 , $n = 4-5$, $P = 0.01$). The maximum depth of ^{137}Cs -labelled (i.e., post-1953) sediment in all three cores of 11 cm yields SAR of 1.7 mm yr⁻¹. This dating estimate assumes that the maximum depth of ^{137}Cs represents initial atmospheric deposition associated with nuclear weapons tests in the early-1950s (Matthews, 1989). The maximum depth of the ^{137}Cs detected in the sediment cores may more closely coincide with the early-1960s when peak atmospheric deposition of ^{137}Cs occurred in NZ (i.e., 1963/64). In that case, ^{137}Cs SAR would be ~2 mm yr⁻¹.

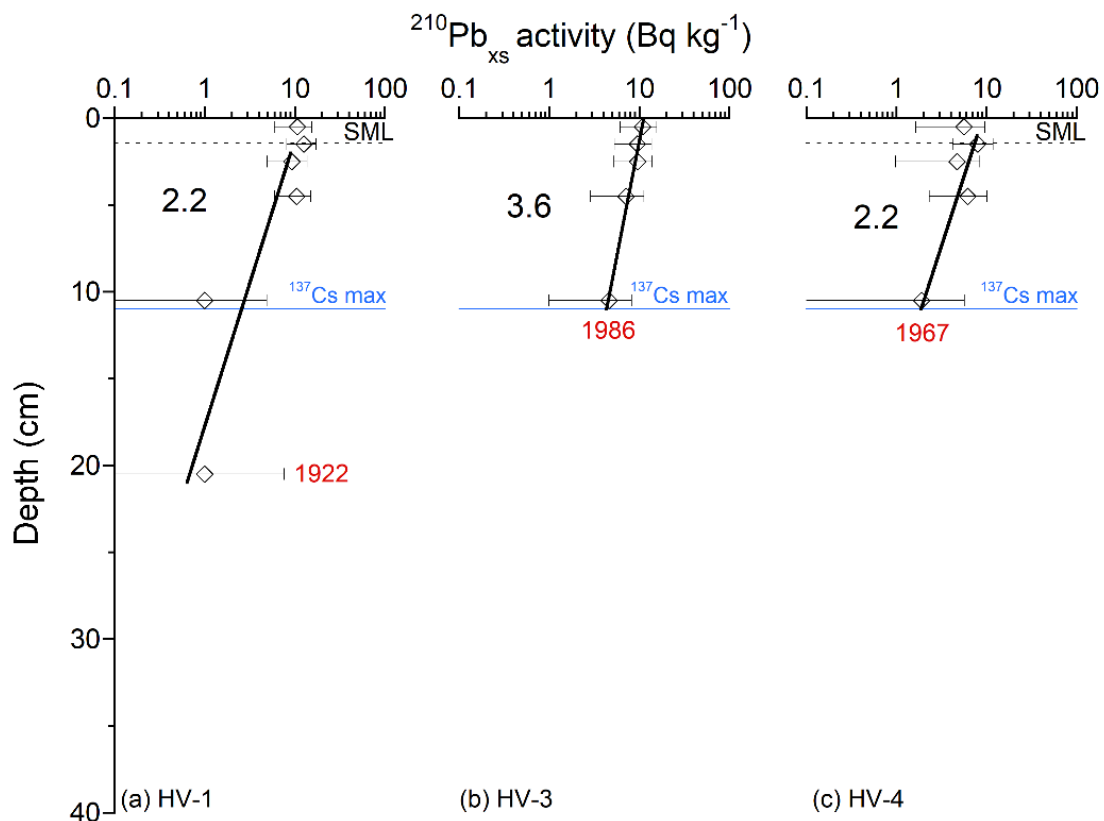


Figure 3-3: Havelock Estuary cores – ages of sediment layers and sediment accumulation rates (SAR). (a) Excess ^{210}Pb activity profiles with 95% confidence intervals shown. Time-averaged SAR (mm yr⁻¹, Black text) derived from regression fit to natural log-transformed ^{210}Pb data. Estimated ages of depth horizons (red text). Surface mixed layer (SML) inferred from excess ^{210}Pb profiles. Maximum depth of caesium-137 (^{137}Cs) indicated. Radioisotope activity expressed in units of Becquerels (Bq).

3.3 Mahau Sound sediment cores

3.3.1 Site MH-1

Core site MH-1 is located at the northern end of the Mahau Sound between 3 and 4 m below chart datum (CD). X-radiographs for core MH-1 indicate that the sediment depositing at this site is primarily composed of fine-grained muds, with traces of mm-scale burrows associated with the feeding and/or burrowing activities of animals being present (Figure 3-4). Gastropod shells, shellfish

valves, small shell fragments (white objects) and wood fragments (black objects) occur in the upper 50-cm of the sediment column. Finely laminated silts occur in lower half of the core, with fragments of organic material. What appears to be a large cm-diameter vertical burrow (100–115 cm depth) can also be observed (Figure 3-4).

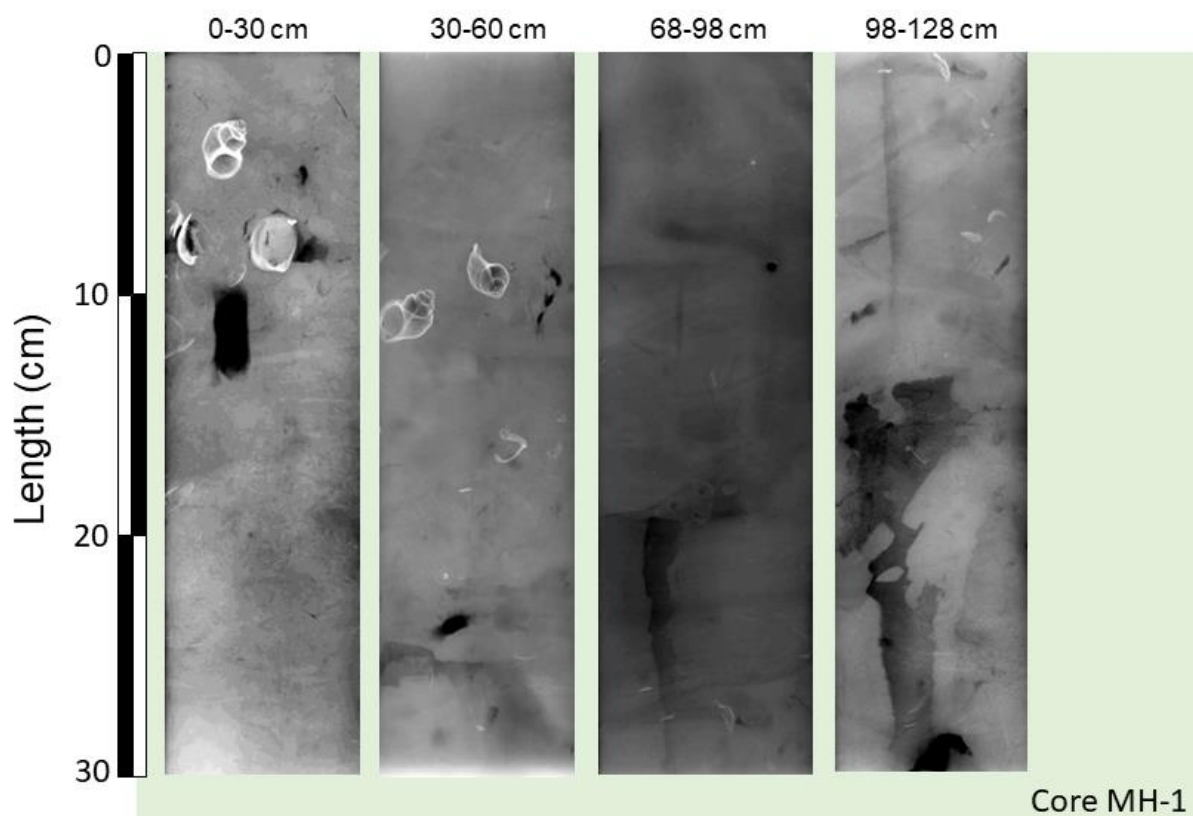


Figure 3-4: Core MH-1 (subtidal: Mahau Sound): 0-128 cm. These images have been inverted so that relatively high-density objects appear white (e.g., shell valves) and low-density materials such as muds or organic material appear as darker areas. Note (i.e., dark coloured sheet) between 115–128 cm depth.

The ^{210}Pb SAR at this site has averaged 4.1 mm yr^{-1} over the last ~ 88 years (i.e., top-most 36 cm of sediment column). The surface-mixed layer, reflecting processes occurring at different time scales, is defined by Beryllium-7 (^7Be , half-life = 53 days) and $^{210}\text{Pb}_{\text{ex}}$ (half-life = 22 years). The vertical distribution of ^7Be in the sediment indicates mixing typically over weeks–months or flood-event deposition (i.e., hours–days). Similar activities of the longer-lived $^{210}\text{Pb}_{\text{ex}}$ in near surface sediment is more usually indicative of intense mixing due to bioturbation by animals (e.g., worms) or bed erosion/redeposition by waves and/or currents. These radioisotope data suggest relatively rapid and shallow mixing (top ~ 3 cm) over time scales of days to weeks and deeper mixing over years–decades due to physical processes, such as wave-driven resuspension and the burrowing and feeding activities of infauna. The residence time of sediment in the $^{210}\text{Pb}_{\text{ex}}$ SML estimated from the SAR is ~ 15 years ($\sim 70\text{mm} / 4.1 \text{ mm yr}^{-1}$). The maximum depth of ^{137}Cs -labelled (i.e., $^{137}\text{Cs}_{\text{max}}$, post-1950s) sediment at 31 cm. Correcting this depth for rapid sediment mixing in the ^7Be SML (i.e., 31 - 3 cm) yields a ^{137}Cs SAR of between 4.4 and 5.2 mm yr^{-1} . (i.e., assuming $^{137}\text{Cs}_{\text{max}}$ year range of 1953–1963). This is in reasonable agreement with the ^{210}Pb SAR (Figure 3-5a) and provides a high level of confidence in the ^{210}Pb geochronology at this site. Dry bulk sediment densities in core MH-1 vary between 0.7 and 1.0 g cm^{-3} and do not display a trend of increasing bulk density with depth (Figure 3-5b). Particle size profiles are relatively uniform with depth, with a narrow range of mean and

median particle diameters (range: 14–24 μm) (Figure 3-5c) for sediment that are composed of clay-rich muds (i.e., 6–16% by volume, Figure 3-5d).

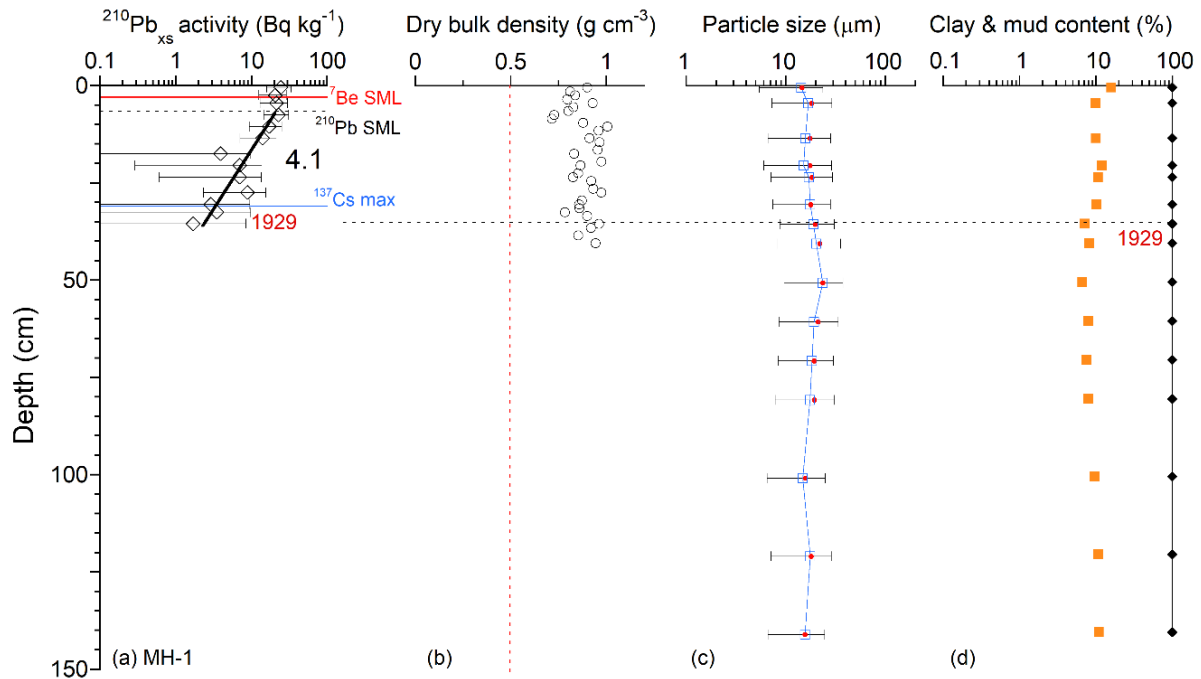


Figure 3-5: Core site MH-1 (Mahau Sound) – ages of sediment layers, sediment accumulation rates (SAR), and sediment properties. (a) Excess ^{210}Pb activity profiles with 95% confidence intervals shown. Time-averaged SAR (mm yr^{-1} , Black text) derived from regression fit to natural log-transformed excess ^{210}Pb data ($r^2 = 0.76$, $n = 10$). Estimated ages of depth horizons (red text). Surface mixed layer (SML) inferred from Beryllium-7 (^7Be , half-life = 53 days) and excess ^{210}Pb (half-life = 22 yr) profiles. Maximum depth of caesium-137 (^{137}Cs) indicated. Radioisotope activity expressed in units of Becquerels (Bq). (b) Sediment dry bulk density, (c) mean (red) and median particle diameters with standard deviation, (d) clay and mud content as percentage of sample by particle volume.

3.3.2 Site MH-2

Core site MH-2 is located in the middle reaches of the Mahau Sound between 3 and 4 m below CD. X-radiographs for core MH-2 indicate that the sediment depositing at this site are primarily composed of fine-grained muds, although with a more complex sedimentary fabric than observed at site MH-1. The x-radiograph clearly show abundant traces of mm-scale and occasional cm-scale burrows cross-cutting silts with weakly developed horizontal bedding/laminations (Figure 3-6). These burrows are associated with the feeding and/or burrowing activities of animals. As also observed at site MH-1, gastropod shells, shellfish (cockle) valves, small shell fragments (white objects) commonly occur in the upper 50-cm of the sediment column and are less abundant in lower section of the core. Wood fragments (black objects) are also present – note that the largest are voids in the sediment slab prepared for x-ray (e.g., 115–120 cm) (Figure 3-6). The $^{210}\text{Pb}_{\text{ex}}$ profile at this site extends to 41 cm, with an apparent change in SAR occurring in the late-1970s. The profile indicates that sediment gradually accumulated, at 1.7 mm yr^{-1} , from the early-1900s until the late 1970s. Subsequently, SAR increased four-fold to average 7.6 mm yr^{-1} until 2017 when the cores were collected (i.e., Figure 3-7a). The ^7Be SML extends to 3-cm depth at site MH-2. This yields an estimated residence time of sediment in the SML of ~ 4 years ($\sim 30 \text{ mm} / 7.6 \text{ mm yr}^{-1}$). No $^{210}\text{Pb}_{\text{ex}}$ SML was observed at site MH-2.

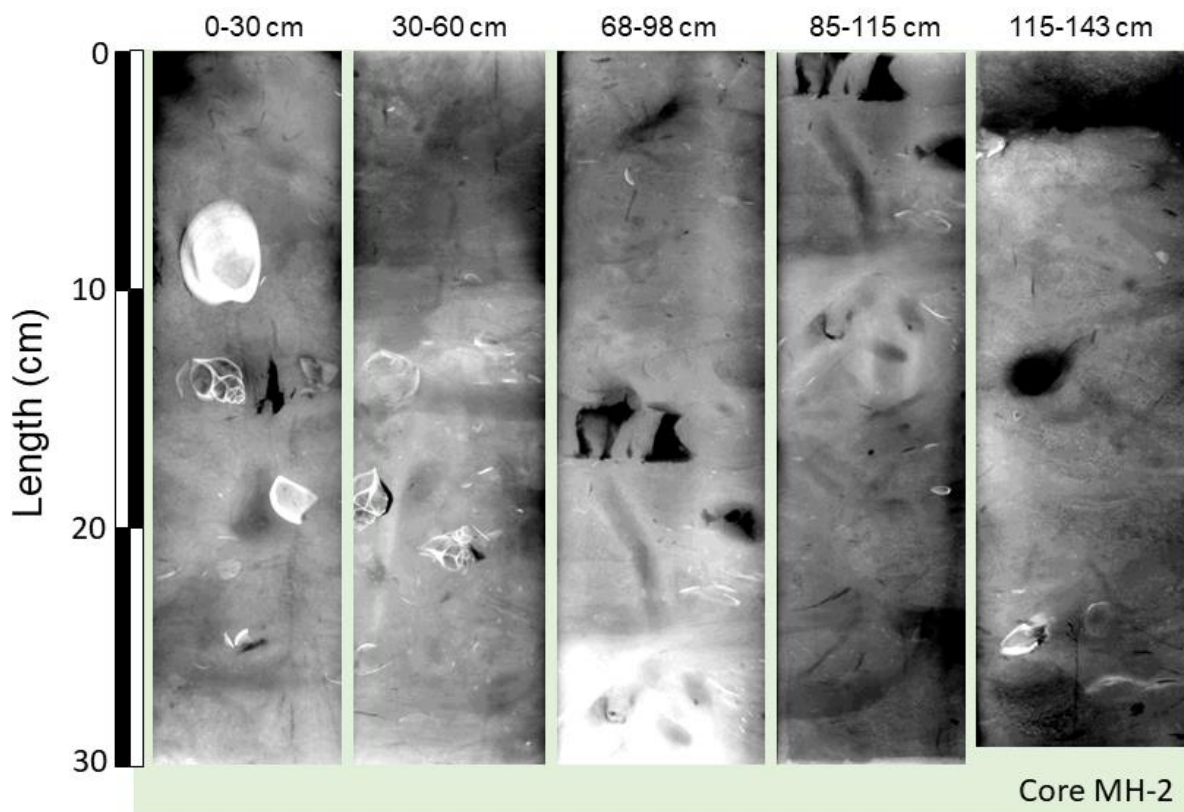


Figure 3-6: Core MH-2 (subtidal: Mahau Sound): 0-143 cm. These images have been inverted so that relatively high-density objects appear white (e.g., shell valves) and low-density materials such as muds or organic material appear as darker areas.

The maximum depth of ^{137}Cs -labelled (i.e., post-1950s) sediment occurs at 31 cm. Correcting this depth for rapid sediment mixing in the ^7Be SML (i.e., 31 – 3 cm) yields a ^{137}Cs SAR of between 4.4 and 5.2 mm yr^{-1} (i.e., assuming $^{137}\text{Cs}_{\text{max}}$ year range of 1953–1963). This is in reasonable agreement with the time-weighted average SAR of 3.9 mm yr^{-1} (Figure 3-7a) given the uncertainty in $^{137}\text{Cs}_{\text{max}}$.

Dry bulk sediment densities in core MH-2 vary between 0.7 and 1.1 g cm^{-3} and do not display a trend of increasing bulk density with depth (Figure 3-7b). Similar to site MH-1, particle size distributions do not substantially vary with depth, with a narrow range of mean and median particle diameters (range: 12–25 μm) (Figure 3-7c) for sediment that is composed of clay-rich muds (i.e., 5–15% by volume, Figure 3-7d).

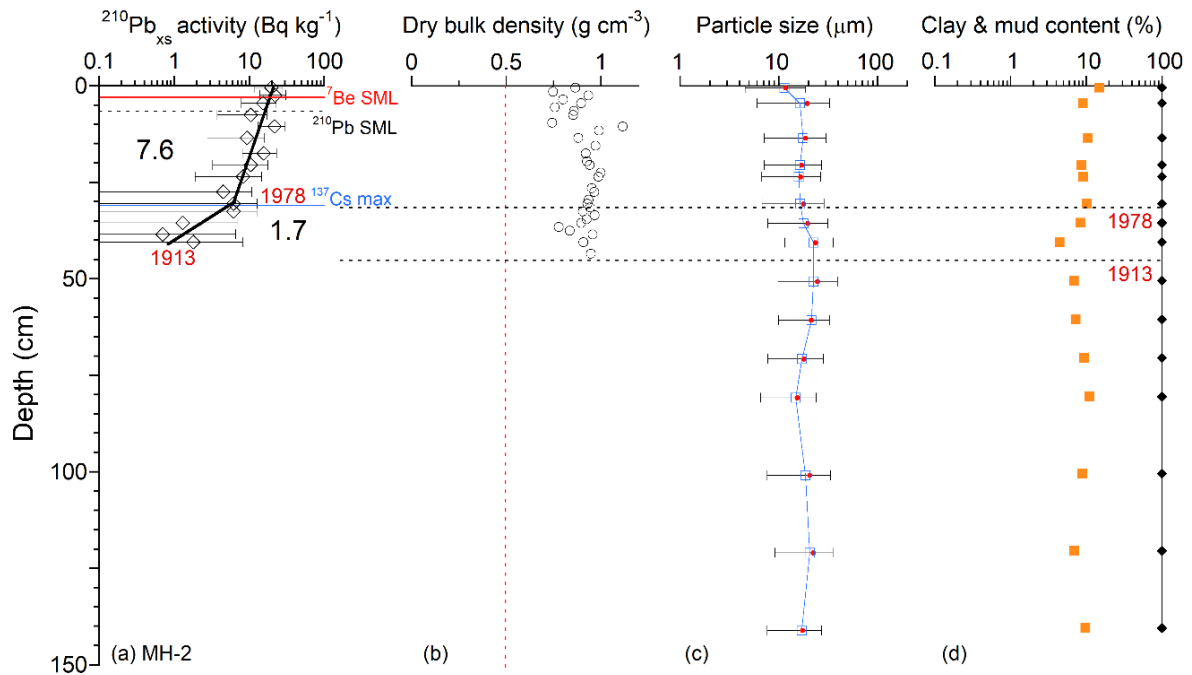


Figure 3-7: Core site MH-2 (Mahau Sound) – ages of sediment layers, sediment accumulation rates (SAR), and sediment properties. (a) Excess ^{210}Pb activity profiles with 95% confidence intervals shown. Time-averaged SAR (mm yr^{-1} , Black text) derived from regression fit to natural log-transformed excess ^{210}Pb data (top fit: $r^2 = 0.73$, $n = 12$, bot fit: $r^2 = 0.63$, $n = 5$). Estimated ages of depth horizons (red text). Surface mixed layer (SML) inferred from Beryllium-7 (^7Be) and excess ^{210}Pb profiles. Maximum depth of caesium-137 (^{137}Cs) indicated. Radioisotope activity expressed in units of Becquerels (Bq). (b) Sediment dry bulk density, (c) mean (red) and median particle diameters with standard deviation, (d) clay and mud content as percentage of sample by particle volume.

3.3.3 Site MH-3

Core site MH-3 is located in Ohingaroa Bay (Mahau Sound) between 3 and 4 m below chart datum. X-radiographs for core MH-3 indicate that the sediment depositing at this site are primarily composed of fine-grained muds, with traces of mm-scale burrows associated with the feeding and/or burrowing activities of animals being present (Figure 3-8). Large shellfish valves and shell fragments (white objects) and wood fragments (black objects) are common. A large cockle shell valve can be observed at 20-cm depth. A layer of closely packed smaller shell valves and fragments can also be seen at 50–55-cm depth. Shell valves and fragments are abundant from 70–110 cm depth, primarily composed of cockle (*Austrovenus stutchburyi*). The layer of large cockle shells (82–91 cm) is identified, many of these remain as intact articulated valves (Figure 3-8). The three cockle valves selected for AMS 14C dating were articulated and had very well-preserved surface ornamentation, which suggests that the animals died in situ rather than transported to the site by tidal currents.

The ^{210}Pb SAR averaging 3.8 mm yr^{-1} over the last ~ 100 years, with excess ^{210}Pb occurring to 38 cm depth. The ^{210}Pb SML extends to 2-cm depth, with a sediment residence time of ~ 5 years ($\sim 20 \text{ mm} / 3.8 \text{ mm yr}^{-1}$). The maximum depth of ^{137}Cs -labelled (i.e., post-1950s) sediment at 24 cm. Correcting this depth for rapid sediment mixing in the ^7Be SML (i.e., 24 -3 cm) yields a ^{137}Cs SAR of between 3.0 and 3.5 mm yr^{-1} (i.e., assuming $^{137}\text{Cs}_{\text{max}}$ year range of 1953–1963). This is in reasonable agreement with the ^{210}Pb SAR (Figure 3-9a) given the uncertainty in $^{137}\text{Cs}_{\text{max}}$. Radiocarbon dating of three shell valves from individual cockles (*Austrovenus stutchburyi*) collected from a shell layer preserved at 82–91-cm depth provides independent ages for the shell layer. The conventional ^{14}C ages are very similar

(i.e., 2,276–2,288 yr B.P), with a 95% confidence interval/range of ~250 years (Table). These results indicate that SAR averaged 0.3 mm yr^{-1} over the ~2000 years prior to the early-1900s (Figure 3-9), being more than ten-fold lower than over the last century.

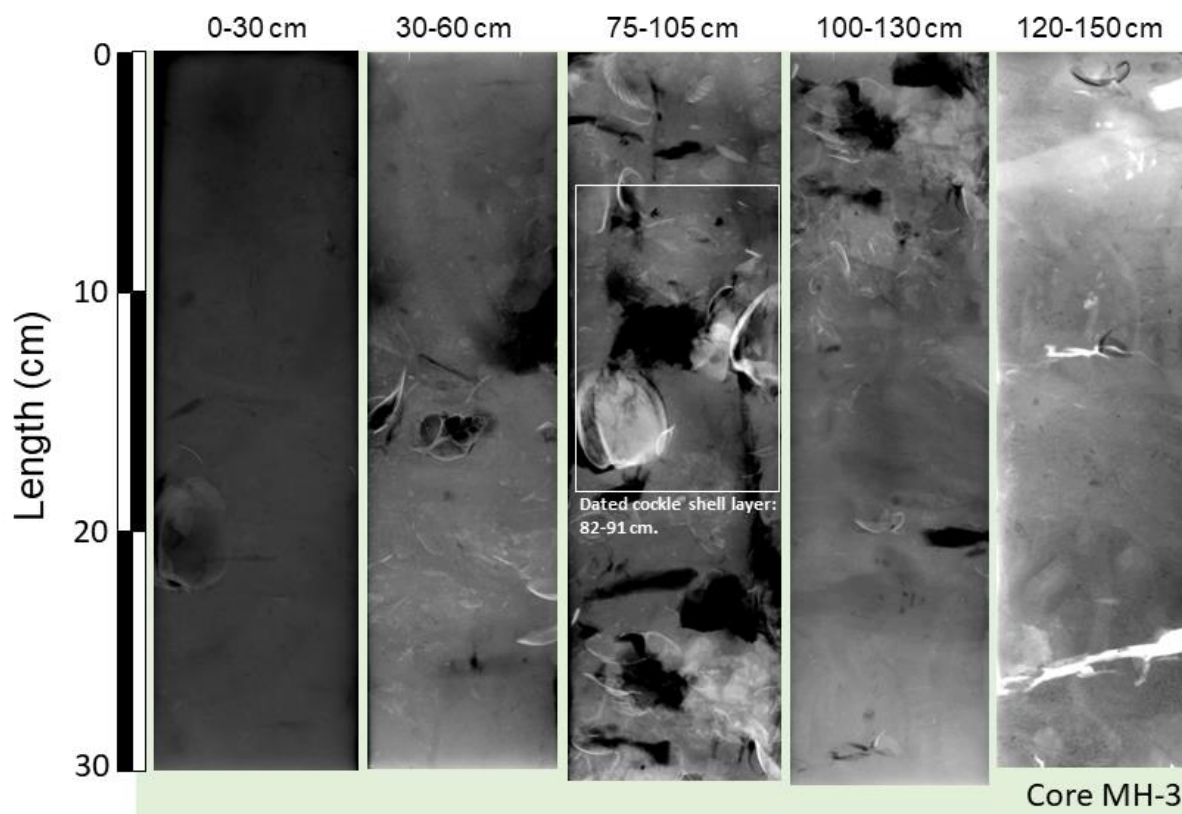


Figure 3-8: Core MH-3 (subtidal: Mahau Sound): 0-150 cm. These images have been inverted so that relatively high-density objects appear white (e.g., shell valves) and low-density materials such as muds or organic material appear as darker areas. The layer of cockle-shell valves used for radiocarbon dating (82–91 cm depth) is labelled.

Dry bulk sediment densities in core MH-3 vary between 0.6 and 1.1 g cm^{-3} and do not display a trend with depth (Figure 3-9b). As reported for the other two core sites in Mahau Sound, particle size distributions do not substantially vary with depth, with a narrow range of mean and median particle diameters (range: 16 – $28 \text{ }\mu\text{m}$) (Figure 3-9c) for sediment that is composed of clay-rich muds (i.e., 3–13% by volume, Figure 3-9d).

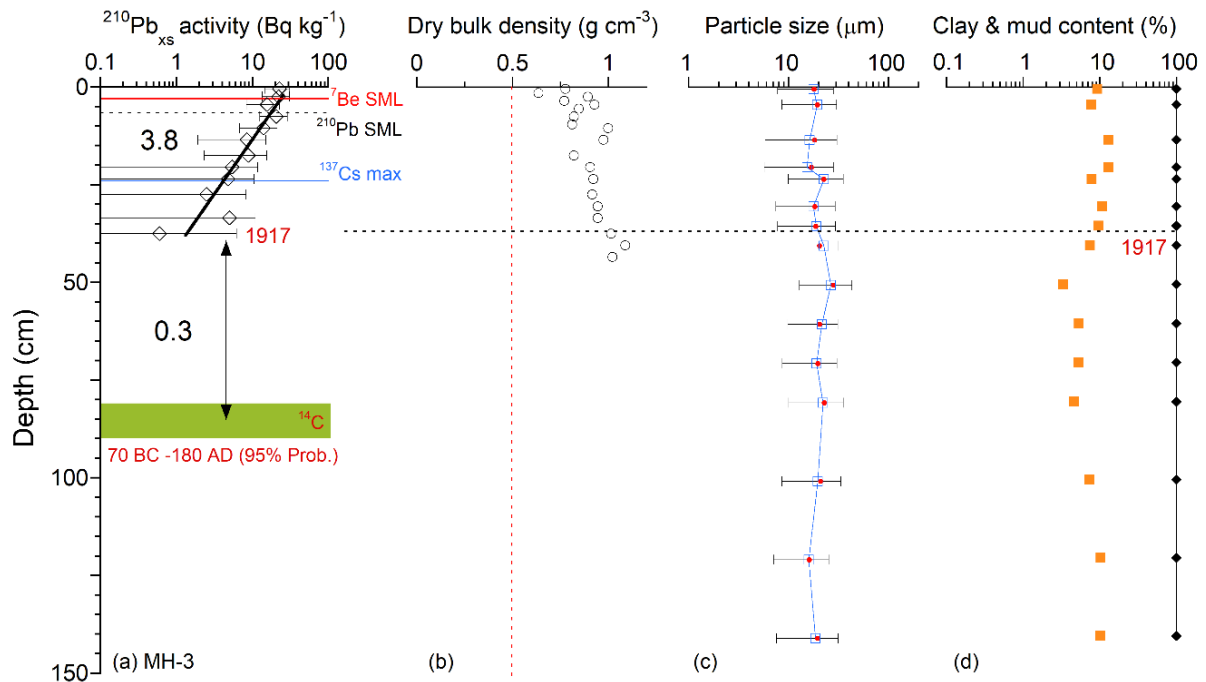


Figure 3-9: Core site MH-3 (Mahau Sound) – ages of sediment layers, sediment accumulation rates (SAR), and sediment properties. (a) Excess ^{210}Pb activity profiles with 95% confidence intervals shown. Time-averaged SAR (mm yr^{-1} , Black text) derived from regression fit to natural log-transformed excess ^{210}Pb data ($r^2 = 0.83$, $n = 11$). Estimated ages of depth horizons (red text). Surface mixed layer (SML) inferred from Beryllium-7 (^7Be) and excess ^{210}Pb profiles. Background SAR for the $\sim 2,000$ years prior to the early-1900s shown (Calibrated ^{14}C ages of cockle shell valves). Maximum depth of caesium-137 (^{137}Cs) indicated. Radioisotope activity expressed in units of Becquerels (Bq). (b) Sediment dry bulk density, (c) mean (red) and median particle diameters with standard deviation, (d) clay and mud content as percentage of sample by particle volume.

The results of the radiocarbon dating, including calculated sediment accumulation rates are presented in **Appendix H**.

3.4 Sources of sediment accumulating in Mahau Sound

CSSI analysis of 15 samples from each of the three cores has yielded data on source contributions at subdecadal time scales. Three replicate mixing model runs were undertaken for core MH-1 to demonstrate the repeatability of the probability distributions of isotopic source proportions generated by Markov Chain Monte Carlo (MCMC) process. These results demonstrate that the modelling of the sediment mixtures (i.e., core samples) using the CSSI data source library generated highly repeatable results (**Appendix J**). Summary statistics reported for the probability distributions of source proportions (%) include the mean, median, standard deviation and credible interval [2.5–97.5% percentile range]).

The results indicate that on average $\sim 30\%$ of the sediment depositing in Mahau Sound has been derived from catchment sources whereas $\sim 70\%$ of the sediment has a signature consistent with the marine end-member source sampled at the Chetwode Islands (Table 3-7). These results are also consistent across all three core sites, with the exception of a single sample from core MH-1 (depth increment: 1-2 cm) with a higher than normal catchment proportion (i.e., 70%, Table 3-7).

The temporal pattern of average sediment contributions from each of the potential major sources, both catchment and the marine endmember, for each core is presented in Figure 3-10. A notable characteristic of these data is the similarity of mean % source contributions, across the three core

sites, to sedimentation in Mahau Sound over the last century. Subsoils are the largest contributor of catchment-derived sediment, averaging 14 to 17% over the three core sites. Erosion of streambanks is the second largest sediment source, on average accounting for ~8 to 10% of sediment accumulation in the Sound. This eroded streambank sediment themselves will be composed of sediment from various upstream sources. Native forest and harvested pine forest (post-1979/1980) account for similar and relatively small proportions of the sediment accumulation at the core sites, averaging 1.8–2.3% of the total sedimentation. Sediment contributions from Kanuka scrub average 1.2–1.6% and the Scrub and Pasture (combined sources) 1.1–1.3%.

Table 3-7: Summary of catchment source contribution (%) to sediment accumulation in Mahau Sound since early 1900s. Statistics for mean catchment source values for each of the three core sites (n =15/core).

Statistic	Site MH-1	Site MH-2	Site MH-3
Mean	31.2	30.7	27.7
Median	29.1	30.7	29.2
Standard deviation	11.4	8.4	8.6
Minimum	20.3	20.7	16.5
Maximum	70.1	53.6	45.4

Appendix J presents box and whisker plots that summarise the probability distributions generated by the isotopic mixing model for each sample analysed from the dated sediment cores. These data highlight the consistent pattern of source contributions over time and between sources at all three core sites. The low uncertainty in the marine source contribution (indicated by the negligible range of the data) largely reflects the relative isotopic distance (i.e., uniqueness) of the isotopic values of the FA biotracers for the marine end member source by comparison with the catchment sources (Figure 2-11 to Figure 2-12).

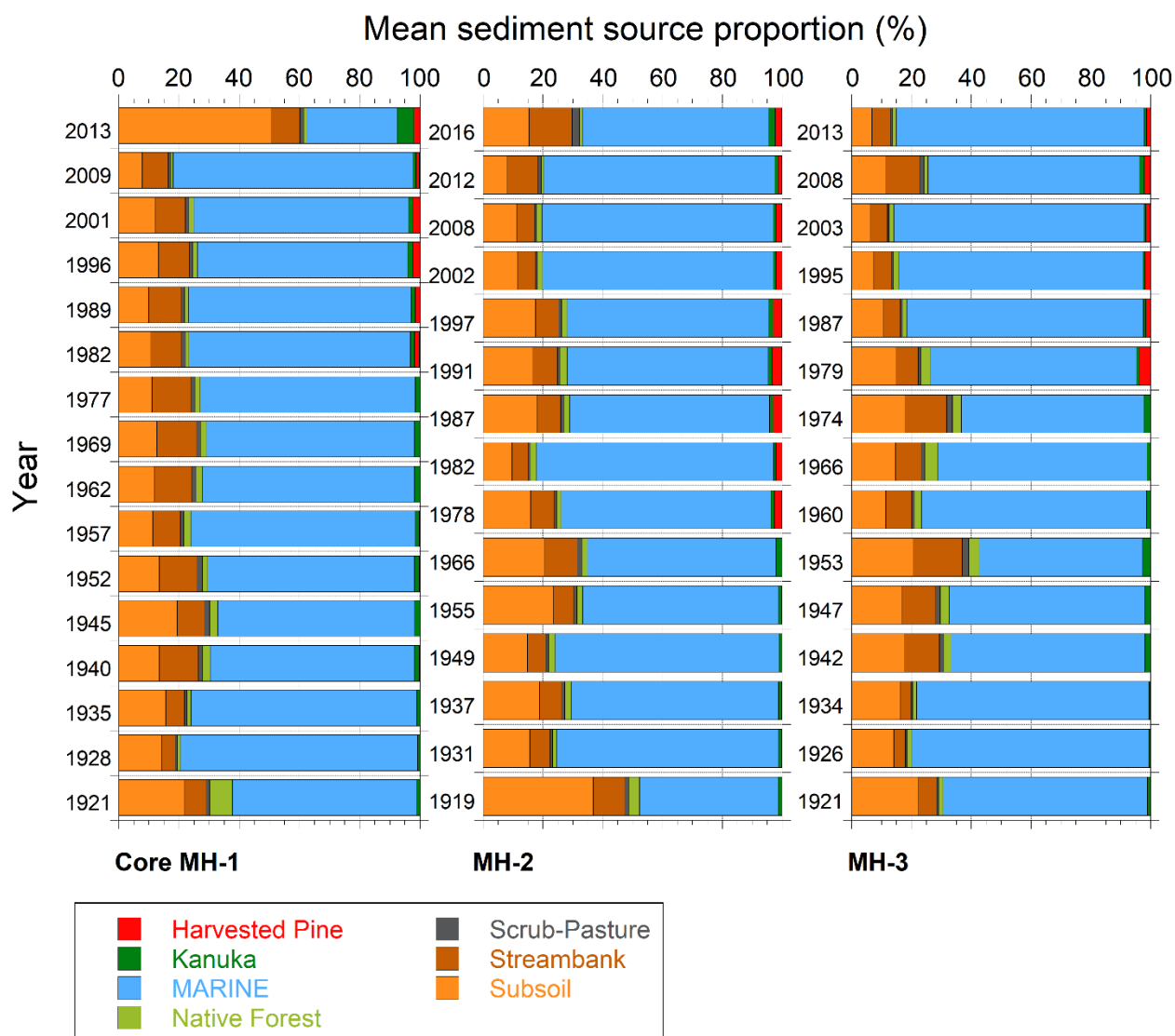


Figure 3-10: All sources of sediment accumulating in Mahau Sound (Inner Pelorus) since the early 20th century determined from CSSI analysis of dated cores. Data shown are the mean sediment source proportions calculated from a probability distribution (n = 3000) generated by the MixSIAR mixing model using the source library.

The temporal pattern of average sediment contributions from each of the catchment sources (i.e., re-scaled catchment sources sum = 100%) for each core is presented in Figure 3-11.

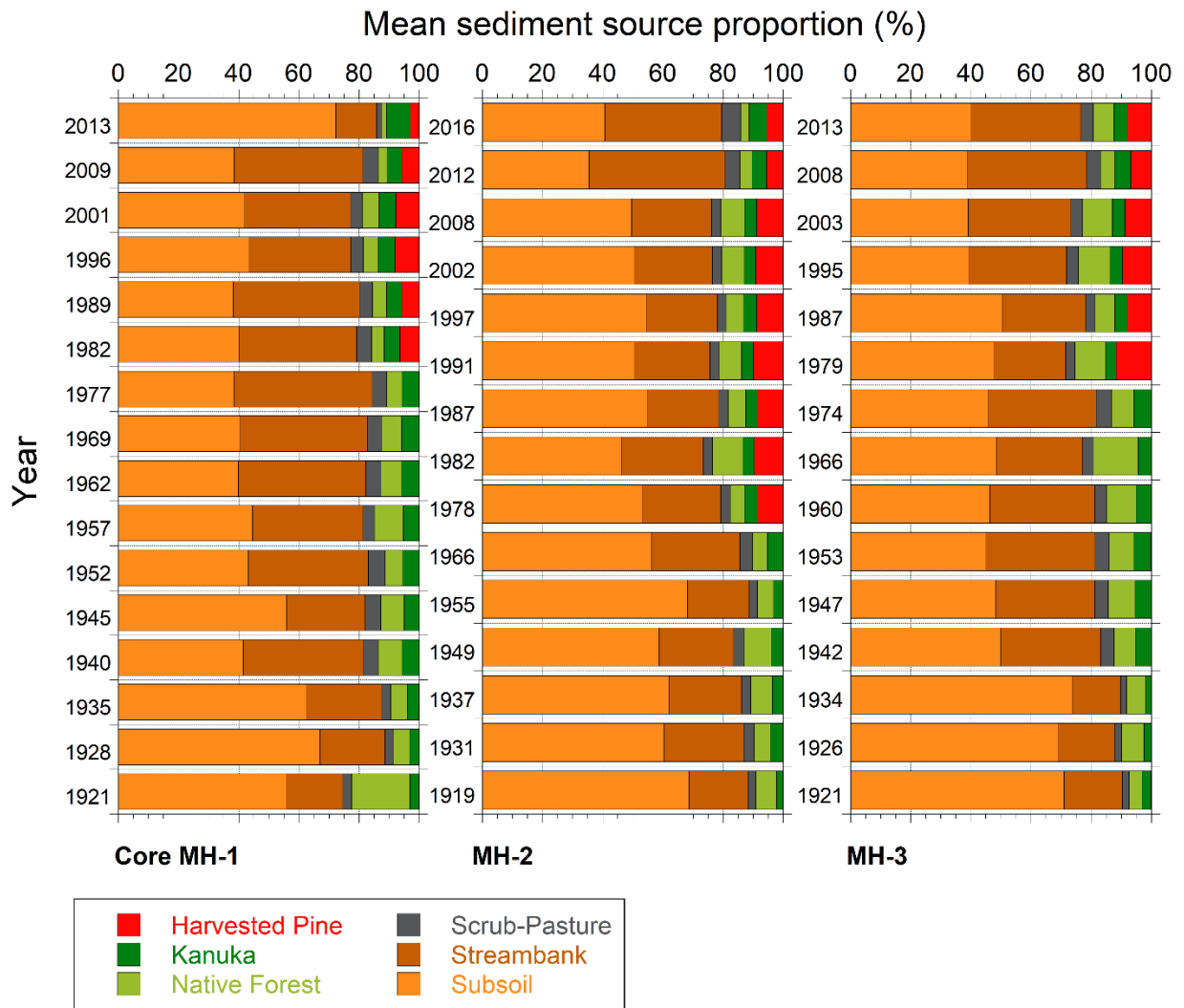


Figure 3-11: Catchment sources of sediment accumulating in Mahau Sound (Inner Pelorus) since the early 20th century determined from CSSI analysis of dated cores. Data shown are the mean sediment source proportions calculated by the MixSIAR mixing model using the source library. Table 3-8 presents the source proportion yields (% km⁻²) for the disturbed catchment land use sources and yield ratios relative to native forest. These calculations, based on the source proportions in each dated core sample and the land use areas, are explained in the methods section 2.6.3. This analysis employs LCDB land use class area data for the entire land catchment of Pelorus Sound (section 2.6.3). For comparison, source proportion yields based on land use area data for the Pelorus-Rai, Kaituna and Cullens Creek catchments only are presented in Appendix K.

Table 3-8: Source proportion yields (% km⁻²) for land use classes and yield ratios relative to native forest based on Land Cover Data Base (LCDB) versions 2 to 4. Source proportion data (%) provided for each core. Land use areas are based on values for the entire land catchment of Pelorus Sound. Source proportion yields provided for mean and credible interval values (2.5%, 97.5%) for the modelled % soil proportion distribution.

LCDB Class	LCDB version Year	Core	Land use class area (km ²)	Source Proportion yield by area (% km ⁻²)			Yield ratio relative to Native Forest			
				Mean	2.5%	97.5%	Mean	2.5%	97.5%	
Harvested Forest	2012/13	MH-1	25.9	0.0772	0.0012	0.4367	65.6	54.5	74.2	
		MH-2		0.0463	0.0012	0.1617	48.1	54.2	45.8	
		MH-3		0.0502	0.0015	0.1601	39.1	48.1	38.2	
			Average				51.0	52.3	52.7	
	2008/09	MH-1	17.7	0.0679	0.0022	0.2349	106.0	137.1	96.9	
		MH-2		0.1132	0.0028	0.3578	58.9	66.2	57.1	
		MH-3		0.1132	0.0045	0.3437	75.7	96.7	64.9	
			Average				80.2	100.0	72.9	
	2001/02	MH-1	11.4	0.2019	0.0070	0.5711	118.1	164.2	92.5	
		MH-2		0.1842	0.0053	0.5632	101.4	98.5	89.8	
		MH-3		0.1316	0.0035	0.4000	77.0	65.7	74.4	
			Average				98.8	109.5	85.6	
	Manuka/Kanuka	2012/13	MH-1	125.9	0.0445	0.0001	0.2374	37.8	6.0	40.3
			MH-2		0.0087	0.0003	0.0319	9.1	14.9	9.0
			MH-3		0.0064	0.0002	0.0222	5.0	5.0	5.3
			Average				17.3	8.6	18.2	
2008/09		MH-1	127.2	0.0079	0.0002	0.0283	12.3	13.7	11.7	
		MH-2		0.0071	0.0002	0.0259	3.7	3.8	4.1	
		MH-3		0.0126	0.0004	0.0432	8.4	8.2	8.1	
			Average				8.1	8.6	8.0	
2001/02		MH-1	130.1	0.0123	0.0003	0.0415	7.2	6.9	6.7	
		MH-2		0.0069	0.0002	0.0244	3.8	2.9	3.9	
		MH-3		0.0054	0.0001	0.0193	3.1	2.3	3.6	
			Average				4.7	4.0	4.7	

LCDB Class	LCDB version Year	Core	Land use class area (km ²)	Source Proportion yield by area (% km ⁻²)			Yield ratio relative to Native Forest		
				Mean	2.5%	97.5%	Mean	2.5%	97.5%
Native Forest	2012/13	MH-1	935.8	0.0012	0.0000	0.0059	–	–	–
		MH-2		0.0010	0.0000	0.0035	–	–	–
		MH-3		0.0013	0.0000	0.0042	–	–	–
	2008/09	MH-1	935.9	0.0006	0.0000	0.0024	–	–	–
		MH-2		0.0019	0.0000	0.0063	–	–	–
		MH-3		0.0015	0.0000	0.0053	–	–	–
	2001/02	MH-1	935.9	0.0017	0.0000	0.0062	–	–	–
		MH-2		0.0018	0.0001	0.0063	–	–	–
		MH-3		0.0017	0.0001	0.0054	–	–	–

Figure 3-11 shows that subsoils are the largest contributor of catchment-derived sediment accumulating in Mahau Sound (averaging 14 to 17% of total sedimentation). The land use sources of these subsoils cannot be discriminated using FA biotracers and are likely to be derived from erosion of subsoils across several land uses. Subsoil erosion will occur on steep lands with disturbed and/or sparse vegetation cover where subsoils are exposed directly to rainfall and surface runoff. Landslides caused by hillslope failures during episodic high-intensity rainstorms will also deliver subsoils to rivers. The LCDB data show that hillslope failures occur in native forest as well as from areas of disturbed land uses.

3.5 Sediment characteristics and mollusc death assemblage

The non-metric multidimensional scaling analysis separated out most replicate core slices by age group based on differences in their sediment characteristics (Figure 3-12a). (Core slices containing the greatest percent of shell carbonate (estimated by volume), lay through the centre of the plot with the sediments deposited since European settlement, correlated with high SARs, gravel, and very fine sand (Figure 3-12a). Since 1950, clay and charcoal are more strongly correlated.

Sediments

Non-metric MDS

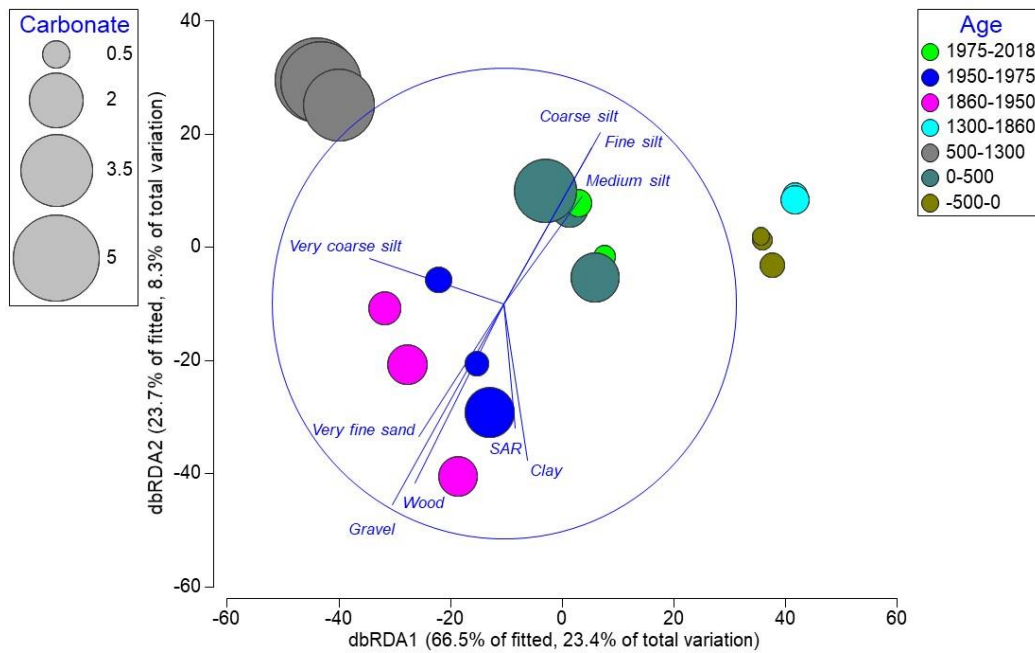
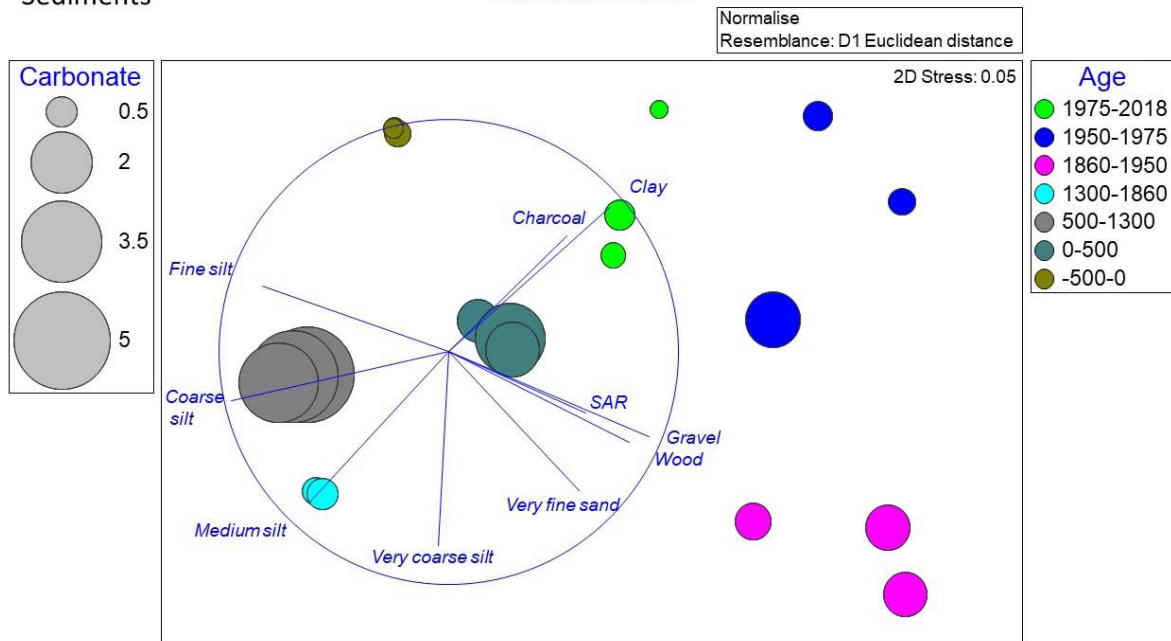


Figure 3-12: a) Results of multivariate death assemblage and sediment analyses. (a - top) Non-metric multidimensional scaling (nMDS) plot of sediment characteristics of Mahau core sections. This analysis is based on time period (i.e., age) and (b - bottom) distance-based redundancy (dbRDA) plot of death assemblage species (shell volumes) and attempts to discriminate time periods against predictor sediment characteristics. The biplot overlay (blue circle) indicates correlations with Pearson correlation coefficients approaching $\rho=1$. The blue lines plotted are for correlates with $\rho > 0.4$ for the measured sediment characteristics. The strongest correlations (i.e., longest blue lines) approach $\rho=1$.

The distance-based redundancy analysis (dRDA) ordination of the death assemblage composition separated most of the time periods with historic and most recent (1975–2018) assemblages correlated with variations in silt content (Fig. 3-12b). In contrast, from European arrival to 1975, changes in species composition were correlated with gravel, wood, very fine sand and clay content along with higher SARs.

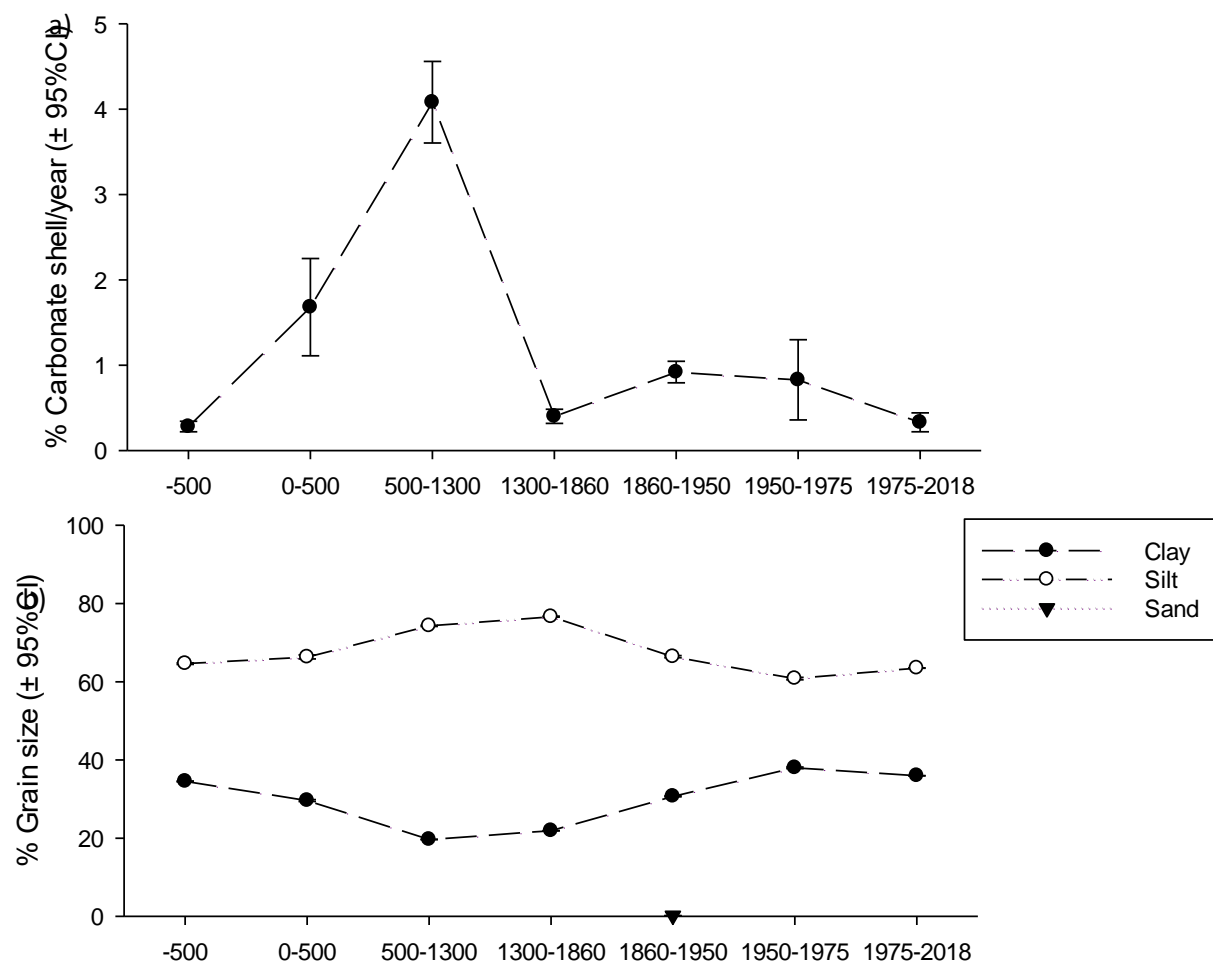


Figure 3-13: Sediment characteristics derived from sections of three replicate cores taken in Mahau Sound, plotted by time-period. . Percent content: a) carbonate shell, b) clay (0–3.9 μm), silt (3.9–62.5 μm), and very fine sand (62.5–125 μm).

As indicated by the size of the “bubbles” in the multivariate analyses plots (Figure 3-12), the percentage of mollusc shell carbonate by volume within each core slice was greatest in pre-human times, except for the oldest (i.e., 500 yr BC to 0 AD) (Figure 3-13a). Mollusc shell deposition was greatest between 500–1300 AD. This maximum proportion of mollusc shell content was consistent with the lowest levels of clay sediment content (Figure 3-13b). The accumulation of shells in the sediment dropped off significantly following arrival of Māori and early Europeans. Sand was completely absent from all core slices except for one of the replicate cores during the European period between 1860–1950.

3.5.1 Death assemblage (DA) species composition and feeding traits

From all core sections, the filter feeding cockle *Austrovenus stutchburyi* was the largest contributor to the death assemblage by weight (71.6%), followed by the bivalve *Cyclomactra ovata*, the ostrich-foot *Pellicaria vermis*, the deposit feeder Tellinidae, and then filter feeding oysters (most likely *Tiostrea chilensis*), *Comminella* and calcareous tube worms (Table 3-9). The cockles were generally large in size (i.e., >5 cm), most numerous in the sediment between 0-1300 AD.

Table 3-9: Mollusc species contributing most of shell by % weight of the total from all three sediment cores.

Species	Total weight (g)	% of total
<i>Austrovenus stutchburyi</i>	527.6	71.6
<i>Cyclomactra ovata</i>	64.2	8.7
<i>Pellicaria vermis</i>	28.2	3.8
Tellinidae	26.6	3.6
Oyster sp.	21.9	3.0
<i>Cominella</i> sp.	16.5	2.2
Calcareous tubeworm case	12.1	1.6

Analysis of functional feeding traits between time periods and replicate cores showed that the greatest mass of shells was from suspension feeder species between 0-1300 AD (Figure 3-14). Deposit feeders became more numerous as a percent of volume following European arrival, co-correlated on the y-axis with the increase in clay, gravel and very fine sand content (see Figure 3-13a above), commencing from 1860 AD.

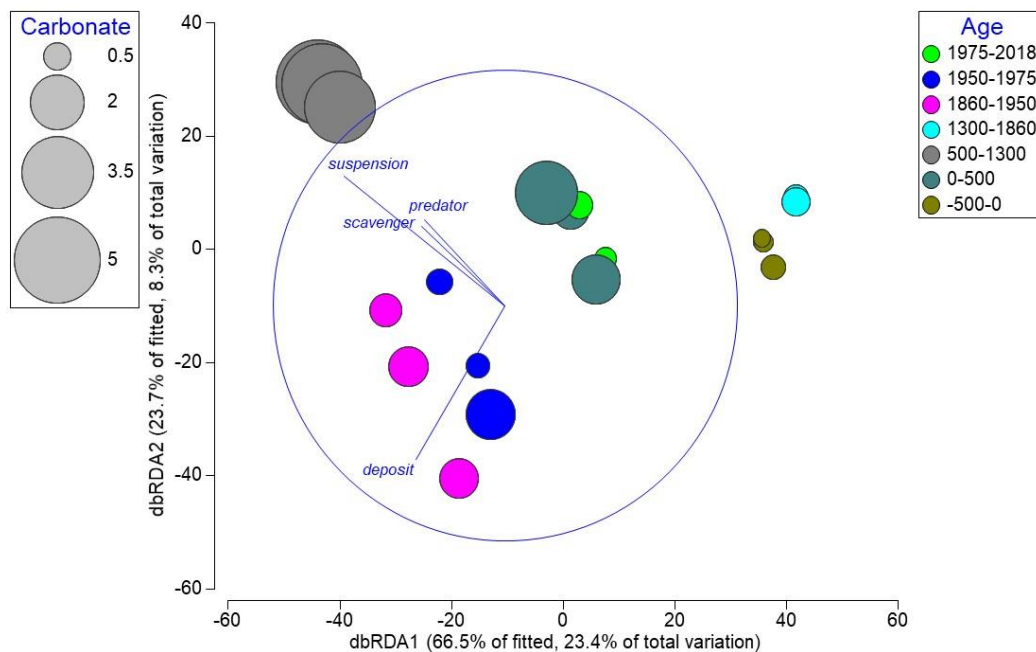


Figure 3-14: Distance based redundancy (dbRDA) plot of death assemblage species (shell volumes) to discriminate time periods against predictor sediment characteristics. The biplot overlay (blue circle and lines) indicates correlations with Pearson correlation coefficients approaching $\rho=1$. The blue lines plotted are for correlates with $P > 0.4$ for the measured sediment characteristics. The strongest correlations (i.e., longest blue lines) approach $\rho=1$.

By multiplying the proportion of each feeding trait by the total shell volume of all identifiable species collected in each date period, suspension feeders (mostly *A. stutchburyi*) were revealed as the dominant feeding trait by shell volume, followed by deposit feeders (Figure 3-15). A comparison of the number of species present in the cores show that species diversity was at its lowest in the most recent sediments (Figure 3-16).

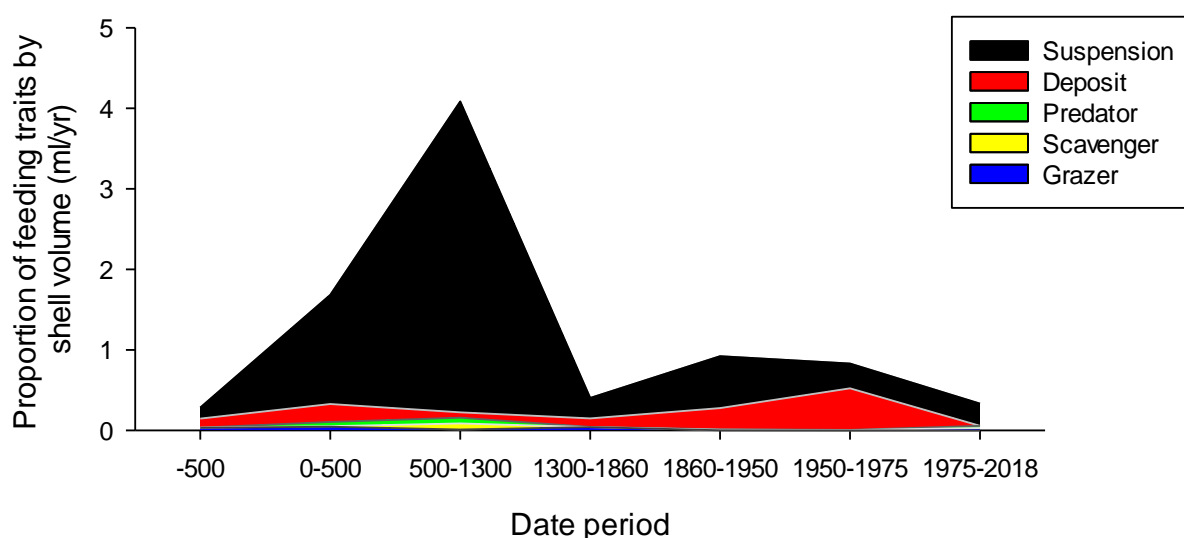


Figure 3-15: The mean proportion of mollusc feeding traits calculated from all cores expressed by shell volume (mL/yr).

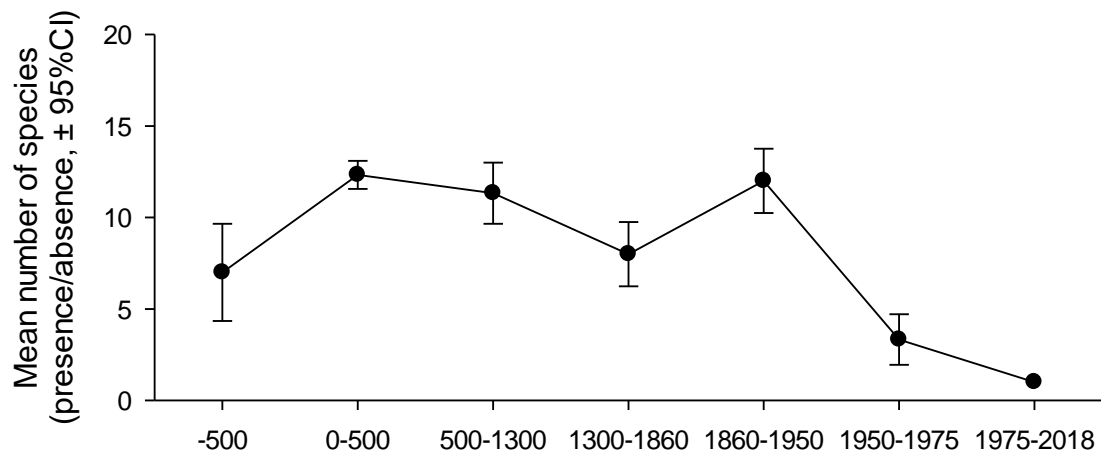


Figure 3-16: Mean number of mollusc species calculated from presence/absence from each date period across all replicate core sections.

4 Discussion

4.1 Changes in sediment accumulation rates

Lead-210 dating of sediment cores indicate that sediment accumulation rates (SAR) in Mahau Sound have averaged 3.8–4.1 mm yr⁻¹ since the early-1900s. These rates are at least ten-times higher than time-average SAR over the previous ~2,000 years (0.2–0.3 mm yr⁻¹) (as estimated from radiocarbon dating of large cockle shells). In Havelock Estuary, apparent SAR on the intertidal flats in the central basin of 2.2–3.6 mm yr⁻¹ are generally lower than average rates on the subtidal flats of the Mahau Sound. The lower rates of sediment accumulation in Havelock Estuary are consistent with a relatively infilled estuary that has more limited accommodation volume for long-term accumulation of fine catchment-derived and marine sediment. The limited sediment accommodation volume of the Havelock Basin reflects:

- proximity to the outlet of the Pelorus River catchment and sediment supply that has formed a large river delta (Carter, 1976) that has infilled the ancestral river valley over the last ~7,000 years or so,
- small present-day tidal prism,
- short hydroperiod (i.e., time period submerged), and
- resuspension of fine sediment deposited on the intertidal flats by a combination of locally-generated waves and export of fine sediment by ebb-tidal currents and river plumes to the middle–outer Sound.

The degree of infilling also suggests that the sediment supplied by rivers has outstripped subsidence (0.7–0.8 mm yr⁻¹) driven by regional tectonic processes in the inner Sound over the last 6,000 to 7,000 years (Hayward et al. 2010), as well as sea level rise around the NZ coast (1.7 mm ± 0.1 yr⁻¹) (Hannah and Bell, 2012) since the early-1900s. This relative sea level rise of ~2.5 mm yr⁻¹ has substantially increased the sediment accommodation volume of the system, being equivalent to about 60% of the sediment accumulation rate in Mahau Sound over the last ~100 years.

The apparent increase in SAR observed in Mahau Sound at site MH-2 from 1.7 mm yr⁻¹ (1913–1978 AD) to 7.6 mm yr⁻¹ (1978–2017) does not occur at the other two Mahau core sites. The time-weighted average SAR for MH-2 is 3.9 mm yr⁻¹, similar to the time-average values at MH-1 and MH-3 (i.e., 3.8 and 4.1 mm yr⁻¹). This suggests that: (1) sedimentation in the Mahau Sound has occurred at a uniform rate since the early-1900s, and (2) the apparent increase in SAR at MH-2 is most likely due to a site-specific process rather than reflecting a general increase in SAR within Mahau Sound as a whole. This local increase in SAR at MH-2 since the late 1970s suggests preferential sediment deposition related to estuarine circulation, river plume transport and/or interaction of these processes. Independent ¹³⁷Cs dating of the Mahau cores yields SAR estimates (3.0–5.2 mm yr⁻¹) that are reasonably similar to the ²¹⁰Pb values. There is likely to be more uncertainty in the ¹³⁷Cs SAR than for ²¹⁰Pb SAR, as the former estimates depend on the year assumed to correspond to maximum ¹³⁷Cs depth (i.e., range 1953–1963). The ²¹⁰Pb SAR observed in Mahau Sound are within the range of rates in Kenepuru Inlet and Beatrix Bay since the late-1800s (1.8–4.6 mm yr⁻¹, Handley et al. 2017). Similarly, SAR in Mahau Sound are as much as ten-fold higher than rates over the previous several thousand years (i.e., Core MH-3, 0.3 mm yr⁻¹) calculated from radiocarbon dating.

Reconstruction of the sedimentation history of Pelorus Sound over the last 800 to 3,400 years by Handley et al. (2017) and from cores collected in the present study indicate that sediment accumulated at a relative low rate (i.e., 0.1–1.1 mm yr⁻¹) prior to European settlement (i.e., mid-1800s). These are similar to pre-human rates measured in Nydia Bay (1.2 mm yr⁻¹) and Tennyson Sound (1.4 mm yr⁻¹, Lauder 1987), tributary arms of Pelorus Sound, and are consistent with the results of previous coring studies conducted in Northland, Auckland and Waikato estuaries (Hume and McGlone 1986, Oldman and Swales 1999, Sheffield et al. 1995, Swales et al. 1997, 2002a, 2002b, 2005, 2012, 2016a).

Large increases in SAR over the last century or so coincide with large-scale catchment deforestation and conversion to pastoral agriculture during the mid–late 1800s. Time-weighted average ²¹⁰Pb SAR of 3.9 and 4.0 mm yr⁻¹ in the Mahau and Kenepuru Sounds and 2.4 mm yr⁻¹ in Beatrix Bay are within the range of values measured for the post-European period in a number of North Island estuaries (range: 2.3–5.5 mm yr⁻¹, Figure 4-1, Handley et al. 2017). The weighting of ²¹⁰Pb SAR values, based on the length of record (years), provides a more representative SAR estimate. The relatively low weighted-average SAR in Beatrix Bay, located in the outer Pelorus Sound, is consistent with the Bay's relative distance from the Pelorus-Rai and Kaituna River catchments – major sources of fine sediment inputs to Havelock Basin.

In many North Island estuaries, an increase in SAR following deforestation has been accompanied by a shift from sand- to mud-dominated systems (e.g., Swales et al. 2002a, 2002b, 2012, 2013). In contrast, the results of the present study indicate that mud-rich sediments have accumulated in the Mahau Sound for at least the last 2,000 years, and for 3,400 years in Kenepuru Sound (Handley et al. 2017). This long-term mud deposition reflects catchment soils that are primarily comprised of silt and silt-clay loams with up to 45% clay content (DSIR 1968, Laffan and Daly 1985). In the Pelorus system, field observations suggest that gravel and sand accumulate in the river channels, whereas suspended sediment yield is primarily discharged to the Sound, with some deposition occurring on low-lying floodplain areas during floods (Figure 1-1). The Pelorus-Rai and Kaituna Rivers transport ~259,000 tonnes per year of suspended sediment to the Havelock Estuary, with ~90% of this sediment load delivered by the Pelorus-Rai River (NZ River Maps national-scale multivariate statistical model, Booker and Whitehead, 2017).

4.2 Sources of river sediment deposits

The relative contributions of land use and major subcatchments to fine sediment deposition in the Pelorus-Rai and Kaituna catchments is summarised in Figure 4-1. The supporting data for this map is presented in Table 3-4 and Table 3-6. Streambank and subsoil contributions have been calculated as separate sources using data from Table 3-4 for the Pelorus River, and Table 3-6 for the Kaituna River. The sampling sites at the outlets of the Pelorus-Rai and Kaituna Rivers (and above the tidal reach) are assumed to contribute 100% of the catchment sediment that is delivered to Havelock Estuary and the inner Pelorus Sound. Cullens catchment represents a small fraction (i.e., less than 3%) of the total 1063 km² land area discharging to the inner Pelorus Sound.

Globally, bank erosion is an important source of suspended sediment in river systems with contributions variously estimated at up to 94% (e.g., Kronvang et al. 2012, Hughes and Hoyle, 2014). The range of bank sediment contributions, however, varies widely. For example, for the glaciolacustrine deposits in New York State, eroded riverbanks contributed 60% (range 46–76%) but less than 46% where these sediment deposits were absent (Nagle et al. 2007). The estimated bank erosion contribution also depends on whether subsoil is included in the estimate (e.g., >90% bank

erosion estimate in a Bay of Plenty (NZ) study, Hughes and Hoyle, 2014), or is estimated as a discrete component (i.e., ~50% (range 41-57%, Waikato River, Hughes 2015). Bank erosion estimates from these previous studies employed erosion pins, fallout radionuclides or time series of aerial photographs (Green et al. 1999). In studies of two New Zealand agricultural catchments used for dairy farming, the bank component of eroded sediment was estimated to be around 64% (range 57-76%, McDowell et al. 2016). The contribution of bank erosion varied seasonally (i.e., summer: 0-17%, autumn: 0-1%, winter: 23-96% and spring: 31-100%, McDowell and Wilcock, 2007). These bank erosion contributions were related to farm management practices, including stock trampling the banks and stream bed. Elsewhere, studies have demonstrated a linear relationship between erosion and bank angle (Laubel et al. 2003). By contrast, the present study employs stable isotopic signatures of biomarkers to identify sediment sources from various land uses (i.e., plant communities). This provides a means to potentially discriminate the sources of sediments in more detail than topsoil vs subsoil.

In the present study, the bulk C and FA tracers have been used to identify the main sources of sediment deposited in the Pelorus-Rai and Kaituna River systems during high flow and flood events, integrated over several years. Sediment deposits in the Pelorus-Rai River are dominated by contributions from streambank and subsoil sources. When modelled as separate sources, streambank erosion contributed on average 37% (range of averages: 26–44%), which is within the range for the literature, albeit at the lower range. This is reasonable because the land use in the Pelorus River catchment is either forested or well fenced to contain stock. Subsoils contributed 32% on average (range of averages: 28–38%, Table 3-4). The sum of the average proportions for the streambank plus subsoil sources was 69% (i.e., Series 1, range of averages: 58–78%) for sediment deposited in the Pelorus River. When the streambank and subsoil components were modelled as a single source, the contribution of the merged sources averaged 63% (i.e., Series 2, range of averages: 41–75%) (Table 3-5, Table 3-6). The lower value for the merged sources reflects the increased uncertainty arising from combining the sources.

This sediment source analysis indicates that the Rai catchment accounts for 54% of the river sediment deposits for the Pelorus-Rai catchment. The upper Pelorus river (above the confluence with the Tinline River) is the other major contributor (~23%).

At the subcatchment scale, some subcatchments appear to be producing larger proportions of sediment than would be expected from their catchment area. Soil erosion on steep land is increased when vegetation cover is reduced exposing soils to direct rainfall impact and loss of root strength (reinforcement) (e.g., Phillips et al. 2012). However, if the rainfall pattern is similar over the whole catchment and the soil type and slope are similar, similar levels of erosion should be expected across the whole catchment (i.e., specific sediment yield), unless the plant communities in those subcatchments affected erosion. Such difference has been demonstrated in a pine forest versus pasture paired catchment study at Pakuratahi (Eyles and Fahey 2006).

To identify soil erosion hot spots (i.e., excessive erosion), SSY values for each subcatchment estimated using the CSSI data were compared with the SSY values estimated using data derived from the NZRM database (Booker and Whitehead, 2017). This comparison indicated that CSSI-estimated SSY values for the Kaiuma and Brown subcatchments were more than 10-fold higher than the NZRM SSY estimates. Conversely, the CSSI SSY estimates for the Upper Pelorus River and Wakamarina River were about half the NZRM SSY values. The elevated specific sediment yields for the Kaiuma and Brown subcatchments may reflect a greater influence by factors including vegetation

removal/disturbance and/or higher annual average rainfall on these western subcatchments compared to subcatchments on the eastern side of the Pelorus catchment.

Annual rainfall at the Tunakino VCSN station (Tunakino Agent No. 30680), adjacent to the Kaiuma catchment, is consistently higher (i.e., ~two-fold) than rainfall on the eastern side of the catchment (Figure A1) at the Wakamarina Twin Falls site (MDC No. 133604) (Figure 2-5) (also Fig. 3, Tait, 2017). Consequently, it is likely that the western subcatchments would produce a higher SSY than the eastern subcatchments from the same land use and thereby account for the higher than expected sediment yield by land area in the Rai River (Table 3-3).

With the exception of sheep pasture, the land uses incorporated in the source modelling for the river sediment deposits were the same for each subcatchment. The sheep pasture source only occurred in the Kaituna River catchment (Table 3-6, Figure 4-1). The summary graph shows all land use soil contribution mean proportions relative to the sediment yield at the mouth of the Pelorus and Kaituna Rivers (Figure 4-1). These results show that streambank and subsoils were the largest sources of sediment, often exceeding 50% of the total sediment yield. It also shows that dairy pasture produced more sediment in the Rai River subcatchments than in the Upper Pelorus and Wakamarina subcatchments. This is consistent with the higher proportion of dairy farming in the Rai River subcatchments. In contrast, sediment yields from harvested pine forest was similar from most subcatchments., except the Kaituna River where harvested pine forest was minimal.

In the summary graph (Figure 4-1), the subsoil and streambank components are shown separately whereas the modelling compared both streambank and subsoils as individual analyses (Table 3-4) and again as a single combined source as streambank+subsoil (Table 3-5). The results for the sum of the individual streambank and subsoil analyses are essentially equivalent to the combined streambank+subsoil source result. Although the preliminary polygon testing showed that there was substantial coincidence between the streambank and subsoil (Figure 2-10), which would allow them to be combined for modelling (c.f. Phillips et al. 2014), these two sediment sources are derived from different erosion processes occurring in the Pelorus River system. Subsoils are primarily from slips where the topsoil removal has left the subsoil exposed or deep-seated mass movement that erodes both topsoil and subsoil. Streambank sediments comprise a blend of all source soils, including subsoils, that have been deposited during overbank flood events. Large flood events are infrequent but not uncommon in the Pelorus River catchment (**Appendix A**). Presenting these two components as separate sources provides an indication of where landslides, the major factor exposing subsoils, were occurring (i.e., across all subcatchments).

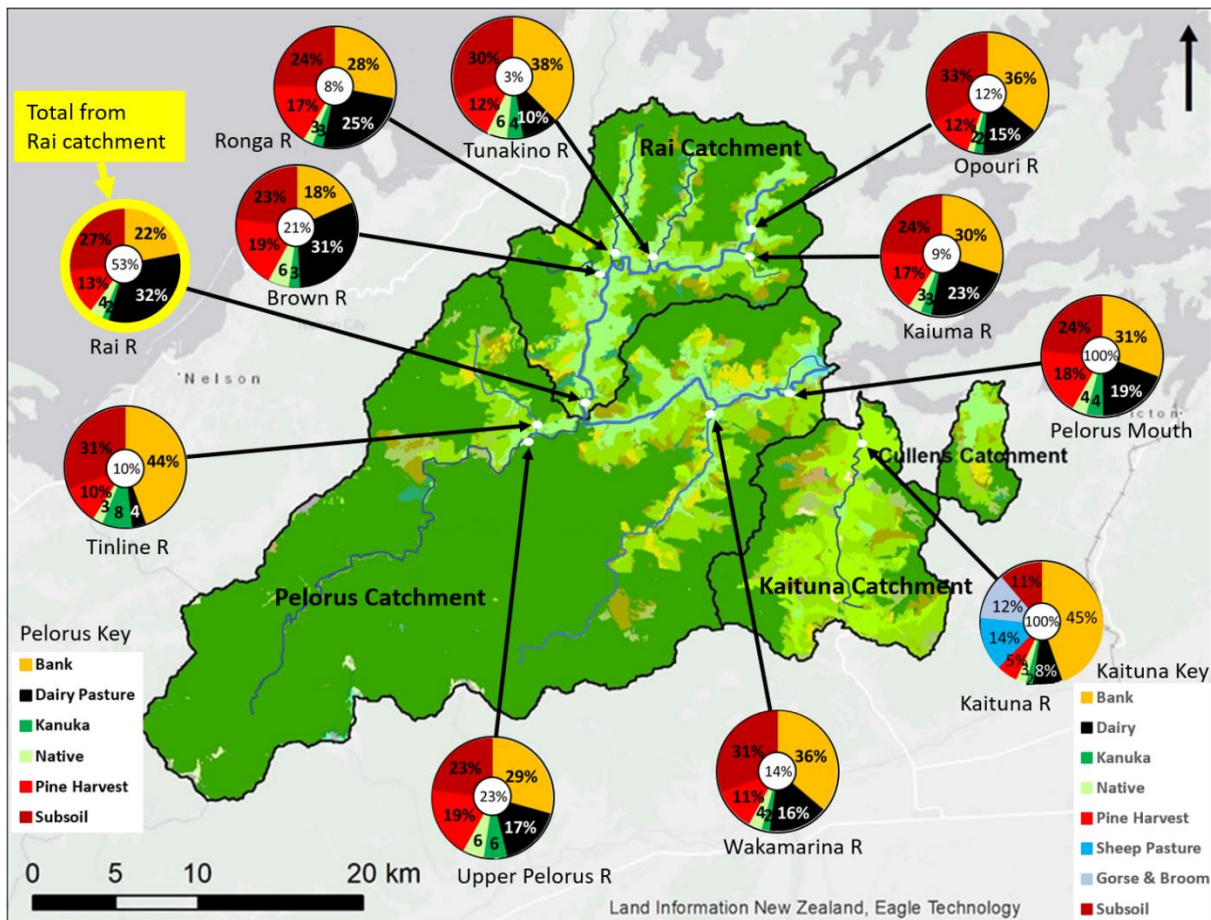


Figure 4-1: Sources of sediment by land use deposited at confluences and contributions (%) from major tributaries in the Pelorus-Rai and Kaituna catchments. The % soil proportions in the centre of each pie chart indicate the contribution of that subcatchment to sediment deposition in the river system (i.e., 100% at the catchment outlet). Data for river sediment collected in April 2016 and May 2018.

The analysis of the river sediment deposited near the outlet of the Pelorus River to Havelock Estuary indicates that 55% of this sediment was sourced from subsoil and streambank erosion. Land use sources were dominated by dairy pasture (23%) and harvested pine (18%). Native forest and kanuka scrub contributed the remaining 6% (Figure 4-1).

Native forest (~640 km², LCDDB-5/2018) and harvested pine (i.e., bare ground post-harvest prior to replanting ~15.7 km²) (Table 1-1) account for 72% and 1.8% of the Pelorus-Rai catchment respectively. Despite the ~40-fold larger area of native forest relative to harvested pine, the sediment deposits at the Pelorus River outlet indicate that the native forest contributes approximately 20% of the amount of topsoil that is derived from harvested pine forest. It is also likely that some fraction of the subsoil source will have originated from the harvested pine area, as well as other land uses. Figure 4-1 shows similar harvested pine/native forest source ratios at many of the sites where river deposits were sampled.

The large differences in the contributions of native forest and harvested pine topsoils to river deposits during the sampling period indicate differences in soil erosion rates. Forested landscapes (including exotic forests) generally generate less sediment than pasture landscapes (e.g., Eyles and Fahey, 2006, Phillips et al. 2012). However, when plantation forests are harvested there is the potential for increased erosion due to soil disturbance, removal of protective ground cover exposing

soils to direct rainfall impact, and loss of root strength (reinforcement) (e.g., Phillips et al. 2012). This 'window of vulnerability' (O'Loughlin and Watson, 1979) to increased soil loss is elevated during the 1- to 6-year period after harvesting (Phillips et al. 2012), when harvested tree root systems decay and the next forest rotation is establishing. In the Pelorus-Rai catchment, the native forest canopy and dense understory with compact root mass largely protects topsoils from rainfall impact (Figure 4-2a). Mature pine forest has a more open understory (Figure 4-2b), which is periodically removed. While these general observations do not prove that there is less erosion from native forest than pine forest, the larger contributions of harvested pine to river sediment deposits in comparison to native forest suggest that this is the case (Figure 4-1). This is also consistent with the literature.

A study of paired native forest vs pine forest catchments (Waikato Region) found little difference between the erosion from both under medium to low rainfall but a three-fold increase in erosion from the pine forest during rainfall events with a greater than 5 year return period (Hughes et al. 2012). Similarly, a study of the aftermath from Cyclone Bola (March 1988, east coast North Island) found that substantially more soil disturbance occurred under pine than native forest (84% vs 67% respectively) during that storm (Hicks, 1991). Marden and Rowan (1993) found that while landslide densities increased in mature indigenous forest following Cyclone Bola, indigenous forest was four times less susceptible to land sliding than areas of regenerating scrubland. In general, New Zealand studies have also found that mature native forest is more effective than pine trees for erosion mitigation (Phillips et al. 2000).



Figure 4-2: Examples of understory plant communities in (a) native forest, and (b) mature pine forest.

LCDB data for the Pelorus-Rai catchment show that landslides also occur in native forest, most likely associated with high-intensity rainstorms. These events will deliver substantially more subsoil to rivers than topsoil. Removal of vegetation on harvested pine areas will expose large areas of subsoils to erosion by rainfall and surface runoff and increase the risk of landslides due to progressive loss of root reinforcement of soils. This soil erosion risk persists for several years after these harvested areas are replanted (Phillips et al. 2012). Our finding that topsoil from harvested pine contributes 190 x more sediment than native forest/indigenous forest also demonstrates the importance of harvested hillslopes as a source sediment.

The soil source proportions calculated here may also reflect local hillslopes, with steeper upper catchment areas having a higher proportion of subsoil and bank erosion than the downstream catchments. Higher erosion rates in the upper catchments of the Pelorus-Rai system will also likely reflect rainfall distribution patterns in this part of the Marlborough Sounds (Figure 1-2).

4.3 Sources of sediment accumulating in the inner Pelorus Sound

4.3.1 Marine sediments

The predominance of marine sediment in Mahau Sound is consistent with the hydrodynamics and sediment-transport processes occurring in the Pelorus system. Freshwater discharges during flood events influence the entire Sound (Carter 1976, Vincent et al. 1989, Gibbs et al. 1991). Surface sediment-laden river plumes transport and deposit catchment-derived sediment along the length of the Sound, fringing embayments, and seaward to the entrance to the Sound. Hydrodynamic model simulations by Hadfield (2015) over a 12-month period at half-hour time steps have been used to determine the potential for sediment resuspension in the Pelorus Sound and adjacent Cook Strait coastal marine area. When critical bed shear stress exceeds 0.1 Pascal ($1 \text{ Pa} = 1 \text{ kg m}^{-2} \text{ s}^{-2}$), unconsolidated/ recently deposited cohesive sediment are likely to be resuspended (e.g., Rinehimer et al. 2007, Fall et al. 2014). The model simulation indicates that near-bed shear stresses exerted by tidal currents are sufficient to resuspend cohesive fine-sediment deposits along most of the length of the main channel, as well as around the headlands and islands at the entrance to Pelorus Sound (Hadfield, 2015). Bed shear-stresses in these areas exceed critical values for sediment entrainment a substantial fraction of the time (i.e., 40–80%, Figure 4-3).

The seabed around the headlands and islands along the coast and within the entrance to Pelorus Sound is also periodically exposed to swell waves, with wave periods sufficient to enhance bed-shear stresses exerted by tidal currents. Bed disturbance by locally generated fetch-limited waves is also likely to occur within the inner Sound (Figure 4-4). Thus, tidal currents and waves provide an effective mechanism to resuspend sediment deposits at the seaward end of Pelorus Sound. Resuspended sediment is transported landward to the head of the Sound by estuarine circulation under the low–average flow conditions that predominate (Broekhuizen et al. 2015). This circulation drives a consistent landward-directed inflow in the bottom layer, with time-averaged (over one-year) current speeds of up to 0.1 m s^{-1} near the seabed, with a seaward-directed outflow at the surface ($\sim 0.2 \text{ m s}^{-1}$) (Fig 3.11, Broekhuizen et al. 2015). Under these average conditions, the travel time of near-bed continuously suspended particles from the Pelorus Sound’s seaward entrance to Havelock Estuary is ~ 6.5 days. Estuarine circulation is weaker during periods of low freshwater inflows, which results in residence times of 50–60 days and favours deposition of fine suspended sediments (Broekhuizen et al. 2015). Thus, Carter’s (1976) description of the Pelorus Sound as a “double-ended sediment trap” is very apt.

Disturbance and resuspension of legacy sediment in the outer Pelorus Sound by tidal currents and/or waves is highly likely to be exacerbated by fishing activities associated with scallop dredging and, less frequent, bottom trawling. These activities have occurred historically and in recent years in the outer Sound prior to the moratorium in 2016. Commercial and recreational scallop-dredging intensities were up to 2017 highest in the Tawhitinui and Waitata Reaches (vicinity of Maud Island) of the outer Sound (Halley, 2018). Ongoing bottom trawling occurs from Beatrix Bay to Waiata Beach and beyond the entrance of Pelorus Sound (Halley, 2018). Catch intensity estimates in this area averaged 100 to $400 \text{ kg km}^2 \text{ yr}^{-1}$ for the period 1997 to 2014 (Appendix 5, Baxter, 2018). Thrush and Dayton (2002) review the environmental effects of dredging and trawling on benthic communities.

Hydrodynamic and sediment-transport processes that re-circulate fine sediment, creating a natural sediment trap within Pelorus Sound point to legacy catchment sediment being the most likely ultimate source of the marine sediment accumulating in Mahau Sound. Sediment accumulation rates in Pelorus Sound (i.e., Mahau, Kenepuru, Beatrix Bay) have averaged $2.4\text{--}4 \text{ mm yr}^{-1}$ over the last

century (present study and Handley et al. 2017). These rates are up to ten-fold higher than over the several thousand years prior to large-scale catchment disturbance that followed European settlement in the mid-1800s. Therefore, the increased rate of sediment deposition in Mahau Sound over the last century coincides with large-scale catchment disturbance.

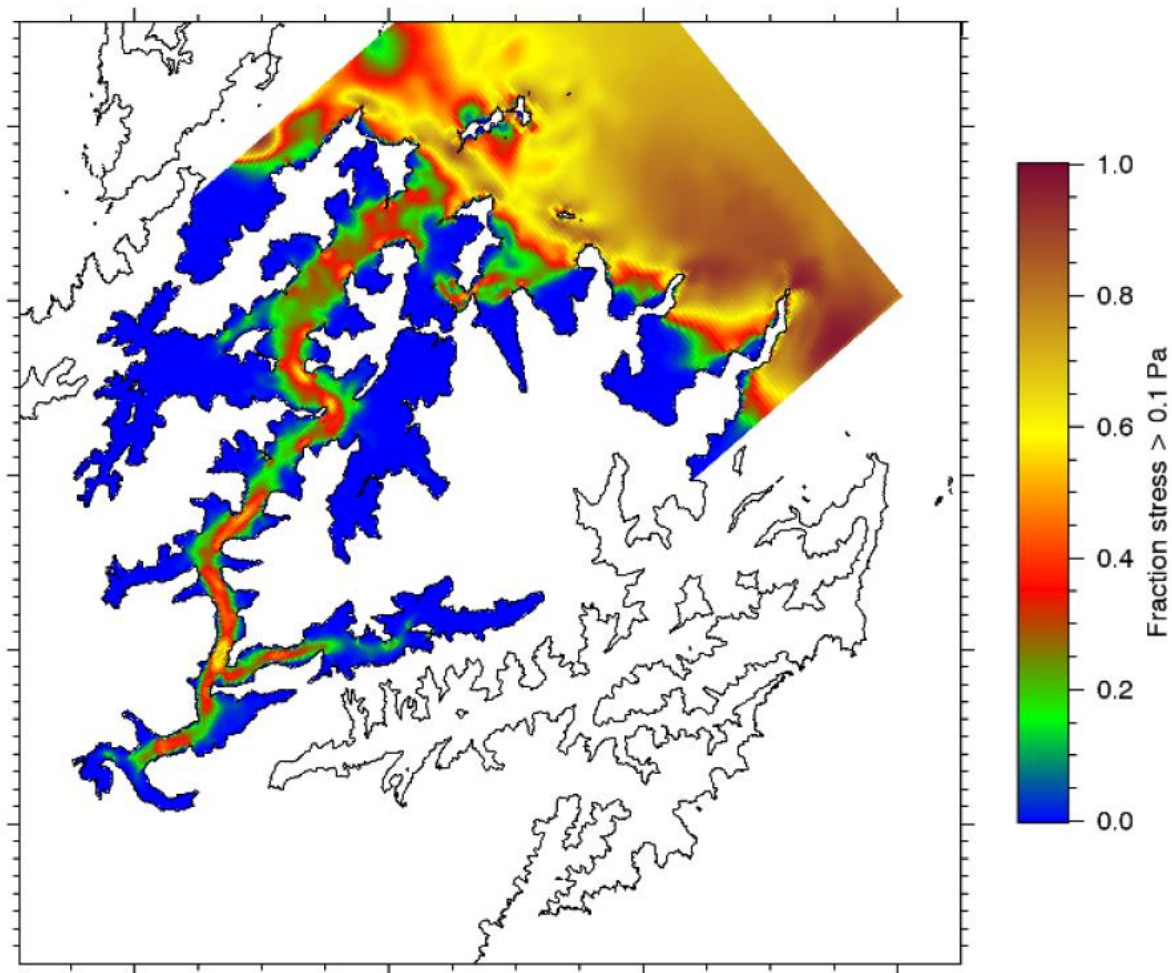


Figure 4-3: Resuspension potential (threshold = 0.1 Pa) for fine sediment in the Marlborough Sounds. The plot shows the fraction of time (0 to 1) during which the modelled bottom shear stress exerted by tidal currents exceeds the threshold value at which sediment entrainment by tidal currents begins. Source: Hadfield (2015).

Potential mechanisms for isotopic enrichment of catchment sediment after deposition in estuarine and marine environments include: (1) in situ primary production by plants (e.g., microphytobenthos, seagrass) (Dalsgaard et al. 2003, Alfaro et al. 2006, Yi et al. 2017), (2) primary production by plants living in/on bed sediment (as above) that is eroded, transported and redeposited elsewhere in the system, and (3) deposition and incorporation of the organic component of marine seston (i.e., dead phytoplankton) into the terrigenous sediment deposits. In the present study, enrichment of legacy catchment sediments deposited in Mahau Sound could potentially occur by all of the mechanisms described above. Fatty acids typically account for 15–25% (C14:0 to C22:6) of the dry biomass of diatoms (single cell algae). The most common FA types found in diatoms include those used in CSSI sediment tracing studies, namely C14:0 and C16:0 (Yi et al. 2017). Carter (1976) also found that the biogenic component of sediment deposits in the outer Sound was primarily composed of individual and colonial diatoms that constitute up to 20–33% of the suspended sediment at the entrance of

Pelorus Sound. Microphytobenthos living in bed sediments typically dominate primary production in shallow estuaries and coastal habitats. Their spatial distribution in estuaries is influenced by light availability at the seabed for photosynthesis. This is primarily influenced by water depth and suspended sediment concentrations (e.g., Thrush et al. 2014, Jones et al. 2017, Pivato et al. 2018).

Handley et al. (2017) determined the $\delta^{13}\text{C}$ FA values for a sediment sample collected from seagrass habitat in Havelock Estuary. The C14:0 FA value for this seagrass sediment was isotopically enriched (i.e., C14:0 -22.4‰ NB: data corrections applied to directly compare with present study) and similar to their sample from the Chetwode Islands (i.e., present study C14:0 mean -23.5‰, SD = 2.3, $n = 6$). The areal extent of seagrass habitat in Pelorus Sound has substantially declined since the 1970s (Bull, 1976), following catchment disturbance and increased sedimentation. Robertson (2019a) reported a 10% (3 ha) decline in seagrass habitat from Havelock Estuary during the period 2014–2019. It is unlikely however that eroded seagrass sediment has substantially contributed to sedimentation in Mahau Sound over the last century. The Estuary has substantially infilled with sediment over the long term, and has continued to function as a net sediment trap over the last 50 years or so (i.e., radioisotope dating, Figure 3-3). The area of seagrass habitat represents only 2% of Havelock Estuary's 8 km² high-tide area. Much of this seagrass habitat is also overlain by soft mud (Robertson, 2019a).

Our conceptual understanding of sediment transport in the Pelorus Sound indicates that isotopically enriched catchment sediment resuspended in the outer Sound is transported into the inner Sound. Isotopic enrichment of catchment sediments deposited in Mahau Sound can also occur by:

- incorporating deposited marine seston (i.e., dead phytoplankton) as well as resuspended inorganic (legacy) sediment transported into the inner Sound by estuarine circulation, and
- in situ primary production and enrichment of catchment sediments by microphytobenthos after deposition in Mahau Sound by microphytobenthos.

The contribution of this latter process is likely to be reduced by the water depth (i.e., 3-4 m below chart datum) and higher suspended sediment concentrations (SSC) in the inner Pelorus Sound. In the outer Sound, water clarity is likely to be higher than in the inner Sound due to lower SSC. Water depths in the outer Sound are typically tens of metres so that suitable areas for microphytobenthos growth will coincide with shallow subtidal banks and flats fringing the channel (e.g., Chetwodes, Foresyth Bay).

Transport of isotopically enriched marine organic matter from the outer to the inner Pelorus Sound is supported by Carter's (1976) observations. Diatom concentrations in suspended sediment at the entrance of Pelorus Sound (i.e., 20–33%) were 10-fold higher than in the inner Sound. The waters of the inner Sound are also consistently the most turbid due to fine sediment discharge from the Pelorus-Rai and Kaituna Rivers. The effects of the catchment sediment load on suspended sediment concentrations in the inner Sound are also enhanced by the substantial import of sediment from the outer Sound by estuarine circulation, as previously described. These considerations suggest that the marine sediment source contribution to deposition in Mahau Sound is substantially composed of isotopically enriched catchment legacy sediments and marine seston.

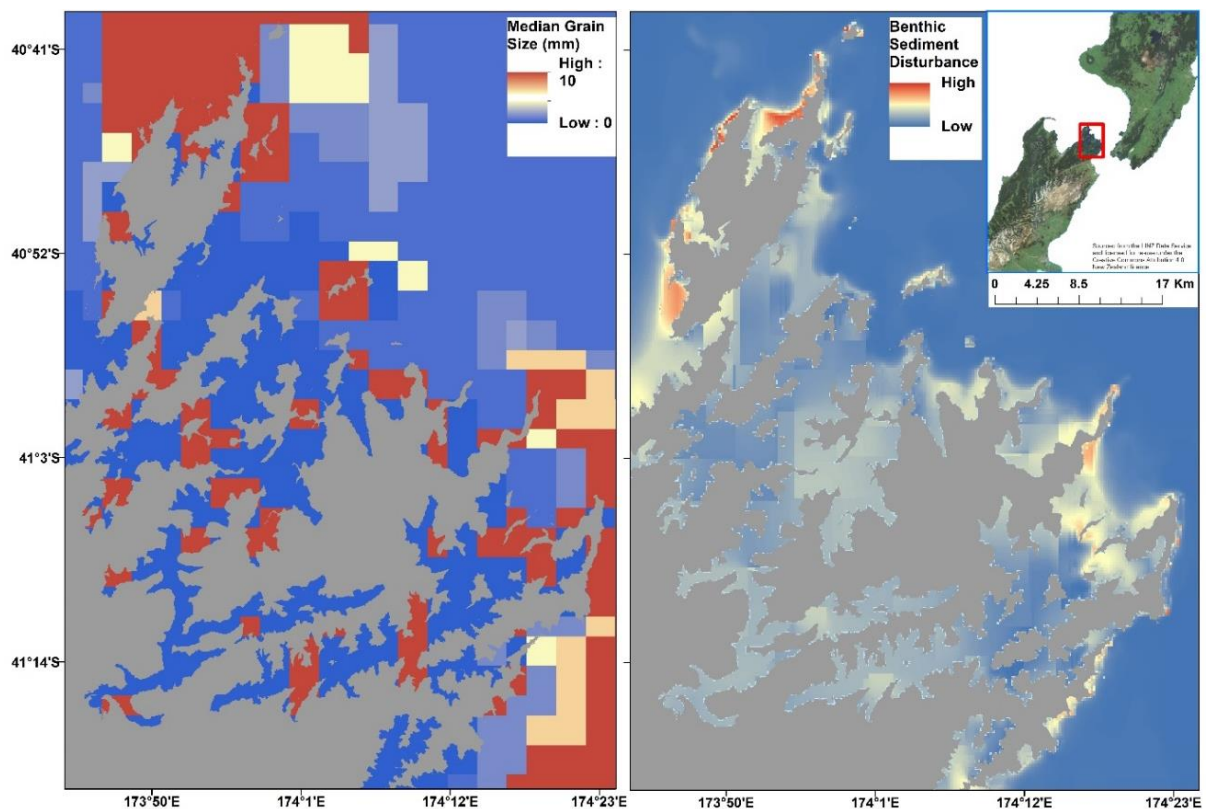


Figure 4-4: Potential for benthic sediment disturbance by waves in the Marlborough Sounds. Analysis based on one year of wave-generated mean friction velocity estimated from hourly surface wave statistics (i.e., significant wave height, peak period). Median particle size (left) and relative bed disturbance potential (right). Data: (1) NZWAVE_NZLAM forecast at 8-km spatial resolution, (2) particle size (median values) at 250-m resolution, (3) water depth at 25-m horizontal resolution. Source: Stephenson et al. (2020).

Water quality monitoring by MDC (July 2012–July 2021) shows that near-surface suspended inorganic solid concentrations in the waters of the inner Pelorus Sound (Median: 6.4 g m^{-3}) are typically three-fold higher than in the outer Sound (Median: 2.5 g m^{-3} , **Appendix K**). Measurements of vertical profiles of water column properties (i.e., conductivity, temperature, turbidity) show that the sediment plumes that disperse through the Sound during river floods (e.g., Figure 1-12) extend through most of the upper water column in the inner Sound (Broekhuizen and Plew, 2018). These consistently higher suspended sediment levels in+ the inner Sound will therefore be less favourable for diatom and seagrass growth due to reduced light availability (i.e., photosynthetically available radiation, PAR).

In the southern Firth of Thames, estuarine muds from the outer Firth of Thames were also found to be important sources of sediment (i.e., 15-27% of total) (Swales et al. 2016a). These isotopically enriched estuarine muds were legacy catchment sediment that had mixed with and/or had been altered over time after deposition by marine primary production.

In the context of sedimentation in Mahau Sound, the preceding observations suggest that the marine sediment is legacy sediment eroded from the entire catchment and deposited in the Pelorus Sound over the last century. Biological processes operating with the Sound have subsequently altered the isotopic signature of this legacy catchment sediment over time. The time scale for isotopic enrichment of catchment sediment in the marine environment is likely to be of the order of years to decades.

4.3.2 The Havelock Inflow – sources

Handley et al. (2017) identified the “Havelock Inflow” as a major source of sediment deposited in Kenepuru Sound and Beatrix Bay (Figure 4-5) over the last several hundred years. This inflow source sediment was sampled from a seagrass meadow in Havelock Estuary, composed of sediment derived from Pelorus and Kaituna Rivers and “the sum total of all sources deposited at the Havelock Estuary delta, that was remobilised by flood scour, waves and tidal currents and transported and deposited at our coring sites over time” (Handley et al. 2017). The inflow source sediment from Handley et al. (2017) has a distinctive highly enriched C14:0 isotopic value (mean -22.4‰) very similar to the marine source in the present study as described above. It is therefore likely that the isotopic signature of the original sediment sources has been overwritten *in situ* by the seagrass.

As discussed in section 4.3.1, it is highly unlikely that eroded seagrass sediments account for the large quantity of marine sediment (i.e., ~70% of total) deposited in Mahau Sound since the early-1900s. Deposition of isotopically enriched “Havelock Inflow” sediment has also occurred in Kenepuru Inlet (i.e., mean ~40%, range 10–80% of source contributions) over last 1,000 years or more (Figure 3-18, Handley et al. 2017). Therefore, deposition of isotopically enriched sediment in Pelorus Sound significantly predates catchment disturbance by people. The Havelock Inflow data has been analysed using the library of catchment and marine sources from the present study. This has enabled the source contributions to the Inflow to be quantified. The modelling indicates that the Havelock Inflow sediment is largely composed of marine (i.e., legacy catchment) sediment as well as marine seston (i.e., dead phytoplankton) transported into the inner Sound by estuarine circulation (mean ~86%) and subsoil (mean ~10%) with total contributions from land use sources being less than 4%. *In situ* isotopic enrichment of seagrass sediment will also occur. The sediment source proportion statistics for this Pelorus Inflow reanalysis are presented in **Appendix K**.

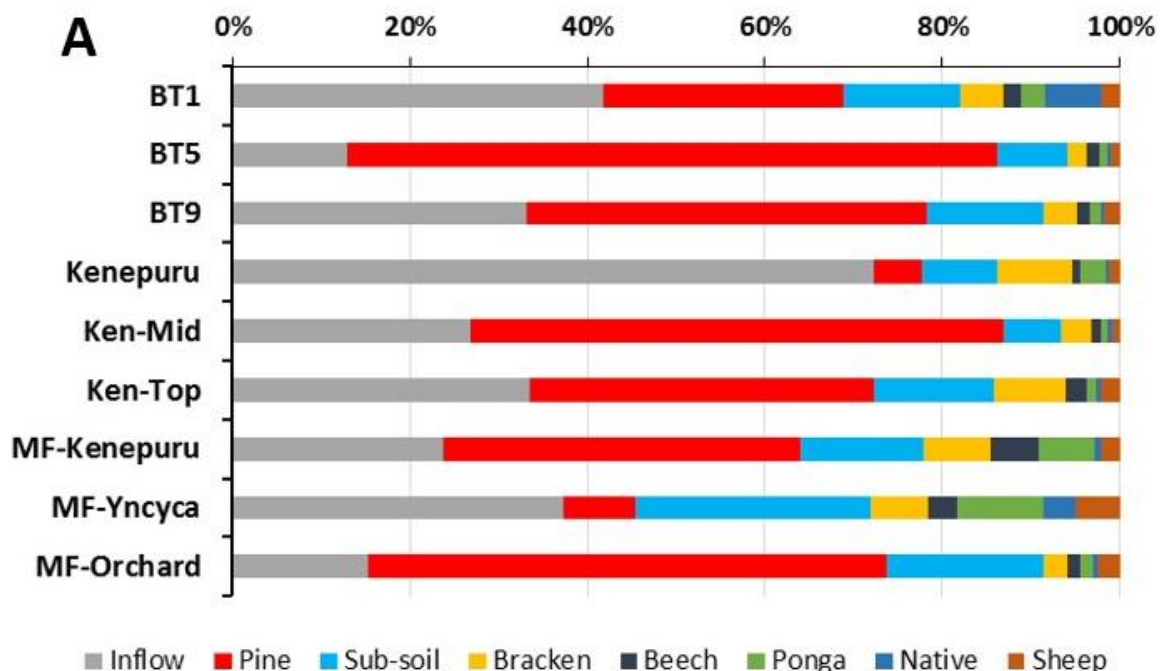


Figure 4-5: Proportional soil contributions from surface sediment from each source. Source: Handley et al. (2017), Figure 3-16.

The analysis of river sediment deposits at the outlets of the Pelorus-Rai (P-R) and Kaituna (K) catchments indicates that eroded streambank sediment (P-R: 31%, K: 45%), subsoil (P-R: 24%, K:

11%), dairy pasture (P-R: 19%, K: 8%) and harvested pine (P-R: 18%, K: 5%) are the major present-day sources of fine sediment discharge to Havelock Estuary (Figure 4-1). The dominance of the marine/legacy source in the Havelock Estuary and Mahau Sound sediment, however, suggests that the present-day catchment sediment contribution is one component of the total annual deposition in the Inner Pelorus Sound.

4.3.3 Subsoils

Subsoils are the largest contributor of catchment-derived sediment depositing in Mahau Sound, averaging 14% to 17% of the total sedimentation across the three core sites. The land use sources of these subsoils cannot be discriminated using the isotopic values of the FA biotracers. These subsoils are, however, likely to be derived from erosion associated with land uses where vegetation removal/soil disturbance occurs and predominantly from steepland areas with bare or sparse vegetation cover, and remobilised legacy sediment deposits temporarily stored in the catchment system. Subsoils at these sites are exposed to erosion by rainfall impact, surface runoff as well as landslides during high-intensity rainfall events (e.g., Basher, 2013, Phillips et al. 2012). Landslides caused by hillslope failures during episodic high-intensity rainstorms will also deliver subsoils to rivers. The LCDB-5 (2018) data (Figure 4-6) indicates that landslides, covering a total area of 0.24 km² (Pelorus-Rai, Kaituna and Cullens Creek catchments) primarily occur in native forest. Disturbed catchment areas with sparse vegetation and/or bare soils cover several tens of square kilometres in the Pelorus-Rai, Kaituna and Cullens Creek catchments. These areas include harvested pine forest (16.5 km²), gorse and broom (9 km²) and erosion hotspots on steepland areas of low producing grassland (50 km²). Roads can also be substantial sources of eroded subsoils (Motha et al. 2003, 2004) and forestry roads may contribute disproportionately to erosion and slips (Fahey and Coker, 1992). Public roads constructed over unstable slopes bordering the Marlborough Sounds also contribute to soil erosion. Miller (2015) documents the contribution of cuttings and sidecast (loose fill) and uncompacted material to slips on the Picton to Linkwater road. An estimated 67,000 m³ of soils and subsoils was eroded from twelve slips along a 21 km section of this road during the period 1985 to 2010 alone.

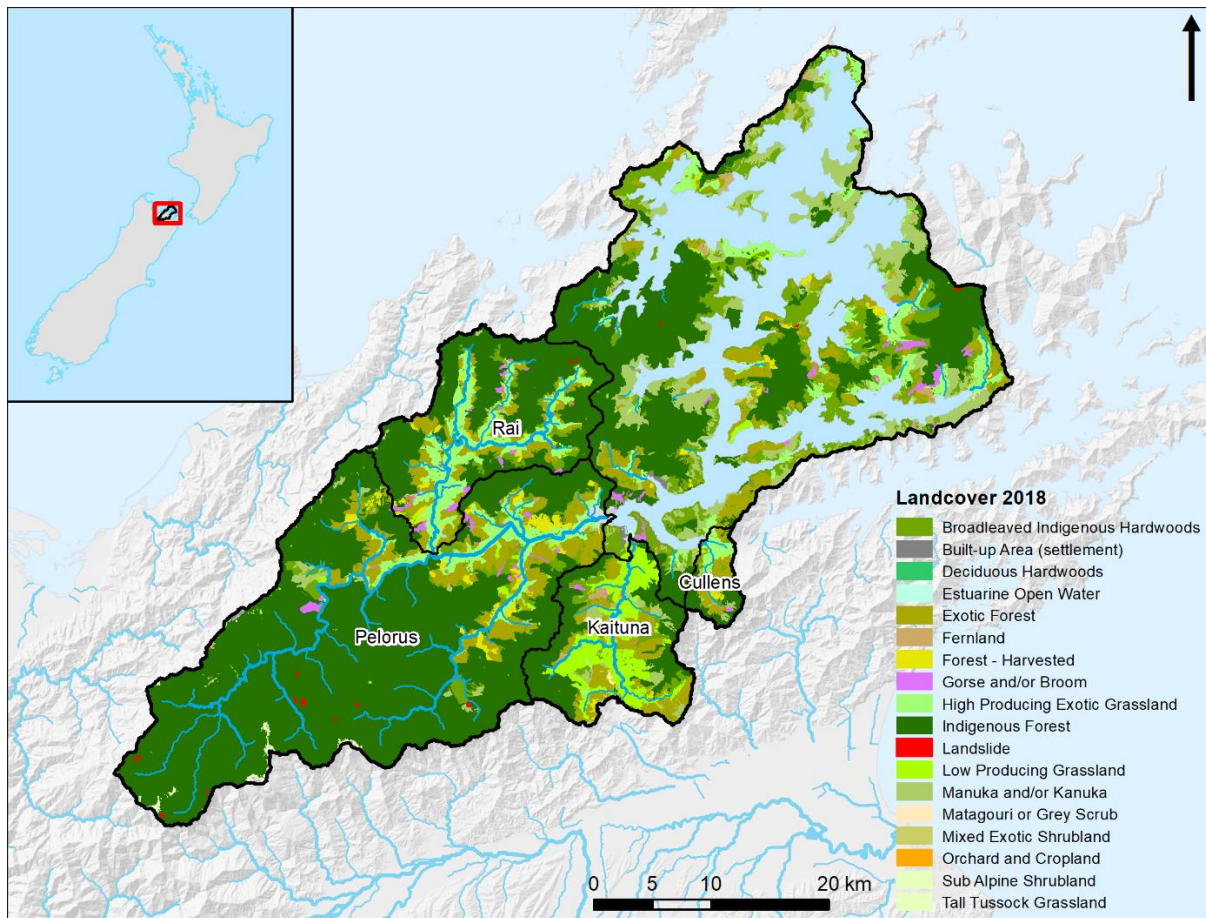


Figure 4-6: LCDB Version 5 (2018) – landcover in the Pelorus Sound catchment.

4.3.4 Streambank sediment

Streambank erosion is the second largest source of catchment-derived sediment accumulating in Mahau Sound, accounting for 8 to 10% of the total. This eroded streambank sediment is itself largely composed of topsoils, subsoils and river sediment from various upstream sources, including sediments eroded over the last ~150 years following large-scale deforestation. The source polygons for the isotopic biplots show that streambank source forms an endmember (Figure 2-11 and Figure 2-12). We speculate that this occurs because the FA biomarkers excreted into the sediment deposits by the streambank plant community continuously “over-writes” the original isotopic signatures of the source soil and sediment after deposition.

4.3.5 Land use sources

Native forest and harvested pine forest (post-1979/1980) account for similar, relatively small proportions of the sediment accumulation in Mahau Sound, averaging 1.8–2.3% of the total. Sediment contributions from Kanuka scrub average 1.2–1.6% and the Scrub and Pasture (combined sources) 1.1–1.3%. Although these sources account for relatively small fraction of the total when the marine source (legacy sediment) is included, large differences in land use areas suggest that sediment yields vary markedly. Total catchment areas for the entire Pelorus Sound system used to estimate land use yields (i.e., LCDB-4) were native forest (936 km²), kanuka/manuka (126 km²), gorse and broom (16.8 km²) and pine harvest (25.9 km²).

Sediment contributions from disturbed catchment land use sources for the entire catchment area of Pelorus Sound relative to native/indigenous forest (2001 – 2012) were based on the average sediment source proportions. This approach was considered most appropriate given the wide-spread dispersal of fine suspended sediment throughout Pelorus Sound by river plumes, tidal currents and estuarine circulation. Data from LCDB versions 2 to 4 (i.e., 2001/2002–2012/13), coincided with dated sediment core layers and their calculated sediment source proportions. Data from LCDB-1 (1996/97) was not included as it does not include harvested pine as a separate land use class. The source proportion yields (% km⁻²) for the disturbed catchment land uses were normalised by the matching values (i.e., year and core) for the native forest (% km⁻²) to enable direct comparisons of the source yields relative to native forest. The calculations of the average source proportion yield ratios relative to native forest are summarised in Table 3-8.

The results suggest that sediment accumulating in the Mahau Sound since the early-1980s (i.e., first rotation harvest) and directly associated with land use activities are disproportionately sourced from harvested pine areas.

4.4 Mollusc death assemblage

Although the Mahau Sound used to support a scallop bed, there was a surprising lack of scallop shells (*Pecten novaezelandiae*) in our sediment cores. The Mahau Sound was one of the first areas in Marlborough to be fished commercially for scallops, starting in 1968 (B. Falconer pers. comm.). The bed was very productive but short lived and never recovered from the initial harvest. The lack of scallop shells in our cores likely reflects that the cores were collected inside the shallower head of the bay, whereas the scallop bed was more offshore, toward the channel (Handley et al. 2017).

The occurrence of large cockles or tuangi (diameter >5 cm) in sediments deposited in pre-human times is significant, indicating that the seabed was likely more stable and less turbid. Cockles often occur in conjunction with subtidal seagrass in a mutualistic relationship. Cockles are also important in starting and maintaining facilitation cascades, where the occurrence of one species allows for the colonisation of other species, including macroalgae (Thomsen et al. 2016, Gribben et al. 2019). Large cockles living subtidally are now rare in the Marlborough Sounds, but they have previously been identified in Deep Bay and Hitaua Bay in Tory Channel (Davidson et al. 2019a, b).

As with the previous report (Handley et al. 2017), the results of work in Mahau Sound showed profound changes to sedimentation rates and shellfish composition since Māori and European settlements. Post-human SAR are an order of magnitude greater than pre-human SAR, however, unlike in the Kenepuru Sound, where shell deposition increased up until the 1950s, analyses of the mollusc death assemblage from the Mahau cores showed a decline in shell deposition (mostly large subtidal filter-feeding cockles/tuangi) following the arrival of Māori in ca. 1300 AD and potentially affected by early European land clearances and mining activities. This decline was correlated with increasing sediment accumulation rates and associated clay content, especially following European arrival in ca. 1860. The functional feeding diversity also declined after this period, with deposit-feeding species becoming more common and forming a greater proportion of the total species composition during the human period. Mollusc species diversity has declined to its lowest point in surficial sediment (1975– 2018).

Additional questions posed by MDC

Marlborough District Council posed several additional questions related to the effects of large storms on estuary sedimentation and potential time lags in storm-sediment delivery (section 1.2). These questions are addressed here.

Can the effects of large storms since 2001 be detected in estuarine sediment?

Several high-intensity rainfall events causing floods that exceeded a 1-in-2-year annual return interval (ARI) have occurred since 2001, in particular 2006, 2008, 2010, 2011 (two events) and 2016. More localised rainfall events are evident in different years (**Appendix A**).

Evidence of these large storms (post-2001) were not detected in the Mahau Sound cores (i.e., SAR and sediment composition). This reflects the temporal resolution of the core records and relatively uniform characteristics of the fine sediment accumulating in Mahau Sound. Factors that influence temporal resolution of the cores include in-situ surface mixing of the sediment deposits, sediment sampling and curve-fitting for dating. Surface-mixed layers (SML i.e., ^7Be), extending to several centimetres' depth, indicate sediment mixing over time scales of weeks to months, surface residence times of several years, followed by progressive burial. The cores were subsampled in one-centimetre thick slices at depth increments to provide sufficient discrete sediment samples for dating (i.e., radioisotope activity). In the Mahau Sound, each 1-cm thick sample represents 0.8 – 2.5 years of average sedimentation from which bulk radioisotope activities are determined, with a resulting loss of fine-scale temporal resolution. Fitting of natural-log – linear profiles to excess ^{210}Pb data is used to calculate SAR estimate over a depth increment below the SML. This again results in time-averaging of the data. These ^{210}Pb SAR were validated using the maximum depth of ^{137}Cs in each core. Based on ^{210}Pb dating, the post-2001 sediment record is contained within the top-most 6–12 cm of the Mahau cores.

Particle size analysis of sediment within these post-2001 sediment was limited to two sampled depth increments (0–1, 4–5 cm). These data did not indicate significant changes in either mud content or particle size. The longer-term record of sedimentation in Mahau Sound and Kenepuru Inlet (Handley et al. 2017) shows that mud-rich sediments have accumulated in the Mahau Sound for at least the last 2,000 years and 3,400 years in Kenepuru Sound (Handley et al. 2017). As previously discussed, this predominance of mud deposition reflects catchment soils that are primarily composed of silt and silt-clay loams with up to 45% clay content (section 4.1). In the Pelorus system, gravel and sand accumulate in the river channels, whereas the finer silt and mud are largely discharged to Pelorus Sound. Hence, the uniformly muddy sediment delivered to the Sound, as well as surface sediment mixing indicated by radioisotope profiles, do not preserve recognisable flood deposits in the estuarine sedimentary record.

What is the relative contribution of these storm events to overall sedimentation?

Although evidence of recent large storms (post-2001) were not detected in the Mahau Sound cores, New Zealand studies show that annual catchment sediment yields are dominated by storm events (e.g., Hicks et al. 2000, Basher et al. 2011, Hughes et al. 2012). Consequently, sediment transport during river floods will dominate sedimentation in receiving marine environments. Degradation of estuarine and coastal marine receiving habitats and ecosystems due to sedimentation has been driven by deposition of fine sediment consisting of clays and silts (diameter ≤ 62.5 microns).

Is there a time-lag in sediment transport from large storms?

Here we consider the potential time-lag in sediment transport [to inner Pelorus Sound] during large storms. New Zealand studies show that annual sediment yields are dominated by storm events (e.g., Hicks et al. 2000, Basher et al. 2011, Hughes et al. 2012), so that sediment transport during river floods will dominate sedimentation in receiving marine environments. The majority of New Zealand catchments are relatively small, so time lags in sediment delivery to estuaries and coastal marine systems will primarily depend on sediment characteristics. During storms, suspended sediment loads consist of fine sediment (mud), consisting of clays and silts (diameter $\leq 62.5 \mu\text{m}$), as well as sand particles (diameter $62.5\text{--}2000 \mu\text{m}$). Time scales for sediment delivery from the catchments discharging to the inner Pelorus Sound will vary primarily due to sediment type.

Fine suspended sediment loads in rivers consists of clays and silts derived from eroded catchment soils. Degradation of estuarine and coastal marine receiving habitats and ecosystems is largely driven by deposition of fine sediment (e.g., Thrush et al. 2004). Fine sediment is readily maintained in suspension in rivers due to their relatively low settling velocities (i.e., $0.1\text{--}2 \text{ mm s}^{-1}$ [quartz], Vanoni, 2006). Mass transport rates of fine sediment in a river are primarily determined by water velocity and suspended sediment concentration. Consequently, a large fraction of this fine sediment will be discharged from the catchment outlet during a flood event (i.e., hours to days), unless retained in a catchment sediment sink during over-bank flow conditions (e.g., flood plain, vegetated areas). Suspended sediment loads transported during flood events also typically include sand-size particles, with settling velocities up to $\sim 30 \text{ cm s}^{-1}$ (quartz). As a rule-of-thumb, sand particles will be retained in suspension when the particle settling velocity exceeds the shear velocity (i.e., function of shear stress) and are transported at the water velocity while suspended. Down-channel variations in flow conditions as well as temporal variations in river (flood) discharge will therefore result in cycles of sand deposition and resuspension, so that sand mass transport rates will typically be lower than those of fine sediment.

Thresholds for sediment entrainment, transport and deposition in rivers as a function of particle size and flow velocity have been described by the Hjulström Curve (Figure 4-7) (e.g., Baring 2011). The Hjulström curve shows that fine sediment (i.e., clay and silt) require much higher flow velocities to erode than to deposit. Again, this demonstrates that the bulk of fine sediment is likely to be transported along the entire length of a river channel network to the catchment outlet without depositing, unless they are trapped in low-energy environments (e.g., riverbank vegetation, flood plain depressions).

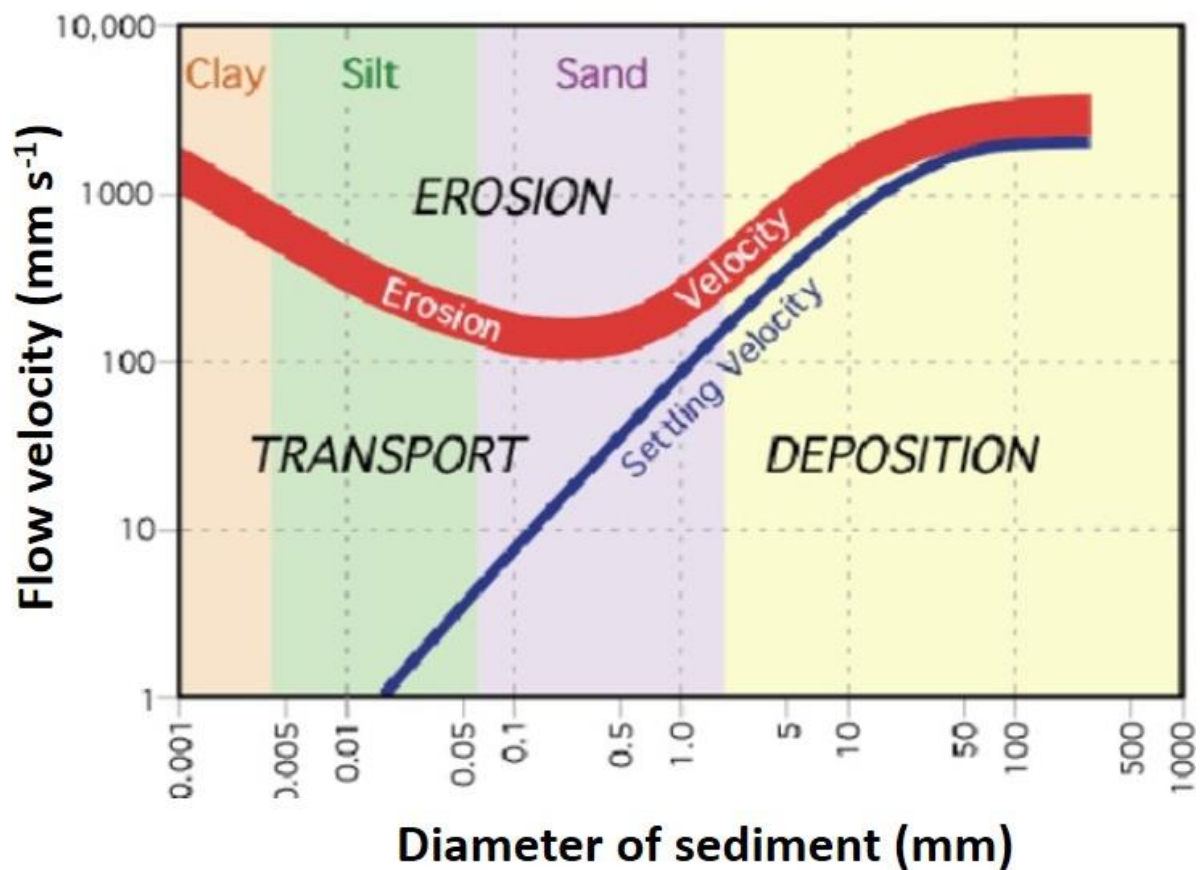


Figure 4-7: Hjulström Curve. Relationship between erosion, deposition and transport as controlled by flow velocity and particle size. Source: Baring (2011).

Data for the Mahau and Kenepuru cores (Handley et al. 2017) show that deposits are composed entirely of fine sediment and that this mud-dominated system has persisted for at least the last several-thousand years. Gravel, sand and muddy-sands have built extensive intertidal flats on the deltas of the Pelorus-Rai and Kaituna Rivers, where they discharge into Havelock Estuary (Figure 1-13). These observations indicate that coarse sediment is trapped within the estuary whereas fine sediment is largely delivered during storms and exported to quiescent subtidal environments in Pelorus Sound where they accumulate.

5 Concluding remarks

This study has provided new insights on sedimentation and the sources of sediment accumulating in the rivers and marine environment of the inner Pelorus Sound/Te Hoiere. It has revealed the cumulative effect of intensive land use in the contributing catchments over historical time. These effects have ranged in scale, from localised impacts on cockle beds from early Māori and European land clearances and mining activities surrounding Mahau Sound, and extensive catchment-wide soil erosion and sedimentation since European settlement. Gold mining, native forest timber clearance, pastoral farming, and more recent widespread harvesting of radiata pine plantations (~1980–present), have all left their legacy in the inner Pelorus Sound. A recurring theme underlying the ten-fold increase in the sediment accumulation rates over the past 100 or so years is that removal of forest and associated soil disturbance from slips, road and track cutting, particularly on hill country exacerbates sediment yields. This information will be valuable to catchment managers and communities working alongside each other in the Te Hoiere restoration project in determining outcomes for the land and coastal environments.

5.1 Legacy sediment and future management

The issue of legacy sediments and how to manage their environmental effects, has been highlighted by this study. Legacy sediments associated with catchment deforestation, mining, and burning (mid-late-1800s) have accumulated as flood plain deposits and throughout Pelorus Sound. This historical catchment disturbance and subsequent land use activities resulted in a ten-fold increase in sediment accumulation rates relative to the previous several thousand years. It is likely that legacy sediments will continue to be a major sediment source for decades to come. Do these order of magnitude increases in sedimentation and resulting effects on aquatic receiving environments render future improvements in land management in the catchment of Pelorus Sound largely ineffectual? To address this question and to identify how the problem of soil erosion and sediment effects may be better managed, it is important to consider cumulative and multiple-stressor effects and broader impacts of human activities on the Pelorus/Te Hoiere system. As well as that, what is a realistic timeframe for restoration?

Fine sediments exert several adverse environmental effects in aquatic receiving environments, both while suspended and after deposition (e.g., Thrush et al. 2004). In rivers and estuaries, sediments reduce visual water clarity, reduce light availability for plant primary production, and smother benthic communities. Soil erosion has also reduced soil fertility due to loss of carbon and nutrients (Schipper et al, 2010) that are exported with sediment to the marine environment. Thus, excessive soil erosion has a cost for both productivity on the land as well as substantial adverse effects in receiving environments. These considerations indicate that implementing improved land management and environmental restoration will have a number of long-term benefits for the Pelorus/ Te Hoiere system.

In rivers, fine sediments degrade habitats by reducing periphyton (food) quantity and productivity, and clogging of interstitial and hyporheic spaces (i.e., within the riverbed) habitat and food resources. This is particularly the case in gravel bed rivers, such as the Pelorus-Rai River. Reduced interstitial flow in riverbeds due to sedimentation can reduce the exchange of organic matter, nutrients and dissolved oxygen and concomitant impoverishment of invertebrate communities (Wood and Armitage, 1996, Mathers et al. 2014). These sediment effects reduce the abundance and diversity of sediment-sensitive invertebrates that underpin river food webs. In the Pelorus system, most of the fine sediment delivered to rivers appears to be exported to the inner Pelorus Sound

during flood events. A proportion of previously eroded soils (i.e., legacy sediments) are however stored in the floodplain. Bank erosion subsequently mobilises these floodplain legacy sediments as well as more recent flood deposits into the river network, as well as constituting a major source of the sediment that accumulates in Mahau Sound, accounting for 8–10% of the total. Effective catchment management activities that include improved land management to reduce soil loss from hillslopes and identifying and managing bank erosion could measurably reduce fine-sediment yields.

In estuaries, adequate visual clarity of water is important to fish and birds for finding prey, as well as for human recreational use. Light penetration into estuarine waters controls the depth of the euphotic zone and therefore the growth and survival of benthic algae and seagrasses, that in turn support food webs and fisheries. Fine sediments also transport other pollutants associated with land use (i.e., microbes, heavy metals, organic compounds, pesticides). Microbial pollution associated with farm animals and sewage/wastewater is primarily delivered to estuaries by river plumes conveying storm waters from runoff. Microbial pollution fundamentally degrades the value of estuaries as food baskets for Iwi and the wider community. Satellite images show that silt-laden river plumes discharged into Havelock Estuary are dispersed throughout Pelorus Sound so that the effects of fine sediment are widespread. Water quality monitoring by MDC also shows that suspended sediment concentrations are consistently higher in the inner Pelorus Sound than in the outer Sound. Loss of seagrass and shellfish from Pelorus Sound is typical of the effects of deposited fine sediments on sensitive benthic plants and animals in other NZ estuaries (Thrush et al., 2004).

Cumulative and multiple stressors cause tipping points in ecological functions and can maintain ecosystems in a highly degraded and altered state. Stressors in Pelorus Sound include excessive sedimentation, seabed disturbance related to fishing activities, as well as the global effects of increasing sea-surface temperatures, rising sea-levels and decreasing pH (i.e., acidification) of marine waters (Handley et al. 2020b, Urlich and Handley, 2020). In addition to excessive sedimentation over the past ~150 years, indicators of degradation include loss of shellfish diversity, large reductions in seagrass cover and kelp, and declines in mussel spat catch, recovery of wild mussel beds, fish abundance (i.e., flatfish, blue cod, rig, snapper, hāpuku), rock lobster, and large rare invertebrates (Handley et al. 2020b, Urlich and Handley, 2020). The damage caused by these cumulative and multiple stressors has left legacies that affect the ecosystems we see today. These stressors need to be addressed in a systematic and integrated way, through the ongoing development and implementation of an Ecosystem-Based Management approach (Urlich and Handley, 2020). Reversing this past damage will take decades, but if we do not start on that journey then there will be no fundamental change. More concerning, the present degraded state of the Pelorus Sound leaves its coastal ecosystems more vulnerable and less resilient to the effects of climate change, manifested by increasing sea-surface temperatures, rising sea-levels and decreasing pH (Urlich and Handley, 2020).

Biodiversity worldwide continues to decline across a wide range of ecosystems (Isbell et al. 2017). Iwi and stakeholders need measures of both long-term and recent environmental changes to understand how stressors have impinged on ecosystem services which affect the social license of primary industries to operate (e.g., Leith et al. 2014). Regardless of whether individual operators are contributing to 'death by a thousand cuts', it is in the interest of primary industries, resource managers and communities that environmental monitoring and metrics are adequate to safeguard ecosystems from 'tipping points' that may significantly impact on ecosystems and the industries and communities they support. This is because the socioeconomic implications of trying to restore a system that has passed a tipping point will likely be costlier and more unpredictable due to long time

lags (i.e., decades) in the recovery of a system to a former stable state (Selkoe et al. 2015). The ongoing global environmental changes expected due to climate change may amplify the consequences of declining biodiversity (e.g. Baert et al. 2018, PCE, 2020). Climate change, along with uncertainties in the cumulative effects of stressors, including sediments, there is therefore a need for land and coastal managers to adopt a precautionary approach to protect estuaries. In the context of the present study, this includes action to adopt land management practices that reduce soil erosion and sediment loads delivered to Pelorus Sound/ Te Hoiere.

Pelorus Sound/Te Hoiere is valued by the people of Marlborough for its natural character, marine habitats, recreational opportunities, economic and social values, and its cultural significance. As this study has shown, these values have been impacted by a century and a half of land-use intensification that has increased sediment, nutrient and microbial loads to the Sound. Marine activities, including dredging and bottom trawling have also disturbed or degraded benthic ecosystems (Robertson and Stevens, 2009, Handley et al., 2017, Ulrich and Handley, 2020b). Integrated catchment and marine management of the Pelorus/Te Hoiere will be required to halt further degradation and realise measurable improvements in the system's environmental state (NPS-FM, 2020) within a generation. The Pelorus/Te Hoiere restoration project provides a platform for the community to come together and begin that process.

6 Acknowledgements

The authors gratefully acknowledge the contributions of several former and present MDC staff: Ms Nicky Eade (Environmental Scientist – Land Resources) liaised with local landowners and assisted with catchment soil sampling, Mr Oliver Wade (MDC Coastal Scientist) and Captain Luke Grogan (MDC Harbour Master) for assistance with sampling of marine sediment at the Chetwode islands. International expert review conducted by Associate-Professor Claudio Bravo Linares (Laboratory of Organic Chemistry and Environmental Forensics, Austral University of Chile). Mr Bruce Lines and his team (Diver Services Ltd, Nelson) undertook sediment coring in Havelock Estuary and Mahau Sound. We thank the landowners in the Pelorus-Rai and Kaituna Catchments who allowed us to sample soils on their properties. Mr Eric Huddleston kindly provided historical photos of the Rai-Whangamoa State Forest that are reproduced in this report. Max Oulton provided cartographic services. Andrew Swales thanks Drs Niall Broekhuizen, Drew Lohrer and Brian Smith (NIWA) for helpful discussions. Ms Stephanie Watson (NIWA) processed GIS layers to create Figure 4-4 (potential benthic disturbance by waves). We also thank Dr Ben Robertson – for reproduction of Figure 1-13 (source: Robertson 2019a). Dr Chris Yarnes (University of California Stable Isotope Facility) undertook the Isotope Ratio Mass Spectrometry of the derivatized fatty acid samples. We also thank Dr Sarah Bury, Ms Julie Brown and the team at NIWA's Greta Point Stable Isotope Facility for bulk-carbon stable isotope analyses. Dr Michael Lechermann and Oksana Golovko (ESR Environmental Radioactivity Laboratory) conducted the gamma spectrometry on sediment core samples for dating.

7 References

- Alewell, C., Birkholz, A., Meusburger, K., Schindler Wildhaber, Y., Mabit, L. (2016) Quantitative sediment source attribution with compound-specific isotope analysis in a C3 plant-dominated catchment (central Switzerland). *Biogeosciences*, 13: 1587–1596.
- Alfaro, A.C., Thomas, F., Sergent, L., Duxbury, M. (2006) Identification of trophic interactions within and estuarine food web (northern New Zealand) using fatty acid biomarkers and stable isotopes. *Estuarine, Coastal and Shelf Science*, 70: 271–286.
- Anderson, M.J., Langton, R.W., Clarke, K.R. (2008) PERMANOVA+ for PRIMER. Guide to software and statistical methods. PRIMER-E, Plymouth, UK.
- Anderson M.J, Willis, T.J. (2003). Canonical analysis of principal coordinates: a useful method of constrained ordination for ecology. *Ecology* 84(2): 511–525.
- Baert, J.M., Eisenhauer, N., Janssen, C.R., De Laender, F. (2018) Biodiversity effects on ecosystem functioning respond unimodally to environmental stress. *Ecology Letters*, 0(0). doi:10.1111/ele.13088
- Baring, N. (2011) Access Geography week 7: Lesson 4: river features section 33. Downloaded from internet site <https://www.slideshare.net/blueboyneda/lesson-4-river-features>
- Bargh, B.J. (1977) *Possible effects of forest harvesting operations in the Brown River catchment on water quality and implications for downstream wildlife, recreation and other uses*. Marlborough Catchment and Regional Water Board Report. Blenheim.
- Basher, L.R., Hicks, D.M., Clapp, B., Hewitt, T. (2011) Sediment yield response to large storm events and forest harvesting, Motueka River, New Zealand. *Journal of Marine and Freshwater Research*, 45(3): 333–356.
- Basher, L.R. (2013) Erosion processes and their control in New Zealand. In: *Dymond J.R. (ed.) Ecosystem services in New Zealand – conditions and trends*. Manaaki Whenua Press, Lincoln, New Zealand: 363–378.
- Baxter, A.S. (2018). Statement of Evidence of Andrew Stephen Baxter on Behalf of the Minister of Conservation regarding marine pressures and ecologically significant marine sites, 2 February 2018. Before the Marlborough District Council. In the matter of the RMA 1991 and the proposed Marlborough Environment Plan – Topic 6 Indigenous Biodiversity, 43 p. Department of Conservation.
- Beggs, J.P. (1962) Farming in Marlborough. *Proceedings of the New Zealand Grassland Association* 24(18): 28.
- Bentley, S.J., Swales, A., Pyeson, B., Dawe, J. (2014) Sedimentation, bioturbation and sedimentary fabric evolution on a modern mesotidal mudflat: a multi-tracer study of processes, rates and scales. *Estuarine, Coastal and Shelf Science* 141: 58–68.
- Blake, W.H., Ficken, K.J., Taylor, P., Russell, M.A., Walling, D.E. (2012). Tracing crop-specific sediment sources in agricultural catchments. *Geomorphology* 139: 3222–329.

- Booker, D.J., Whitehead, A.L. (2017) NZ River Maps: An interactive online tool for mapping predicted freshwater variables across New Zealand. NIWA, Christchurch.
<https://shiny.niwa.co.nz/nzrivermaps/>
- Bourbonniere, R.A., Meyers, P.A. (1996) Sedimentary geolipid records of historical changes in the watersheds and productivities of Lakes Ontario and Erie. *Limnology and Oceanography* 41(2): 352–359.
- Bowie, L.J.S. (1963) Land utilisation in the Marlborough Sounds. *Unpublished MA thesis*. University of Canterbury.
- Bray, J.R. (1991) Growth, biomass, and productivity of a bracken (*Pteridium esculentum*) infested pasture in Marlborough Sounds, New Zealand. *New Zealand Journal of Botany* 29: 169–176.
- Brayshaw, N.H. (1964) *Canvas and gold: a history of the Wakamarina goldfields and lower Pelorus Valley*. Blenheim, Brayshaw: 253.
- Broekhuizen, N., Hadfield, M., Plew, D. (2015) A biophysical model for the Marlborough Sounds, Part 2: Pelorus Sound. *NIWA Christchurch*. CHC2014-130. (Version 2 dated 10 June 2015).
- Broekhuizen, N., Plew, D. (2018) Marlborough Sounds Water Quality Monitoring: review of Marlborough District Council monitoring data 2011-2018. Hamilton, National Institute for Water and Atmospheric Research Ltd: 186.
- Carter, L. (1976) Seston transport and deposition in Pelorus Sound, South Island, New Zealand. *New Zealand Journal of Marine and Freshwater Research* 10(2): 263–282.
- Challis, A.J. (1991) Archaeological research and management strategy: The Nelson-Marlborough Region. *Department of Conservation*: 41.
- Chappell, P.R. (2016) The climate and weather of Marlborough. *NIWA Science and Technology Series* 69.
- Clark, K.J., Hayward, B.W., Cochran, U.A., Wallace, L.M., Power, W.L., Sabaa, A.T. (2015) Evidence for past subduction earthquakes at a plate boundary with widespread upper plate faulting: southern Hikurangi Margin, New Zealand. *Bulletin of the Seismological Society of America*, 105: 1661-1690.
- Clarke, K.R., Gorley, R.N. (2015). PRIMER v7: User Manual/Tutorial software package. PRIMER-E Ltd, 296 Coker, R.J. (1994) Sedimentation and forest harvesting in the Marlborough Sounds. A report prepared in partial fulfillment of the degree of Master of Forestry Science at the University of Canterbury: 37.
- Cotton C.A. (1955). *New Zealand geomorphology: reprints of selected papers 1912–1925*. Wellington, New Zealand University Press.
- Dalsgaard, J., St. John, M., Kattner, G., Müller-Navarra, D., Hagen, W. (2003) Fatty acid trophic markers in the pelagic marine environment. *Advances in Marine Biology*, 46: 225–340.

- Davidson, R., Baxter, A., Duffy, C., Handley, S., Gaze, P., Fresne, S.D., Courtney, S. (2019a) Expert panel review of selected significant marine sites surveyed during the summer of 2018-2019 – Research, survey and monitoring report number 972. Davidson Environmental, A report prepared for: Marlborough District Council and Department of Conservation C/o Seymour Square Blenheim: 33.
- Davidson, R.J., Rayes, C.T., Scott-Simmonds (2019b) Re-survey of subtidal cockles located at the head of Deep Bay, Tory Channel. Prepared by Davidson Environmental Ltd. for Marlborough District Council. *Survey and monitoring report* 934.
- de Rose, R.C., Trustrum, N.A., Blaschke, P.M. (1993). Post-deforestation soil loss from steep land hillslopes in Taranaki. *Earth Surface Processes and Landforms* 18(2): 131–144.
- Didyk, B.M., Simoneit, B.R.T., Brassell, S.C., Eglinton, G. (1978) Organic geochemical indicators of palaeoenvironmental conditions of sedimentation. *Nature* 272: 216–222.
- Drury, A. (1854) *Revised sailing directions for the northern part of the colony of New Zealand*. Williamson and Wilson. Auckland.
- Department of Scientific and Industrial Research (1968). General survey of the soils of South Island, New Zealand. *DSIR Soil Bureau Bulletin* 27. Wellington.
<https://doi.org/10.7931/dl1-sbb-027>
- Eklöf, J., Austin, Å., Bergström, U., Donadi, S., Eriksson, B.D., Hansen, J., Sundblad, G. (2017). Size matters: relationships between body size and body mass of common coastal, aquatic invertebrates in the Baltic Sea. *PeerJ*, 5: e2906.
- Eyles, G., Fahey, B. (2006) The Pakuratahi Land Use Study: A 12-year paired catchment study of the environmental effects of *Pinus radiata* forestry. *Landcare report* to Hawke's Bay Regional Council: 128.
- Fahey, B.D., Coker, R.J. (1992) Sediment production from forest roads in Queen Charlotte Forest and potential impact on marine water quality, Marlborough Sounds, New Zealand. *New Zealand Journal of Marine and Freshwater Research*, 26(2): 187-195.
- Gibbs, M., James, M., Pickmere, S., Woods, P., Shakespeare, B., Hickman, R., Illingworth, J. (1991) Hydrodynamic and water column properties at six stations associated with mussel farming in Pelorus Sound, 1984–85. *New Zealand journal of marine and freshwater research*, 25(3): 239-254.
- Gibbs, M. (2008) Identifying source soils in contemporary estuarine sediments: a new compound specific isotope method. *Estuaries and Coasts*, 31: 344–359.
- Gibbs, M.M. (2014a). Protocols on the use of Compound-Specific Stable Isotopes to identify and apportion soil sources from land use. Revised 2013. Contract report to Joint FAO/IAEA Division of Nuclear Techniques in Food and Agriculture: 126.
<http://www-naweb.iaea.org/nafa/swmn/public/CSSI-technique-protocols-revised-2013.pdf>
- Gibbs, M.M., Swales, A., Olsen, G. (2014b) Suess Effect on biomarkers used to determine sediment provenance from land-use changes. In: L.K. Heng, K. Sakadevan, G. Dercon, M.L. Nguyen (eds). *Proceedings – International Symposium on Managing Soils for food*

- Security and Climate Change Adaptation and Mitigation*. Food and Agriculture Organization of the United Nations Rome, 2014: 371–375.
- Gibbs M., Leduc D., Nodder S.D., Kingston A., Swales A., Rowden A.A., Mountjoy J., Olsen G., Ovenden R., Brown J., Bury S., Graham B. (2020) Novel application of a compound-specific stable isotope (CSSI) tracking technique demonstrates connectivity between terrestrial and deep-sea ecosystems via submarine canyons. *Frontiers in Marine Science*, 7(608): doi: 10.3389/fmars.2020.00608
- Glaser, B. (2005) Compound-specific stable-isotope (δ C-13) analysis in soil science. *Journal of Plant Nutrition and Soil Science* 1685: 633–648.
- Goff, J.R., Chague-Goff, C. (1999) A late Holocene record of environmental changes from coastal wetlands: Abel Tasman National Park, New Zealand. *Quaternary International*, 56: 39-51.
- Goff, J.R., McFadgen, B.G. (2001) Nationwide tsunami during prehistoric Maori occupation, New Zealand. *Proceedings of International Tsunami Symposium, 2001*: 469-476. Seattle, A, NOAA/PEML.
- Green M.O., Coco, G. (2014) Review of wave-driven sediment resuspension and transport in estuaries. *Reviews of Geophysics* 52: 77–117.
- Green, T.R., Beavis, S.G., Dietrich, C.R., Jakeman, A.J. (1999). Relating stream-bank erosion to in-stream transport of suspended sediment. *Hydrological processes* 13(5): 777–787.
- Gribben, P.E., Angelini, C., Altieri, A.H., Bishop, M.J., Thomsen, M.S., Bulleri, F. (2019) *H3 Facilitation Cascades in Marine Ecosystems, Oceanography and Marine Biology*. Taylor and Francis.
- Hadfield, M., Broekhuizen, N., Plew, D. (2014) A biophysical model for the Marlborough Sounds. *Part 1: Queen Charlotte Sound and Tory Channel*.
- Hadfield, M. (2015) An assessment of potential for resuspension of fine sediments in Marlborough Sounds. *NIWA Client Report WLG2015-53* prepared for Marlborough District Council: 10.
- Halley, S.A. (2018). Brief of evidence of Stephen Ashley Halley on behalf of The Ministry of Primary Industries, MPI, Wellington, 38 p.
- Hancock G.J., Revill, A.T. (2013) Erosion source discrimination in a rural Australian catchment using compound-specific isotope analysis (CSIA). *Hydrological Processes* 27(6): 923–932.
- Handley, S.J. (1998) Power to the oyster: do spionid-induced blisters affect condition in subtidal oysters? *Journal of Shellfish Research*, 17(4): 1093-1099.
- Handley, S.J., Willis, T.J., Cole, R.G., Bradley, A., Cairney, D.J., Brown, S.N., Carter, M.E. (2014) The importance of benchmarking habitat structure and composition for understanding the extent of fishing impacts in soft sediment ecosystems. *Journal of Sea Research*, 86(0): 58-68.

- Handley, S. (2015) The history of benthic change in the Pelorus Sound (Te Hoiere), Marlborough. *NIWA Client Report* NEL2015-001 for Marlborough District Council.
- Handley, S., Gibbs, M., Swales, A., Olsen, G., Ovenden, R., Bradley, A. (2017) A 1,000 year seabed history Pelorus Sound/Te Hoiere, Marlborough. *NIWA Client report* Prepared for Marlborough District Council, Ministry of Primary Industries and the Marine Farming Association. No. 2016119NE, MDC15401, April 2017: 117.
- Handley, S.J., Swales, A., Horrocks, M., Gibbs, M., Carter, M., Ovenden, R., Stead, J. (2020) Historic and contemporary anthropogenic effects on granulometry and species composition detected from sediment cores and death assemblages, Nelson Bays, Aotearoa-New Zealand. *Continental Shelf Research* 202: 104-147.
- Handley, S.J., Morrisey, D., Depree, C., Carter, M., Mejía Torres, L.A. (2020b) Relative macrofaunal biomass reduced under an enriched salmon farm, Pelorus Sound, Aotearoa-New Zealand. *Marine Pollution Bulletin*, 157: 111303.
- Hannah, J., Bell, R.G. (2012) Regional sea level trends in New Zealand. *Journal of Geophysical Research* 117: C01004, doi:10.1029/2011JC007591.
- Hayward, B.W., Grenfell, H.R., Sabaa, A.T., Kay, J., Daymond-King, R., Cochran, U. (2010) Holocene subsidence at the transition between strike-slip and subduction on the Pacific-Australian plate boundary, Marlborough Sounds, New Zealand. *Quaternary Science Reviews*, 29(5-6): 648-661.
- Hector, J. (1872) Report on the gold mines in the province of Marlborough. *NZ Geological Survey Reports of Geological Explorations*.
- Hegan, C. (1993) "Radiata, prince of pines". *New Zealand Geographic* 20. October-December. Retrieved from (<https://www.nzgeo.com/stories/radiata-prince-of-pines/>) on 21 November 2019.
- Hicks, D.L. (1991). Erosion under pasture, pine plantations, scrub and indigenous forest: a comparison from Cyclone Bola. *New Zealand Forestry* November 1991: 21-22.
- Hicks, D.M., Gomez B., Trustrum N.A. (2000) Erosion thresholds and suspended sediment yields, Waipaoa River Basin, New Zealand. *Water Resources Research* 36(4): 1129–1142.
- Hicks, D.M., Shankar, U., McKerchar, A.I., Basher, L., Jessen, M., Lynn, I., Page, M. (2011) Suspended sediment yields from New Zealand rivers. *Journal of Hydrology (New Zealand)* 50(1): 81–142.
- Hogg, A.G., Higham, T.F.G., Dahm, J. (1998) Radiocarbon dating of modern marine and estuarine shellfish. *Radiocarbon*, 40: 975–984.
- Hughes, A.O., Quinn, J.M., McKergow, L.A. (2012) Land use influences on suspended sediment yields and event sediment dynamics within two headwater catchments, Waikato, New Zealand. *New Zealand Journal of Marine and Freshwater Research* 46(3): 315–333.

- Hughes, A., Hoyle, J. (2014) The importance of bank erosion as a source of suspended sediment within the Kopurererua catchment. NIWA Client Report No: HAM2014-064 prepared for Bay of Plenty Regional Council.
- Hughes, A. (2015) Waikato River suspended sediment: loads, sources, and sinks. Waikato Regional Council report TR 2018/65.
- Hume, T.M., McGlone, M.S. (1986) Sedimentation patterns and catchment use changes recorded in the sediments of a shallow tidal creek, Lucas Creek, Upper Waitemata Harbour, New Zealand. *Journal of the Royal Society of New Zealand*, 19: 305–317.
- Hunt, S. (2019) Summary of historic estuarine sedimentation measurements in the Waikato region and formulation of a historic baseline sedimentation rate. Waikato Regional Council Technical Report 2019/08. ISSN2230-4363 (online): 30.
- IAEA (2019) Guidelines for sediment tracing using the compound specific stable isotope technique, International Atomic Energy Agency (IAEA) TECDOC-1881, ISBN 978-92-0-158519-6. Prepared by the Joint FAO/IAEA Division of Nuclear Techniques in Food and Agriculture, Vienna, Austria: 68.
- Isbell, F., Gonzalez, A., Loreau, M., Cowles, J., Díaz, S., Hector, A., Mace, G.M., Wardle, D.A., O'Connor, M.I., Duffy, J.E. (2017) Linking the influence and dependence of people on biodiversity across scales. *Nature*, 546(7656): 65–72.
- Jantschik, R., Nyffeler, F., Donard, O.F.X. (1992) Marine particle size measurement with a stream-scanning laser system. *Marine Geology* 106: 239–250.
- Johnston, A. Mace, J. Laffan, M. (1981) "The saw, the soil, and the Sounds". *Soil and Water*, Aug/Oct 1981: 4-8.
- Johnston, M.R. (1993) Gold in a tin dish. Volume Two: the history of the eastern Marlborough goldfields, Nikau Press, Nelson: 456.
- Jones, H.F.E., Pilditch, C.A., Hamilton, D.P., Bryan, K.R. (2017) Impacts of a bivalve mass mortality event on an estuarine food web and bivalve grazing pressure. *N. Z. Journal of Marine and Freshwater Research* 51(3): 370–392.
- Kohn, M.J. (2010) Carbon isotope compositions of terrestrial C3 plants as indicators of (paleo)ecology and (paleo)climate. *PNAS*, 107(46): 19691–19695
www.pnas.org/cgi/doi/10.1073/pnas.1004933107
- Kronvang, B., Andersen, H.E., Larsen, S.E., Audet, J. (2012) Importance of bank erosion for sediment input, storage and export at the catchment scale. *Journal of Soils and Sediments* DOI 10.1007/s11368-012-0597-7
- Kruskal, J.B., Wish, M. (1978) Multidimensional scaling. Sage. ISBN: 0803909403
- Laffan, M.D. (1980) Some observations of regoliths and landslides in the Marlborough Sounds. *Soil News*, 28 (2): 96-102.
- Laffan, M.D., Daly, B.K. (1985) Soil resources of the Marlborough Sounds and implications for exotic production forestry. *New Zealand Journal of Forestry*, 30: 54-69.

- Laubel, A., Kronvang, B., Hald, A.B., Jensen, C. (2003) Hydromorphological and biological factors influencing sediment and phosphorus loss via bank erosion in small lowland rural streams in Denmark. *Hydrol. Processes* 17: 3443–3463.
- Lauder, G.A. (1987) Coastal landforms and sediments of the Marlborough Sounds. *Unpublished PhD Thesis*. University of Canterbury, Christchurch: 327.
- Legendre, P., Anderson, M.J. (1999) Distance-based redundancy analysis: testing multispecies responses in multifactorial ecological experiments. *Ecological monographs* 69: 1-24.
- Leith, P., Ogier, E., Haward, M. (2014). Science and Social License: Defining Environmental Sustainability of Atlantic Salmon Aquaculture in South-Eastern Tasmania, Australia. *Social Epistemology*, 28(3-4): 277–296.
- Li, G., Wan, L., Cui, M., Wu, B., Zhou, J. (2019). Influence of canopy interception and rainfall kinetic energy on soil erosion under forests. *Forests* 10(6): 509
- Lochhead, L. (2012) The battle for Rai Valley 1898. *ENNZ: Environment and Nature in New Zealand* 7(1-2): 25-40. Retrieved 28 August 2019. <https://envirohistorynz.com/tag/lynne-lochhead/>.
- MacDiarmid, A., McKenzie, A., Sturman, J., Beaumont, J., Mikaloff-Fletcher, S., Dunne, J. (2012) Assessment of anthropogenic threats to New Zealand marine habitats. Wellington, New Zealand: Ministry of Agriculture and Forestry.
- Marden, M., Rowan, D. (1993) Protective value of vegetation on tertiary terrain before and during Cyclone Bola, East Coast, North Island, New Zealand. *New Zealand Journal of Forestry Science* 23: 255–263.
- Marlborough District Council (1992) *Issues and Options for Forestry and Farming in the Marlborough Sounds*. Blenheim, NZ.
- Marlborough District Council (1994). State of the environment report. Blenheim, NZ.
- Marlborough District Council (2008). State of the environment report 2008. Blenheim, NZ
- Marlborough District Council (2016). State of the environment report 2015. Blenheim, NZ.
- Mathers, K.L., Millet, J., Robertson, A.L., Stubbington, R., Wood, P.J. (2014) faunal response to benthic and hyporheic sedimentation varies with direction of vertical hydrological exchange. *Freshwater Biology*, 59: 2278–2289.
- Matthews, K.M. (1989) Radioactive fallout in the South Pacific: a history. Part 1: Deposition in New Zealand. *Report NRL1989/2*, National Radiation Laboratory, Christchurch, New Zealand.
- McArdle, B.H., Anderson, M.J. (2001) Fitting multivariate models to community data: a comment on distance-based redundancy analysis. *Ecology* 82: 290-297.
- McDowell, R.W., Norris, M., Cox, N. (2016) Using the provenance of sediment and bioavailable phosphorus to help mitigate water quality impact in an agricultural catchment. *Journal of Environmental Quality*, 45(4): 1276-1285.

- McDowell, R.W., Wilcock, R.J. (2007) Sources of sediment and phosphorus in stream flow of a highly productive dairy farmed catchment. *Journal of Environmental Quality*, 36(2): 540-548.
- McGlone, M.S., Wilmshurst, J.M., Leach, H.M. (2005) An ecological and historical review of bracken (*Pteridium esculentum*) in New Zealand, and its cultural significance. *New Zealand Journal of Ecology*, 29(2): 165–184.
- McIntosh, A.D. (Ed) (1940) Marlborough: A provincial history. Marlborough Provincial Historical Committee. Blenheim: 431.
- Miller, D. (2015) Some impacts of roading and flood damage on sounds roads. Part only – Queen Charlotte Drive and Kenepuru Road, period 1985-2010. No. 105 p. www.marlborough.govt.nz/Environment/Coastal/Reports-and-Special-Investigations.aspx
- Moore, J.W., Semmens, B.X. (2008) Incorporating uncertainty and prior information into stable isotope mixing models. *Ecology Letters*, 11: 470–480.
- Motha, J.A., Wallbrink, P.J., Hairsine, P.B., Grayson, R.B. (2003) Determining the Sources of Suspended Sediment in a Forested Catchment in Southeastern Australia. *Water Resources Research*, 39: 1056-1069.
- Motha, J.A., Wallbrink P.J, Hairsine P.B., Grayson, R.B. (2004) Unsealed Roads as Suspended Sediment Sources in an Agricultural Catchment in South-Eastern Australia. *Journal of Hydrology*, 286: 1-18.
- Nagle, G.N., Fahey, T.J., Ritchie, J.C., Woodbury, P.B. (2007) Variations in sediment sources and yields in the Finger Lakes and Catskills regions of New York. *Hydrological Processes* 21, 828–838, DOI: 10.1002/hyp.6611
- Neal, R. (2018) Dairyshed effluent and stream crossing survey 2017/18. Technical Report 18-006. Marlborough District Council: 26.
- Nicol, A. (2011) Landscape history of the Marlborough Sounds, New Zealand. *NZ Journal of Geology and Geophysics*, 54: 195-208.
- NZ Soil Bureau (1968) General survey of the soils of the South Island, New Zealand. *New Zealand Soil Bureau Bulletin* 27. Includes maps at 1:250 000.
- Oldman, J.W., Swales, A. (1999) Maungamaungaroa Estuary numerical modelling and sedimentation. *NIWA Client Report* ARC70224, prepared for Auckland Regional Council.
- O’Loughlin, C.L. (1979) Near-shore seawater quality study, Marlborough Sounds. NZ Forest Service, unpublished Forest Research Institute Report (available from library@scionresearch.com), and reported in *New Zealand Journal of Ecology*, Vol 3. Resumes. <http://newzealandecology.org/nzje/1495.pdf>.
- O’Loughlin, C.L. Watson, A.J. (1979) Root-wood strength deterioration in Radiata pine after clear-felling. *New Zealand Journal of Forestry Science*, 9(3): 284-293.

- Olsen, C.R., Simpson, H.J., Peng, T.H., Bopp, R.F., Trier, R.M. (1981) Sediment mixing and accumulation rate effects on radionuclide depth profiles in Hudson Estuary sediments. *Journal of Geophysical Research: Oceans*, 86(C11): 11,020-11,028.
- Owens, P.N., Blake, W.H., Gaspar, L., Garteuille, D., Koiter, A.J., Lobbb, D.A., Petticrew, E.L., Reiffarth, D.G., Smith, H.G., Woodward, J.C. (2016) Fingerprinting and tracing the sources of soils and sediments: Earth and ocean science, geoarchaeological, forensic, and human health applications. *Earth Science Reviews* 162: 1–23.
- Parnell, A., Phillips, D.L., Bearhop, S., Semmens, B.X., Ward, E.J., Moore, A.L., Jackson, J., Grey, D.J., Kelly, D.J., Inger, R. (2013) Bayesian stable isotope mixing models. *Environmetrics*, 24: 387–399.
- Paton, B.R. (1982) Sawmill pioneers in the Pelorus. Diploma in Parks and Recreation dissertation. Lincoln College. Canterbury: 58.
- Peden, R. (2008) Farming in the economy – the golden years, 1950s to 1980s. *Te Ara – the Encyclopaedia of New Zealand*.
<https://teara.govt.nz/en/photograph/17637/topdressing-trials>. Accessed 5 September 2019
- Pellegrini, A.F.A., Hobbie, S.E., Reich, P.B., Jumpponen, A., Brookshire, E.N.J., Caprio, A.C., Coetsee, C., Jackson, R.B. (2020) Repeated fire shifts carbon and nitrogen cycling by changing plant inputs and soil decomposition across ecosystems. *Ecological Monographs*, 00(00):e01409. 10.1002/ecm.1409.
- Petchy, F., Anderson, A., Zondervan, A., Ulms, S., Hogg, A. (2008) New marine ΔR values for the South Pacific Subtropical Gyre Region. *Radiocarbon* 50(3): 373–397.
- Phillips, D.L., Gregg, J.W. (2003) Source partitioning using stable isotopes: coping with too many sources. *Oecologia*, 136: 261-269.
- Phillips, C. Pruden, C. Coker, R. (1996) Forest harvesting in the Marlborough Sounds – flying in the face of a storm? *New Zealand Journal of Forestry* 41(1): 27-31.
- Phillips, C., Marden, M., Basher, L. (2012) Plantation forest harvesting and landscape response – what we know and what we need to know. *New Zealand Journal of Forestry* 56(4): 4–12.
- Phillips, C., Marden, M., Miller, D. (2000) Review of plant performance for erosion control in the East Coast Region. *Landcare Research Contract Report LCD9900/111* prepared for the Ministry Agriculture and Forestry: 128.
- Phillips, D.L., Inger, R., Bearhop, S., Jackson, A.L., Moore, J.W., Parnell, A.C., Semmens, B.X., Ward, E.J. (2014). Best practices for use of stable isotope mixing models in food-web studies. *Canadian Journal of Zoology* 92: 823–835.
- Pivato M., Carniello, L., Moro, I., D’Odorico, P. (2018) On the feedback between water turbidity and microphytobenthos growth in shallow tidal environments. *Earth Surface Processes and Landforms* 44: 1192–1206.

- Prickett, N. (ed) (1982) *The first thousand years: regional perspectives in New Zealand archaeology*. Dunmore Press. Palmerston North.
- Rattenbury, M.S., Copper, R.A., Johnston, M.R. (1998). *Geology of the Nelson Area*. Institute of Geological and Nuclear Sciences, 1:250,000 geological map 9. 1 sheet + 67 Lower Hutt, New Zealand.
- Richie, J.C., McHenry, J.R. (1989) Application of radioactive fallout cesium-137 for measuring soil erosion and sediment accumulation rates and patterns: a review with bibliography. *Hydrology Laboratory, Agriculture Research Service, U.S. Department of Agriculture, Maryland*.
- Rieley, G., Collier, R.J., Jones, D.M., Eglinton, G., Eakin, P.A., Fallick, A.E. (1991) Sources of sedimentary lipids deduced from stable carbon-isotope analyses of individual compounds. *Nature* 352: 425–427.
- Robbins, J.A., Edgington, D.N. (1975) Determination of recent sedimentation rates in Lake Michigan using ^{210}Pb and ^{137}Cs . *Geochemica et Cosmochimica Acta*, 39: 285–304.
- Robertson (2019a). Havelock Estuary, Marlborough. Broad Scale Habitat Mapping and Ecological Assessment: 81.
- Robertson (2019b) Havelock Estuary, Marlborough. Fine Scale Habitat Mapping and Ecological Assessment: 73.
- Robertson, B., Stevens, L. (2009) Rai Valley Sustainable Farming Project: Preliminary assessment of river and coastal issues. Report for NZ Landcare Trust. Wriggle Coastal Management, Nelson.
- Schipper, L.A., Parfitt, R.L., Ross, C., Baisden, W.T., Claydon, J.J., Fraser, S. (2010) Gains and losses in C and N stocks of New Zealand pasture soils depend on land use. *Agriculture, Ecosystems and Environment*, 139: 611–617.
- Selkoe, K.A., Blenckner, T., Caldwell, M.R., Crowder, L.B., Erickson, A.L., Essington, T.E., Estes, J.A., Fujita, R.M., Halpern, B.S., Hunsicker, M.E., Kappel, C.V., Kelly, R.P., Kittinger, J.N., Levin, P.S., Lynham, J.M., Mach, M.E., Martone, R.G., Mease, L.A., Salomon, A.K., Samhouri, J.F., Scarborough, C., Stier, A.C., White, C., Zedler, J. (2015) Principles for managing marine ecosystems prone to tipping points. *Ecosystem Health and Sustainability*, 1(5): 1-18.
- Sheffield, A.T., Healy, T.R., McGlone, M.S. (1995) Infilling rates of a steep-land catchment estuary, Whangamata, New Zealand. *Journal of Coastal Research*, 11(4): 1294–1308.
- Skilton, J., Thompson, N. (2017) Mahakipawa Estuary: Fine-Scale Monitoring and Broad-Scale Habitat Mapping 2017. Report for Marlborough District Council. SLR Consulting NZ, Nelson.
- Smith, H.G., Karam, D.S., Lennard, A.T. (2018) Evaluating tracer selection for catchment sediment fingerprinting. *Journal of Soils and Sediments* 18: 3005–3019.

- Smith, H.G., Spiekermann, R., Dymond, J., Basher, L. (2019) Predicting spatial patterns in riverbank erosion for catchment sediment budgets. *New Zealand Journal of Marine and Freshwater Research* 53: 338–362. <https://doi.org/10.1080/00288330.2018.1561475>
- Smith, J.N. (2001). Why should we believe ^{210}Pb geochronologies? *Journal of Environmental Radioactivity* 55: 121–123.
- Sommerfield, C.K., Nittrouer, C.A., Alexander, C.R. (1999) ^7Be as a tracer of flood sedimentation on the northern California continental margin. *Continental Shelf Research* 335–361.
- Staff, G., Powell, E.N., R.J., S., Cummins, H. (1985). Biomass: is it a useful tool in paleocommunity reconstruction? *Lethaia*, 18(3): 209-232.
- Statistics New Zealand (2021). Total dairy cattle, Marlborough region 1993–2020. Available from www.statistic.govt.nz
- Stephens, J. (2009) Wakamarina Gold in The Prow: ngā kōrero o te tau ihu. Accessed 30 April 2020. <http://www.theprow.org.nz/enterprise/wakamarina-gold/#.XqpGRqgzY2w>
- Stephenson F., Bulmer, R., Leathwick, J., Brough, T., Clark, D., Rowden, A., Greenfield, B., Bowden, D., Tuck, I., Hewitt, J., Neill, K., Mackay, K., Pinkerton, M., Anderson, O., Gorman, R., Mills, S., Watson, S., Nelson, W., Lundquist, C. (2020) Development of a New Zealand Marine Habitat Classification. *NIWA Client Report* prepared for Department of Conservation.
- Stevens, L., Robertson, B. (2014) Havelock estuary 2014: Broad-scale habitat mapping. Prepared for Marlborough District Council. Wriggle Coastal Management, Nelson.
- Stock, B.C., Jackson, A., Ward, E.J., Parnell, A.C., Phillips, D.L., Semmens, B.X. (2018). Analyzing mixing systems using a new generation of Bayesian tracer mixing models. *PeerJ* 6: e5096: DOI 10.7717/peerj.5096.
- Stuiver, M., Polach, H.A. (1977) Discussion: reporting ^{14}C data. *Radiocarbon* 19(3): 355–363.
- Sutherland, B.K. (2000) *The effects of changing resource use in the Marlborough Sounds*. Unpublished MSc thesis in Geography, University of Canterbury. Christchurch.
- Sutherland, R. (2011) Forestry: seeing the wood for the trees. In (Eds) Brooks C, McKendry L, Olliver D. *Marlborough – Celebrating 150 years*. Marlborough District Council and Marlborough Electric Power Trust.
- Swales, A., Hume, T.M., Oldman, J.W., Green, M.O. (1997) Holocene sedimentation and recent human impacts in a drowned-valley estuary: 895–900. In: J. Lumsden (ed.). *Proceedings of the 13th Australasian Coastal and Ocean Engineering Conference*, Centre for Advanced Engineering, University of Canterbury, Christchurch, New Zealand.
- Swales, A., Williamson, R.B., Van Dam, L.F., Stroud, M.J. (2002a) Reconstruction of urban stormwater contamination of an estuary using catchment history and sediment profile dating. *Estuaries*, 25(1): 43–56.

- Swales, A., Hume, T.M., McGlone, M.S., Pilvio, R., Ovenden, R., Zviguina, N., Hatton, S., Nicholls, P., Budd, R., Hewitt, J., Pickmere, S., Costley, K. (2002b) Evidence for the physical effects of catchment sediment runoff preserved in estuarine sediments: Phase II (field study). ARC Technical Publication 221. *NIWA Client Report* HAM2002-067.
- Swales, A., Bentley, S.J., McGlone, M.S., Ovenden, R., Hermansphan, N., Budd, R., Hill, A., Pickmere, S., Haskew, R., Okey, M.J. (2005) Pauatahanui Inlet: effects of historical catchment landcover changes on estuary sedimentation. *NIWA Client Report* HAM2004-149, for Wellington Regional Council and Porirua City Council.
- Swales, A., Gibbs, M., Hewitt, J., Hailes, S., Griffiths, R., Olsen, G., Ovenden, R., Wadhwa, S. (2012) Sediment sources and accumulation rates in the Bay of Islands and implications for macro-benthic fauna, mangrove and saltmarsh habitats. *NIWA Client Report* HAM2012-048.
- Swales, A., Gibbs, M., Stephens, T., Olsen, G., Budd, R., Ovenden, R., Costley, K. (2016a) Sources of eroded soils and their contribution to long-term sedimentation in the Firth of Thames. *NIWA Client Report* HAM2016-001 prepared for Waikato Regional Council and Dairy NZ: 68.
- Swales, A., Denys, P., Pickett, V.I., Lovelock, C.E. (2016b). Evaluating deep subsidence in a rapidly accreting mangrove forest using GPS monitoring of surface-elevation benchmarks and sedimentary records. *Marine Geology* 380: 205–218.
- Swales, A., Gibbs, M. (2020). Transition in the isotopic signatures of fatty-acid soil biomarkers under changing land use: insights from a multi-decadal chronosequence. *Science of the Total Environment* 722: 137850 (on-line)
<https://doi.org/10.1016/j.scitotenv.2020.137850>
- Tait, A. (2017). Interpolation of mean annual rainfall for Marlborough District. Prepared for Marlborough District Council. Prepared for Marlborough District Council. *NIWA Client Report* 2017004WN.
- Te Ara – The Encyclopedia of New Zealand. (2020): Story: Marlborough Places 2. Pelorus Valley. <https://teara.govt.nz/en/marlborough-places/page-2> retrieved 29 April 2020.
- Te Tau Ihu Statutory Acknowledgments (2014) Nelson City Council, Tasman District Council, Marlborough District Council.
- The Rai Valley Centennial Committee. (1981) The Rai and its people: a centennial history of the Rai Valley District 1881-1981. The Rai Valley Centennial Committee. Blenheim, NZ: Express Printing.
- Thomsen, M.S., Hildebrand, T., South, P.M., Foster, T., Siciliano, A., Oldach, E., Schiel, D.R., (2016) A sixth-level habitat cascade increases biodiversity in an intertidal estuary. *Ecology and evolution* 6: 8291-8303.
- Thrush, S.F., Dayton, P. K. (2002). Disturbance to marine benthic habitats by trawling and dredging: implications for marine biodiversity. *Annual Review of Ecological Systems* 33: 449–473.
- Thrush, S.F., Hewitt, J.E., Cummings, V.J., Ellis, J.I., Hatton, C., Lohrer, A., Norkko, A. (2004) Muddy waters: elevating sediment input to coastal and estuarine habitats. *Frontiers in Ecology and the Environment* 2: 299–306.

- Thrush, S.F., Hewitt, J.E., Parkes, S., Lohrer, A.M. et al. (2014) Experimenting with ecosystem interaction networks in search of threshold potentials in real-world marine ecosystems. *Ecology* 95(6): 1451–1457.
- Townsend, M., Lohrer, A. (2015) ANZECC guidance for estuary sedimentation. NIWA Client Report HAM2015-096 prepared for Ministry for the Environment: 45.
- Upadhayay, H.R., Smith, H.G., Griepentrog, M., Bodé S., Bajracharya, R. M., Blake, W., Cornelis, W., Boeckx P. (2018) Community managed forests dominate the catchment sediment cascade in the mid-hills of Nepal: a compound-specific stable isotope analysis. *Science of the Total Environment* 637–638: 306–317.
- Urlich, S.C. (2015) Mitigating fine sediment from forestry in coastal waters of the Marlborough Sounds. No. *MLDC Technical Report*, No: 15-009: 61.
- Urlich, S.C. (2020) Opportunities to manage sediment from forestry more effectively in the Marlborough Sounds and contributing catchments. *New Zealand Journal of Forestry* 65(2): 25-32.
- Urlich, S.C., Handley, S.J. (2020) History of pine forestry in the Pelorus/Te Hoiere catchment and the Marlborough Sounds. *New Zealand Journal of Forestry* 65(2): 19-24.
- Urlich, S.C., Handley, S.J. (2020b, In press) From ‘clean and green’ to ‘brown and down’: a synthesis of historical changes to biodiversity and marine ecosystems in the Marlborough Sounds, New Zealand. *Ocean and Coastal Management*.
- Verburg, P. (2007) The need to correct for the Suess effect in the application of $\delta^{13}\text{C}$ in sediment of autotrophic Lake Tanganyika, as a productivity proxy in the Anthropocene. *Journal of Paleolimnology*, 37: 591–602.
- Vincent, W.F., Clive Howard-Williams, C., Downes, M.T., Dryden, S.J. (1989). Underwater light and photosynthesis at three sites in Pelorus Sound, New Zealand. *New Zealand Journal of Marine and Freshwater Research*, 23:1: 79-91.
- Waitangi Tribunal (2008) Te Tau Ihu o Te Waka a Maui. Report on northern South Island claims. Volume III. Waitangi Tribunal. Ministry of Justice. Wellington: 442.
- Walls, G.Y., Laffan, M.D. (1986) Native vegetation and soil patterns in the Marlborough Sounds, South Island, New Zealand. *New Zealand Journal of Botany*, 24: 293-313.
- Ward, J. (1840) Supplementary information relative to New Zealand comprising despatches and journals of the Company’s offices of the first expedition and the first report of the directors. Smith, Elder and Co. Cornhill. London. Retrieved from www.enzb.auckland.ac.nz on 12 December 2018.
- Wastney, N. (2006) The valleys beyond: early Rai Valley and upper Opouri. Self-published. Nelson: 143.
- Whitehead, A.L., Booker, D.J. (2019) Communicating biophysical conditions across New Zealand’s rivers using an interactive webtool. *New Zealand Journal of Marine and Freshwater Research* 53 (2): 278–287.

- Wildhaber, Y.S., Liechti, R., Alewell, C. (2012) Organic matter dynamics and stable isotopes for tracing sources of suspended sediment. *Biogeosciences Discuss.* 9: 453–483.
- Wilmshurst, J.M., Anderson, A.J., Higham, T.F., Worthy, T.H. (2008) Dating the late prehistoric dispersal of Polynesians to New Zealand using the commensal Pacific rat. *Proceedings of the National Academy of Sciences*, 105: 7676-7680.
- Wise, S. (1977) The use of radionuclides ^{210}Pb and ^{137}Cs in estimating denudation rates and in soil measurement. *Occasional paper No. 7 University of London, Kings College, Department of Geography, London.*
- Wood, P.J., Armitage, P.D. (1997) Biological effects of fine sediment in the lotic environment. *Environmental Management*, 21:203–217.
- Yi, Z., Xu, M., Di, X., Brynjolfsson, S., Fu, W. (2017) Exploring valuable lipids in Diatoms. *Frontiers in Marine Science* 4:17. doi: 10.3389/fmars.2017.00017.

Appendix A Historical record of severe weather events

Table A-1 presents information on historical weather events that have resulted in flooding and erosion in the Pelorus-Rai catchment since the late-1860s. Flood discharges exceeding 2000 m³ s⁻¹ are significant as these events typically result in severe flooding of lowland areas, road closures and widespread land sliding on hillslopes.

Table A-1: Historical records of severe weather events (1868-2000) in the Pelorus/Te Hoiere and Kaituna catchments and Pelorus Sound. Source: NIWA Historical Weather Events Catalogue (<https://hwe.niwa.co.nz/>).

Date	Location	Rainfall and duration	Description
1 Feb 1868	Pelorus		The flood at Pelorus was unprecedented in the memory of the oldest Māori settlers there.
28 Oct 1900			All the rivers were very high.
18 March 1904			Biggest flood ever recorded at Canvastown at that time. Bridges washed out at Canvastown, Wakamarina, Pelorus Bridge and Rai. Numerous landslides.
24 June 1905			Floods occurred in Pelorus, Wakamarina, and Kaituna.
5 May 1923			All bridges in the district were gone.
2 April 1931	Rai Valley	28.9 cm in 14 hours	Estimated well over 150 years return period. Torrential rain also hit Ronga and Opouri Valley. Rai river rose 6.1m (biggest flood for over 20 years).
	Yncyca Bay	34.3 cm in 48 hours	
31 Jan 1933	Rai Valley	51.1 cm in 56 hours	Estimated well over 150 years return. Ronga and Opouri Rivers in flood. Several bridges washed away in district.
12 April 1938	Havelock	5.1 cm in 5 hours 14.7 cm over 3 days	The Marlborough Sounds area experienced the most intense falls of rains. Many slips fell across creek beds.
30 Nov 1939			Flooding in the Pelorus and Wakamarina blocked Nelson road.
13 Feb 1940	Rai Valley	12.7 cm in 36 hours	Floodwater blocked Havelock Nelson road at Canvastown. Serious flooding in Opouri and much of valley underwater.
17 Mar 1941	Opouri	11.5 cm in 24 hours	Kaituna River overflowed, inundated farmland and properties.
29 Sep 1947	Opouri	14.5 cm in 24 hours	

Date	Location	Rainfall and duration	Description
22 Feb 1949	Rai Valley Havelock	13.4 cm in 12 hours 11.3 cm in 12 hours	Pelorus and Wakamarina rivers were in high flood, and heavy flooding to Rai Valley and Canvastown
25 Nov 1952	Havelock Mahakipaoa	15.2 cm in 24 hours 18.1 cm in 24 hours	
19 July 1958	Pelorus Canvastown		Pelorus river in high flood, covered most of the valley floor between Havelock and Canvastown (1116 m ³ /s at peak discharge).
31 July 1962	Pelorus Kaituna		Pelorus river at Dalton's Bridge 1247 m ³ /s at peak, Kaituna River discharge (140 m ³ /s).
22 May 1966	Havelock	12.7 cm	Kaituna river was in a raging flood. Worst flood since 1902. All reclaimed land underwater. There was water in places last seen 50 years ago. Numerous slips occurred.
10 Mar 1975	Kenepuru		Heavy rain and strong winds were experienced.
8 July 1983	Opouri	50.1 cm	Slips damaged roads from Canvastown to Havelock. multiple slips in the Pelorus catchment (1 in 11.7-year event at peak flow in Pelorus catchment (source: MDC hydrologist), 8–10 July.
21 Oct 1983	Opouri	70 cm over 61 hours	Heavy flooding in Canvastown, Whakamarino, and Rai Valley. Ronga and Opouri rivers and tributaries flooded. Slips in the Rai, Canvastown and Havelock areas (and Pelorus according to Ron Sutherland <i>pers comm</i>).
11 Aug 1990			Several dropouts and slips in steep country of the Marlborough Sounds which closed a number of roads.
30 June 1997			Rural areas of the Marlborough Sounds were badly affected. Flooding and slips affected roads and properties.
1 July 1998			
8 July 1998			
8 Oct 1998	Pelorus Sound	10 cm in 24 hours	

Date	Location	Rainfall and duration	Description
27 Oct 1998	Pelorus Sound	16.7 cm in 24 hours	

More recent records of high intensity rainfall events from 1998-2018 are shown in Figure 1-1. There were seven catchment-wide storms during this period: in 1998, 2006, 2008, 2010, 2011 (twice) and 2016, which exceeded a 1- in 2-year annual return interval (ARI). More localised rainfall events are evident from different catchments in different years. The maximum ARI was a 1-in 65-year event or greater in July 1998. This coincided with floodwaters in excess of $2000 \text{ m}^3 \text{ s}^{-1}$ calculated at Dalton's Bridge for the Pelorus River, upstream of the Whakamarino confluence. Other floods that exceeded $2000 \text{ m}^3/\text{s}$ occurred in 2008, 2010 and 2012, as denoted by the arrows (Figure 1-1).

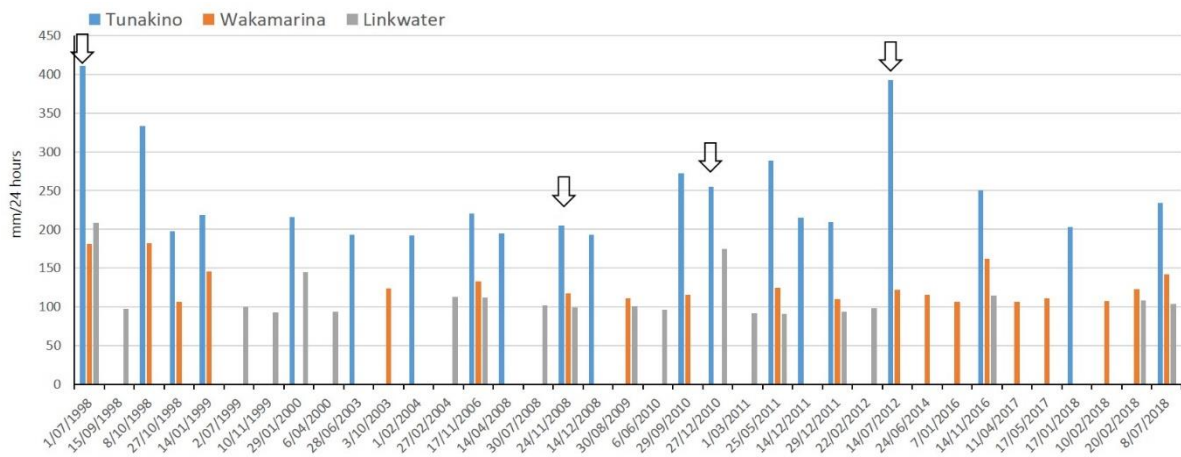


Figure A1: Twenty largest rainfall events (1998–2018) in three subcatchments discharging to Havelock Estuary. Arrows denote flood volumes of the Pelorus/Te Hoiere River that exceeded $2000 \text{ m}^3/\text{s}$ as calculated from the Dalton's Bridge upstream of the confluence of the Whakamarino (Wakamarina) River. Data source: Val Wadsworth (MDC).

HAVELOCK HARBOUR BOARD

Phone.....

HAVELOCK,
20th April, 1953

T. P. Shand, M. P.,
Wellington.

Channel & Harbour Improvements.

Dear Mr Shand,

Further to our recent conversation I forward herewith V.D.M. Jacobson's report on the history of the Havelock Harbour.

This report was prepared by request and placed before the meeting of the Board held on Saturday last, 18th Inst.

The conclusion reached, after discussion, was that, after turning the Kaituna into its original course, a dredged navigation channel to the wharf would last some considerable time.

The first dredged channel, even with the Kaituna coming into it well down from the wharf, lasted twenty years.

The later experiment of the river to come in past the wharf was disastrous. turning part of

THE PROPOSALS ARE:-

- A. To turn the Kaituna back into its original channel where it has run for the last fifty years.
- B. Then to dredge a channel to the wharf, and, if finance allows, to the new heavy goods jetty and the sheep yards. 40,000 sheep this season.
- C. To provide other needed improvements and amenities according to the finance available.

Dredging details left to the Engineer, probably from Nelson.

The turning of the Kaituna is to be done in accordance with advice being obtained from the Wairau River Board's Engineer.

At the meeting, in addition to the members, were Dr V.D.M. Jacobson, Messrs N. Weston, J. Shand and B. Garnham.

In support of these proposals the Sounds Settlers have, through Mr J. Shand, offered the Board an interest free loan of one thousand pounds, immediately available, repayable within ten years.

In addition the launch men, and some public spirited local residents, have such faith in the efficacy of these proposals that they have offered free gifts of money, so far totalling £300, towards the cost of the job. This figure will probably reach £500.

THE BOARD HAS DECIDED TO ACCEPT THESE WONDERFUL OFFERS OF HELP AND GET ON WITH THE JOB.

It was indicated to the Board, that in order to obtain the services of the Nelson dredge, speed would be necessary.

A deputation consisting of Dr V.D.M. Jacobson, Messrs N.A. Foote, J. Shand, and either the secretary or Chairman was appointed to wait on the Minister for Marine and the Minister for Works seeking a £ for £ subsidy on the money raised, say £1500.

It is requested that Dr Jacobson's report be presented to the Ministers in the presence of the Deputation.

I respectfully draw your attention to a very important aspect of the proposals:-

1. The emergency road to Cullen's Point estimated cost is £20,000

HAVELOCK HARBOUR BOARD

Phone

HAVELOCK,

2. With 24hrs access to the wharf the agitation for a £70,000¹⁹ Causeway will practically disappear for many years to come. Continued.
3. The proposals now put forward involve an expenditure of only about £3,000.

Politically, support of these proposals by your Government is a very good proposition.

Supplementary to the above I may add that about five years ago a few plants of Spartina Grass were experimentally planted in the mud flats. These did so well that a further 1500 were planted last Spring. These have all grown and even seeded. Odd plants are now scattered over a wide area.

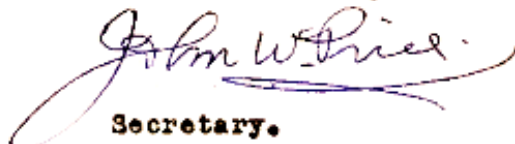
It is considered that, long before the new channel silts up, these plants will have so multiplied and covered the mud flats as to hold up most of the silt brought down by floods.

A letter is being sent Nelson Harbour Board to arrange use of the dredge.

A grant towards the sealing of the wharf road, Cook St, is being sought by the Town Board through the Marlborough County Council. Estimated cost £800. This matter will also be referred to.

I would be glad for you to arrange and advise date suitable for the deputation. Not too early in the day.

Yours faithfully,


Secretary.

HAVELOCK HARBOUR BOARD

Rhone

HAVELOCK,

19

REPORT ON HISTORY OF HAVELOCK HARBOUR. Prepared by Dr V.D.M.Jacobson.

Part 1. Description of Harbour.

Tidal Estuary with Ka ituna River flowing into it.

<u>Tidal Range</u>	High water, Springs, Approx 14ft.
	" " Neaps, " 8 to 16 ft.
<u>Mudflats.</u>	Consisting of silt, shingle and soft sand with varying surface depths averaging one foot.
<u>Channels</u>	(A) River channel
	(B) Launch Channel
	(C) Blind Channels 1. To Cullen's Point
	2. Parallel to Main Road.

(A). RIVER CHANNEL

This has been the river channel for at least the last 50 years. It is over 80 years since the river ran in what is now the Cullen's Point blind channel.

The River channel, with the tide out, is about twenty yards wide and carries an average of about 1 ft of water. It has broken through the stop bank which was designed to return to the river that water which now flows into the launch channel. About two thirds of the ~~river~~ river runs down to the wharf channel.

(B) LAUNCH CHANNEL

This channel, from beacon to wharf, is under half a mile and cuts straight to Cullen's point. It is navigable to small launches (about 2'6" draught) at low water neaps. There is about 6" water at the wharf at low water, springs. This channel built up after a flood in the KAITUNA and is kept at present depth by launch traffic. There are constantly changing banks of river silt in the upper reaches.

(C) BLIND CHANNELS.

CULLEN'S POINT. For 100 yards from the Point channel depth at low water, springs, about 14ft. This channel shallows and runs for about half a mile into the mud flats on the Mahakipawa side of the harbour. The river ran here over 80 yrs ago, Channel depth has not changed within the memory of the older inhabitants,

Parallel to Main Road. Takes off from the wharf channel ~~about 300 yds~~ about 300 yds from the wharf and runs up to the rushes parallel to the main road, a distance of about half a mile. Depth has not varied for the last 30 or 40 years,

IN THE PAST.

Before the river was brought into it, the Launch channel ran from Cullen's Point into the mud flats, thence to the wharf, there being two bends in this channel. It was narrow with steep banks not ~~sixxxx~~ disturbed by the small powered launches then in use.

The cut to the wharf from the river channel was started with the idea of scooping out the wharf channel, but has been found to cause considerable harm by depositing silt.

PREVIOUS DREDGING OPERATIONS.

1910. Before river was let into wharf channel.

Priestman Grab dredge with half to one ton grab. A channel was cut 6ft depth half way to Cullens Point. There a hard bottom made the lift small and operations were suspended. From here the channel went off at angle to Cullen's Point to leave an isthmus partially covered with tide. This was eventually deepened in places by hand shoveled to give a small cut in the line of the present channel. The TIDAL scour opened this small cut and gave the present channel. After this the channel lasted twenty years.

1930. Small suction dredge.

Channel was taken to a depth of four feet out to the hard area, that stopped previous dredging; Even though a bar was left this lasted well until the Kaituna was brought into it shortly after dredging. This lasted approximately five years.

1947. Dragline .Dragline on Punt.

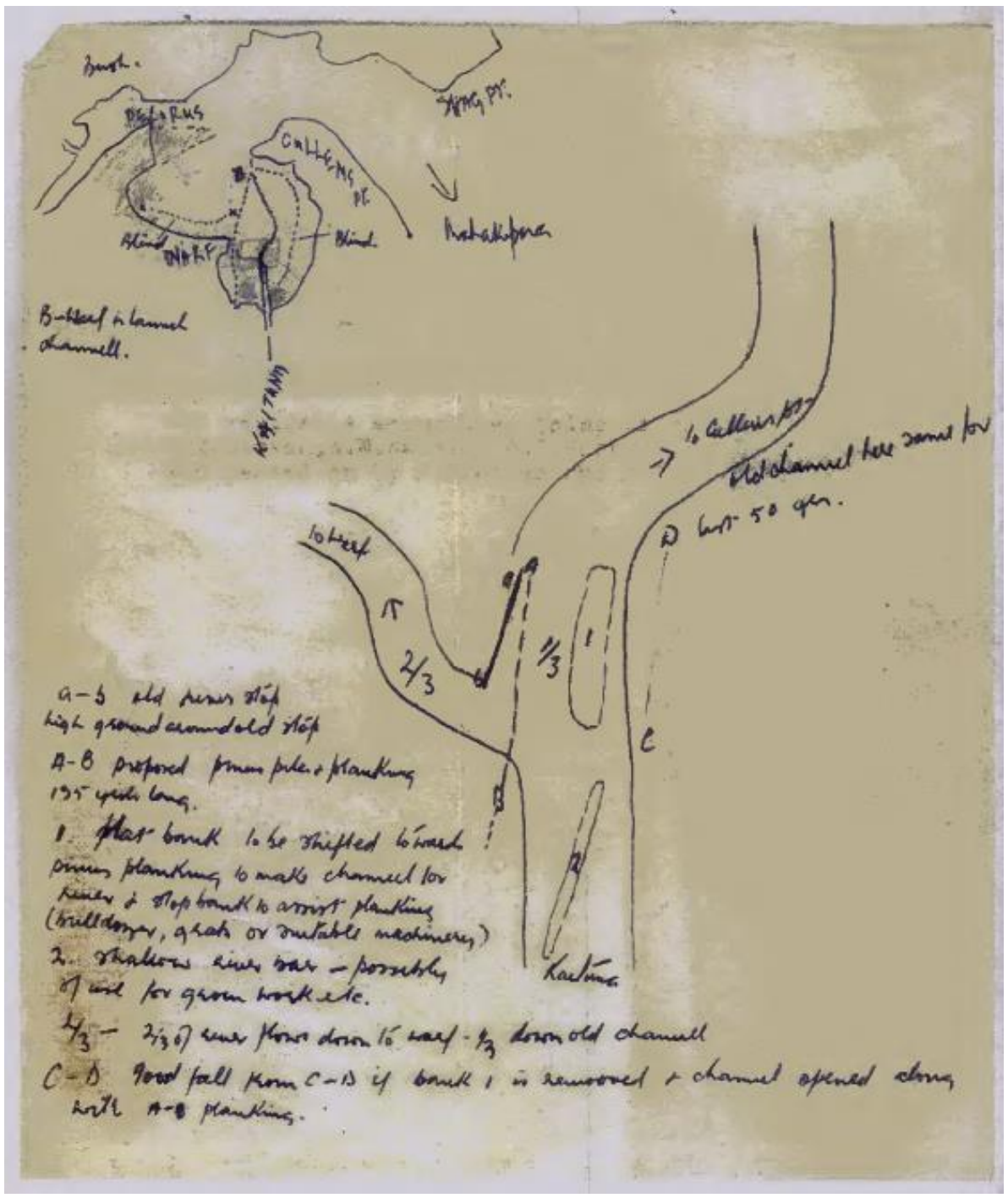
Difficulty was experienced in mooring ~~the~~ engine Punt against the dragline. Small success.

PRESENT SCHEME.

- (A). River Works. Open up river channel immediately beyond old River stop-bank. Divert wharf cut overflow back into the River Channel, by means of pine insignis piles and planking, 135 yds long, extending well up stream beyond the present cut. Bulldozer or power grab will readily open the river channel.

DREDGE. Grab Dredge with a five ton grab.

The Captain of the Grab Dredge, who has looked over the area, states that the proposed work is possible and that the material would be easy dredging. With this dredge the daily minimum load is 370 tons. It is estimated about 18 loads a re required to be shifted



a-b old river stop
 high ground around old stop
 A-B prepared from pile & planking
 175 yards long.
 1. flat bank to be shifted toward
 river planking to make channel for
 river & stop bank to assist planking
 (bulldozers, grubs or suitable machinery)
 2. shallow river bar - possibly
 of use for ground work etc.
 4/3 - 2/3 of river flows down to east - 1/3 down old channel
 C-D good fall from C-D if bank 1 is removed & channel opened along
 with A-B planking.

SUMMARY.

1. The river channel has been stationary for the last fifty years apart from the man made cut to the wharf.
2. Blind channels have remained in status quo for over fifty years
3. Wharf Channel remained stationary until river was led into it.
4. The first grab cut channel remained workable for twenty years.
5. Adverse criticism of dredging the harbour channels has been expressed by those who do not live in Havelock and, over the years, have not had the opportunity of observing local conditions.

The information contained in this report has been gleaned from old residents among them being Messrs A.J.Brown, T.Hutchinson, W. Hutchinson, N.W.Naylor, R.J.Horton, D.Pickering, E.A.Johnson, A.J.Jones, and passed on by J.Shetter who died at 84 yrs of age ~~four~~ years ago.

84

three

Appendix C Summary of CSSI method

In this section we describe how stable isotopes are used to identify the sources of catchment sediments deposited in lakes, estuaries and coastal waters and explain how isotopic data are interpreted.

Stable isotopes are non-radioactive and are a natural phenomenon in many elements. In the NIWA Compound Specific Stable Isotope (CSSI) method, carbon (C) stable isotopes are used to determine the provenance of sediments (Gibbs, 2008). About 98.9% of all carbon atoms have an atomic weight (mass) of 12. The remaining ~1.1% of C atoms have an extra neutron in the atomic structure, giving it an atomic weight (mass) of 13. These are the two stable isotopes of carbon. Naturally occurring carbon also contains an extremely small fraction (about two trillionths) of radioactive carbon-14 (^{14}C). Radiocarbon dating is also used in the present study to determine long-term sedimentation rates.

To distinguish between the two stable isotopes of carbon, they are referred to as light (^{12}C) and heavy (^{13}C) isotopes. Both of these stable isotopes of carbon have the same chemical properties and react in the same way. However, because ^{13}C has the extra neutron in its atom, it is slightly larger than the ^{12}C atom. This causes molecules with the ^{13}C atoms in their structure to react slightly slower than those with ^{12}C atoms, and to pass through cell walls in plants or animals at a slower rate than molecules with ^{12}C atoms. Consequently, more of the ^{12}C isotope passes through the cell wall than the ^{13}C isotope, which results in more ^{12}C on one side of the cell wall than the other. This effect is called isotopic fractionation and the difference can be measured using a mass spectrometer. Because the fractionation due to passage through one cell-wall step is constant, the amount of fractionation can be used to determine chemical and biological pathways and processes in an ecosystem. Each cell wall transfer or “step” is positive and results in enrichment of the ^{13}C content.

The amount of fractionation is very small (about one thousandth of a percent of the total molecules for each step) and the numbers become very cumbersome to use. A convention has been developed where the difference in mass is reported as a ratio of heavy-to-light isotope. This ratio is called “delta notation” and uses the symbol “ δ ” before the heavy isotope symbol to indicate the ratio i.e., $\delta^{13}\text{C}$. The units are expressed as “per mil” which uses the symbol “‰”. The delta value of a sample is calculated using the equation:

$$\delta^{13}\text{C} = \left[\left(\frac{R_{\text{sample}}}{R_{\text{standard}}} \right) - 1 \right] 1000$$

where R is the molar ratio of the heavy to light isotope $^{13}\text{C}/^{12}\text{C}$. The international reference standard for carbon was a limestone, Pee Dee Belemnite (PDB), which has a $^{13}\text{C}/^{12}\text{C}$ ratio of 0.0112372 and a $\delta^{13}\text{C}$ value of 0 ‰. As all of this primary standard has been consumed, secondary standards calibrated to the PDB standard are used. Relative to this standard most organic materials have a negative $\delta^{13}\text{C}$ value.

Atmospheric CO_2 , which is taken up by plants in the process of photosynthesis, presently has a $\delta^{13}\text{C}$ value of about -8.5. In turn, the $\delta^{13}\text{C}$ signatures of organic compounds produced by plants partly depends on their photosynthetic pathway, primarily either C_3 or C_4 . During photosynthesis, carbon passes through a series of reactions or trophic steps along the C_3 or C_4 pathways. At each trophic step, isotopic fractionation occurs and organic matter in the plant (i.e., the destination pool) is depleted by 1 ‰. The C_3 pathway is longer than the C_4 pathway so that organic compounds produced by C_3 plants have a more depleted $\delta^{13}\text{C}$ signature. There is also variation in the actual amount of

fractionation between plant species having the same photosynthetic pathway. This results in a range of $\delta^{13}\text{C}$ values, although typical bulk values for C_3 and C_4 plants vary around -26‰ and -12‰ respectively. The rate of fractionation also varies between the various types of organic compounds produced by plants. Thus, by these processes a range of organic compounds each with unique $\delta^{13}\text{C}$ signatures are produced by plants that can potentially be used as natural tracers or biomarkers.

The instruments used to measure stable isotopes are called “isotope ratio mass spectrometers” (IRMS) and they report delta values directly. However, because they have to measure the amount of ^{12}C in the sample, and the bulk of the sample C will be ^{12}C , the instrument also gives the percent C (%C) in the sample.

When analysing the stable isotopes in a sample, the $\delta^{13}\text{C}$ value obtained is referred to as the bulk $\delta^{13}\text{C}$ value. This value indicates the type of organic material in the sample and the level of biological processing that has occurred. (Biological processing requires passage through a cell wall, such as in digestion and excretion processes and bacterial decomposition.) The bulk $\delta^{13}\text{C}$ value can be used as an indicator of the likely source land cover of the sediment. For example, fresh soil from forests has a high organic content with %C in the range 5% to 20% and a low bulk $\delta^{13}\text{C}$ value in the range -28‰ to -40‰ . As biological processing occurs, bacterial decomposition converts some of the organic carbon to carbon dioxide (CO_2) gas which is lost to the atmosphere. This reduces the %C value and, because microbial decomposition has many steps, the bulk $\delta^{13}\text{C}$ value increases by $\sim 1\text{‰}$ for each step. Pasture land cover and marine sediments typically have bulk $\delta^{13}\text{C}$ values in the range -24‰ to -26‰ and -20‰ to -22‰ , respectively. Wastewater and dairy farm effluent have bulk $\delta^{13}\text{C}$ values more enriched than -20‰ . Consequently, a dairy farm where animal waste has been spread on the ground as fertilizer, will have bulk $\delta^{13}\text{C}$ values higher (more enriched) than pasture used for sheep and beef grazing.

There are occasions when the inorganic component of the soil imparts a highly modified $\delta^{13}\text{C}$ isotopic signature to the soil such that the $\delta^{13}\text{C}$ value cannot be used for modelling of soil sources. This phenomenon occurs for example in Karst (limestone) soils, such as in the upper Whangarei Harbour associated with the Portland sediment.

In addition to the bulk $\delta^{13}\text{C}$ value, organic carbon compounds in the sediment can be extracted and the $\delta^{13}\text{C}$ values of the carbon in each different compound can be measured. These values are referred to as compound-specific stable isotope (CSSI) values. A forensic technique recently developed to determine the provenance of sediment uses both bulk $\delta^{13}\text{C}$ values and CSSI values from each sediment sample in a deposit for comparison with signatures from a range of potential soil sources for different land cover types. This method is called the CSSI technique (Gibbs, 2008).

The CSSI technique is based on the concepts that:

1. land cover is primarily defined by the plant community growing on the land, and
2. all plants produce the same range of organic compounds but with slightly different CSSI values because of differences in the way each plant species grows and also because each land cover type has a characteristic composition of plant types that contribute to the CSSI signature.

The compounds commonly used for CSSI analysis of sediment sources are natural plant fatty acids (FAs) which bind to the soil particles as labels called biomarkers. While the amount of a biomarker may decline over time, the stable isotope values of the FA biomarkers do not change.

These stable isotope values for the suite of FA biomarkers in a soil provides positive identification of the source of the soil by land cover type.

The sediment at any location in an estuary or harbour can be derived from many sources including river inflows, coastal sediments and harbour sediment deposits that have been mobilised by tidal currents and wind-waves. The contribution of each sediment source to the sediment mixture at the sampling location will be different. To separate and apportion the contribution of each source to the sample, a mixing model is used. The CSSI technique uses the mixing model IsoSource (Phillips and Gregg, 2003). The IsoSource mixing model is described in more detail in a following section.

While the information on stable isotopes above has focused on carbon, these descriptions also apply to nitrogen (N), which also has two stable isotopes, ^{14}N and ^{15}N . The bulk N content (%N) and bulk isotopic values of N, $\delta^{15}\text{N}$, also provide information on land cover in the catchment but, because the microbial processes of nitrification and denitrification can cause additional fractionation after the sediment has been deposited, bulk $\delta^{15}\text{N}$ cannot be used to identify sediment sources. The fractionation step for N is around +3.5‰ with bulk $\delta^{15}\text{N}$ values for forest soils in the range +2‰ to +5‰. Microbial decomposition processes result in bulk $\delta^{15}\text{N}$ values in the range 6‰ to 12‰ while wastewater and dairy effluent can produce bulk $\delta^{15}\text{N}$ values up to 20‰. However, the use of synthetic fertilizers such as urea, which has $\delta^{15}\text{N}$ values of -5‰, can result in bulk $\delta^{15}\text{N}$ values <0‰.

Sample analyses

An aliquot of each dry sediment sample was acidified with 1 N hydrochloric acid to remove inorganic carbonate before analysing for bulk organic C and N stable isotopes. About 50 mg of each acidified sample was combusted in a helium gas stream in a Fisons N1500 Elemental Analyser coupled via a ConFlo-II interface to a Thermo-Finnegan Continuous Flow Isotope Ratio Mass Spectrometer (CF-IRMS).

For $\delta^{13}\text{C}$, CF-IRMS measurements typically have a precision of ± 0.1 ‰ or better and the instrument also provides the proportion of organic C and N (%) in each sample.

Aliquots (20 to 40 g) of the non-acidified dry sediment were extracted with hot dichloromethane (100 °C) under high pressure (2000 psi) in a Dionex Accelerated Solvent Extractor (ASE 2000) to extract the fatty acids bound to the sediment particles. The FAs were methylated using 5% boron trifluoride catalyst in methanol to produce fatty acid methyl esters (FAMES). These FAMES were analysed by gas chromatography (GC)-combustion-IRMS to produce compound-specific stable isotope $\delta^{13}\text{C}$ values i.e., CSSI values. Method details and data interpretation protocols were described previously by Gibbs (2008).

Fatty acids are highly polar, so they cannot be analysed directly as they will bind to the gas chromatograph (GC) column during analysis. Consequently, they must be derivatised into their methyl esters, which are non-polar, using a catalyst such as boron trifluoride (BF_3) in methanol (MeOH). Each FA methyl ester (FAME) consists of the FA carbons plus one carbon from the MeOH used for the derivatisation step. The analytical values from the GC-combustion-isotope ratio mass spectrometer (GC-C-IRMS) were corrected for the added carbon in a methyl-group from the methanol used in the derivatisation to obtain the CSSI value for each FA using the equation:

$$\delta^{13}\text{C}_{\text{FA}} = (\delta^{13}\text{C}_{\text{FAME}} - (1-X) * \delta^{13}\text{C}_{\text{Methanol}}) / X$$

where FA is the fatty acid and X is the fractional contribution of the FA to the FAME. X can be calculated from the number of carbons in the FA molecule divided by the number of carbon atoms in the FAME derived from the FA. For example, the FA stearic acid (C18:0) has 18 carbon atoms

whereas the FAME produced, methyl stearate, has 19 carbon atoms, including one added carbon from the methanol, and thus has an X value of 18/19 or 0.9474. $\delta^{13}\text{C}_{\text{FA}}$ is the FA CSSI value corrected for the methyl- group, $\delta^{13}\text{C}_{\text{FAME}}$ is the uncorrected isotopic value for the FAME and $\delta^{13}\text{C}_{\text{Methanol}}$ is the isotopic value for the methanol used in the derivatisation step.

The CG-C-IRMS analysis uses FA standards, both internal and external, of known CSSI $\delta^{13}\text{C}$ value for the calibration of the soil FAMES and uses the retention times of the standards to confirm the identity of each FA being measured. This methyl-group correction was applied to all FAMES.

Several corrections are applied to the raw data to enable direct comparison of data between batches and for samples of varying ages (in the case of the sediment cores):

- Methyl-group (MeOH, FAME only) corrections to the $\delta^{13}\text{C}$ signature of each batch.
- Soil and sediment samples are often analysed in batches. This requires inter-batch corrections for individual FAs were to be applied relative to a master batch. These corrections account for slight differences arising from sample processing (extraction and derivatisation) and IRMS instrument set up and/or setting values for internal lab calibration standards between batches. The master batch maybe the first batch or the largest batch in a series. These inter-batch corrections are made using a NIWA FAME standard that are analysed with each batch.
- These inter-batch and methyl-corrected $\delta^{13}\text{C}$ FA data were finally adjusted for the Suess Effect to the year 2015 AD (i.e., sediment cores only). The Suess Effect describes the progressive depletion of the atmospheric CO_2 $\delta^{13}\text{C}$ signature, which is largely due to the combustion of fossil fuels since the early 1700s. This process also results in a depletion of soil $\delta^{13}\text{C}$ signatures as plants utilise CO_2 in photosynthesis and subsequently label potential soil sources (Verburg, 2007, Gibbs et al. 2014b). The annual rate of $\delta^{13}\text{C}$ CO_2 depletion in New Zealand is -0.025‰ (per mil) per year (source: NIWA).

This Suess Effect correction is critical to enable direct comparison of sediment deposits with sources of varying ages, which has resulted in a $\sim 2.15\%$ depletion in $\delta^{13}\text{C}$ values since 1700.

Data processing and presentation

The %C and suite of CSSI values for the extracted FAMES were assembled into a matrix table and modelled using IsoSource to estimate the number (n) of isotopically feasible proportions of the main sediment sources at each sampling location. In successive model iterations, potential sources were added or removed to find an isotopic balance where the confidence level was high (lowest n value) and uncertainty was low. The isotopically feasible proportions of each soil source are then converted to soil proportions using the %C of each soil on a proportional basis. That is, the higher the %C in the soil, the less of that soil source is required to obtain the isotopic balance. In general, soil proportions less than 5% were considered possible but potentially not present. Soil proportions $>5\%$ were considered to be present within the range of the mean \pm SD.

CSSI Method

The CSSI method applies the concept of using the $\delta^{13}\text{C}$ signatures of organic compounds produced by plants to distinguish between soils that develop under different land-cover types. With the exception of monocultures (e.g., wheat field), the $\delta^{13}\text{C}$ signatures of each land-cover type reflects the combined signatures of the major plant species that are present.

For example, the isotopic signature of a lowland native forest in the upper North Island will be dominated by kauri, rimu, totara and tānekaha. A monoculture, such as pine forest, by comparison will impart an isotopic signature that largely reflects the pine species, as well as, potentially, any understory plants.

The application of the CSSI method for sediment-source determination involves the collection of sediment samples from potential subcatchment and/or land cover sources as well as sampling of sediment deposits in the receiving environment. These sediment deposits are composed of mixtures of terrigenous sediments, with the contribution of each source potentially varying both temporally and spatially. The sampling of catchment soils provides a library of isotopic signatures of potential sources that is used to model the most likely sources of sediments deposited at any given location and/or time.

Straight-chain FAs with carbon-chain lengths of 12 to 26 atoms (C12:0 to C26:0) have been found to be particularly suitable for sediment-source determination as they are bound to fine sediment particles and long-lived (i.e., decades to millennia). Fatty acids including myristic (C14:0): palmitic (C16:0), stearic (C18:0), arachidic (C20:0) and behenic (C22:0) have commonly been used to evaluate present and historical sources of terrigenous sediments. Although breakdown of these FA to other compounds eventually occurs, the signature of a remaining FA in the mixture does not change.

The stable isotope compositions of N and C and the CSSI of carbon in the suite of fatty acid (FA) biomarkers are extracted from catchment soils and marine sediments. It is the FA signatures of the soils and marine sediments that are used in this study to determine sediment sources. Gibbs (2008) describes the CSSI method in detail.

Correction of the CSSI signatures for the Suess Effect

The reconstruction of changes in sources of terrigenous sediment deposited in a freshwater or marine receiving environment can be determined from dated cores using the FA isotope signatures preserved in the sediments. Before the feasible sources of these sediments could be evaluated using the IsoSource package, the isotope (i.e., input) data required correction for the effects of the release of “old carbon” into the biosphere over the last 300 years, associated with the burning of fossil fuels and deforestation.

Specifically, the release of old carbon with a depleted $\delta^{13}\text{C}$ signature has resulted in a decline in $\delta^{13}\text{C}$ in atmospheric CO_2 ($\delta^{13}\text{CO}_2$). The changing abundance of carbon isotopes in a carbon reservoir associated with human activities is termed the Suess Effect (Keeling 1979). This depletion in atmospheric $\delta^{13}\text{CO}_2$ is of the order of 2 ‰ since 1700 and has accelerated substantially since the 1940s (Verburg 2007). Thus, the $\delta^{13}\text{C}$ signatures of plant biomarkers, such as Fatty Acids have also changed due to the Suess Effect. Consequently, the isotopic signatures of estuarine sediments (i.e., the mixture) deposited in the past must be corrected to match the isotopic signatures of present-day source soils. The release of this fossil carbon is associated with anthropogenic activity (the so-called Suess Effect). Figure C-1 presents the atmospheric $\delta^{13}\text{C}$ curve reconstructed by Verburg (2007) using data collected in earlier studies and includes measurements of material dating back to 1570 AD. These data indicate that the atmospheric $\delta^{13}\text{C}$ signature was stable until 1700 AD, with subsequent depletion of $\delta^{13}\text{C}$ due to release of fossil carbon.

In the present study, we use this atmospheric $\delta^{13}\text{C}$ curve to correct the isotopic values of the FAs in sediment samples of varying ages taken from cores to equivalent modern values.

This is required because the $\delta^{13}\text{C}$ values of the FAs from the potential catchment sources are modern (i.e., 2010 AD), and are therefore depleted due to the Suess Effect. For example, the $\delta^{13}\text{C}$ value of a Fatty Acid derived from a kauri tree growing today will be depleted by -2.15 ‰ in comparison to a kauri that grew prior to 1700 AD (Fig. 8.1). It can be seen that the isotopic correction for the period since 1700 is variable depending on age. Examples of this correction process for isotopic data for sediments taken from a sediment core collected in the Bay of Islands are presented in Table C-1

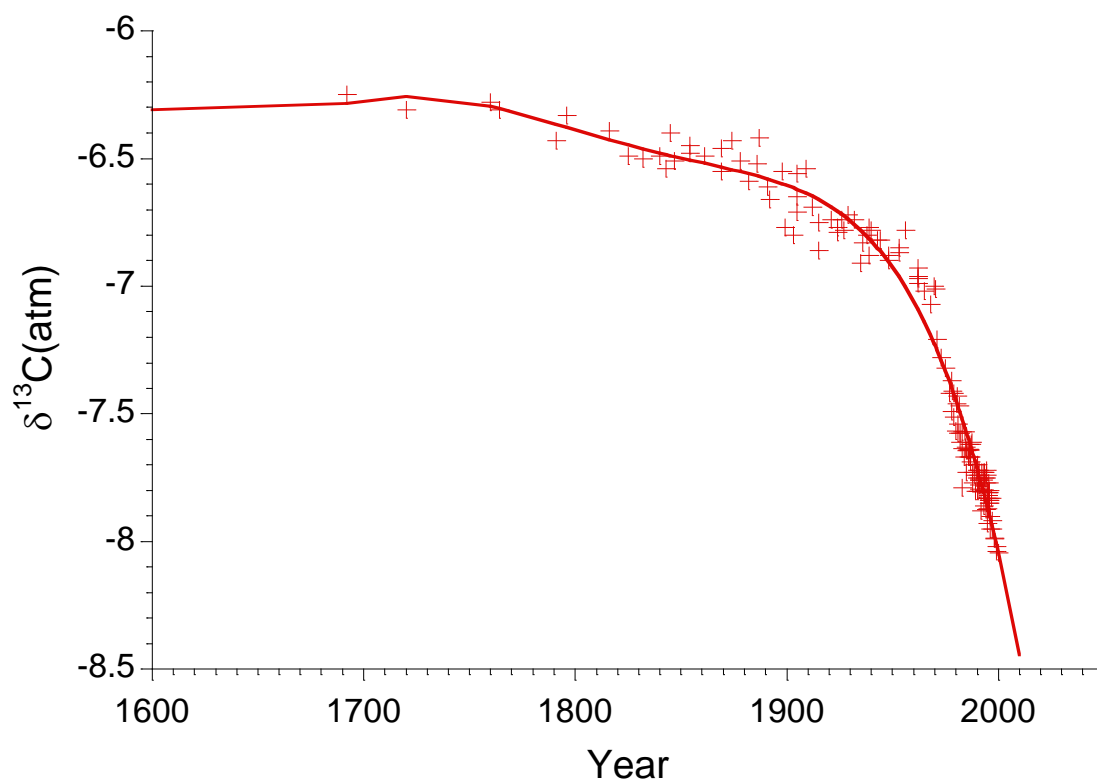


Figure C-1: Historical change in atmospheric $\delta^{13}\text{C}$ (per mil) (1570–2010 AD) due to release of fossil carbon. The release of this fossil carbon is associated with anthropogenic activity (the so-called Suess Effect). Source: Verburg (2007).

Conversions of isotopic proportions to soil proportions

The IsoSource model provides estimates of the isotopic-proportional contributions of each land-cover (i.e., soil) type in each marine sample. Thus, these results are in terms of carbon isotopic proportions and not source soil proportions. Furthermore, the stable isotope tracers account for a small fraction, typically less than 2%, of total organic carbon (OC) in the soil and OC accounts for typically <10% of the soil by weight. These factors mean that the contribution of each source soil to a sediment mixture will scale with the soil carbon content. Consequently, a linear correction based on the soil OC is required to estimate the proportion of each soil source in a sediment sample from a receiving environment (Gibbs 2008).

To convert the isotopic proportions to soil proportions ($S_n\%$) the simple linear correction equation below was used:

$$S_n\% = \frac{I_n/C_n\%}{\sum_n^1 (I_n/C_n\%)} * 100$$

Where I_n is the mean feasible isotopic proportion of source soil n in the mixture estimated using an isotopic mixing model and $C_n\%$ is the percentage organic carbon in the source soil.

Because this calculation only uses the OC% in the source soils for linear scaling, the proportional contribution of each source soil is not influenced by any loss of carbon (e.g., total carbon, FAs etc.) in the sediment mixture due to biodegradation. The level of uncertainty in the mean soil proportion is the same as that defined by the standard deviation about the mean isotopic proportion.

A simple example of this linear correction is illustrated here by considering a solution composed of a mixture of three different sodium (Na) salts which provide equal proportions of Na to the mixture (3 x 1/3 each): sodium chloride (NaCl, molecular weight 58.45), sodium nitrate (NaNO₃, mw 85.0), and sodium sulphate (Na₂SO₄, mw 142.0). Consider each of these salts to represent a different source soil, each of which are present in a sediment mixture. The %Na represents the % carbon in each source soil. The %Na in each salt is calculated by dividing the atomic weight of sodium (23) by the molecular weight of each salt compound, but also recognising how many atoms of sodium are present in the molecule.

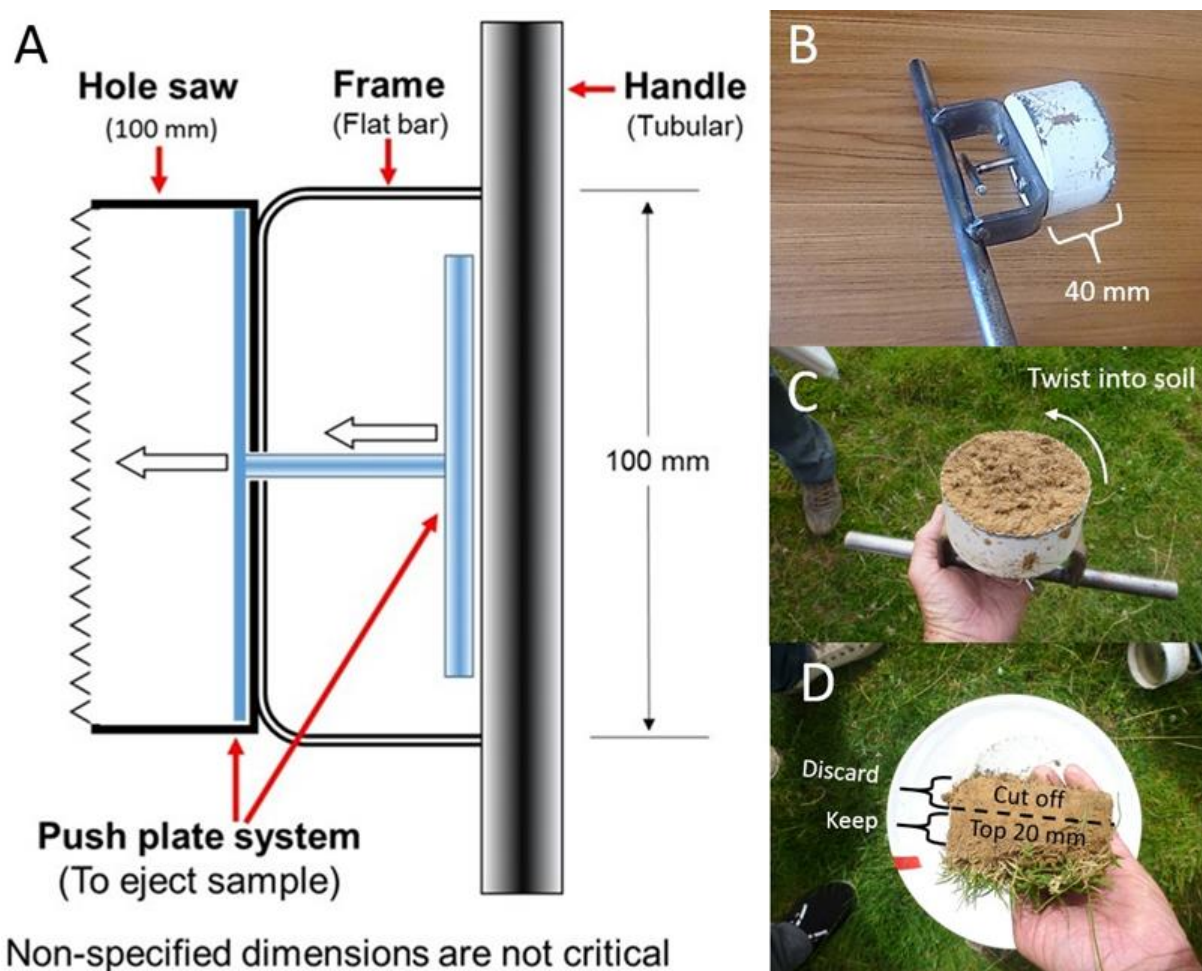
Table C-1 below presents the calculations required to apply the linear correction equation using the sodium salts example in order to determine how much of each salt is in the mixture. The ratio M%/S% for each salt and sum of this ratio (3.11) represent the numerator and denominator respectively in the conversion equation. Thus, for example the proportion of NaCl salt in the mixture is given by $(0.85/3.11) \times 100 = 27.3\%$.

Table C-1: Example of the linear correction method to convert the isotopic proportions to soil proportions. Using sodium (Na) salt compounds as analogies to various soil sources present in a mixture.

Salt type	%Na in salt (S%)	%Na in mixture (M%)	M%/S%	% salt in mixture
NaCl	39.4	33.3	0.85	20.5
NaNO ₃	27.1	33.3	1.23	29.8
Na ₂ SO ₄	32.4	33.3	1.03	33.1
SUM			3.11	

Appendix D Soil sampling method

Topsoil and subsoil samples were collected at sampling sites using a purpose-built hand corer to ensure equivalent soil volumes were collected to prevent any bias in the composite sample. The hand corer was cleaned of any residual soil prior to use at each site. Soil plugs were obtained by twisting the corer into the soil that was then extruded. The saw teeth effectively cut through the root sward in the ground. The core barrel is about 40 mm long and provides enough friction for the soil plug to come out of the ground inside the corer (Figure D-1). Each soil plug was partially extruded leaving the 0–20 mm depth section inside the corer and allowing the exposed 20–40 mm depth section to be cut off and discarded. The soil in the upper 0–20 mm depth layer was crumbled from the plant root mass and combined into a bulk composite sample in a 20-L plastic bucket. Coarse plant material (twigs, leaves, roots), stones, seeds, worms and insects were removed by hand picking. The composite soil sample was mixed thoroughly by hand before a 200–400 g aliquot of the mixture was sealed in zip-lock type sealable plastic bag for laboratory analysis.



Non-specified dimensions are not critical

Figure D-1: Hand corer used for land use sampling. A) Schematic cross section showing the push plate system used to extrude the soil from the corer after collection, B) side view of the hand corer showing the push plate handle ready for coring, C) a view of the inverted corer after collecting a pasture core, and D) the soil plug extruded from the corer ready for trimming to 20 mm thickness before combining in the composite sample. Note: this soil plug would normally be retained in the corer until the soil sample in the 20–40 mm core section had been removed.

Appendix E Estuarine core sites and composition analysis

Table E-1: Details of estuarine sediment cores collected. Havelock Estuary and Mahau Sound, March and December 2017.

Site	Environment	Date	Time (NZDT)	Water depth (m)	NZTM-E	NZTM-N	Retained core lengths A-B-C- (cm)
Havelock	High tide: 1051						
HV-1	Intertidal	28/03/17	0845	2.3	1664001	5431334	75/104/88
HV-2	Intertidal		1020		1663797	5430931	94/84/90
HV-3	Intertidal		1130		1664029	5430712	56/54
HV-4	Intertidal		1225		1664356	5430798	64/69/62
HV-5	Intertidal		1325		1664195	5431140	57/69
Mahau							
MH-1	Subtidal	12/12/17	0950	4.1	1674380	5435058	140/151/145/151/141
MH-2	Subtidal		1350	4.7	1674191	5434476	148/158 x 5 replicates
MH-3	Subtidal		1600	5.2	1673897	5433729	159/159/158/161/154/157

Sediment cores selected for radioisotope dating were cut open lengthwise using a skill saw with a 125 mm diameter blade. After cutting the core barrels along their entire lengths on both sides, thin stainless-steel sheets were pushed through the sediment to split the core into two separate halves. The cores were first logged, including description of any obvious sediment layers before subsampling for radioisotope, particle size and bulk density analyses.

X-radiographs were made of each sediment core prior to dating. To do this, cores were split lengthways and sectioned into 40 cm long and 2 cm thick longitudinal slabs. These slabs were then imaged using a Varian PaxScan 4030E amorphous silicon digital detector panel (Figure E-1). X-rays were generated using an Ultra EPX-F2800 portable x-ray source with a typical exposure of 25 mAs (milliamp seconds) and 50–60 kiloelectron Volts (keV). The raw x-ray images were post-processed using the Image-J software package.



Figure E-1: NIWA digital x-ray system. A sediment slab mounted on the x-ray detector plate ready for imaging. Photo: Ron Ovenden, NIWA.

Dry bulk sediment density (ρ_b) was calculated as the dry mass per unit volume of sediment in each 1-cm thick core slice prepared for radioisotope dating. The slice volume was 78 cm^3 for the 10-cm diameter cores. Samples were processed by first weighing on a chemical balance to the nearest 0.01 g, dried at 70°C for 24 hours and reweighed to obtain the dry-sample weight. The ρ_b is expressed in units of grams per cubic centimetre (g cm^{-3}) and was calculated from the dry sample weight and sample volume. The ρ_b reflects the bulk characteristics of the sediment deposit, in particular sediment porosity (i.e., proportion of pore-space volume) and particle characteristics, such as size distribution and mineralogy. For example, the ρ_b of an estuarine sand deposit is of the order of $1.5\text{--}1.7 \text{ g cm}^{-3}$, whereas a mud deposit with high water content can typically have a ρ_b of $\sim 0.5 \text{ g cm}^{-3}$.

Appendix F Source library for Pelorus River and Mahau Sound

Table F-1: Land use library isotopic data from sites as shown in Figure 2-4. Mean data are the isotopic values of the fatty acids extracted from the land use soils. Std deviations are for the mean data by land use.

Note: sources listed in alphabetical order as output by MixSIAR model.

Land use	%C	$\delta^{13}\text{C}$	C14:0	C16:0	C18:0	C20:0	C22:0	C24:0	C26:0
Mean values	%	‰	‰	‰	‰	‰	‰	‰	‰
Bracken	12.24	-28.83	-32.97	-30.43	-34.30	-34.44	-35.21	-35.52	-34.30
Dairy	8.85	-29.38	-33.65	-32.53	-34.09	-34.42	-35.17	-35.92	-34.09
Gorse and Broom	13.34	-29.19	-33.49	-30.80	-34.56	-34.19	-35.92	-36.71	-34.56
Harvested Pine	6.03	-28.81	-38.33	-32.43	-33.05	-32.49	-33.39	-33.71	-33.05
Kanuka	20.87	-28.02	-29.65	-31.00	-31.23	-31.36	-31.72	-31.59	-31.23
Native Forest	23.28	-28.13	-31.57	-28.36	-28.35	-29.82	-30.69	-30.84	-28.35
Stream Bank	1.42	-27.30	-30.20	-29.11	-32.86	-32.01	-33.05	-35.59	-32.86
Subsoil	0.72	-27.01	-30.94	-31.28	-33.75	-32.87	-33.45	-35.83	-33.75
Std Deviation									
Bracken		0.29	0.86	0.24	0.55	0.29	0.86	0.24	0.55
Dairy		0.55	0.79	0.95	1.56	0.55	0.79	0.95	1.56
Gorse and Broom		0.03	0.94	0.68	0.15	0.03	0.94	0.68	0.15
Harvested Pine		0.78	1.73	1.64	1.14	0.78	1.73	1.64	1.14
Kanuka		0.14	1.33	1.75	0.46	0.14	1.33	1.75	0.46
Native Forest		0.53	1.22	1.16	0.08	0.53	1.22	1.16	0.08
Stream Bank		0.56	1.67	1.10	0.45	0.56	1.67	1.10	0.45
Subsoil		1.07	1.02	1.06	0.41	1.07	1.02	1.06	0.41

Table F-2: Sediment source library of FA isotopic data used for modelling sources of sediment deposited at Mahau core sites. Data for individual samples and mean and standard deviation values for % carbon, and isotopic values ($\delta^{13}\text{C}$ ‰) of fatty acids extracted from the catchment and marine sources are presented. There are some differences between the river and Mahau sound source libraries due to the fact that the Sound potentially receives sediment from all sources, and (2) some sources were merged as their isotopic signatures were similar. Notes: [1] harvested pine included as a potential source for sediments deposited post-1979, [2] sources listed in alphabetical order as output by MixSIAR model.

Source	Description	NZTM-East	NZTM-North	Sample ID	%C	C14:0 (‰)	C20:0 (‰)	C22:0 (‰)	C24:0 (‰)	C26:0 (‰)
Harvested Pine	Clifton Lodge Forest Rd	1660219	5430787	196/37	9.94	-29.86	-40.34	-34.44	-32.87	-32.04
	Golden Age Wakamarina Valley Rd	1654592	5421402	196/38	6.00	-38.84	-32.75	-30.53	-32.18	-33.29
	Tunakino Valley	1694197	5373045	196/39	3.44	-36.21	-33.84	-33.18	-33.85	-33.02
	Pine (Recent harvest)	1651448	5426938	204/22	4.76	-37.94	-31.41	no data	no data	-33.10
				Mean	6.03	-38.33	-33.05	-32.49	-33.39	-33.71
			SD	2.80	1.73	1.25	1.72	1.06	1.14	
Kanuka	Kanuka Maungatapu Rd	1649868	5428299	204/27B	17.97	-30.58	-32.86	-32.19	-32.56	-32.14
	Kanuka Tinline Rd Pratts-1	1641080	5426295	204/28B	27.39	-28.13	-31.32	-30.89	-31.43	-31.27
	Kanuka Tinline Rd Pratts-2	1641080	5426295	204/29B	17.26	-30.25	-29.50	-30.98	-31.17	-31.37
				Mean	20.87	-29.65	-31.23	-31.36	-31.72	-31.59
				SD	5.65	1.33	1.68	0.73	0.74	0.47
Marine	Chetwode-1 (32 m depth)	1692898.3	5472291.3	196/66	0.80	-24.45	-30.07	-29.29	-28.02	-28.30
	Chetwode-2 (31 m)	1691654.5	5471876.6	196/67	0.85	-25.30	-25.54	-28.63	-27.23	-23.70
	Chetwode-3 (18 m)	1691185.7	5471573.2	196/68	0.63	-24.43	-26.27	-27.07	-27.22	-28.50
	Chetwode-4 (30 m)	1690592.3	5471223	196/69	0.78	-24.92	-24.48	-29.00	-27.10	-25.51
	Chetwode-5 (18 m -near 2015 site)	1690283.9	5471231.6	196/70	0.69	-19.28	-25.13	-28.60	-27.64	-28.15
	Chetwode-7 (21 m)	1689586.9	5471014.9	196/71	0.99	-22.69	-25.64	-29.09	-27.85	-29.01
				Mean	0.79	-23.51	-26.19	-28.62	-27.51	-27.19
				SD	0.13	2.26	1.99	0.80	0.38	2.10

Source	Description	NZTM-East	NZTM-North	Sample ID	%C	C14:0 (‰)	C20:0 (‰)	C22:0 (‰)	C24:0 (‰)	C26:0 (‰)
Native Forest	Beech forest-Pelorus bridge	1648030.2	5427218.9	183/160	9.74	-32.43	-28.97	-29.08	-30.31	-29.39
	Beech forest-Double Bay-Kenepuru			183/169	12.48	-30.71	-27.73	-30.56	-31.07	-32.28
	Beech forest-Nydia Bay			183/178	4.72	-34.83	-29.89	-28.23	-30.12	-31.17
	Rimu, tawa, Native-Pelorus Bridge	1647973	5427215	183/161	36.81	-31.48	-30.77	-30.70	-30.84	-30.66
				Mean	15.94	-32.36	-29.34	-29.64	-30.59	-30.88
			SD	14.28	1.79	1.30	1.19	0.44	1.20	
Scrub and Pasture	Gorse and Broom Rai Hill	1647165	5438485	204/1	10.27	no data	-35.47	-35.34	-37.42	-37.69
	Gorse and Broom Rai (Upper)	1649248	5429724	204/14	5.28	-34.16	-35.30	-34.66	-36.06	-36.27
	Gorse and Broom Pelorus	1651381	5428568	204/19	24.47	-32.83	-32.92	-32.58	-34.29	-36.17
	Gorse and Broom Havelock Estuary	1665108	5429332	204/26	5.87	-32.05	-32.87	-32.75	-33.35	-34.71
	Bracken-Rai Valley Roadside	1648374	5433945	196/35	7.70	-32.34	-34.49	-34.52	-35.45	-34.68
	Bracken-Opouri Valley Roadside	1658346	5439916	196/36	7.45	-32.62	-35.48	-36.04	-36.17	-35.85
	Bracken Rai Upper	1649030	5429747	204/15	21.57	-33.95	-32.92	-32.77	-34.00	-36.03
	Dairy grazing-Pelorus Rd.	1653873	5429763.3	183/187	8.50	-32.86	-32.66	-33.53	-34.15	-35.72
	Dairy grazing-Opouri River	1656521.5	5437737.6	183/188	14.36	-34.60	-33.91	-34.65	-35.28	-35.84
	Zilwood Dairy landuse	1653572	5429026	196/26	7.67	-33.22	-34.98	-34.47	-35.42	no data
	Opouri Rd Dairy landuse	1657156	5438334	196/27	7.08	-33.19	-35.16	-34.69	-35.32	no data
	Dairy-Wratts (Kaituna)	1664364	5426738	196/43	6.64	-34.39	-33.71	-34.78	-35.67	-36.22
	Sheep-Newtons Lwr hillslope (Kaituna)	1664998	5427249	196/31	6.81	-32.77	-35.73	-35.35	-36.18	-36.03
	Sheep-Newtons Upp terrace (Kaituna)	1664970	5426563	196/32	3.80	-32.84	-33.68	-34.50	-35.33	-35.48
	Sheep-Footes (Kaituna)	1663507	5424460	196/33	5.07	-33.98	-35.99	-35.33	-36.02	-36.09
	Sheep and Beef Kaituna	1663141	5419678	204/12	4.78	-33.26	-34.72	-33.01	-34.63	-35.64
	Scrub and Pasture				Mean	9.21	-33.27	-34.37	-34.31	-35.30
				SD	5.95	0.77	1.14	1.06	1.02	0.72

Source	Description	NZTM-East	NZTM-North	Sample ID	%C	C14:0 (‰)	C20:0 (‰)	C22:0 (‰)	C24:0 (‰)	C26:0 (‰)
Stream Bank	Bank Erosion in Opouri River	1657308	5438310	196/17B	1.23	-28.33	-32.49	-32.07	-33.07	-38.19
	Bank Erosion in Tunakino River	1652318	5437440	196/18B	1.22	-30.73	-32.83	-31.55	-32.79	-33.63
	Bank Erosion in Kaiuma Stream	1652187	5437527	196/20B	1.61	-31.55	-33.27	-32.42	-33.29	-34.96
				Mean	1.42	-30.20	-32.86	-32.01	-33.05	-35.59
				SD	0.28	1.67	0.39	0.44	0.25	2.35
Subsoil	Subsoil-Footes Farm (Kaituna)	1663424	5424320	196/40	1.73	-33.45	-33.13	-33.18	-33.68	-33.24
	Subsoil-Tunakino Valley (Kaituna)	1663055	5423794	196/41	0.99	-31.66	-33.15	-31.72	-32.44	-34.68
	Subsoil-Clifton Lodge Forest Rd (Pelorus)	1660243	5430693	196/42	0.46	-30.22	-34.35	-34.02	-34.46	-36.98
	Kaituna (upper) subsoil steep slope	1663141	5419678	204/13	0.60	-34.77	-32.59	-32.10	-38.93	-34.27
	Pelorus subsoil Hughes block Rd	1651224	5426010	204/23	1.84	-35.11	-31.63	-30.76	-29.76	-32.27
				Mean	1.12	-33.04	-32.97	-32.36	-33.85	-34.29
			SD	0.64	2.08	0.99	1.27	3.35	1.77	

Appendix G Mixing models

Two-endmember model

The two-endmember mixing model assumes that the FA isotopic values of a well-mixed sediment mixture downstream of a river confluence is the sum of the proportional contribution of the FA isotopic values of inputs from each upstream source, **A** and **B**, where A can be the tributary and B can be the main stem of the river.

$$\delta^{13}\text{C}_{\text{mixture}} = f_A\delta^{13}\text{C}_A + f_B\delta^{13}\text{C}_B \quad (1)$$

Where f_A and f_B are the fractions or proportions of each source. This equation can also be rewritten

$$1 = f_A + f_B \quad (2)$$

To solve for f_A , the equation is rewritten as:

$$f_A = (\delta^{13}\text{C}_{\text{mixture}} - \delta^{13}\text{C}_B) / (\delta^{13}\text{C}_A - \delta^{13}\text{C}_B) \quad (3)$$

and for f_B , the equation is rewritten as:

$$f_B = (\delta^{13}\text{C}_{\text{mixture}} - \delta^{13}\text{C}_A) / (\delta^{13}\text{C}_B - \delta^{13}\text{C}_A) \quad (4)$$

The caveat for the two-endmember mixing model is that the isotopic value of each FA tracers in the mixture must be between the values of the sources A and B. Theoretically, this should be the case where only tributaries upstream contribute to the mixture downstream, and where both upstream sources are dissimilar. In the case were the downstream mixture has similar $\delta^{13}\text{C}$ tracer values to one of the upstream sources then modelling of the A and B source contributions will not be valid. This situation indicates incomplete mixing of the two source sediments and the mixture (i.e., flood sediment deposit) should be resampled further downstream.

MixSIAR model

The Bayesian mixing model, MixSIAR (Stock et al. 2018), employed in the study is used to construct the probability distributions of sources to a sediment mixture. A key advantage of MixSIAR is that it can account for uncertainty in the isotopic signatures of each source and resulting estimates of source contributions to a sediment mixture.

Probability model-fitting to the observed data is based on a Markov Chain Monte Carlo (MCMC) method whereby the isotopic proportions of potential sources are estimated by repeated random sampling and discarding those which are not “*probabilistically consistent with the data*” (Phillips et al. 2014). Subsequent estimates are required to be similar to previous ones, thereby creating a Markov Chain (Phillips et al. 2014). Model output consists of a sample of the posterior proportions derived from the MCMC simulation and represent true probability distributions of source proportions that can be summarised by various descriptive statistics, including the 95% credible interval. MixSIAR includes diagnostic tests to determine convergence of the MCMC on the posterior distributions for all variables in the model.

The repeatability of source proportions calculated by the MCMC model fitting process was also demonstrated for the Mahau Sound sediment core MH-1 by conducting three model runs for each of the 15 samples. Statistics for the modelled isotopic source proportions from this assessment

indicated that the MCMC process produced outputs with very good repeatability. The results of these tests are presented in **Appendix J**.

The MCMC settings for the modelling were: three chains, chain lengths of 300,000, “burn in” of 200,000 and “thin” value of 100. This generated model output containing 3000 samples of posterior source proportions (sum = 1). Typical model run times (run length: long) for seven sources and five FA tracers were ~3 minutes using a laptop computer with an Intel i7 processor. A continuous effects model, with a process only (i.e., $n = 1$) error structure, was employed to estimate the posterior distributions of sources for each individual sediment mixture sampled from the river sediment or dated cores. This process-only error structure implements the MixSIR model (Moore and Semmens, 2008) within the MixSIAR suite, so that uncertainty includes the source variance only and no distinction is made from sources of variance associated with the trophic discrimination factors (TDF) (Stock and Semmens, 2015; 2016). Specification of TDF to account for differences in the isotopic values of consumers’ tissues and diet is a major source of uncertainty in estimating source contributions in food-web applications (Phillips et al. 2014, Stock and Semmens 2016). In the context of the present study, the fact that TDF are not required for sediment tracing studies, as well as the application of historical land use information to constrain potential sources, are key advantages. Bayesian estimates of source proportions can be informed by reliable priors based on data and thereby constrain the model and reduce uncertainty. For example, in food web studies, the gut contents of fish (i.e., prey species and relative abundance) can be used to construct priors in MixSIAR. In the present study, reliable/semi-quantitative information on the relative contributions of various sediment sources at the river sites and in Mahau sound were unknown so that an “uninformative prior” was applied. An uninformative prior is one where all combinations of isotopic proportions (sum = 1) are equally likely (Stock and Semmens 2015).

MixSIAR model convergence diagnostics

Diagnostic tests of convergence of the Markov chain to a stationary distribution for all variables and measures of model fit provided with MixSIAR output are used to evaluate model performance for each sediment mixture analysed. These diagnostics are described here:

Gelman-Rubin test: the Gelman-Rubin test requires more than one Markov Chain Monte Carlo (MCMC) to be calculated (default number of chains = 3), with a value of 1 at convergence. A value of less than 1.1 is generally acceptable (Stock and Semmens, 2015). In the present study, most model variables had Gelman-Rubin values of less than 1.05.

Geweke test: the Geweke test is a two-sided z-test that compares the means of the first and second halves of each MCMC chain (i.e., expect 5% of model variables to be outside +/- 1.96). At model convergence these means should be the same, with large z-scores indicating rejection (Stock and Semmens, 2015).

DIC: the deviance information criterion (DIC, Spiegelhalter et al. 2002) provides another measure of model fit to the data and is commonly applied to Bayesian models where the posterior distributions have been estimated using MCMC methods. Model fit improves inversely with the DIC value. The DIC assumes that the posterior distribution is approximately multivariate normal.

The diagnostic model convergence information for the Pelorus River and Mahau Sound sediment core samples are presented below.

Table G-1: Pelorus River summary of MixSIAR model convergence. Results for diagnostic tests of convergence of the Markov chain to a stationary distribution for all variables and measures for tributary model runs estimating source soil contributions from their catchments.

Tributary	Gelman-Rubin			Geweke			DIC
	>1.01	>1.05	>1.10	Chain 1	Chain 2	Chain 3	
Upper Pelorus R.	0	0	0	2	0	0	6.00
Tinline R.	0	0	0	2	0	2	8.99
Rai R.	0	0	0	1	3	0	8.05
Wakamarina R.	0	0	0	0	0	0	8.18
Pelorus R. (at mouth)	0	0	0	1	3	0	8.04
Brown R.	0	0	0	0	0	0	8.24
Ronga R.	0	0	0	0	0	0	7.76
Tunakino R.	0	0	0	0	0	1	5.19
Kaiua R.	0	0	0	0	0	0	6.73
Opouri R.	0	0	0	2	5	2	11.69

Table G-2: Mahau core MH-1 summary of MixSIAR model convergence. Mahau core MH-1 summary of MixSIAR model convergence. Results for diagnostic tests of convergence of the Markov chain to a stationary distribution for all variables and measures of fit for three replicate model runs for each dated sediment mixture.

Sample depth (cm)	²¹⁰ Pb Year	Gelman-Rubin (n >1.05, out of 27 variables)			Geweke Chains n1/n2/n3			DIC		
		Run 1	Run 2	Run 3	Run 1	Run 2	Run 3	Run 1	Run 2	Run 3
1-2	2013	0	2	0	0/2/0	0/0/0	0/0/1	37.14	37.79	38.08
3-4	2009	0	0	0	0/7/1	0/3/3	4/0/3	19.31	19.52	19.00
6-7	2001	0	0	0	0/0/0	2/2/0	0/0/8	13.41	13.65	13.31
8-9	1996	0	0	0	0/0/0	1/3/3	2/3/1	14.71	14.93	14.54
11-12	1989	0	0	0	0/0/0	0/2/1	0/0/0	11.53	11.19	11.45
14-15	1982	0	0	0	6/3/0	0/0/1	5/0/0	12.31	12.41	12.56
16-17	1977	0	0	0	1/4/1	3/2/5	0/0/0	11.58	11.65	11.60
19-20	1969	0	0	0	0/0/0	3/5/0	0/5/0	10.89	10.80	11.22
22-23	1962	0	0	0	4/5/0	1/0/0	2/2/0	9.91	9.94	9.93

Sample depth (cm)	²¹⁰ Pb Year	Gelman-Rubin (n >1.05, out of 27 variables)			Geweke Chains n1/n2/n3			DIC		
24-25	1957	0	0	0	0/2/3	0/1/3	1/1/1	12.04	12.52	12.39
26-27	1952	0	0	0	2/0/0	0/0/0	5/0/1	11.83	11.83	11.98
29-30	1945	0	0	0	0/0/3	3/0/0	4/0/0	20.60	20.71	20.63
31-32	1940	0	0	0	2/1/0	2/3/0	1/2/0	11.23	11.39	11.35
33-34	1935	0	0	0	2/2/0	5/1/0	2/0/0	16.18	16.33	16.19
36-37	1928	0	0	0	0/0/1	0/3/0	0/1/0	17.89	17.82	17.46
39-40	1921	0	0	0	0/1/2	0/3/0	1/3/3	28.21	28.25	28.48

Table G-3: Mahau core MH-2 summary of MixSIAR model convergence. Mahau core MH-2 summary of MixSIAR model convergence. Results for diagnostic tests of convergence of the Markov chain to a stationary distribution for all variables and measures of fit for a single model run for each dated sediment mixture.

Sample depth (cm)	²¹⁰ Pb Year	Gelman-Rubin (n >1.05, out of 27 variables)			Geweke Chains n1/n2/n3			DIC		
		Run 1	Run 2	Run 3	Run 1	Run 2	Run 3	Run 1	Run 2	Run 3
1-2	2016	0	-	-	6/0/0	-	-	19.42	-	-
3-4	2012	0	-	-	0/0/3	-	-	12.66	-	-
6-7	2008	0	-	-	0/1/4	-	-	15.68	-	-
11-12	2002	0	-	-	0/0/0	-	-	15.75	-	-
15-16	1997	0	-	-	0/0/0	-	-	19.68	-	-
19-20	1991	0	-	-	1/3/2	-	-	13.75	-	-
22-23	1987	0	-	-	3/0/5	-	-	14.49	-	-
26-27	1982	0	-	-	0/1/0	-	-	14.71	-	-
29-30	1978	0	-	-	0/0/1	-	-	18.96	-	-
31-32	1966	0	-	-	0/0/0	-	-	14.13	-	-
33-34	1955	0	-	-	2/1/0	-	-	18.39	-	-
34-35	1949	0	-	-	5/10/0	-	-	17.70	-	-
36-37	1937	0	-	-	3/2/3	-	-	17.93	-	-
37-38	1931	0	-	-	7/3/6	-	-	15.08	-	-
39-40	1919	0	-	-	0/1/3	-	-	20.83	-	-

Table G-4: Mahau core MH-3 summary of MixSIAR model convergence. Mahau core MH-3 summary of MixSIAR model convergence. Results for diagnostic tests of convergence of the Markov chain to a stationary distribution for all variables and measures of fit for a single model run for each dated sediment mixture.

Sample depth (cm)	²¹⁰ Pb Year	Gelman-Rubin (n >1.05, out of 27 variables)			Geweke Chains n1/n2/n3			DIC		
		Run 1	Run 2	Run 3	Run 1	Run 2	Run 3	Run 1	Run 2	Run 3
0-1	2013	0	-	-	0/0/2	-	-	11.49	-	-
3-4	2008	0	-	-	0/0/0	-	-	11.15	-	-
5-6	2003	0	-	-	6/5/0	-	-	14.63	-	-
8-9	1995	0	-	-	6/1/4	-	-	13.85	-	-
11-12	1987	0	-	-	2/0/2	-	-	12.93	-	-
14-15	1979	0	-	-	1/1/1	-	-	15.69	-	-
16-17	1974	0	-	-	0/0/6	-	-	12.09	-	-
19-20	1966	0	-	-	0/1/0	-	-	15.48	-	-
21-22	1960	0	-	-	1/0/0	-	-	12.45	-	-
24-25	1952	0	-	-	0/0/0	-	-	12.88	-	-
26-27	1947	0	-	-	0/0/1	-	-	12.42	-	-
28-29	1942	0	-	-	0/0/2	-	-	12.85	-	-
31-32	1934	0	-	-	2/0/0	-	-	25.00	-	-
34-35	1926	0	-	-	0/2/0	-	-	25.23	-	-
36-37	1921	0	-	-	0/0/0	-	-	18.87	-	-

Appendix H Radioisotope dating

Radioisotopes as geological clocks

Radioisotopes are unstable atoms that release excess energy in the form of radiation (i.e., gamma rays, alpha particles) in the process of radioactive decay. The radioactive-decay rate can be considered fixed for each type of radioisotope and it is this property that makes them very useful as geological clocks. The half-life ($t_{1/2}$) of a radioisotope is one measure of the radioactive decay rate and is defined as the period of time taken for the quantity of a substance to reduce by exactly half. Therefore, after two half-lives only 25% of the original quantity remains.

The $t_{1/2}$ value of radioisotopes also defines the timescale over which they are useful for dating. For example, ^{210}Pb (naturally occurring radioisotope) has a half-life of 22 years and can be used to date sediments up to seven half-lives old or about 150 years. Dating by ^{210}Pb is based on the rate of decrease in unsupported or excess ^{210}Pb activity with depth in the sediment. Excess ^{210}Pb is produced in the atmosphere and is deposited continuously on the earth's surface, where it falls directly into the sea or on land. Like other radioisotopes, ^{210}Pb is strongly attracted to fine sediment particles (e.g., clay and silt), which settle out of the water column and are deposited on the seabed. ^{210}Pb also falls directly on land and is attached to soil particles. When soils are eroded, they may eventually be carried into estuaries and the sea and provide another source of excess ^{210}Pb . As these fine sediments accumulate on the seabed and bury older sediments over time, the excess ^{210}Pb decays at a constant rate (i.e., the half-life). The rate of decline in excess ^{210}Pb activity with depth also depends on the local SAR. Slow declines in ^{210}Pb activity with depth indicate rapid sedimentation whereas rapid declines indicate that sedimentation is occurring more slowly. More details of ^{210}Pb dating are described below.

Although radioisotopes can occur naturally, others are manufactured. Caesium-137 ($t_{1/2} = 30$ yr) is an artificial radioisotope that is produced by the detonation of nuclear weapon or by nuclear reactors. In New Zealand, the fallout of caesium-137 associated with atmospheric nuclear weapons tests was first detected in 1953, with peak deposition occurring during the mid-1960s. Therefore, caesium-137 occurs in sediments deposited since the early 1950s. The feeding and burrowing activities of benthic animals (e.g., worms and shellfish) can complicate matters due to downward mixing of younger sediments into older sediments. Repeated reworking of seabed sediments by waves also mixes younger sediment down into older sediments. X-ray images and short-lived radioisotopes such as ^7Be ($t_{1/2} = 53$ days) can provide information on sediment mixing processes.

^{210}Pb dating

^{210}Pb ($t_{1/2} = 22.3$ yr) is a naturally occurring radioisotope that has been widely applied to dating recent sedimentation (i.e., last 150 yrs) in lakes, estuaries and the sea (Figure H-1). ^{210}Pb is an intermediate decay product in the uranium-238 (^{238}U) decay series and has a radioactive decay constant (k) of 0.03114 yr^{-1} . The intermediate parent radioisotope radium-226 (^{226}Ra , half-life 1622 years) yields the inert gas radon-222 (^{222}Rn , half-life 3.83 days), which decays through several short-lived radioisotopes to produce ^{210}Pb . A proportion of the ^{222}Rn gas formed by ^{226}Ra decay in catchment soils diffuses into the atmosphere where it decays to form ^{210}Pb . This atmospheric ^{210}Pb is deposited at the earth surface by dry deposition or rainfall. The ^{210}Pb in estuarine sediments has two components: supported ^{210}Pb derived from *in situ* ^{222}Rn decay (i.e., within the sediment column) and an unsupported ^{210}Pb component derived from atmospheric fallout. This unsupported ^{210}Pb component of the total ^{210}Pb concentration in excess of the supported ^{210}Pb value is estimated from the ^{226}Ra assay (see below). Some of this atmospheric unsupported ^{210}Pb component is also

incorporated into catchment soils and is subsequently eroded and deposited in estuaries. Both the direct and indirect (i.e., soil inputs) atmospheric ^{210}Pb input to receiving environments, such as estuaries, is termed the unsupported or excess ^{210}Pb .

The activity profile of unsupported ^{210}Pb in sediments is the basis for ^{210}Pb dating. In the absence of atmospheric (unsupported) ^{210}Pb fallout, the ^{226}Ra and ^{210}Pb in estuary sediments would be in radioactive equilibrium, which results from the substantially longer ^{226}Ra half-life. Thus, the ^{210}Pb activity profile would be uniform with depth. However, what is typically observed is a reduction in ^{210}Pb activity with depth in the sediment column. This is due to the addition of unsupported ^{210}Pb directly or indirectly from the atmosphere that is deposited with sediment particles on the bed. This unsupported ^{210}Pb component decays with age ($k = 0.03114 \text{ yr}^{-1}$) as it is buried through sedimentation. In the absence of sediment mixing, the unsupported ^{210}Pb activity decays exponentially with depth and time in the sediment column. The validity of ^{210}Pb dating rests on how accurately the ^{210}Pb delivery processes to the estuary are modelled, and in particular the rates of ^{210}Pb and sediment inputs (i.e., constant versus time variable).

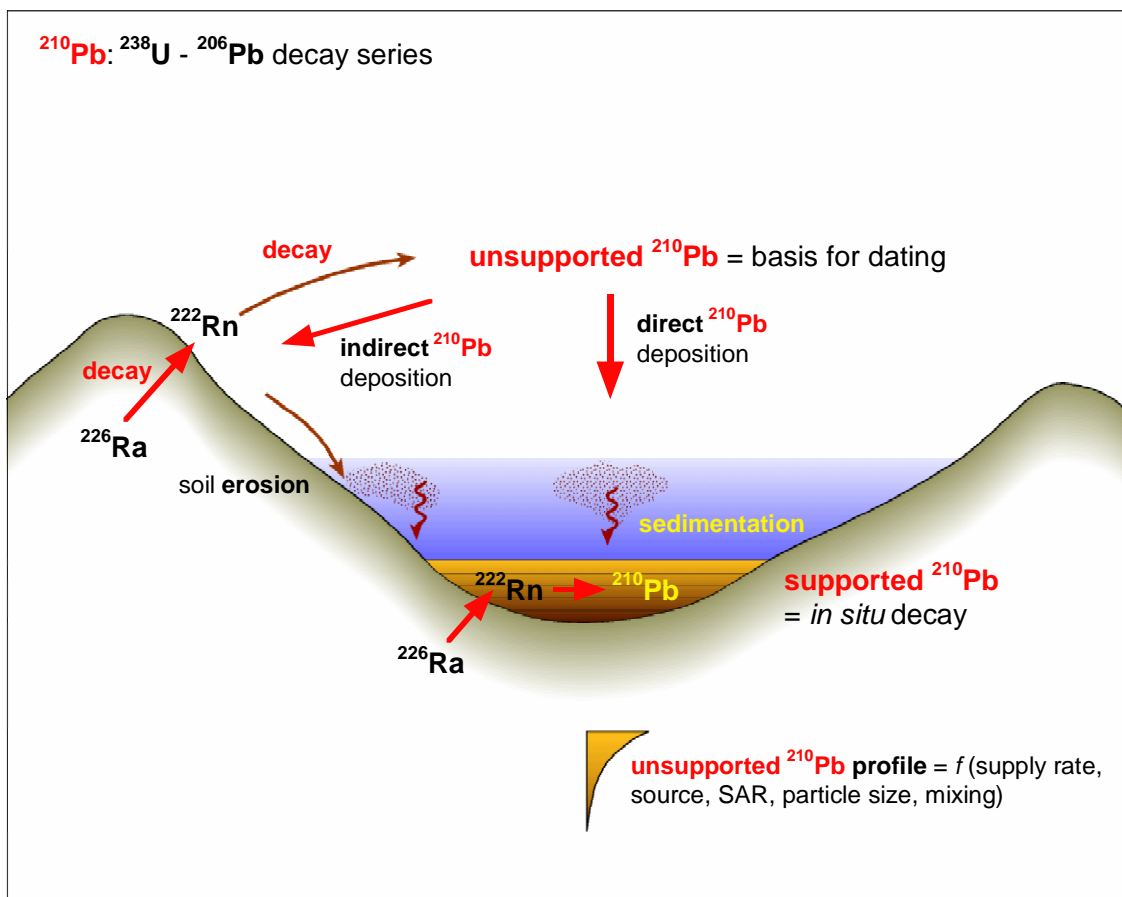


Figure H-1: ^{210}Pb pathways to estuarine sediments.

¹³⁷Cs dating

¹³⁷Cs was introduced to the environment by atmospheric nuclear weapons tests in 1953, 1955–1956 and 1963–1964. Peaks in annual ¹³⁷Cs deposition corresponding to these dates are the usual basis for dating sediments (Wise, 1977, Ritchie and McHenry, 1989). Although direct atmospheric deposition of ¹³⁷Cs in estuaries is likely to have occurred, ¹³⁷Cs was also incorporated into catchment soils, some of which have been eroded and deposited in estuaries (Figure H-2). In New Zealand, ¹³⁷Cs deposition was first detected in 1953 and its annual deposition was measurable at several locations until 1985. Annual ¹³⁷Cs deposition can be estimated from rainfall using known linear relationships between rainfall and Strontium-90 (⁹⁰Sr) and measured ¹³⁷Cs/⁹⁰Sr deposition ratios (Matthews, 1989). Experience in a number of NZ estuaries shows that ¹³⁷Cs profiles measured in estuarine sediments bear no relation to the record of annual ¹³⁷Cs deposition (i.e., 1955–1956 and 1963–1964 ¹³⁷Cs-deposition peaks absent), but rather preserve a record of direct and indirect (i.e., soil erosion) atmospheric deposition since 1953 (e.g., Swales et al. 2002a,b, 2012).

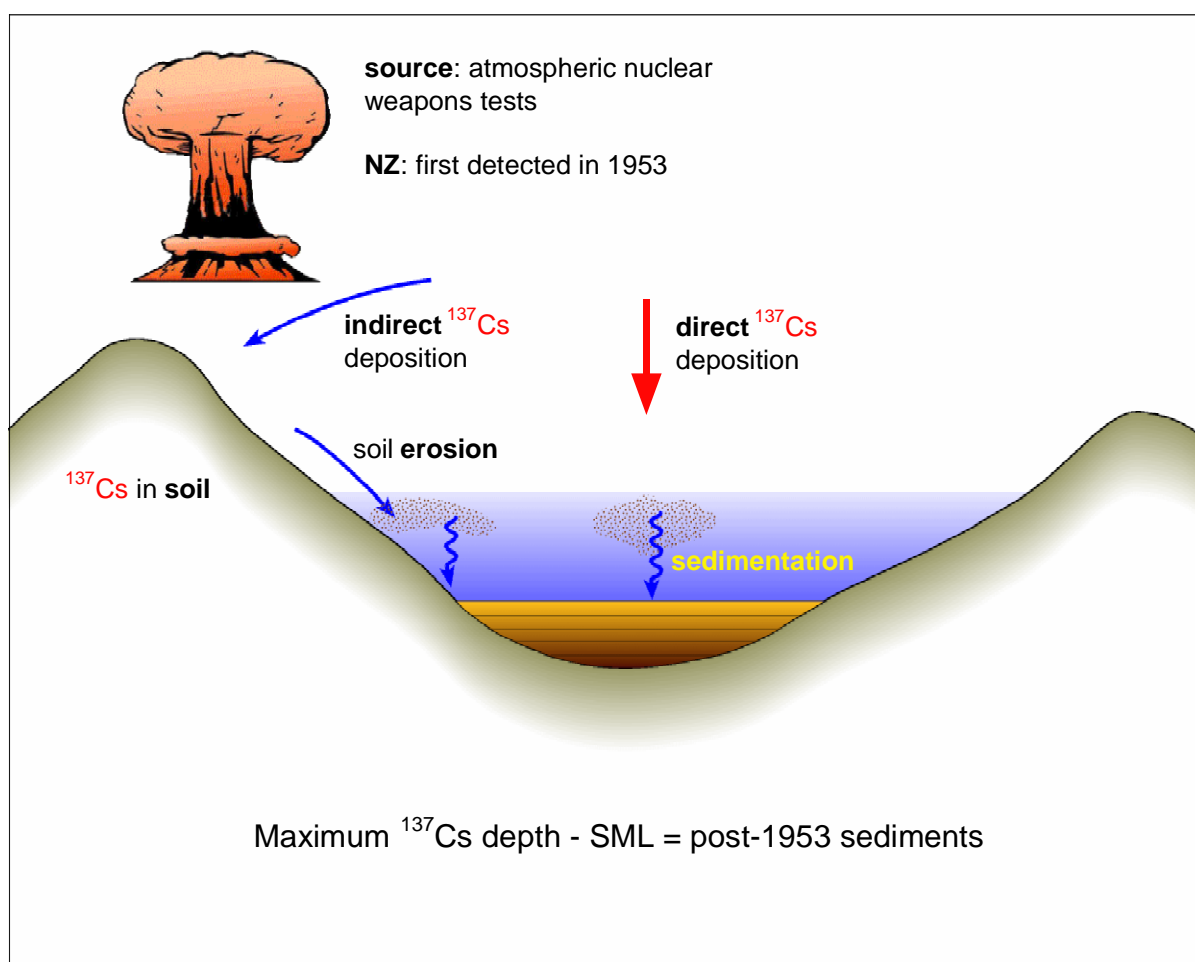


Figure H-2: ¹³⁷Cs pathways to estuarine sediments.

The maximum depth of ¹³⁷Cs in sediment deposits is the usual basis for dating in New Zealand estuaries as ¹³⁷Cs is derived from eroded catchment soils as well as direct atmospheric deposition. The maximum possible depth of ¹³⁷Cs occurrence in sediment cores (corrected for sediment mixing) is taken to coincide with the year 1953, when ¹³⁷Cs deposition was first detected in New Zealand. This

assumes that there was negligible delay in initial atmospheric deposition of ^{137}Cs in estuarine sediments (e.g., ^{137}Cs scavenging by suspended particles), whereas time-lag in ^{137}Cs input to estuaries associated with topsoil erosion are likely.

Due to the low initial ^{137}Cs activities in the 1950s and subsequent radioactive decay since that time (i.e., ~ 2 half-life's, [$t_{1/2} = 30$ years]), the detectable maximum ^{137}Cs depth will date to sometime during 1952–1963 period, and more likely towards the end of this period. Uncertainty in the maximum depth of ^{137}Cs also results from: (1) the depth interval between sediment samples and (2) minimum detectable activity of ^{137}Cs , which is primarily determined by sample size and counting time. If a surface mixed layer (SML) is evident in a core, as shown by an x-ray image and/or a tracer profile (e.g., ^7Be , ^{210}Pb) then ^{137}Cs is likely to have been rapidly mixed through the SML. Therefore, to calculate time-averaged sedimentation rates, the maximum depth of ^{137}Cs occurrence is reduced by the maximum depth of the SML.

Sediment accumulation rates

Time-averaged SAR were estimated from the unsupported ^{210}Pb ($^{210}\text{Pb}_{\text{ex}}$) concentration profiles preserved in cores. The rate of $^{210}\text{Pb}_{\text{ex}}$ concentration decrease with depth can be used to calculate a net sediment accumulation rate. The $^{210}\text{Pb}_{\text{ex}}$ concentration at time zero (C_0 , Bq kg^{-2}), declines exponentially with age (t):

$$C_t = C_0 e^{-kt} \quad (1)$$

where k is the radioactive decay constant for ^{210}Pb ($k = 0.03114 \text{ yr}^{-1}$). Assuming that within a finite time period, sedimentation (S) or SAR is constant then $t = z/S$ (where z is depth in the sediment column) can be substituted into Eq. 2 and by re-arrangement:

$$\frac{\ln \left[\frac{C_t}{C_0} \right]}{z} = -k/S \quad (2)$$

Because $^{210}\text{Pb}_{\text{ex}}$ concentration decays exponentially and assuming that sediment age increases with depth, a vertical profile of natural log(C) should yield a straight line of slope $b = -k/S$. We fitted a linear regression model to natural-log transformed ^{210}Pb concentration data to calculate b . The SAR over the depth of the fitted data is given by:

$$S = -(k)/b \quad (3)$$

An advantage of the ^{210}Pb -dating method is that the SAR is based on the entire $^{210}\text{Pb}_{\text{ex}}$ profile rather than a single layer, as is the case for ^{137}Cs . Furthermore, if the ^{137}Cs tracer is present at the bottom of the core then the estimated SAR represents a minimum value.

The ^{137}Cs profiles were also used to estimate time-averaged SAR based on the maximum depth of ^{137}Cs in the sediment column, corrected for surface mixing. The ^{137}Cs SAR is calculated as:

$$S = (M - L)/T - T_0 \quad (4)$$

where S is the ^{137}Cs SAR, M is the maximum depth of the ^{137}Cs profile, L is the depth of the surface mixed layer (SML) indicated by the ^7Be profile and/or x-ray images, T is the year cores were collected and T_0 is the year (1953) ^{137}Cs deposition was first detected in New Zealand.

Pre 20th century time-average SAR, over time scales of several hundred years, were estimated from the radiocarbon dates (¹⁴C) obtained from pairs of shell samples collected below the maximum depth of excess ²¹⁰Pb in each core. The time averaged ¹⁴C SAR (mm yr⁻¹) was calculated as:

$$S_B = (D_{Pb} - D_C) / (T_{Pb210} - T_{C14}) \quad (5)$$

Where D_{Pb} and D_C are respectively the depths (mm) below the top of each core of the maximum penetration of the ²¹⁰Pb_{ex} profile and mean ¹⁴C age from Accelerator Mass Spectrometry (AMS) dating of the dated shell samples. The matching ages of these layers (T_{Pb210} , T_{C14}) are estimates as years A.D., with the AMS ¹⁴C age (before present [BP = 1950]), adjusted to the year of core collection (2015). The time averaged ¹⁴C SAR (S_B) estimate integrates the effects of land disturbance and soil erosion by Māori and early Europeans over several hundred years as well as background SAR prior to human arrival.

Radiocarbon dating – sample details and results

Cockle shell valves (*Austrovenus stutchburyi*) from three individual animals were analysed and dated as follows. Shell samples were acid-washed in 0.1 N hydrochloric acid, rinsed, and dried prior to Atomic Mass Spectrometry (AMS) dating analysis. The dating results are expressed as radiocarbon age in years before present (B.P., 1950 AD, Stuiver and Polach, 1977). Duplicate samples were analysed from the same depth interval in several cores to evaluate the likelihood of shell material being reworked from its original stratigraphic position. The results of the radiocarbon dating, including the calculated time-average sediment accumulation rates, are included in Table H-1.

Table H-1: Radiocarbon dating results for cockle shell samples and calculated sediment accumulation rates for core MH-3. The ¹⁴C age ±1 standard deviation (Before Present [BP] = 1950) is based on the Libby half-life (5,568 yr) with correction for isotopic fractionation. The laboratory calibration used OxCal v4.3.2 (Bronk Ramsay, 2017): r5 Marine 13 marine curve (Reimer et al. 2013) and a marine reservoir correction (ΔR -7.45). The 95% probability age range is used to calculate the time average sediment accumulation rate (SAR). is calculated from the vertical depth increment and ages of shell sample and the sediment at the base of the excess ²¹⁰Pb sediment layer (i.e., early-1900s, 38 cm depth). The time period also includes the number of years between 1950 AD and core collection in 2017 (i.e., 67 yr). The Wk number is the Waikato University Radiocarbon Dating Laboratory sample identification.

Core	Depth (cm)	Sample ID	¹⁴ C (radiocarbon) age (Years Before Present)	Calibrated ¹⁴ C age range (cal. yr BP, 95% probability)	¹⁴ C SAR (mm yr ⁻¹)	Time period
MH-3	82-85	Wk-49167	2,278 ±15	1,770	0.25	1918–180 AD
				2,040	0.22	1918–23 BC
	87-91	Wk-49372	2,288 ±15	1,780	0.28	1918–170 AD
				2,050	0.24	1918–100 BC
	87-91	Wk-49373	2,276±15	1,760	0.28	1918–190 AD
				2,040	0.24	1918–90 BC

Table H-2: Summary of sediment accumulation rates (SAR) in Mahau Sound. Time-average SAR (mm yr^{-1}) estimated from ^{137}Cs , excess ^{210}Pb and ^{14}C dating from historical to pre-human periods. Information on linear regression fits to log-transform $^{210}\text{Pb}_{\text{ex}}$ data included. The ^{137}Cs SAR is estimate assuming deposition since 1953.

Core site	^{137}Cs max (cm)	^{137}Cs SAR (post-1953)	^{210}Pb and ^{14}C depth and age ranges (cm, AD)	^{210}Pb SAR (r^2, n)	^{14}C SAR (range)	Time span (Years) (mean range)
MH-1	31	4.8	7-36 (2017–1929 AD)	4.1 (0.76, 10)	–	
MH-2	31	4.8	0-30 (2017–1978 AD)	7.6 (0.72, 12)	–	
			30-41 (1978–1913 AD)	1.7 (0.63, 5)	–	
MH-3	24	3.8	2-38 (2017–1917 AD)	3.8 (0.83, 11)	0.22–0.28	1,738–2,058

Appendix I River sediment source proportion statistics from mixing model results

Two-endmember mixing model

Table I-1: Soil proportion statistics from two-endmember mixing model analysis of the river confluences (tributaries and main stem). Each run represents a different set of tributary sources for the downstream mixture.

Confluence/Tributaries	Two-endmember model results					Mean (%)	Rounded (%)
	Run 1	Run 2	Run 3	Run 4	Run 5		
Pelorus below Tinline							
% from	0.259	0.381	0.315	0.222	0.308	0.297	30.0
% from	0.741	0.619	0.685	0.778	0.692	0.703	70.0
N	5	3	1	2	2	13	13
SD	0.133	0.065		0.043	0.031	0.068	6.8
Pelorus below Rai							
% from	0.50	0.56	0.65	0.66		0.595	60.0
% from	0.50	0.44	0.35	0.34		0.405	40.0
N	6	4	4	3		17	17
SD	0.27	0.09	0.20	0.09		0.162	16.2
Pelorus below Wakamarina							
% from	0.15	0.144	0.136			0.144	14.0
% from	0.85	0.856	0.864			0.856	86.0
N	3	1	1			5	5
SD	0.068					0.068	6.8
Rai below Brown							
% from	0.37	0.41				0.389	39.0
% from	0.63	0.59				0.611	61.0
N	3	2				5	5
SD	0.21	0.02				0.115	11.5

Confluence/Tributaries	Two-endmember model results			Mean (%)	Rounded (%)
Rai below Opouri					
% from	0.24			0.240	24.0
% from	0.76			0.760	76.0
N	3			3	3
SD	0.14			0.140	14.0
Opouri below Tunakino					
% from	0.11	0.192	0.101	0.135	14.0
% from	0.89	0.808	0.899	0.865	86.0
N	2	1	1	4	4
SD	0.02			0.020	20.0
Opouri below Kauima					
% from	0.44	0.43		0.434	43.0
% from	0.56	0.57		0.566	57.0
N	5	3		8	8
SD	0.26	0.07		0.163	16.3
Kaituna below Atahaua					
% from	0.21	0.36	0.35	0.307	31.0
% from	0.79	0.64	0.65	0.693	69.0
N	2	3	4	9	9
SD	0.12	0.10	0.09	0.104	10.4

MixSIAR model

Table I-2: MixSIAR statistics from modelling the source contribution of each land use in the tributaries to the Pelorus River system. The Rai River system is a major tributary of the Pelorus River.

Pelorus River system	Statistic	Dairy Pasture	Kanuka	Native	Pine Harvest	Subsoil+Streambank
Upper Pelorus R.	Mean	16.8	6.3	5.7	19.0	52.2
	Median	14.1	4.6	3.8	15.4	55.6
	Std Dev	12.6	5.7	6.0	15.3	23.1
	2.5% (percentile)	0.86	0.17	0.14	0.72	4.57
	97.5% (percentile)	48.32	21.21	21.81	59.57	88.37
Tinline_R	Mean	3.8	8.0	2.7	10.2	75.2
	Median	2.6	6.4	1.5	6.2	81.0
	Std Dev	4.1	6.8	3.7	12.0	18.7
	2.5% (percentile)	0.10	0.43	0.05	0.27	21.60
	97.5% (percentile)	14.71	27.14	12.94	46.12	95.22
Rai_R	Mean	32.5	1.9	3.8	13.1	48.8
	Median	30.0	1.3	2.8	9.4	51.6
	Std Dev	17.1	1.9	3.5	12.4	22.0
	2.5% (percentile)	5.34	0.06	0.11	0.32	4.22
	97.5% (percentile)	70.50	6.89	12.93	47.38	84.12
Wakamarina R	Mean	16.0	2.2	3.6	11.4	66.8
	Median	14.0	1.6	2.9	7.9	71.1
	Std Dev	10.7	2.1	3.2	11.4	17.7
	2.5% (percentile)	1.71	0.08	0.12	0.33	19.57
	97.5% (percentile)	44.11	7.75	11.55	43.86	89.35
Lower Pelorus R (Before it discharges into Mahau Sd)	Mean	19.1	4.5	3.9	18.1	54.4
	Median	16.8	3.5	2.9	14.4	58.3
	Std Dev	13.3	3.8	3.6	14.3	21.8
	2.5% (percentile)	1.42	0.14	0.14	0.88	5.50
	97.5% (percentile)	52.06	14.14	13.72	54.19	86.77

Table I-3: MixSIAR statistics from modelling the source contribution of each land use in the tributaries to the Rai River system.

Rai_River system	Statistic	Dairy Pasture	Kanuka	Native	Pine Harvest	Subsoil+Streambank
Opouri_R	Mean	15.5	2.4	1.8	11.9	68.4
	Median	13.2	1.7	1.3	8.5	72.8
	Std Dev	11.3	2.4	1.8	11.7	17.2
	2.5% (percentile)	1.07	0.05	0.04	0.33	19.89
	97.5% (percentile)	45.72	9.49	6.68	46.27	89.93
Kaiuma_	Mean	22.9	2.9	3.5	16.6	54.1
	Median	20.5	2.1	2.7	13.3	58.0
	Std Dev	15.3	2.8	3.3	14.0	21.9
	2.5% (percentile)	1.82	0.08	0.12	0.63	6.36
	97.5% (percentile)	61.29	10.66	11.75	53.90	86.87
Tunakino River	Mean	9.9	4.3	5.5	12.4	67.8
	Median	8.2	2.8	3.6	8.7	73.6
	Std Dev	8.1	4.6	6.0	11.8	19.8
	2.5% (percentile)	0.46	0.13	0.14	0.40	14.80
	97.5% (percentile)	30.90	16.84	22.58	45.15	91.54
Ronga River	Mean	25.1	2.9	2.6	16.9	52.4
	Median	22.1	2.1	1.9	13.5	57.0
	Std Dev	16.7	2.8	2.6	14.2	22.2
	2.5% (percentile)	1.52	0.08	0.07	0.70	4.39
	97.5% (percentile)	64.44	10.88	9.22	55.46	86.26
Brown River	Mean	30.8	3.0	5.6	19.3	41.3
	Median	29.0	2.1	4.2	15.7	42.2
	Std Dev	16.4	2.9	4.9	15.4	21.7
	2.5% (percentile)	3.62	0.08	0.16	0.73	2.38
	97.5% (percentile)	66.68	11.08	18.17	57.35	80.66
Rai River (At confluence with Pelorus River)	Mean	32.5	1.9	3.8	13.1	48.8
	Median	30.0	1.3	2.8	9.4	51.6
	Std Dev	17.1	1.9	3.5	12.4	22.0
	2.5% (percentile)	5.34	0.06	0.11	0.32	4.22
	97.5% (percentile)	70.50	6.89	12.93	47.38	84.12

Table I-4: MixSIAR statistics from modelling the source contribution of each land use in the tributaries to the Kaituna River system.

Kaituna_River	Statistic	Dairy	GorseandBr	Kanuka	Native	Pine Harvest	Sheep and Brack	Subsoil and Streambank
Lower Kaituna R (At Havelock Estuary)	Mean	7.9	12.2	1.8	2.7	5.5	14.2	55.8
	Median	6.4	9.2	1.2	1.6	3.7	11.4	59.1
	Std Dev	7.0	10.8	1.8	3.1	5.7	11.4	18.8
	2.5% (percentile)	0.29	0.38	0.04	0.05	0.14	0.78	10.33
	97.5% (percentile)	25.31	39.66	6.53	11.28	20.90	42.93	84.01

Appendix J MDC Pelorus Sound TSS Monitoring

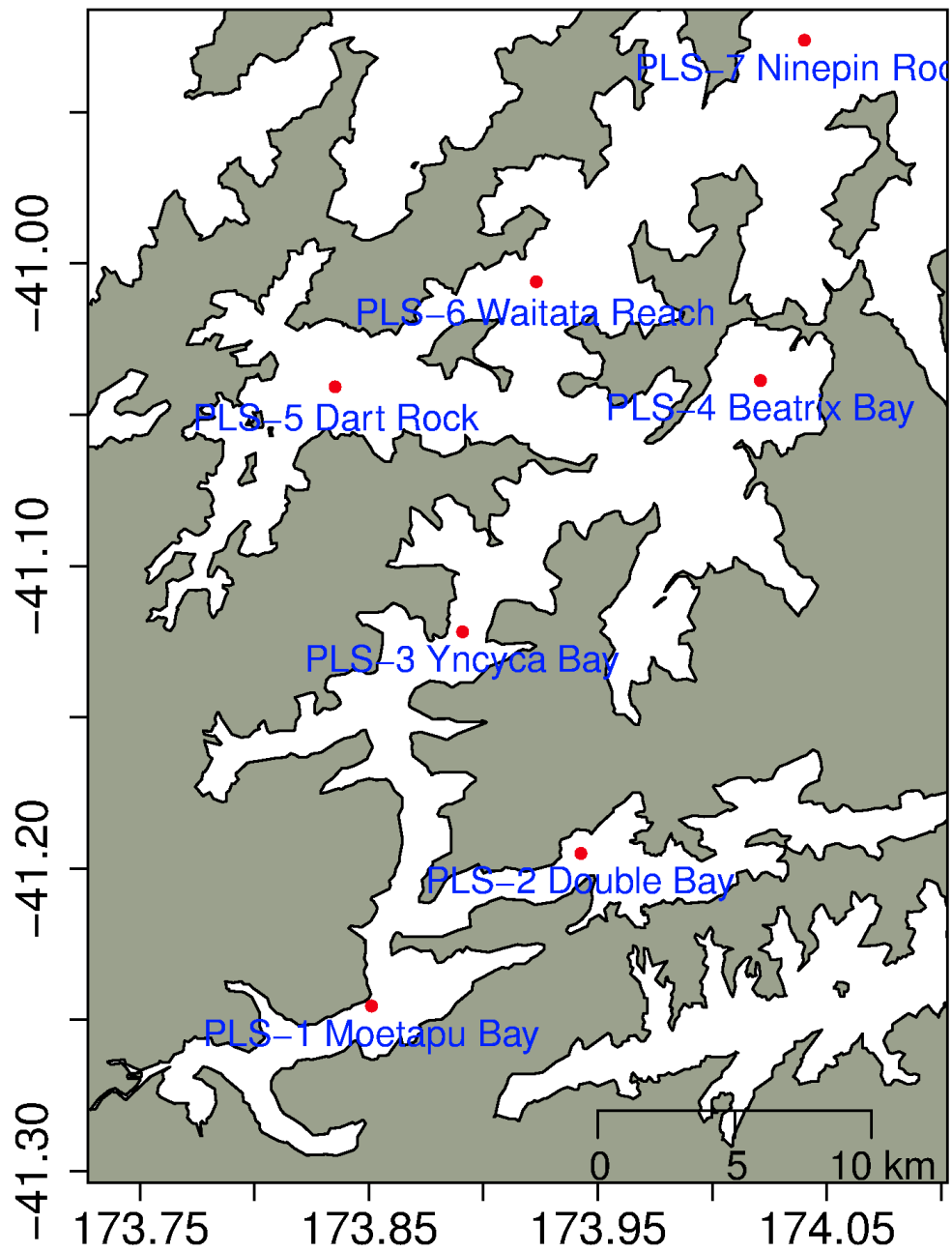


Figure J-1: Locations of MDC water quality monitoring sites in Pelorus Sound. Source: Dr Niall Broekhuizen (NIWA).

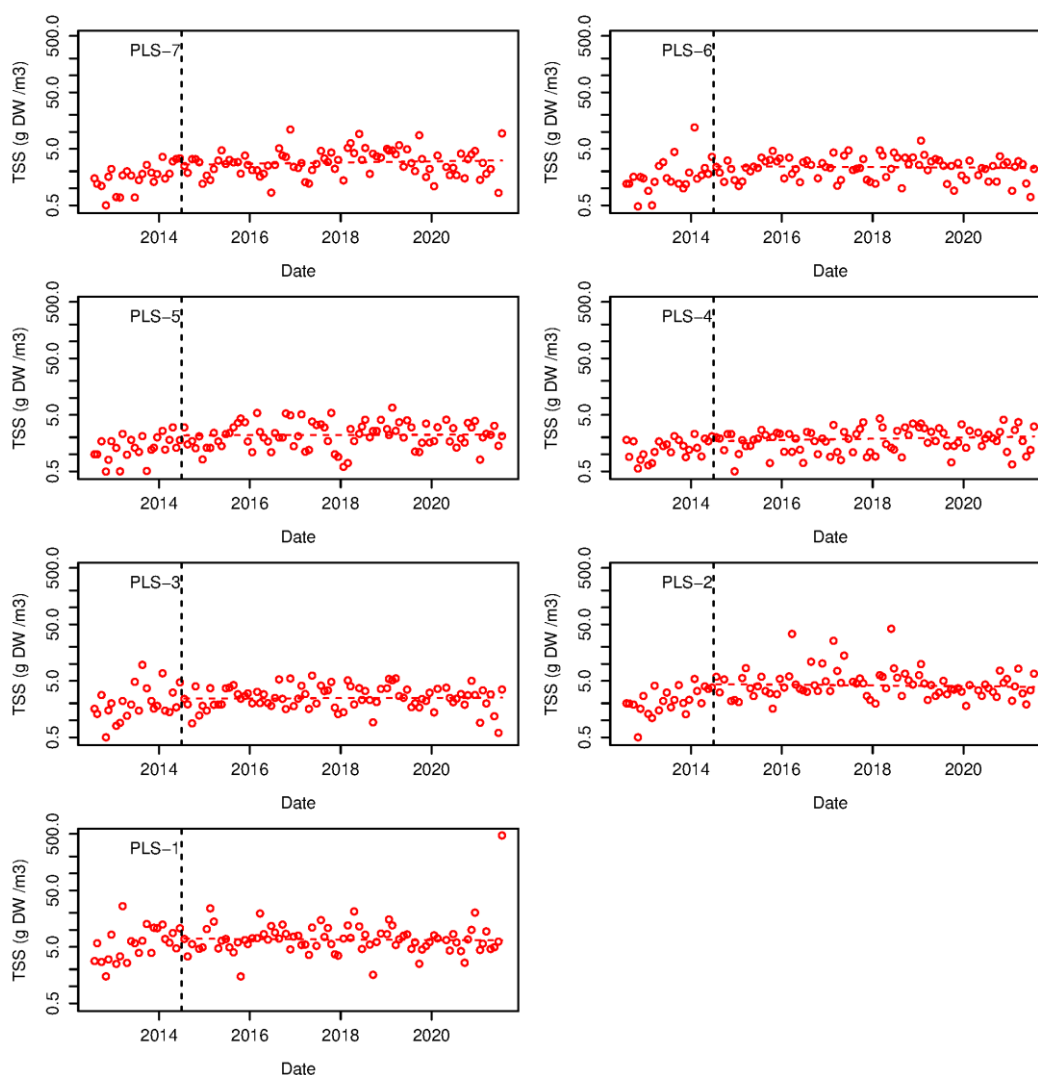


Figure J-2: Time series of total suspended solids (TSS, g m^{-3}) at MDC water quality monitoring sites in Pelorus Sound (July 2012 to July 2021). Notes: (1) Y-axis plotted on a log scale, (2) Vertical dotted line denotes a change in sampling method. Pre-2015: grab sample at $\sim 2\text{-m}$ depth, Post: depth-integrated sample from top 12-m of water column where water depth allows and shallow sample where depth $< 12\text{ m}$. Source: Dr Niall Broekhuizen (NIWA).

Table J-1: Summary statistics for TSS (g m^{-3}) at selected MDC WQ monitoring sites. Source: N. Broekhuizen (NIWA).

Site	Median	Mean	Max
PLS-1 (Mahau Sound)	6.4	11.8	470 (July 2021)
PLS-4 (Beatrix Bay)	1.7	1.8	4.3
PLS-7 (Nine-pin Rock)	2.5	2.9	11.0

Appendix K Soil proportion (%) statistics for Mahau cores

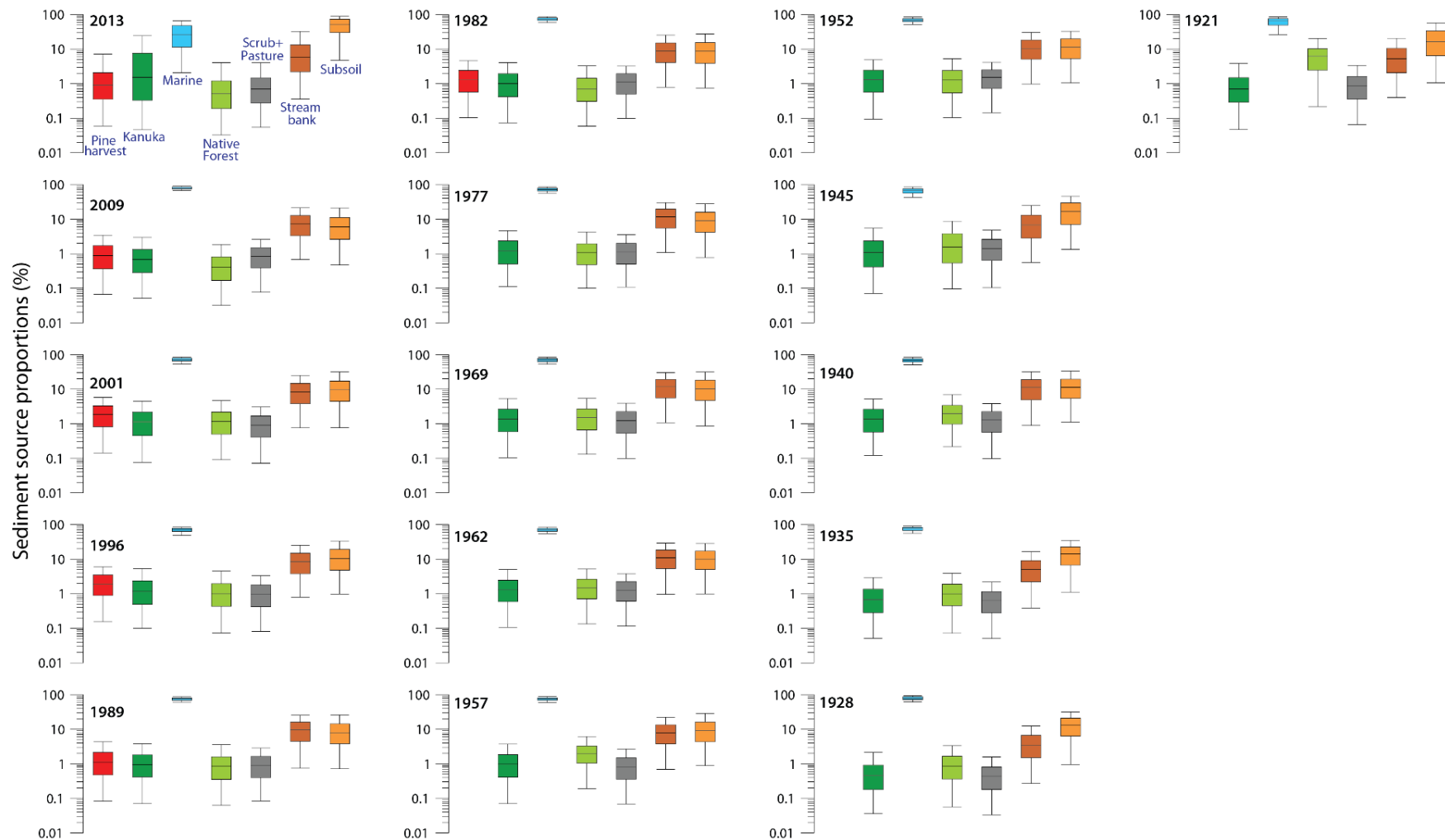


Figure K-1: Core MH-1 source proportion distribution (%) for dated samples. Box and whisker plots showing median, lower and upper interquartile and 5% and 95%-ile values of sediment source proportions (%) for each sample ($n = 3000$). The year of deposition estimated from ^{210}Pb dating is shown in the top left of each sub-plot. Representative results from one of three runs (run 3) of the mixing model performed for each dated sample. **Notes:** (1) top of core at top left, (2) y-axis is plotted on a log₁₀ scale, (3) Harvested pine was not included as a source prior to 1978.

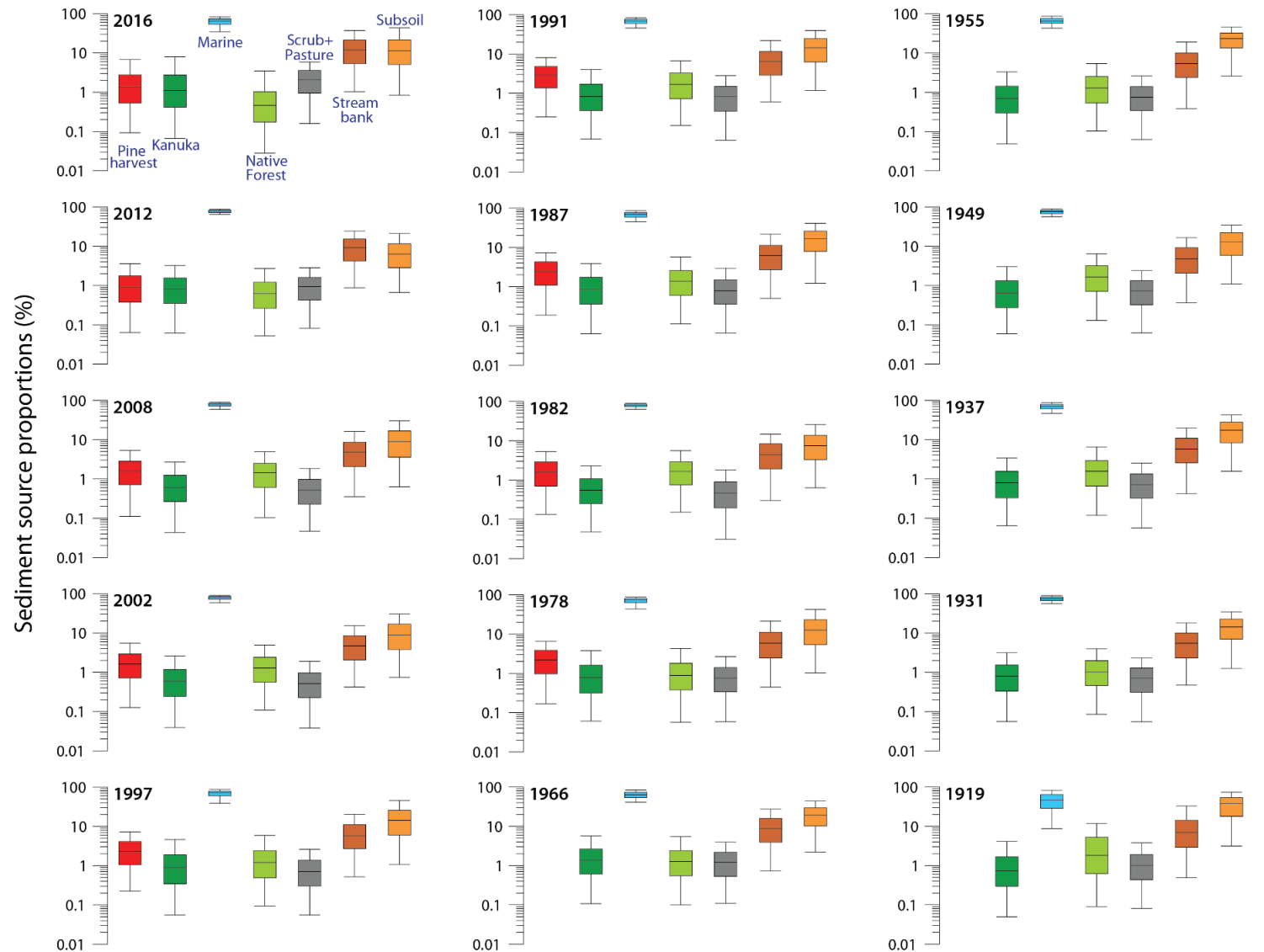


Figure K-2: Core MH-2 source proportion distribution (%) summaries for dated samples. Box and whisker plots showing median, lower and upper interquartile and 5% and 95% values of sediment source proportions (%) for each sample (n = 3000). The year of deposition estimated from ^{210}Pb dating is shown in the top left of each sub-plot. Representative results from one of three runs (run 3) of the mixing model performed for each dated sample. **Notes:** (1) top of core at top left, (2) y-axis is plotted on a \log_{10} scale, (3) Harvested pine was not included as a source prior to 1978.

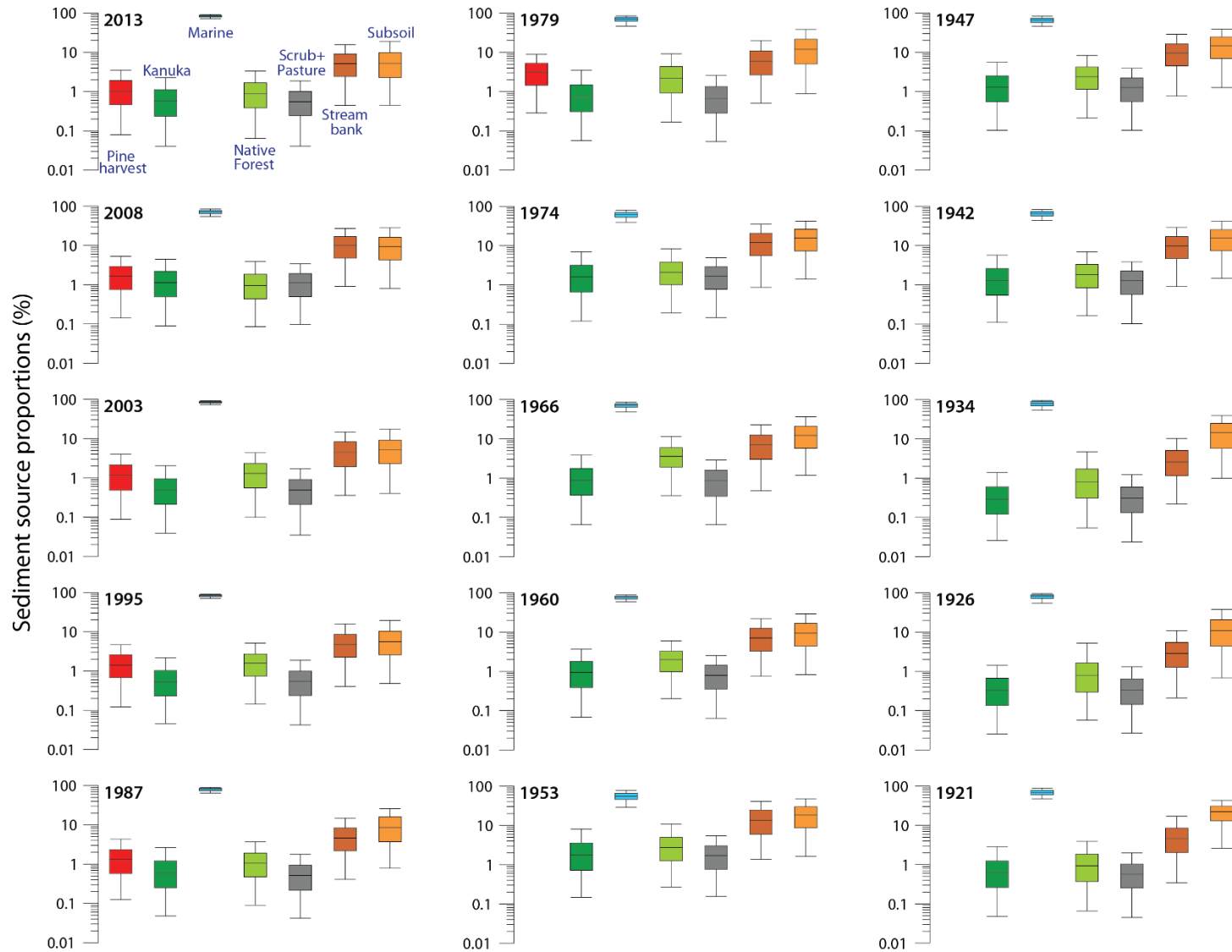


Figure K-3: Core MH-3 source proportion distribution (%) summaries for dated samples. Box and whisker plots showing median, lower and upper interquartile and 5% and 95% values of sediment source proportions (%) for each sample (n = 3000). The year of deposition estimated from ^{210}Pb dating is shown in the top left of each sub-plot. Representative results from one of three runs (run 3) of the mixing model performed for each dated sample. **Notes:** (1) top of core at top left, (2) y-axis is plotted on a \log_{10} scale, (3) Harvested pine was not included as a source prior to 1978.

Table K-1 (core MH-1) sediment source proportions (%). Statistics for repeat model runs (R1 –R3): inc. standard deviation (SD) and credible interval (2.5%– 97.5%).

Depth (cm)	²¹⁰ Pb Year	Statistic RUN >>	Pine Harvest			Kanuka			Marine			Native Forest			Scrub and Pasture			Streambank			Subsoil		
			R1	R2	R3	R1	R2	R3	R1	R2	R3	R1	R2	R3	R1	R2	R3	R1	R2	R3	R1	R2	R3
1–2	2013	Mean	2.0	2.1	2.0	5.6	5.1	5.2	29.9	29.8	30.1	1.1	1.0	1.0	1.2	1.2	1.1	9.6	9.1	9.8	50.6	51.7	50.8
		Median	0.9	0.9	0.9	1.5	1.3	1.3	26.5	26.2	26.3	0.5	0.5	0.5	0.7	0.7	0.7	5.9	5.7	6.3	52.2	54.2	51.7
		SD	3.8	4.8	4.4	8.5	8.2	8.3	20.9	20.7	21.1	1.8	1.7	1.5	1.5	1.8	1.5	10.5	10.2	10.7	26.5	26.0	26.4
		2.5%	0.03	0.04	0.03	0.02	0.03	0.02	1.09	1.09	1.10	0.02	0.01	0.02	0.03	0.02	0.02	0.14	0.19	0.24	1.95	2.78	2.30
		97.5%	11.3	12.9	10.2	29.9	28.8	31.8	70.7	70.3	70.8	5.5	5.4	5.3	5.5	6.4	5.6	39.2	38.5	41.3	91.5	91.7	92.0
3–4	2009	Mean	1.2	1.2	1.2	1.0	1.0	1.0	79.7	79.7	80.1	0.6	0.6	0.6	1.0	1.0	1.1	8.6	8.6	8.4	7.8	7.8	7.6
		Median	0.9	0.9	0.9	0.7	0.7	0.7	80.5	80.5	80.8	0.4	0.4	0.4	0.8	0.8	0.9	7.2	7.2	7.0	6.0	6.0	5.9
		SD	1.1	1.1	1.1	1.0	1.0	1.0	7.4	7.4	7.3	0.7	0.7	0.9	0.8	0.8	0.8	6.6	6.6	6.5	6.9	6.9	6.7
		2.5%	0.04	0.04	0.04	0.03	0.03	0.03	63.6	63.6	63.9	0.02	0.02	0.02	0.04	0.04	0.05	0.34	0.34	0.25	0.22	0.22	0.23
		97.5%	4.2	4.2	4.1	3.6	3.6	3.7	91.5	91.5	92.0	2.3	2.3	2.3	2.9	2.9	3.0	23.9	23.9	24.0	25.2	25.2	25.1
6–7	2001	Mean	2.3	2.3	2.3	1.6	1.5	1.6	71.3	71.0	71.4	1.6	1.6	1.6	1.2	1.2	1.2	10.1	10.1	10.1	12.0	12.3	11.9
		Median	1.9	1.8	1.8	1.1	1.1	1.2	72.4	72.0	72.5	1.2	1.1	1.1	0.9	0.9	0.9	8.4	8.4	8.3	9.9	10.0	9.6
		SD	1.8	1.8	1.9	1.5	1.5	1.6	10.1	10.2	10.1	1.6	1.6	1.7	1.0	1.0	1.0	7.8	7.7	7.7	9.8	10.0	10.0
		2.5%	0.08	0.09	0.08	0.04	0.04	0.04	48.8	48.1	49.1	0.04	0.04	0.06	0.03	0.05	0.04	0.42	0.33	0.33	0.40	0.40	0.38
		97.5%	6.51	6.4	6.9	5.40	5.4	5.5	87.3	87.5	87.3	5.8	5.9	5.8	3.6	3.6	3.6	29.0	28.7	28.7	36.1	36.4	35.8

Core MH-1: sediment source proportions (%). Statistics for repeat model runs (R1 –R3): inc. standard deviation (SD) and credible interval (2.5%– 97.5%).

Depth (cm)	²¹⁰ Pb Year	Statistic RUN >>	Pine Harvest			Kanuka			Marine			Native Forest			Scrub and Pasture			Streambank			Subsoil		
			R1	R2	R3	R1	R2	R3	R1	R2	R3	R1	R2	R3	R1	R2	R3	R1	R2	R3	R1	R2	R3
8–9	1996	Mean	2.4	2.4	2.4	1.7	1.6	1.7	69.8	70.1	70.1	1.5	1.5	1.6	1.2	1.3	1.2	10.2	9.9	9.9	13.2	13.2	13.1
		Median	1.9	1.9	2.0	1.2	1.1	1.2	71.4	71.7	71.4	1.0	1.0	1.0	1.0	1.0	1.0	8.6	8.1	7.8	10.5	10.5	10.4
		SD	1.9	2.0	1.9	1.8	1.7	1.8	11.1	11.2	11.1	1.6	1.9	1.8	1.0	1.0	1.0	7.9	7.8	7.9	10.6	10.7	10.7
		2.5%	0.08	0.08	0.12	0.06	0.03	0.05	44.0	43.7	44.70	0.03	0.05	0.05	0.03	0.05	0.05	0.41	0.32	0.40	0.59	0.57	0.52
		97.5%	7.1	7.2	7.0	6.4	6.1	6.0	86.9	87.5	86.9	5.7	5.7	6.1	3.8	3.8	3.9	28.6	28.8	29.0	38.0	38.5	39.6
11–12	1989	Mean	1.5	1.5	1.6	1.3	1.3	1.3	74.1	74.7	74.6	1.2	1.2	1.2	1.1	1.1	1.1	10.9	10.5	10.8	9.9	9.7	9.4
		Median	1.1	1.1	1.2	0.9	0.9	0.9	74.5	75.3	75.2	0.9	0.9	0.9	0.9	0.9	0.9	9.7	8.9	9.4	8.0	7.8	7.3
		SD	1.4	1.3	1.4	1.2	1.3	1.2	8.3	8.4	8.3	1.3	1.3	1.2	0.9	0.9	0.9	7.7	7.7	7.7	8.0	7.9	7.8
		2.5%	0.04	0.05	0.05	0.04	0.03	0.03	56.8	57.12	56.87	0.03	0.04	0.04	0.05	0.05	0.04	0.40	0.40	0.50	0.34	0.34	0.42
		97.5%	5.2	4.9	5.1	4.4	4.5	4.4	88.6	88.6	88.4	4.5	4.6	4.3	3.3	3.4	3.4	28.1	28.0	28.5	29.4	29.1	28.6
14–15	1982	Mean	1.7	1.7	1.7	1.4	1.4	1.4	73.5	73.7	73.6	1.1	1.1	1.1	1.3	1.3	1.3	10.3	10.4	10.4	10.6	10.4	10.5
		Median	1.3	1.3	1.4	1.0	1.1	1.0	74.3	74.7	74.1	0.7	0.7	0.7	1.1	1.0	1.1	8.7	9.0	8.8	8.7	8.4	8.3
		SD	1.5	1.5	1.5	1.4	1.3	1.4	8.9	8.9	9.0	1.2	1.1	1.2	1.0	1.0	1.0	7.7	7.6	7.9	8.5	8.6	8.5
		2.5%	0.05	0.07	0.06	0.04	0.05	0.05	55.0	54.07	53.94	0.03	0.03	0.02	0.05	0.04	0.04	0.45	0.45	0.38	0.41	0.20	0.27
		97.5%	5.5	5.5	5.4	5.1	5.0	4.9	88.3	88.1	88.7	4.2	4.1	4.1	3.7	3.8	3.7	28.5	28.0	28.5	30.8	31.3	31.8

Core MH-1: sediment source proportions (%). Statistics for repeat model runs (R1 –R3): inc. standard deviation (SD) and credible interval (2.5%– 97.5%).

Depth (cm)	²¹⁰ Pb Year	Statistic RUN >>	Pine Harvest			Kanuka			Marine			Native Forest			Scrub and Pasture			Streambank			Subsoil		
			R1	R2	R3	R1	R2	R3	R1	R2	R3	R1	R2	R3	R1	R2	R3	R1	R2	R3	R1	R2	R3
16–17	1977	Mean	NA	NA	NA	1.6	1.6	1.6	71.4	71.1	71.4	1.5	1.5	1.5	1.4	1.3	1.4	13.1	13.5	13.2	11.0	11.0	10.9
		Median	NA	NA	NA	1.2	1.1	1.2	71.4	71.1	71.8	1.1	1.0	1.0	1.1	1.1	1.1	11.6	11.9	11.8	8.9	9.2	9.0
		SD	NA	NA	NA	1.5	1.6	1.5	9.1	9.2	9.1	1.5	1.7	1.5	1.1	1.1	1.1	9.2	9.2	9.1	8.7	8.5	8.6
		2.5%	NA	NA	NA	0.06	0.05	0.05	53.5	52.22	52.5	0.05	0.05	0.05	0.06	0.04	0.04	0.60	0.55	0.64	0.41	0.47	0.31
		97.5%	NA	NA	NA	5.5	5.7	5.7	87.8	87.0	88.1	5.4	5.3	5.5	4.0	3.9	3.9	32.9	33.9	33.8	31.8	31.0	31.8
19–20	1969	Mean	NA	NA	NA	1.9	1.9	1.8	69.0	68.8	68.6	2.0	1.9	1.9	1.5	1.5	1.5	13.1	13.0	12.7	12.6	12.8	13.5
		Median	NA	NA	NA	1.4	1.4	1.3	69.4	69.6	69.4	1.5	1.4	1.4	1.2	1.2	1.2	11.6	11.4	11.2	10.3	10.7	11.1
		SD	NA	NA	NA	1.7	1.8	1.7	10.0	10.0	10.4	2.0	1.9	1.9	1.2	1.1	1.2	9.1	9.2	9.2	9.9	9.9	10.4
		2.5%	NA	NA	NA	0.05	0.05	0.05	48.5	47.21	45.44	0.06	0.09	0.07	0.05	0.05	0.05	0.48	0.63	0.44	0.42	0.55	0.52
		97.5%	NA	NA	NA	6.6	6.6	6.2	87.0	86.0	86.2	7.0	6.6	6.5	4.4	4.1	4.3	33.1	34.0	33.1	36.5	37.1	38.3
22–23	1962	Mean	NA	NA	NA	1.8	1.8	1.8	70.4	70.3	70.9	2.0	2.0	2.0	1.5	1.5	1.6	12.5	12.7	12.3	11.8	11.7	11.6
		Median	NA	NA	NA	1.3	1.3	1.3	70.4	70.7	71.0	1.5	1.5	1.5	1.3	1.3	1.3	11.0	11.2	10.6	10.1	9.8	9.6
		SD	NA	NA	NA	1.6	1.7	1.6	9.2	9.1	9.1	2.0	2.1	2.0	1.2	1.1	1.2	8.9	8.9	8.8	8.7	9.0	8.8
		2.5%	NA	NA	NA	0.06	0.04	0.06	51.9	52.05	52.61	0.07	0.07	0.08	0.06	0.06	0.07	0.46	0.53	0.51	0.51	0.53	0.41
		97.5%	NA	NA	NA	6.0	6.3	6.0	87.1	86.6	87.1	6.7	6.5	6.7	4.3	4.2	4.4	32.3	32.4	32.7	32.3	33.7	32.3

Core MH-1: sediment source proportions (%). Statistics for repeat model runs (R1 –R3): inc. standard deviation (SD) and credible interval (2.5%– 97.5%).

Depth (cm)	²¹⁰ Pb Year	Statistic RUN >>	Pine Harvest			Kanuka			Marine			Native Forest			Scrub and Pasture			Streambank			Subsoil		
			R1	R2	R3	R1	R2	R3	R1	R2	R3	R1	R2	R3	R1	R2	R3	R1	R2	R3	R1	R2	R3
24–25	1957	Mean	NA	NA	NA	1.3	1.3	1.3	74.7	74.3	74.6	2.4	2.4	2.4	1.0	1.0	1.0	9.2	9.3	9.3	11.3	11.6	11.4
		Median	NA	NA	NA	1.0	0.9	0.9	75.3	75.0	75.6	2.0	2.0	1.9	0.8	0.8	0.8	7.8	7.9	7.9	9.3	9.6	9.1
		SD	NA	NA	NA	1.2	1.2	1.2	8.6	9.1	9.2	1.9	2.0	2.0	0.8	0.9	0.8	6.8	7.0	7.0	8.8	9.2	9.2
		2.5%	NA	NA	NA	0.04	0.03	0.03	55.7	54.27	54.91	0.10	0.11	0.10	0.03	0.02	0.03	0.33	0.46	0.36	0.45	0.41	0.39
		97.5%	NA	NA	NA	4.4	4.5	4.5	89.1	89.3	89.4	7.2	7.4	7.4	3.1	3.2	3.1	24.9	25.4	25.6	33.0	33.8	33.6
26–27	1952	Mean	NA	NA	NA	1.7	1.7	1.8	68.7	68.9	69.1	1.8	1.8	1.7	1.7	1.8	1.8	12.5	12.4	12.5	13.5	13.4	13.1
		Median	NA	NA	NA	1.3	1.3	1.3	69.1	69.5	69.5	1.3	1.3	1.3	1.5	1.5	1.5	10.5	10.6	10.5	11.4	11.3	11.0
		SD	NA	NA	NA	1.6	1.7	1.7	10.1	10.3	10.2	1.9	1.8	1.8	1.3	1.3	1.3	9.3	9.4	9.4	10.1	10.1	9.9
		2.5%	NA	NA	NA	0.05	0.04	0.05	47.5	47.98	48.43	0.06	0.05	0.06	0.08	0.07	0.08	0.50	0.36	0.41	0.55	0.53	0.57
		97.5%	NA	NA	NA	5.9	6.1	6.2	86.7	87.0	87.0	6.6	6.5	6.2	4.6	4.7	4.7	33.9	34.2	34.0	37.1	38.0	36.3
29–30	1945	Mean	NA	NA	NA	1.7	1.8	1.7	65.4	65.6	65.5	2.7	2.8	2.8	1.8	1.8	1.8	9.0	8.8	8.9	19.4	19.3	19.3
		Median	NA	NA	NA	1.1	1.0	1.0	66.5	66.7	67.0	1.5	1.7	1.6	1.4	1.4	1.4	6.8	6.8	6.7	16.6	16.2	16.8
		SD	NA	NA	NA	1.9	2.1	1.9	13.5	13.2	13.3	3.2	3.4	3.3	1.5	1.5	1.5	7.9	7.5	7.8	14.4	14.3	14.2
		2.5%	NA	NA	NA	0.04	0.04	0.04	36.7	38.16	36.26	0.04	0.06	0.04	0.05	0.06	0.06	0.28	0.29	0.26	0.55	0.66	0.69
		97.5%	NA	NA	NA	6.9	7.2	7.0	87.3	87.4	86.7	10.6	11.3	11.4	5.5	5.5	5.4	29.1	27.4	28.6	49.9	49.9	50.3

Core MH-1: sediment source proportions (%). Statistics for repeat model runs (R1 –R3): inc. standard deviation (SD) and credible interval (2.5%– 97.5%).

Depth (cm)	²¹⁰ Pb Year	Statistic RUN >>	Pine Harvest			Kanuka			Marine			Native Forest			Scrub and Pasture			Streambank			Subsoil		
			R1	R2	R3	R1	R2	R3	R1	R2	R3	R1	R2	R3	R1	R2	R3	R1	R2	R3	R1	R2	R3
31–32	1940	Mean	NA	NA	NA	1.8	1.8	1.9	67.7	67.7	67.4	2.6	2.6	2.5	1.5	1.5	1.5	12.9	13.1	13.1	13.4	13.3	13.5
		Median	NA	NA	NA	1.3	1.4	1.4	68.2	68.1	67.9	2.0	1.9	1.9	1.3	1.3	1.2	11.1	11.2	11.4	11.3	11.0	11.3
		SD	NA	NA	NA	1.8	1.8	1.8	10.5	10.7	10.6	2.5	2.5	2.4	1.2	1.2	1.2	9.7	9.8	9.6	10.2	10.3	10.2
		2.5%	NA	NA	NA	0.05	0.06	0.05	45.9	45.67	45.64	0.11	0.10	0.11	0.05	0.05	0.04	0.42	0.52	0.48	0.57	0.47	0.64
		97.5%	NA	NA	NA	6.2	6.7	6.4	86.1	86.6	85.6	8.7	8.8	8.6	4.4	4.4	4.5	34.8	35.7	35.0	38.2	38.4	38.4
33–34	1935	Mean	NA	NA	NA	1.0	1.0	1.0	75.0	74.7	75.2	1.4	1.4	1.4	0.8	0.8	0.8	6.2	6.2	6.3	15.6	16.0	15.4
		Median	NA	NA	NA	0.7	0.7	0.7	76.0	75.4	76.0	1.0	1.0	1.0	0.6	0.6	0.6	5.0	4.8	4.9	14.4	15.0	14.1
		SD	NA	NA	NA	1.0	1.0	1.0	10.8	10.8	10.5	1.3	1.3	1.3	0.7	0.7	0.7	5.1	5.3	5.3	10.7	10.7	10.4
		2.5%	NA	NA	NA	0.03	0.02	0.02	52.4	52.08	52.88	0.03	0.04	0.03	0.02	0.03	0.02	0.18	0.19	0.21	0.50	0.76	0.60
		97.5%	NA	NA	NA	3.6	3.6	3.8	92.3	92.3	92.0	4.6	4.8	4.8	2.6	2.6	2.6	19.3	19.3	19.0	38.9	38.9	38.2
36–37	1928	Mean	NA	NA	NA	0.7	0.7	0.7	78.7	78.5	78.9	1.2	1.2	1.2	0.6	0.6	0.6	4.6	4.5	4.6	14.2	14.6	14.1
		Median	NA	NA	NA	0.4	0.5	0.5	79.2	79.5	79.5	0.9	0.9	0.9	0.4	0.4	0.4	3.5	3.4	3.5	13.3	13.7	13.2
		SD	NA	NA	NA	0.7	0.7	0.8	9.9	9.9	9.5	1.2	1.1	1.1	0.5	0.5	0.5	4.1	3.8	4.0	9.6	9.7	9.4
		2.5%	NA	NA	NA	0.02	0.02	0.02	58.4	58.39	58.97	0.03	0.04	0.03	0.02	0.02	0.02	0.13	0.15	0.15	0.40	0.45	0.47
		97.5%	NA	NA	NA	2.6	2.6	2.6	94.8	94.2	94.0	4.1	4.1	4.0	1.9	1.9	1.9	14.9	14.3	14.4	34.9	35.2	34.0

Core MH-1: sediment source proportions (%). Statistics for repeat model runs (R1 –R3): inc. standard deviation (SD) and credible interval (2.5%– 97.5%).

Depth (cm)	²¹⁰ Pb Year	Statistic RUN >>	Pine Harvest			Kanuka			Marine			Native Forest			Scrub and Pasture			Streambank			Subsoil		
			R1	R2	R3	R1	R2	R3	R1	R2	R3	R1	R2	R3	R1	R2	R3	R1	R2	R3	R1	R2	R3
39–40	1921	Mean	NA	NA	NA	1.2	1.2	1.2	61.2	61.1	61.0	7.5	7.6	7.7	1.2	1.2	1.2	7.3	7.6	7.5	21.7	21.3	21.4
		Median	NA	NA	NA	0.7	0.7	0.7	64.3	64.9	64.3	6.3	6.3	6.4	0.9	0.8	0.8	5.3	5.3	5.6	16.4	16.1	16.6
		SD	NA	NA	NA	1.5	1.6	1.7	18.4	18.7	18.4	7.0	7.2	6.9	1.1	1.1	1.2	7.1	7.7	7.1	18.2	18.1	18.1
		2.5%	NA	NA	NA	0.02	0.02	0.02	16.7	14.58	15.3	0.09	0.09	0.11	0.04	0.03	0.03	0.21	0.18	0.18	0.52	0.46	0.49
		97.5%	NA	NA	NA	5.2	5.4	5.2	87.5	87.7	86.9	26.1	25.7	25.7	4.1	4.1	4.2	24.9	27.1	25.2	64.0	63.6	63.2

Table K-2 (core MH-2) sediment source proportions (%). Statistics for repeat model runs (R1 –R3): inc. standard deviation (SD) and credible interval (2.5%– 97.5%).

Depth (cm)	²¹⁰ Pb Year	Statistic RUN >>	Pine Harvest			Kanuka			Marine			Native Forest			Scrub and Pasture			Streambank			Subsoil		
			R1	R2	R3	R1	R2	R3	R1	R2	R3	R1	R2	R3	R1	R2	R3	R1	R2	R3	R1	R2	R3
1–2	2016	Mean	2.1	–	–	2.2	–	–	62.4	–	–	1.0	–	–	2.4	–	–	14.5	–	–	15.3	–	–
		Median	1.4	–	–	1.1	–	–	64.4	–	–	0.5	–	–	2.1	–	–	12.0	–	–	11.5	–	–
		SD	2.3	–	–	3.0	–	–	15.0	–	–	2.0	–	–	1.8	–	–	11.4	–	–	13.7	–	–
		2.5%	0.04	–	–	0.03	–	–	26.8	–	–	0.01	–	–	0.08	–	–	0.56	–	–	0.48	–	–
		97.5%	8.3	–	–	10.2	–	–	85.3	–	–	5.9	–	–	6.3	–	–	42.2	–	–	50.8	–	–
3–4	2012	Mean	1.2	–	–	1.1	–	–	77.2	–	–	0.9	–	–	1.1	–	–	10.3	–	–	8.1	–	–
		Median	0.9	–	–	0.8	–	–	77.7	–	–	0.6	–	–	0.9	–	–	9.1	–	–	6.4	–	–
		SD	1.2	–	–	1.1	–	–	7.5	–	–	1.0	–	–	0.9	–	–	7.4	–	–	6.9	–	–
		2.5%	0.03	–	–	0.04	–	–	61.5	–	–	0.02	–	–	0.04	–	–	0.46	–	–	0.33	–	–
		97.5%	4.2	–	–	4.0	–	–	90.0	–	–	3.3	–	–	3.2	–	–	27.1	–	–	24.9	–	–
6–7	2008	Mean	2.0	–	–	0.9	–	–	77.3	–	–	1.8	–	–	0.7	–	–	6.0	–	–	11.2	–	–
		Median	1.6	–	–	0.6	–	–	79.3	–	–	1.4	–	–	0.5	–	–	4.8	–	–	8.8	–	–
		SD	1.7	–	–	0.9	–	–	9.7	–	–	1.7	–	–	0.6	–	–	5.1	–	–	9.5	–	–
		2.5%	0.05	–	–	0.02	–	–	54.6	–	–	0.04	–	–	0.02	–	–	0.18	–	–	0.32	–	–
		97.5%	6.3	–	–	3.3	–	–	91.0	–	–	5.9	–	–	2.2	–	–	18.8	–	–	33.6	–	–

Core MH-2: sediment source proportions (%). Statistics for repeat model runs (R1 –R3): inc. standard deviation (SD) and credible interval (2.5%– 97.5%).

Depth (cm)	²¹⁰ Pb Year	Statistic RUN >>	Pine Harvest			Kanuka			Marine			Native Forest			Scrub and Pasture			Streambank			Subsoil		
			R1	R2	R3	R1	R2	R3	R1	R2	R3	R1	R2	R3	R1	R2	R3	R1	R2	R3	R1	R2	R3
11–12	2002	Mean	2.1	–	–	0.9	–	–	77.3	–	–	1.7	–	–	0.7	–	–	5.9	–	–	11.5	–	–
		Median	1.6	–	–	0.6	–	–	78.8	–	–	1.3	–	–	0.5	–	–	4.7	–	–	8.9	–	–
		SD	1.7	–	–	0.9	–	–	9.7	–	–	1.7	–	–	0.6	–	–	4.9	–	–	9.6	–	–
		2.5%	0.06	–	–	0.02	–	–	53.8	–	–	0.05	–	–	0.02	–	–	0.24	–	–	0.38	–	–
		97.5%	6.4	–	–	3.2	–	–	91.1	–	–	5.9	–	–	2.3	–	–	17.9	–	–	34.9	–	–
15–16	1997	Mean	2.8	–	–	1.4	–	–	67.7	–	–	1.8	–	–	0.9	–	–	7.7	–	–	17.6	–	–
		Median	2.3	–	–	0.9	–	–	70.9	–	–	1.2	–	–	0.7	–	–	5.8	–	–	14.1	–	–
		SD	2.3	–	–	1.7	–	–	14.8	–	–	2.1	–	–	0.8	–	–	6.6	–	–	14.5	–	–
		2.5%	0.11	–	–	0.03	–	–	29.9	–	–	0.05	–	–	0.03	–	–	0.27	–	–	0.55	–	–
		97.5%	8.5	–	–	5.9	–	–	87.7	–	–	7.4	–	–	3.0	–	–	23.0	–	–	54.7	–	–
19–20	1991	Mean	3.3	–	–	1.3	–	–	67.2	–	–	2.4	–	–	1.0	–	–	8.2	–	–	16.6	–	–
		Median	2.9	–	–	0.8	–	–	68.7	–	–	1.7	–	–	0.8	–	–	6.5	–	–	14.4	–	–
		SD	2.5	–	–	1.4	–	–	12.3	–	–	2.5	–	–	0.9	–	–	6.9	–	–	12.2	–	–
		2.5%	0.13	–	–	0.03	–	–	39.7	–	–	0.09	–	–	0.03	–	–	0.31	–	–	0.58	–	–
		97.5%	9.1	–	–	4.8	–	–	86.0	–	–	8.5	–	–	3.4	–	–	25.9	–	–	44.0	–	–

Core MH-2: sediment source proportions (%). Statistics for repeat model runs (R1 –R3): inc. standard deviation (SD) and credible interval (2.5%– 97.5%).

Depth (cm)	²¹⁰ Pb Year	Statistic RUN >>	Pine Harvest			Kanuka			Marine			Native Forest			Scrub and Pasture			Streambank			Subsoil		
			R1	R2	R3	R1	R2	R3	R1	R2	R3	R1	R2	R3	R1	R2	R3	R1	R2	R3	R1	R2	R3
22–23	1987	Mean	2.9	–	–	1.3	–	–	66.9	–	–	1.9	–	–	1.0	–	–	7.9	–	–	18.1	–	–
		Median	2.4	–	–	0.8	–	–	68.5	–	–	1.4	–	–	0.8	–	–	6.2	–	–	16.6	–	–
		SD	2.3	–	–	1.4	–	–	12.6	–	–	2.0	–	–	0.9	–	–	6.8	–	–	12.4	–	–
		2.5%	0.09	–	–	0.03	–	–	40.4	–	–	0.06	–	–	0.03	–	–	0.24	–	–	0.65	–	–
		97.5%	8.28	–	–	4.73	–	–	86.9	–	–	6.9	–	–	3.4	–	–	24.6	–	–	45.0	–	–
26–27	1982	Mean	2.0	–	–	0.8	–	–	79.3	–	–	2.1	–	–	0.6	–	–	5.6	–	–	9.6	–	–
		Median	1.6	–	–	0.6	–	–	80.9	–	–	1.6	–	–	0.5	–	–	4.4	–	–	7.5	–	–
		SD	1.7	–	–	0.8	–	–	8.5	–	–	1.8	–	–	0.6	–	–	4.7	–	–	8.1	–	–
		2.5%	0.07	–	–	0.03	–	–	59.6	–	–	0.07	–	–	0.02	–	–	0.16	–	–	0.35	–	–
		97.5%	6.20	–	–	2.9	–	–	91.3	–	–	6.7	–	–	2.2	–	–	17.4	–	–	29.5	–	–
29–30	1978	Mean	2.6	–	–	1.2	–	–	70.1	–	–	1.4	–	–	1.0	–	–	7.8	–	–	15.9	–	–
		Median	2.2	–	–	0.8	–	–	73.1	–	–	0.9	–	–	0.7	–	–	5.8	–	–	12.6	–	–
		SD	2.1	–	–	1.4	–	–	14.1	–	–	1.9	–	–	0.8	–	–	7.1	–	–	13.4	–	–
		2.5%	0.08	–	–	0.03	–	–	34.2	–	–	0.03	–	–	0.03	–	–	0.22	–	–	0.49	–	–
		97.5%	7.7	–	–	4.8	–	–	88.8	–	–	5.4	–	–	3.1	–	–	25.1	–	–	48.3	–	–

Core MH-2: sediment source proportions (%). Statistics for repeat model runs (R1 –R3): inc. standard deviation (SD) and credible interval (2.5%– 97.5%).

Depth (cm)	²¹⁰ Pb Year	Statistic RUN >>	Pine Harvest			Kanuka			Marine			Native Forest			Scrub and Pasture			Streambank			Subsoil		
			R1	R2	R3	R1	R2	R3	R1	R2	R3	R1	R2	R3	R1	R2	R3	R1	R2	R3	R1	R2	R3
31–32	1966	Mean	NA	NA	NA	2.0	–	–	63.2	–	–	1.8	–	–	1.5	–	–	10.8	–	–	20.7	–	–
		Median	NA	NA	NA	1.4	–	–	63.6	–	–	1.3	–	–	1.2	–	–	8.8	–	–	19.2	–	–
		SD	NA	NA	NA	2.0	–	–	13.0	–	–	2.1	–	–	1.2	–	–	8.6	–	–	13.1	–	–
		2.5%	NA	NA	NA	0.04	–	–	36.5	–	–	0.04	–	–	0.05	–	–	0.31	–	–	1.07	–	–
		97.5%	NA	NA	NA	7.1	–	–	86.0	–	–	6.9	–	–	4.5	–	–	31.7	–	–	49.6	–	–
33–34	1954	Mean	NA	NA	NA	1.1	–	–	65.6	–	–	1.9	–	–	1.0	–	–	7.0	–	–	23.4	–	–
		Median	NA	NA	NA	0.7	–	–	65.7	–	–	1.3	–	–	0.7	–	–	5.4	–	–	23.1	–	–
		SD	NA	NA	NA	1.1	–	–	13.6	–	–	2.1	–	–	0.8	–	–	6.2	–	–	13.2	–	–
		2.5%	NA	NA	NA	0.02	–	–	37.9	–	–	0.05	–	–	0.03	–	–	0.18	–	–	1.30	–	–
		97.5%	NA	NA	NA	4.1	–	–	89.6	–	–	7.0	–	–	3.0	–	–	22.6	–	–	51.1	–	–
34–35	1949	Mean	NA	NA	NA	1.0	–	–	74.8	–	–	2.3	–	–	0.9	–	–	6.2	–	–	14.8	–	–
		Median	NA	NA	NA	0.6	–	–	76.0	–	–	1.7	–	–	0.7	–	–	4.8	–	–	12.9	–	–
		SD	NA	NA	NA	1.0	–	–	10.5	–	–	2.2	–	–	0.8	–	–	5.2	–	–	10.7	–	–
		2.5%	NA	NA	NA	0.03	–	–	51.9	–	–	0.07	–	–	0.03	–	–	0.20	–	–	0.58	–	–
		97.5%	NA	NA	NA	3.70	–	–	91.1	–	–	7.9	–	–	2.8	–	–	19.3	–	–	38.3	–	–

Core MH-2: sediment source proportions (%). Statistics for single model run of dated sediment sample: inc. standard deviation (SD) and credible interval (2.5%– 97.5%).

Depth (cm)	²¹⁰ Pb Year	Statistic RUN >>	Pine Harvest			Kanuka			Marine			Native Forest			Scrub and Pasture			Streambank			Subsoil		
			R1	R2	R3	R1	R2	R3	R1	R2	R3	R1	R2	R3	R1	R2	R3	R1	R2	R3	R1	R2	R3
36–37	1937	Mean	NA	NA	NA	1.1	–	–	69.3	–	–	2.2	–	–	0.9	–	–	7.4	–	–	19.0	–	–
		Median	NA	NA	NA	0.8	–	–	70.4	–	–	1.6	–	–	0.7	–	–	5.8	–	–	17.4	–	–
		SD	NA	NA	NA	1.2	–	–	13.2	–	–	2.2	–	–	0.8	–	–	6.3	–	–	13.0	–	–
		2.5%	NA	NA	NA	0.04	–	–	42.3	–	–	0.05	–	–	0.03	–	–	0.20	–	–	0.81	–	–
		97.5%	NA	NA	NA	4.3	–	–	90.2	–	–	8.0	–	–	2.9	–	–	22.9	–	–	47.7	–	–
37–38	1931	Mean	NA	NA	NA	1.1	–	–	74.2	–	–	1.4	–	–	0.9	–	–	6.8	–	–	15.6	–	–
		Median	NA	NA	NA	0.8	–	–	75.2	–	–	1.0	–	–	0.7	–	–	5.5	–	–	14.3	–	–
		SD	NA	NA	NA	1.0	–	–	10.6	–	–	1.5	–	–	0.7	–	–	5.7	–	–	10.5	–	–
		2.5%	NA	NA	NA	0.03	–	–	52.3	–	–	0.04	–	–	0.03	–	–	0.23	–	–	0.60	–	–
		97.5%	NA	NA	NA	3.7	–	–	91.2	–	–	4.7	–	–	2.7	–	–	20.7	–	–	38.5	–	–
39–40	1919	Mean	NA	NA	NA	1.3	–	–	46.4	–	–	3.6	–	–	1.4	–	–	10.4	–	–	36.9	–	–
		Median	NA	NA	NA	0.7	–	–	46.0	–	–	1.8	–	–	1.0	–	–	7.0	–	–	37.8	–	–
		SD	NA	NA	NA	1.8	–	–	22.6	–	–	4.7	–	–	1.3	–	–	10.6	–	–	22.2	–	–
		2.5%	NA	NA	NA	0.02	–	–	4.8	–	–	0.04	–	–	0.04	–	–	0.26	–	–	1.49	–	–
		97.5%	NA	NA	NA	5.4	–	–	85.5	–	–	15.7	–	–	4.6	–	–	40.7	–	–	78.8	–	–

Table K-3 (core MH-3) sediment source proportions (%). Statistics for single model run of dated sediment samples: inc. standard deviation (SD) and credible interval (2.5%– 97.5%).

Depth (cm)	²¹⁰ Pb Year	Statistic RUN >>	Pine Harvest			Kanuka			Marine			Native Forest			Scrub and Pasture			Streambank			Subsoil		
			R1	R2	R3	R1	R2	R3	R1	R2	R3	R1	R2	R3	R1	R2	R3	R1	R2	R3	R1	R2	R3
1–2	2013	Mean	1.3	–	–	0.8	–	–	83.0	–	–	1.2	–	–	0.7	–	–	6.2	–	–	6.8	–	–
		Median	1.0	–	–	0.6	–	–	83.7	–	–	0.9	–	–	0.5	–	–	5.1	–	–	5.2	–	–
		SD	1.1	–	–	0.8	–	–	6.2	–	–	1.1	–	–	0.6	–	–	4.8	–	–	5.9	–	–
		2.5%	0.04	–	–	0.02	–	–	68.6	–	–	0.03	–	–	0.02	–	–	0.20	–	–	0.21	–	–
		97.5%	4.2	–	–	2.8	–	–	92.8	–	–	3.9	–	–	2.2	–	–	17.7	–	–	22.0	–	–
3–4	2008	Mean	2.0	–	–	1.6	–	–	70.8	–	–	1.4	–	–	1.3	–	–	11.5	–	–	11.3	–	–
		Median	1.6	–	–	1.1	–	–	71.6	–	–	1.0	–	–	1.1	–	–	10.0	–	–	9.4	–	–
		SD	1.6	–	–	1.4	–	–	9.3	–	–	1.4	–	–	1.0	–	–	8.4	–	–	8.9	–	–
		2.5%	0.08	–	–	0.05	–	–	50.8	–	–	0.04	–	–	0.05	–	–	0.44	–	–	0.37	–	–
		97.5%	6.1	–	–	5.5	–	–	86.5	–	–	5.0	–	–	3.9	–	–	30.3	–	–	33.3	–	–
5–6	2003	Mean	1.5	–	–	0.7	–	–	83.5	–	–	1.6	–	–	0.6	–	–	5.6	–	–	6.4	–	–
		Median	1.1	–	–	0.5	–	–	84.2	–	–	1.3	–	–	0.5	–	–	4.5	–	–	5.1	–	–
		SD	1.2	–	–	0.7	–	–	5.7	–	–	1.4	–	–	0.5	–	–	4.6	–	–	5.4	–	–
		2.5%	0.04	–	–	0.02	–	–	70.6	–	–	0.05	–	–	0.02	–	–	0.19	–	–	0.24	–	–
		97.5%	4.6	–	–	2.5	–	–	92.6	–	–	5.0	–	–	2.0	–	–	16.4	–	–	20.6	–	–

Core MH-3: sediment source proportions (%). Statistics for repeat model runs (R1 –R3): inc. standard deviation (SD) and credible interval (2.5%– 97.5%).

Depth (cm)	²¹⁰ Pb Year	Statistic RUN >>	Pine Harvest			Kanuka			Marine			Native Forest			Scrub and Pasture			Streambank			Subsoil		
			R1	R2	R3	R1	R2	R3	R1	R2	R3	R1	R2	R3	R1	R2	R3	R1	R2	R3	R1	R2	R3
8–9	1995	Mean	1.8	–	–	0.7	–	–	81.6	–	–	2.0	–	–	0.7	–	–	6.0	–	–	7.2	–	–
		Median	1.4	–	–	0.5	–	–	82.3	–	–	1.6	–	–	0.5	–	–	4.8	–	–	5.6	–	–
		SD	1.4	–	–	0.7	–	–	6.2	–	–	1.6	–	–	0.6	–	–	4.9	–	–	6.0	–	–
		2.5%	0.07	–	–	0.03	–	–	68.0	–	–	0.07	–	–	0.02	–	–	0.19	–	–	0.23	–	–
		97.5%	5.3	–	–	2.6	–	–	91.5	–	–	6.2	–	–	2.2	–	–	18.1	–	–	22.2	–	–
11-12	1987	Mean	1.6	–	–	0.9	–	–	79.2	–	–	1.4	–	–	0.7	–	–	5.8	–	–	10.5	–	–
		Median	1.3	–	–	0.6	–	–	80.2	–	–	1.1	–	–	0.5	–	–	4.6	–	–	8.6	–	–
		SD	1.4	–	–	0.9	–	–	8.1	–	–	1.3	–	–	0.6	–	–	4.6	–	–	8.1	–	–
		2.5%	0.06	–	–	0.02	–	–	61.5	–	–	0.05	–	–	0.02	–	–	0.20	–	–	0.40	–	–
		97.5%	5.2	–	–	3.2	–	–	91.8	–	–	4.6	–	–	2.1	–	–	16.8	–	–	29.3	–	–
14–15	1979	Mean	3.6	–	–	1.1	–	–	69.0	–	–	3.1	–	–	0.9	–	–	7.5	–	–	14.8	–	–
		Median	3.1	–	–	0.7	–	–	70.9	–	–	2.2	–	–	0.7	–	–	6.0	–	–	11.9	–	–
		SD	2.7	–	–	1.4	–	–	12.3	–	–	3.2	–	–	0.9	–	–	6.2	–	–	12.0	–	–
		2.5%	0.16	–	–	0.03	–	–	39.4	–	–	0.09	–	–	0.02	–	–	0.28	–	–	0.42	–	–
		97.5%	10.2	–	–	4.3	–	–	86.7	–	–	11.4	–	–	3.1	–	–	23.0	–	–	43.5	–	–

Core MH-3: sediment source proportions (%). Statistics for repeat model runs (R1 –R3): inc. standard deviation (SD) and credible interval (2.5%– 97.5%).

Depth (cm)	²¹⁰ Pb Year	Statistic RUN >>	Pine Harvest			Kanuka			Marine			Native Forest			Scrub and Pasture			Streambank			Subsoil		
			R1	R2	R3	R1	R2	R3	R1	R2	R3	R1	R2	R3	R1	R2	R3	R1	R2	R3	R1	R2	R3
16–17	1974	Mean	NA	NA	NA	2.3	–	–	61.0	–	–	2.9	–	–	2.0	–	–	14.0	–	–	17.8	–	–
		Median	NA	NA	NA	1.6	–	–	61.7	–	–	2.1	–	–	1.7	–	–	12.0	–	–	15.5	–	–
		SD	NA	NA	NA	2.4	–	–	12.8	–	–	2.8	–	–	1.5	–	–	10.7	–	–	12.9	–	–
		2.5%	NA	NA	NA	0.06	–	–	34.9	–	–	0.10	–	–	0.06	–	–	0.42	–	–	0.75	–	–
		97.5%	NA	NA	NA	8.7	–	–	83.3	–	–	10.6	–	–	5.7	–	–	39.2	–	–	47.0	–	–
19–20	1966	Mean	NA	NA	NA	1.3	–	–	69.9	–	–	4.5	–	–	1.1	–	–	8.7	–	–	14.6	–	–
		Median	NA	NA	NA	0.9	–	–	71.8	–	–	3.6	–	–	0.9	–	–	7.0	–	–	12.2	–	–
		SD	NA	NA	NA	1.3	–	–	12.1	–	–	4.0	–	–	1.0	–	–	7.2	–	–	11.2	–	–
		2.5%	NA	NA	NA	0.04	–	–	41.8	–	–	0.17	–	–	0.03	–	–	0.23	–	–	0.52	–	–
		97.5%	NA	NA	NA	4.9	–	–	88.6	–	–	14.6	–	–	3.6	–	–	26.1	–	–	41.8	–	–
21–22	1960	Mean	NA	NA	NA	1.3	–	–	75.2	–	–	2.4	–	–	1.0	–	–	8.6	–	–	11.5	–	–
		Median	NA	NA	NA	0.9	–	–	76.3	–	–	2.0	–	–	0.8	–	–	7.1	–	–	9.4	–	–
		SD	NA	NA	NA	1.2	–	–	8.9	–	–	2.0	–	–	0.8	–	–	6.7	–	–	8.9	–	–
		2.5%	NA	NA	NA	0.03	–	–	55.5	–	–	0.09	–	–	0.03	–	–	0.38	–	–	0.47	–	–
		97.5%	NA	NA	NA	4.3	–	–	89.6	–	–	7.0	–	–	2.9	–	–	24.8	–	–	32.8	–	–

Core MH-3: sediment source proportions (%). Statistics for repeat model runs (R1 –R3): inc. standard deviation (SD) and credible interval (2.5%– 97.5%).

Depth (cm)	²¹⁰ Pb Year	Statistic RUN >>	Pine Harvest			Kanuka			Marine			Native Forest			Scrub and Pasture			Streambank			Subsoil		
			R1	R2	R3	R1	R2	R3	R1	R2	R3	R1	R2	R3	R1	R2	R3	R1	R2	R3	R1	R2	R3
24–25	1952	Mean	NA	NA	NA	2.6	–	–	54.6	–	–	3.7	–	–	2.1	–	–	16.5	–	–	20.5	–	–
		Median	NA	NA	NA	1.8	–	–	55.4	–	–	2.7	–	–	1.7	–	–	13.5	–	–	18.4	–	–
		SD	NA	NA	NA	2.9	–	–	15.2	–	–	3.8	–	–	1.7	–	–	12.7	–	–	14.5	–	–
		2.5%	NA	NA	NA	0.08	–	–	20.6	–	–	0.13	–	–	0.08	–	–	0.75	–	–	0.86	–	–
		97.5%	NA	NA	NA	10.3	–	–	80.7	–	–	13.5	–	–	6.2	–	–	45.6	–	–	53.6	–	–
26-27	1947	Mean	NA	NA	NA	1.8	–	–	65.5	–	–	3.1	–	–	1.5	–	–	11.4	–	–	16.7	–	–
		Median	NA	NA	NA	1.3	–	–	66.3	–	–	2.4	–	–	1.3	–	–	9.6	–	–	14.7	–	–
		SD	NA	NA	NA	1.9	–	–	11.6	–	–	2.8	–	–	1.2	–	–	8.6	–	–	11.8	–	–
		2.5%	NA	NA	NA	0.05	–	–	41.3	–	–	0.10	–	–	0.05	–	–	0.41	–	–	0.66	–	–
		97.5%	NA	NA	NA	6.7	–	–	85.1	–	–	10.4	–	–	4.5	–	–	32.0	–	–	42.3	–	–
28–29	1942	Mean	NA	NA	NA	1.9	–	–	64.8	–	–	2.5	–	–	1.5	–	–	11.7	–	–	17.6	–	–
		Median	NA	NA	NA	1.3	–	–	65.7	–	–	1.8	–	–	1.3	–	–	9.8	–	–	15.7	–	–
		SD	NA	NA	NA	2.0	–	–	12.4	–	–	2.7	–	–	1.2	–	–	9.0	–	–	12.6	–	–
		2.5%	NA	NA	NA	0.06	–	–	38.8	–	–	0.08	–	–	0.05	–	–	0.50	–	–	0.67	–	–
		97.5%	NA	NA	NA	7.2	–	–	85.8	–	–	8.6	–	–	4.4	–	–	32.8	–	–	46.5	–	–

Core MH-3: sediment source proportions (%). Statistics for repeat model runs (R1 –R3): inc. standard deviation (SD) and credible interval (2.5%– 97.5%).

Depth (cm)	²¹⁰ Pb Year	Statistic RUN >>	Pine Harvest			Kanuka			Marine			Native Forest			Scrub and Pasture			Streambank			Subsoil		
			R1	R2	R3	R1	R2	R3	R1	R2	R3	R1	R2	R3	R1	R2	R3	R1	R2	R3	R1	R2	R3
31–32	1934	Mean	NA	NA	NA	0.4	–	–	77.7	–	–	1.4	–	–	0.4	–	–	3.6	–	–	16.4	–	–
		Median	NA	NA	NA	0.3	–	–	79.6	–	–	0.8	–	–	0.3	–	–	2.6	–	–	14.4	–	–
		SD	NA	NA	NA	0.5	–	–	13.5	–	–	1.9	–	–	0.4	–	–	3.6	–	–	12.5	–	–
		2.5%	NA	NA	NA	0.01	–	–	48.6	–	–	0.03	–	–	0.01	–	–	0.11	–	–	0.48	–	–
		97.5%	NA	NA	NA	1.7	–	–	96.2	–	–	6.7	–	–	1.5	–	–	12.7	–	–	44.7	–	–
34–35	1926	Mean	NA	NA	NA	0.5	–	–	79.5	–	–	1.5	–	–	0.5	–	–	3.9	–	–	14.1	–	–
		Median	NA	NA	NA	0.3	–	–	83.0	–	–	0.8	–	–	0.3	–	–	2.8	–	–	10.9	–	–
		SD	NA	NA	NA	0.6	–	–	13.7	–	–	2.9	–	–	0.5	–	–	3.7	–	–	12.4	–	–
		2.5%	NA	NA	NA	0.01	–	–	46.2	–	–	0.03	–	–	0.01	–	–	0.11	–	–	0.34	–	–
		97.5%	NA	NA	NA	1.9	–	–	95.9	–	–	7.8	–	–	1.6	–	–	12.8	–	–	43.4	–	–
36–37	1921	Mean	NA	NA	NA	1.0	–	–	68.4	–	–	1.4	–	–	0.7	–	–	6.1	–	–	22.4	–	–
		Median	NA	NA	NA	0.6	–	–	68.4	–	–	0.9	–	–	0.6	–	–	4.6	–	–	22.1	–	–
		SD	NA	NA	NA	1.2	–	–	12.8	–	–	1.5	–	–	0.6	–	–	5.5	–	–	12.5	–	–
		2.5%	NA	NA	NA	0.02	–	–	43.0	–	–	0.03	–	–	0.02	–	–	0.17	–	–	1.20	–	–
		97.5%	NA	NA	NA	3.7	–	–	91.6	–	–	5.1	–	–	2.4	–	–	20.4	–	–	47.5	–	–

Source proportion statistics for the reanalysed Havelock Inflow sediment

Table K-3: Sources of sediment contributing to the “Havelock Inflow” Handley et al. (2017). Analysis based on catchment and marine source library developed for the present study. Statistics for soil source proportions (%). Mixing model results for three model runs – range of values shown where they differ between runs. Model convergence diagnostics [run1/2/3]: DIC = [31.3/30.9/31.2], Gelmin-Rubin = [all 0/27 >1.05], Geweke = [(0/1/4), (1,5,0), (0/0/3)].

Land use source	Mean	Median	SD	2.5% (percentile)	97.5% (percentile)
Harvested pine	0.5	0.3	0.5	0.01	1.8
Kanuka	0.2–0.3	0.1–0.2	0.2–0.4	0.01	0.9–1.2
Marine	86.0	87.0–87.2	8.5–8.6	67.0–67.3	97.8–98.0
Native forest	0.3	0.2	0.4–0.5	0.01	1.2–1.3
Scrub and pasture	0.3	0.2	0.3	0.01	0.9–1.0
Streambank	2.4–2.5	1.7–1.8	2.4	0.06	8.6–8.9
Subsoil	10.1–10.3	9.0–9.3	8.1–8.2	0.17–0.22	28.0–28.9

Appendix L Source proportion yields (% km⁻²) by land use area for Pelorus-Rai, Kaituna and Cullens Creek catchments.

To compare the relative sediment contributions of disturbed catchment land use sources with the native/indigenous forest sediment contributions (2001 – 2012), the average sediment source proportions (%), run 3) calculated from analysis of the Mahau cores were normalised using land use area data (km²). Landuse areas were extracted from the Land Cover Data Base (Manaaki Whenua Landcare [LCDB], <https://www.landcareresearch.co.nz/publications/innovation-stories/2014-stories/lcdb>) versions 2 through 4. The disturbed land use sources included were gorse and broom (class 51), manuka and/or kanuka (class 52) and forest – harvested (class 64). Soil proportion (%) results for dated sediment core samples that coincided in time with LCDB-2 (2001/2002), LCDB-3 (2008/2009) and LCDB-4 (2012/13) were included. Data from LCDB-1 (1996/97) does not identify harvested pine as a separate land use class. Likewise, data from LCDB-5 (2018/19) was not included because the Mahau cores were collected in 2017, prior to that LCDB update. The source proportion yields (% km⁻²) for the disturbed catchment land uses were then normalised by the matching values (i.e., year and core) for the native forest (% km⁻²) to enable direct comparisons of the source yields relative to native forest.

Two separate analyses were undertaken using: **(1)** LCDB land use area data for the Pelorus-Rai, Kaituna and Cullens Creek catchments that discharge to the upper reaches of Pelorus Sound, and **(2)** land use area data for the entire catchment of the Sound to its seaward boundary at Te Akaroa (west point) – Kaitira (east point). **Table K-1** presents the results of the analysis for option 1 (i.e., LCDB land use area data for Pelorus-Rai, Kaituna and Cullens Creek catchments).

Although the second option is considered most appropriate (i.e., land use area for entire Pelorus Sound catchment) as described in the results section, table H1 is presented here to enable comparison with results based on land use data for the entire catchment of the Pelorus Sound.

Table L-1: Source proportion yields (% km⁻²) for land use classes and yield ratios relative to native forest based on Land Cover Data Base (LCDB) versions 2 to 4. Sediment source proportions (%) for model run 3. Land use areas are based on the combined values for the Pelorus-Rai, Kaituna and Cullens Creek catchments.

LCDB Class	Year	Core	Area (km ²)	Source proportion yield by area (% km ⁻²)			Yield relative to Indigenous Forest		
				Mean	2.5%	97.5%	Mean	2.5%	97.5%
Harvested Forest	2012/13	MH-1	21.2	0.0945	0.0014	0.5347	59.7	49.6	67.4
		MH-2		0.0567	0.0014	0.1979	43.8	49.2	41.7
		MH-3		0.0614	0.0019	0.1960	35.6	43.8	34.8
		Average					46.3	47.5	48.0
	2008/09	MH-1	11.8	0.1691	0.0042	0.5342	196.2	190.3	163.8
		MH-2		0.1691	0.0042	0.5342	65.4	73.6	63.4
		MH-3		0.1691	0.0068	0.5131	84.1	107.4	72.0
		Average					115.2	123.8	99.7
	2001/02	MH-1	5.7	0.4044	0.0141	1.1441	176.0	244.7	137.8
		MH-2		0.3691	0.0105	1.1283	151.1	146.8	133.8
		MH-3		0.2636	0.0070	0.8014	114.7	97.9	110.9
		Average					147.3	163.1	127.5
Manuka/Kanuka	2012/13	MH-1	21.6	0.2590	0.0007	1.3821	163.6	26.0	174.3
		MH-2		0.0509	0.0019	0.1855	39.3	64.3	39.1
		MH-3		0.0370	0.0009	0.1290	21.4	21.4	22.9
		Average					74.8	37.2	78.7
	2008/09	MH-1	22.2	0.0657	0.0016	0.2219	76.3	71.1	68.0
		MH-2		0.0406	0.0009	0.1483	15.7	16.2	17.6
		MH-3		0.0721	0.0022	0.2474	35.9	34.9	34.7
		Average					42.6	40.7	40.1
	2001/02	MH-1	24.3	0.0657	0.0016	0.2219	28.6	27.5	26.7
		MH-2		0.0370	0.0008	0.1302	15.1	11.4	15.4
		MH-3		0.0288	0.0007	0.1031	12.5	9.2	14.3
		Average					18.8	16.0	18.8
Native Forest	2012/13	MH-1	694.9	0.0016	0.0000	0.0079	–	–	–
		MH-2		0.0013	0.0000	0.0047	–	–	–

LCDB Class	Year	Core	Area (km ²)	Source proportion yield by area (% km ⁻²)			Yield relative to Indigenous Forest		
		MH-3		0.0017	0.0000	0.0056	–	–	–
	2008/09	MH-1	696.2	0.0009	0.0000	0.0033	–	–	–
		MH-2		0.0026	0.0001	0.0084	–	–	–
		MH-3		0.0020	0.0001	0.0071	–	–	–
	2001/02	MH-1	696.2	0.0023	0.0001	0.0083	–	–	–
		MH-2		0.0024	0.0001	0.0084	–	–	–
		MH-3		0.0023	0.0001	0.0072	–	–	–